ANAEROBIC DIGESTION of FISCHER-TROPSCH REACTION WATER

Submerged Membrane Anaerobic Reactor Design, Performance Evaluation & Modeling

By

Pierrie Jakobus van Zyl

This Thesis is Presented for the Degree of
DOCTOR OF PHILOSOPHY
In the Department of Civil Engineering
UNIVERSITY OF CAPE TOWN

Water Research Group
Department of Civil Engineering
University of Cape Town

Supervisors:
Prof GA Ekama
Prof MC Wentzel

June 2008

Abstract

ANAEROBIC DIGESTION of FISCHER-TROPSCH REACTION WATER - Submerged membrane Anaerobic Reactor Design, Performance Evaluation & Modeling

- Pierrie Jakobus van Zyl
(August 2008)

The aim of this project is to develop and evaluate an anaerobic membrane bio-reactor for the treatment of Fischer-Tropsch Reaction Water originating in Sasol's coal to fuel synthesis process. It was hypothesized that an anaerobic membrane bio-reactor fitted with submerged flat panel ultra filtration membranes to induce a 100% solids-liquid-separation and biogas recycle for membrane scour will be able to treat Fischer-Tropsch Reaction Water to a higher standard and more economically than currently available systems. A down-flow anaerobic packed bed reactor was also operated to benchmark the performance of the anaerobic membrane bio-reactor.

During the anaerobic membrane bio-reactor evaluation period of 680 days, the two systems were operated at a steady state organic loading rate (OLR) of 15 kgCOD/m^3_{Vr}/d for a period of 60 days and their performance compared. The anaerobic membrane bioreactor yielded a total effluent COD of <100 mgCOD/L compared with the packed bed reactor 1750 mgCOD/L, of which 770 mgCOD/L was particulate organics. The alkalinity requirement of the anaerobic membrane reactor (0.067 kgNaOH/$kgCOD_{removed}$) was 25% lower than that of the packed bed reactor (0.11 mgNaOH/$kgCOD_{removed}$). The mixed liquor suspended solids concentration in the membrane system could be increased to >30gTSS/L resulting in organic loading rates double (30 kgCOD/m^3_{Vr}/d) the maximum viable limit of the packed bed system (OLR = 15 kgCOD/m^3_{Vr}/d). The sludge production of the membrane reactor (0.022 gTSS/$gCOD_{removed}$) was significantly lower than that of the packed bed (0.031 gTSS/$gCOD_{removed}$) resulting in low nutrient requirements.

In the second part of the project, a steady state and dynamic simulation model were developed for the anaerobic conversion for Fischer-Tropsch Reaction Water. The two models were calibrated and validated on the data collected in the 680 day experimental phase of the project. From the experimental phase it was found that, if the anaerobic membrane bioreactor is implemented, savings in capital and main operating costs are; reactor volume (50%), alkalinity (25%), sludge incineration (30 %) and downstream processing (± 95%). From the modeling section it was concluded that pH, temperature, effluent short chain fatty acids and hydrogen partial pressure play pivotal roles in the stability of the anaerobic system treating Fischer-Tropsch Reaction Water, if one of these parameters deviates from the prescribed range the treatment capability of the system deteriorates dramatically.

Declaration

This decleration is to certify this is essentially my own work and that this thesis has not been submitted in partially or in full to another institute of higher learning for a post graduate degree.

…….
Pierrie J van Zyl
August 2008

Synopsis

The Fischer-Tropsch (FT) process converts coal and natural gas (mostly methane) to synthetic fuels and other value added polymers. Irrespective of the feedstock and catalysts used, the FT process produces three major effluent streams, namely Oily Sewer Water (known as API), Stripped Gas Liqour (SGL) and Fischer-Tropsch Reaction Water (FTRW). At Sasol's Secunda plant situated in South Africa, the three streams have a combined flow and organic load of 128 ML/d and 677 tonCOD/d respectively. The combined waste water stream is currently treated in an activated sludge plant, requiring 705 tonsO_2/d (480 tonO_2/d for sludge activation and 225 tonO_2/d for electricity generation from coal) and producing in the order of 150 tonTSS/d of dry solids. FTRW contributes 77% of the organic load and consists mostly of C_2 to C_6 Short Chain Fatty Acids (SCFA). The aerobic treatment of SCFA streams is problematic because of the tendency to produce biomass with poor settling properties, has high aeration demand, high sludge production as well as poor effluent quality and high solid liquid separation costs.

As early as 1986 research on the Anaerobic Digestion of Fischer-Tropsch Reaction Water (AD-FTRW) was investigated and it was shown that this high organic strength (18 000 mgCOD/L), low pH (3.77), industrial waste water is in fact amenable to anaerobic digestion. Anaerobic digestion can be defined as the stepwise decomposition of a biodegradable substrate mediated by micro-organisms that proliferate under oxygen deficient (anaerobic) conditions. The biodegradable substrate undergoes a stepwise decomposition process with the final products being carbon dioxide, methane and biomass. However, some major issues hampered the full scale application of the AD-FTRW process, viz. (i) poor sludge settleability and solids-liquid-separation and (ii) the alkalinity requirements to raise the influent pH to within the range of optimal anaerobic digestion (±7). Nevertheless, the significance of energy recovery from biogas produced in the AD-FTRW was identified early on and sustainable long term evaluation of fixed-bed anaerobic technologies were initiated by Sasol in 1987.

From the pilot-scale work, alkalinity requirements were identified as the main constraints in the applicability of the AD-FTRW. Other concerns were the high TSS and total SCFA concentration (~500 mgAc/L) in the effluent. The result was that an aerobic polishing step would be enquired to decrease the effluent COD and solids to levels that is acceptable for reverse osmosis and recycling for water re-use.

From literature it was concluded that a possible solution to the high effluent TSS and SCFA and possibly also to the high alkalinity requirements, was a combination of anaerobic digestion and membrane technologies. Membranes provide a 100% solids-liquid separation, producing effluents completely free of TSS. Secondly, membranes also un-couple the hydraulic and solids retention times so that high reactor solids concentrations can be achieved, resulting in a lowering in effluent biodegradable COD (and SCFA). The lower the effluent SCFA (and resultant acidity), the lower the alkalinity requirements to maintain pH neutrality.

Apart from the expected gains in effluent quality and lowered alkalinity consumption with an Anaerobic Membrane Bioreactor (AnMBR) specifically designed for AD-FTRW, a few other advantages were identified. These include:

- Anaerobic systems relying on granulation like the Up-flow Anaerobic Sludge Bed Reactor (USAB), Extended Granular Sludge Bed Reactor (EGSB) and Internal Circulation (IC) reactors show poor process performance in the long term treatment of SCFA streams. This problem is overcome by the 100% solids-liquid separation imposed by the membranes in the AnMBR.
- The capital cost around membrane acquisition and installation has traditionally been one of the main factors hampering the full-scale implementation of MBRs. However, from the early 90's membrane costs have shown a >95% decrease. The same has also been observed for the operating cost of MBR plants. If these trends continue membrane technologies will become the preferred waste water treatment option and its use will increase dramatically in the next five years.
- In the early 90's there was a dramatic increase in the research outputs generated by research facilities investigating aerobic MBRs. In response to these research outputs and skills developments, full-scale aerobic MBR plants rapidly increased in number in the past decade. For the AnMBR, a 10 fold increase in publications has been observed over the past 4 years. It is thus expected that the AnMBR will follow the same path to full-scale application as the Aerobic MBR.

Currently, non-woven polymer ultra-filtration (0.5 µm – 2 nm) membranes are the most popular membrane pore size in waste water treatment because these operate under more economical Trans Membrane Pressures (TMPs), and retains bacteria and viruses while allowing soluble constituents to pass through. AnMBR research is currently dominated by two reactor configurations; (i) the cross-flow system, in which an external membrane module is mounted on a completely mixed anaerobic reactor and (ii) the submerged configuration in which flat panel membranes are submerged in the mixed liquor and recycles biogas for membrane scour. The submerged configuration has gained significant popularity in research in the past few 3 years.

The aim of this study is to investigate the Anaerobic Digestion of Fischer-Tropsch Reaction Water (AD-FTRW). The investigation consists of four major parts:

1. The design, commission, start-up and operate a laboratory-scale Submerged Anaerobic Membrane Reactor (AnMBR) using A4-size flat panel Kubota® membranes for the treatment of FTRW.

2. The design, commission, start-up and operate a laboratory-scale Anaerobic Packed Bed Reactor (AnPBR) to serve as benchmark for the AnMBR's performance. The AnPBR design is a scale-down of a pilot plant AnPBR currently also under evaluation by Sasol for the AD-FTRW.

3. Develop a steady state design model for the AD-FTRW, calibrated on the data obtained in (1) and (2) predicting design parameters like; (i) reactor volume, (ii) operational MLSS, (iii) biogas production and (iv) feedstock consumption (alkalinity and nutrients) for a given organic load of FTRW.

4. Develop of a dynamic simulation model for the AD-FTRW, again calibrated on the steady sate model and data obtained in (1) and (2). Once the reactor volumes and feedstock requirements for a given organic load has been identified by the steady state model, the dynamic model can be used to predict the designed reactor's (i) response to dynamic flow and load variations, (ii) the effluent quality that can be expected for a given reactor volume and sludge age and (iii) the effect of inhibitory substances on the microbial performance.

The 23 L laboratory-scale AnMBR includes 3 200x300 mm (A4-size) submerged flat panel ultra filtration membranes to induce a 100% solids-liquid-separation. Membrane scour to minimize membrane fouling is provided by a biogas recirculation system (750 $L/m^2/h$). Biogas is extracted from biogas headspace above the mixed liquor and reintroduced through a coarse bubble diffuser below the membranes. Advantages of anaerobic membrane FTRW treatment are that (i) zero suspended solids effluent for reuse, (ii) very low (< 0.03 gCOD/gCOD) sludge production, (iii) zero oxygen demand and (iv) recovery of 2/3 of the carbon and > 98% of the COD and energy in methane for beneficial use – recycling for membrane scour and energy generation. The AnMBR is fed a synthetic FTRW conditioned with nutrients and some alkalinity (~800 $mgCaCO_3/L$) to raise the pH to that of actual FTRW (3.77).

.

Start-up from an un-adapted municipal anaerobic biomass from an OLR of 2 $kgCOD/m^3_{Vr}/d$ to the desired steady state value of 15 $kgCOD/m^3_{Vr}/d$ was achieved in less than 4 months. From the nutrient optimization after start-up it was shown that N, P, S and Fe are of primary importance in the AD-FTRW system and should be dosed as macro nutrients (~ 50, 10, 4, 1 mg/L_{feed} respectively).

In the membrane performance evaluation of the AnMBR it was found that inorganic foulants can be removed by rinsing and back-flushing the membranes. However, for biological foulants, a chemical clean is required. Membrane life span was estimated at upwards of 7 years, but conclusive results will require an investigation period significantly longer than 680 days. A critical flux of 4.3 $L/m^2/h$ was identified. At fluxes higher than this critical value, biological cake layer formation could not be controlled by biogas scour resulting in excessively high TMPs (>1000 mmH_2O) to maintain flux. The low critical flux observed in the AnMBR is probably due to the accumulation of extra cellular polymers and/or endogenous biomass in the MLSS due to the very long sludge age. Research done by Hu & Stuckey (2007) has shown that the addition of powdered activated carbon can increase the critical flux to > 20 $L/m^2/h$ in a submerged AnMBR.

Apart from membranes, another means of achieving a high degree of solid-liquid-separation in the AD-FTRW environment has been identified as fixed film anaerobic technologies. For a direct comparison between the performance of the membrane and packed bed technologies for AD-FTRW, a laboratory-scale replica of the AnPBR pilot plant was designed and constructed to serve as control reactor for the performance evaluation of the AnMBR. The constructed lab-scale AnPBR system was operated at the exact same laboratory conditions as the AnMBR and fed the same feed and nutrient mix as the AnMBR. The final design of the scaled down AnPBR was a 23 L, the down flow velocity in the lab-scale unit was kept the same as the pilot plant at 0.884 m/h requiring a recycle flow of 20.05 L/h. The same pilot-plant packing material (Flocor Rings) as was used in the pilot plant was used in the lab scale unit. Since the diameter of the lab-scale system was selected so that the down flow velocity and the packing densities are the same as in the pilot plant, the

hydrodynamics experienced by the micro-organisms inside the lab scale unit should be similar to that of the pilot plant.

The AnMBR effluent is free of particulates and TSS compared with the AnPBR where 57 % of the effluent COD (1750 mgCOD/L) is in particulate form. Furthermore the total COD of the AnMBR is only 2% (35 mgCOD/L) of the total effluent COD of the AnPBR at an OLR of 15 kgCOD/m^3/d. The result would be a significantly reduced operating and capital cost for the downstream processing system. Due to the retention of biomass in the AnMBR and its long sludge age, the dead biomass in the reactor gets hydrolyzed and is reintroduced as substrate to be utilized by the anaerobic biomass. This re-utilization of biomass results in a 30% lower sludge production (0.022 gTSS/$gCOD_{removed}$ vs. 0.031 gTSS/$gCOD_{removed}$) and nutrient dosage - and hence sludge disposal cost - compared with the AnPBR.

The main operating cost in anaerobic systems treating acidic waste water is the alkalinity dosing cost. Because of the high effluent SCFA and slightly higher reactor pH of the AnPBR, the alkalinity consumption of this system was 25% higher (0.11 gNaOH/$gCOD_{removed}$ vs. 0.067 gNaOH/$gCOD_{removed}$) than that of the AnMBR under the same operating conditions. However, the AnPBR can handle far larger (3 times) shock loads than the AnMBR and still show a 30% shorter recovery period (8 days).

Provided the membranes can be maintained below the critical flux, the AnMBR was operated at a maximum OLR of 30 kgCOD/m^3_{Vr}/d, compared with 8 kgCOD/m^3_{Vr}/d for the AnPBR. This implies a 3 times smaller reactor volume than required with the AnPBR for the same organic loading. This and the significant savings in fixed capital and main operating costs namely; reactor volume (60%) alkalinity (25%), sludge incineration (30 %) and downstream processing (± 95%) indicates that the AnMBR might be a financially competitive treatment option for FTRW, despite the high ultra filtration membrane costs and more complex control strategies.

A steady state model was developed for the anaerobic conversion FTRW with Urea and hydroxide dosing, to their metabolic products; (i) biomass, (ii) carbon dioxide, (iii) methane, (iv) alkalinity and (v) ammonia. The primary use of this model is reactor design, i.e. the calculation of (i) mixed liquor concentration (MLSS), (ii) reactor volume, (iii) reactor operational pH, (iv) alkalinity, (v) nutrient requirements and (vi) biogas production and composition.

This model comprises three parts (i) a COD mass balance based kinetic part from which the methane gas and biomass COD production are determined for a given sludge age, (ii) a C, H, O, N, charge and COD mass balance based stoichiometry part from which the gas composition (or partial pressure of CO_2) and alkalinity generated are calculated from the COD concentration utilized and its x, y and z and a composition in $C_xH_yO_z$ of the biodegradable organics, the urea dosed for nitrogen and the alkalinity requirements and (iii) a carbonate weak/acid base chemistry part from which the pH of the digester is obtained from the partial pressure of CO_2 and alkalinity generated. The model takes into account dissociation of the SCFA substrate, hydrolysis of urea (for N requirements) and alkalinity dosing to maintain a reactor pH at 7.0, since it was found that these processes have a significant effect reactor pH. Because the FTRW are all readily biodegradable, it could be assumed that the biodegradable substrate is utilized to completion (S_{be} = 0). The model was calibrated on steady state experimental data recorded on the AnMBR. The model was validated against datasets of 200 days each from the AnMBR and the AnBPR operated under the same laboratory conditions.

Biogas and pH are predicted to well within 10% of the actual measured values. The mixed liquor concentration predictions can vary as much as 30%, but yields results typically within 15% of the measured results under normal operating conditions. The steady state model was found to be sufficiently accurate to judge the health of the system. If parameters – including biogas production and pH – deviate from the predicted values, it is usually an early sign of system instability. Steady state models are (i) practical for design, because they allow reactor sizes to be simply calculated in a spreadsheet and (ii) provide a basis for crosschecking for simulation model outputs and (iii) can predict initial values for dynamic simulation models, like biomass concentrations and reactor volumes. However, steady state models cannot predict effluent biodegradable COD concentration (S_{be}), bioprocess inhibition, response to organic over-loading or digester failure conditions. For this, the time dependant metabolic intermediate production by the individual organism groups is required.

The dynamic simulation AD-FTRW model was developed to overcome the restrictions of the steady state model. The dynamic AD-FTRW model was developed from balanced stoichiometric reactions describing the anaerobic metabolism of each biodegradable organic type of the feed by its corresponding Functional Organism Group (FOG). The yield values of the individual FOGs were calibrated against the steady state model with an automated parameter optimization using the water treatment simulation package West®. Similarly, the half saturation constants for the individual FOGs were calibrated with West® against batch test experimental data on sludge harvested from the AnMBR on which individual SCFA concentrations profiles were measured.

After calibration, the dynamic AD-FTRW was validated against dynamic flow and load experimental data. The model shows less variability in the predicted outputs than the experimental data. The model only calculates daily averages, whereas the experimental data are grab samples obtained from the experimental system. Nevertheless parameters (i) alkalinity, (ii) pH, (iii) biogas production and (iv) composition and (v) MLSS are predicted within the ± 10 % error margin. The experimental vs. predicted outputs for S_{be} and effluent SCFA are 190^S vs. 224^S mgCOD/L (P_{90} = 65%) and 134^S vs. 112^S mgAc/L (P_{90} = 75%) respectively. Although the dynamic AD-FTRW model slightly over predicts the effluent COD (18%) and SCFA (20%), the effluent COD is less than 1% of the influent COD and a 20% error in effluent COD is < 0.2% of the influent COD. This slight over prediction is advantageous, since it will result in a more conservative design of downstream processes.

A literature survey was conducted to find the required inhibition functions for mesophillic anaerobic digestion. Inhibitory parameters include pH, temperature, high Short Chain Fatty Acid (SCFA) concentrations and dissolved hydrogen gas ($H_{2(aq)}$) inhibition. It was found that a temperature and pH variation of ± 4 ^oC and ± 0.3 pH units respectively can lead to catastrophic system failure. Also a rapid (1 day) OLR increase of 17% also leads to a catastrophic failure. These findings correspond well with observations on the experimental system. The inhibition functions were obtained from literature and applied 'as is' and should be validated experimentally if this research is continued.

Irrespective of the inhibition type (pH, T, SCFA or OLR increase) the dissolved hydrogen gas pressure ($H_{2(aq)}$) always shows a fluctuation before the system fails catastrophically. It can also be noted that, if the $H_{2(aq)}$ recovers, the system also recovers from the inhibition of shock load. Secondly the $H_{2(aq)}$ also recovers far quicker than other parameters like effluent SCFA or S_{be}. Thus the $H_{2(aq)}$ concentration appears to the ideal pre-emptive parameter for predicting (i) inhibitions, (ii) imminent

reactor failure and also (iii) reactor recovery. Traditionally, the $H_{2(aq)}$ and the gas phase hydrogen partial pressure could not be measured economically due to its low concentrations. However, due to recent advances in hydrogen fuel cell technology inexpensive $H_{2(aq)}$-probes that can measure $H_{2(aq)}$ concentrations as low as 90 nano-mols are currently available. It has also been proven that these probes can survive long term use in anaerobic digestion mixed liquor.

It is estimated that if the AnMBR technology is implemented at full scale and the entire FTRW stream is treated anaerobically, a 77% reduction in oxygen demand and a 63% reduction on sludge production is expected on the entire water (AnMBR and Activated Sludge) treatment system. Since energy can be recovered from the anaerobically produced methane, the electricity requirements of the aerobically treated API and SGL wastewater streams will be met with a surplus of roughly 400 MWh will be produced.

Since sludge incineration and energy requirements for aeration are the major contributors to the overall operating cost of the activated sludge plant, it is estimated that a saving of 60 million Rand/year can be made with the anaerobic digestion of FTRW. Furthermore, it the methane in the biogas is converted to electricity it will produce approximately 571 MWh/d or 23 MW (at 33% thermal efficiency), enough to power 17000 average South African house holds. The carbon footprint of the AS-AnMBR plant will also be 48% less than that of the current waste water treatment system. Alternatively, the biogas can be blended into the natural gas line before auto-thermal reforming which will then be converted to synthesis gas and polymerized via the FTRW process. It is estimated that if the 127.8 ton/d of methane is converted to diesel, 52 000 L/d can be produced extra, resulting in a further capital gain of ~ 65 R million per year.

Table of Contents

List of Figures

List of Tables

Abbreviation List

Abbreviation

Ac	Acetic Acid	[mol/L]
AD- FTRW	Anaerobic Digestion of Fischer-Tropsch Reaction Water	
AD-PS/WAS	Anaerobic Digestion of Primary Sludge/Waste Activated Sludge	
AnFBR	Anaerobic Fluidised Bed Reactor	
AnMBR	Anaerobic Membrane Bioreactor	
AnPBR	Anaerobic Packed Bed Reactor	
API	American Petroleum Industries Wastewater	
AS	Activated Sludge	
b	Rate of Endogenous Decay	[1/d]
B	Boron	
Bu	Butyric Acid	[mol/L]
C	Carbon Chain Length	
Ca	Calcium	
$CaCO_3$	Calcium Carbonate	
CH_4	Methane	
Co	Cobalt	
COD	Chemical Oxygen Demand	[mgCOD/L]
CO_2	Carbon Dioxide	
CTL	Coal to Liquid	
Cu	Copper	
$C_xH_yO_z$	Generic Composition of Substrate	
$C_2H_4O_2$	Acetic Acid (Ac)	
$C_3H_6O_2$	Propionic Acid (Pr)	
$C_4H_8O_2$	Butyric Acid (Bu)	
$C_5H_{10}O_2$	Valeric Acid (Va)	
$C_6H_{12}O_2$	Hexanoic Acid (Hx)	
$C_5H_7O_2N$	Generic Composition of Biomass	
Da	Daltons	
D_b	Electron Accepting Capacity of the Biomass	
D_s	Electron Donating Capacity of the Substrate	
DSVI	Diluted Sludge Volume Index	[mL/g]
Dyn	Dynamic	
E	Fraction of the Biodegradable COD that is Converted to Biomass	
EGSB	Extended Granular Sludge Bed Reactor	

EtOH	Ethanol	[mol/L]
f	Unbiodegradable Fraction of Endogenous Mass	
F	Fraction of Organic Acid in Dissociated Form	
f_{cv}	COD to VSS Ratio of Biomass	[gCOD/gVSS]
Fe	Iron	
f_i	VSS to TSS Ratio of Biomass	[gVSS/gTSS]
f_n	TKN to VSS Ration of Biomass	[gTKN/gVSS]
FOG	Functional Organism Group	
FSA	Free and Saline Ammonia	[mgN/L]
FT	Fischer-Tropsch	
FTRW	Fischer Tropsch Reaction Water	
GTL	Gas to Liquid	
HCl	Hydrochloric Acid	
HPLC	High Pressure Liquid Chromatography	
HRT	Hydraulic Retention Time	[d]
Hx	Caproic (Hexanoic) Acid	[mol/L]
$H_{2(aq)}$	Dissolved Hydrogen Gas Concentration	[mol/L]
I	Inhibition	
IC	Internal Circulation Reactor	
ISS	Inorganic Suspended Solids	[mgISS/L]
K_a	Dissociation Constant for Weak Acid/Base	
K_{c1}	H_2CO_3/HCO_3^- Equilibrium Constant	
K_{c2}	HCO_3^-/CO_3^{2-} Equilibrium Constant	
K_h	Henry's Law Equilibrium Constant	
K_s	Half Saturation Constant	[mol/L]
KWh	Kilo Watt Hour	
M	Mass	[g]
MBR	Membrane Bio Reactor	
MeOH	Methanol	[mol/L]
Mg	Magnesuim	
Mn	Manganese	
MLSS	Mixed Liquor Suspended Solids	[gTSS/L]
MLVSS	Mixed Liqour Volatile Suspended Solids	[gVSS/L]
MW	Mega Watt	
MWh	Mega Watt Hour	
N	Nitrogen	[mgN/L]
NaOH	Sodium Hydroxide	
Ni	Nickel	
ODE	Ordinary Differential Equation	

OLR	Organic Loading Rate	[kgCOD/m^3_{Vr}/d]
OrthoP	Ortho Phosphates	
P	Phosphorous	[mgP/L]
pH	Proton Activity	
pH_2	Hydrogen Partial Pressure	[atm]
pK_a	Log10 of Dissociation Constant (K_a)	
PM	Petersen Matrix	
Pr	Propionic Acid	[mol/L]
PS	Primary Sludge	
P&ID	Piping & Instrumentation Diagram	
Q	Flow Rate	[L/d]
r	Process Rate	
Rh	Hydraulic Retention Time	[d]
Rs	Sludge Age/Mean Cell Residence Time/SRT	[d]
R/O	Reverse Osmosis	
S	COD	[mgCOD/L]
SAS	Sasol Advanced Synthol	
SCFA	Short Cahin Fatty Acid	[mgAc/L]
SGL	Stripped Gas Liqour	
SPD	Slurry Phase Distillate	
SRT	Solids Retention Time	[d]
SS	Steady State	
$SO_4^{--}S$	Sulphur	[mgS/L]
T	Temperature	
TDS	Total Dissolved Solids	
TKN	Total Kedjal Nitrogen	
TMP	Trans Membrane Pressure	[mmH_2O]
TSS	Total Settlable Solids	[mgTSS/L]
UASB	Up-flow Anaerobic Sludge bed Reactor	
Va	Valeric (Pentanoic) Acid	[mol/L]
VFA-5pt	Total SCFA Concentration as Acetic Acid	[mgAc/L]
VHI	Visual Health Indicator	
Vr	Reactor Volume	[L]
VSS	Volatile Suspended Solids	[mgVSS/L]
WABC	Weak Acid/Base Chemistry	
WAS	Waste Activated Sludge	
X	MLSS Concentration	[gTSS/L]

Y	Yield	[mol/mol]
Z	Biomass	[mol/L]
Zn	Zink	
μ	Growth Rate	[1/d]
μ_{max}	Maximum Specific Growth Rate	[1/d]
$(NH_2)_2CO$	Urea	

Subscript

ac	Acetogenic Biomass
acBu	Butyric Acid Acetogenesis
acEt	Ethanol Acetogenesis
acHx	Hexanoic Acid Acetogenesis
acPr	Propionic Acid Acetogenesis
acVa	Valeric Acid Acetogenesis
ad	Acidogenic Biomass
AD	Anaerobic Digestion
Alk	Alkalinity
am	Acetoclastic Methanogenesis
AR	Active Representative Organism Mass
Atm	Atmospheric
b	Biodegradable
bp	Biodegradable Particulate
bs	Biodegradable Soluble
bsf	Biodegradable Soluble Fermentable (Glucose)
C	Degrees Celsius
d	death/endogenous respiration
e	Effluent
ER	Endogenous Representative Organism Mass
g	gas
i	Influent
K	Degrees Kelvin
m	Methane
mm	Methanol Methanogenesis
t	total
up	Unbiodegradable Particulate
us	Unbiodegradable Soluble
w	Waste
x	SCFA Carbon Chain Length 2-6

Acknowledgements

- **George Ekama** – Thank you for giving me the opportunity to be part of the UCT Water Research Group. Conducting this project under your expert guidance was a truly enlightening and life changing experience.

- **Mark Wentzel** – Your patience and ability to explain complex concepts in the simplest way is truly admirable. Thank you for all the hours I could spend in your office conversing about ideas and concepts, I will never forget it.

- **Taliep Lakey** – 'Jou hande staan vir niks verkeerd nie' Thank you for all the help in the construction, commissioning and operation of my reactors, but more than that thank you for being there through all the failures and successes in this project.

- **Eike von Geurhard** – Your workshop produced some of the best lab-scale reactors I have ever seen. It was a true pleasure having you to back us up on this project.

- **My Father and Mother; Pierrie and Rina van Zyl** – If I had to write another 300 pages I would still not have enough words to completely thank you for all the love and support through my life. But above all I would like to thank you for the love of nature you instilled in my being from very young age, without it, this thesis would never have happened.

- **My Brothers; Andre and Jacques van Zyl** – Thank you for all the support and friendship through years, but most of all thank you for those cheerful phone calls when I needed it the most.

- **Dryer and Jaco van Zyl** – Thank you for all the enthusiastic interest you show in what I do. And always remember; if you value the importance of school work and studies you will have the world at you feet.

- **Karl-Heinz Riedel** – Thank you for all the support and for removing hurdles (some even unknown to me) to streamline this research project. I can only hope that I will fulfill your expectations as an employee of Sasol Limited.

- **Corporate Acknowledgements:** Sasol Environmental Science and Technology, The National Research Foundation, The Water Institute of South Africa, The International Water Association and The University of Cape Town.

- Finally, humble thanks to The Almighty, for without his guidance love and compassion this thesis would never have been

THIS THESIS IS DEDICATED TO ALL THE INHABITANTS OF THE Van Zyl-FARM, VRYHEID IN THE SOUTHERN CAPE –

May you have walls for the wind and a roof for the rain and drinks bedside the fire, laughter to cheer you and those you love near you and all that your heart may desire

CHAPTER 1

1. Introduction

The Fischer-Tropsch (FT) process has been under development over the past six decades at Sasol. The FT process is the catalytic conversion of coal and natural gas to synthetic fuels and other value-added polymers (Chapter 2, Figure 2.1). In this process the feedstock (coal/natural gas) undergoes gasification/reforming to produce synthesis gas (CO and H_2) and a wastewater called Stripped Gas Liquor (SGL). The purified synthesis gas enters the FT reactors and is catalytically polymerized to form long chain hydrocarbons, methane and water (Eq 1.1).

$$nCO + 2nH_2 \rightarrow C_nH_{2n} + nH_2O + CH_4 \qquad (1.1)$$

From Eq 1.1 it can be noted that on a molar basis, the FT reaction produces more water than actual product (C_nH_{2n}). In the next step of the Sasol process called Product Recovery, the methane, the water produced in the FT reaction and the actual product are separated. The methane is separated and recycled back to the gasification/reforming step for re-polymerization. The polymerized products (C_nH_{2n}, Eq 1.1) are then further upgraded to petrol, diesel, jet fuel and a range of other products.

The water produced in the FT reaction contains significant amounts of Short Chain Fatty Acids (SCFAs). These cannot be separated from the water economically. This wastewater stream is known as Fischer-Tropsch Reaction Water (FTRW). FTRW, SGL and a third major organic stream namely American Petroleum Industries (API) - which is an oily sewer water from the petrochemical plant - is combined and treated in the second largest activated sludge (AS) plant in the world, situated at Secunda (South Africa). The combined flow of the FTRW (29 ML/d), SGL (62 ML/d) and the API (37 ML/d) is 128 ML/d with an organic load of 677 tonCOD/d. This amounts to a 7 million person equivalent organic load treated in a single fully aerobic activated sludge plant.

The FTRW stream comprises 23 % of the total flow and 77 % of the total organic load entering the Secunda activated sludge plant. The FTRW stream is unique, in that it is chemically produced water with virtually no dissolved salts or particulates, comprising mostly of readily biodegradable SCFAs. Early studies conducted by Britz & Nel (1986), indicated that FTRW can be treated anaerobically provided sufficient alkalinity is dosed to neutralize this streams acidity.

If the FTRW stream is kept separate from the SGL and API streams and treated anaerobically, currently experienced problems with aerobic activated sludge treatment such as aeration costs and sludge production costs will be significantly reduced. Furthermore it is estimated that anaerobic digestion of the SCFAs in FTRW will take place rapidly, resulting in low Hydraulic Retention Times (HTRs) of < 24 hours for a production scale anaerobic reactor.

However, one major problem hampers the implementation of anaerobic systems on FTRW, namely the poor settling characteristics due to the dispersed nature of the biomass produced on the SCFAs in this stream. A state-of-the-art technology namely the polymeric ultra filtration membrane might provide a means of separating the hydraulic and solids retention times in a high rate anaerobic reactor. Membranes provide a positive barrier – completely independent of sludge settleability – which retains particulates and biomass in the reactor while allowing treated effluent to exit it.

It is hypothesized that Fischer-Tropsch Reaction Water can be treated in a laboratory-scale Anaerobic Membrane Bio-Reactor (AnMBR) specifically designed for this purpose. The laboratory-scale AnMBR will use 200x300 mm flat panel ultra filtration membranes to induce a 100% solids-liquid-separation. The membranes will be submerged in the AnMBR mixed liquor. Membrane scour to minimize membrane fouling is provided by a biogas recirculation system - biogas is extracted from a biogas headspace situated above the mixed liquor, recycled and reintroduced through a coarse bubble diffuser below the membranes. It is expected that the AnMBR will operate at HRTs < 1 day and produce an effluent quality superior to other technologies currently under evaluation for FTRW treatment. The advantages of anaerobic membrane FTRW treatment are that (i) zero suspended solids effluent for reuse; (ii) very low (< 3% gCOD/gCOD) sludge production, (iii) zero oxygen demand and (iv) recovery of 2/3 of the carbon to methane for beneficial use – recycling for membrane scour and energy generation.

If the first part of the hypothesis is met, the AnMBR performance will be evaluated against a laboratory-scale Anaerobic Packed Bed Reactor (AnPBR) also under evaluation for the treatment of FTRW. The two reactors will be compared on parameters like; (i) maximum attainable organic loading rate, (ii) alkalinity and nutrient requirements, (iii) effluent quality, (iv) start-up time, (v) membrane/packing performance and (vi) response to overloading conditions.

The experimental data collected in the performance evaluation period will used to construct a steady state design model for the anaerobic treatment of FTRW. The primary use of this model will be the prediction of design parameters like (i) reactor volume for a given operational MLSS (a requirement for effective membrane scour), (ii) alkalinity and nutrient requirements, and (iii) biogas production. The experimental data will further be used to construct a dynamic simulation model to predict; (i) the AnMBR's response to influent flow and load variations, (ii) effluent quality and (iii) the effects of substances that might have an inhibitory effect on the microbial activity in the reactor.

The final project outcome is anticipated to be a laboratory-scale AnMBR prototype capable of treating FTRW at short HRTs with a Reverse Osmosis (R/O) ready effluent (i.e. no effluent polishing required between the AnMBR and the R/O plant). The second part of the project outcome will be a computer design package for the reactor size, feedstock requirements, simulation of system performance and prediction of effluent quality for an AnMBR treating FTRW at any given flow and organic loading rate. It is estimated that if the entire FTRW stream is treated anaerobically in a production scale AnMBR, a 77% reduction in oxygen demand and a 63% reduction on sludge production is expected on the entire water treatment system (Table 1.1).

Table 1.1, Current AS Compared with Proposed AS-AnMBR Reagent & Product Requirements

Total Production		Current	Proposed	Reduction [%]
Coal	[ton/d]	-170	0	100
Oxygen	[ton/d]	-705	-110	84
Energy	[MWh/d]	-320	+571	-
TSS	[ton/d]	+150	+55.3	63
Carbon Dioxide	[ton/d]	+970	+503	48

Figure 1.1, represents the in- and outputs of the purposed AS-AnMBR plant (compare to Chapter 2 Figure 2.2 representing the in- and outputs of the current AS plant).

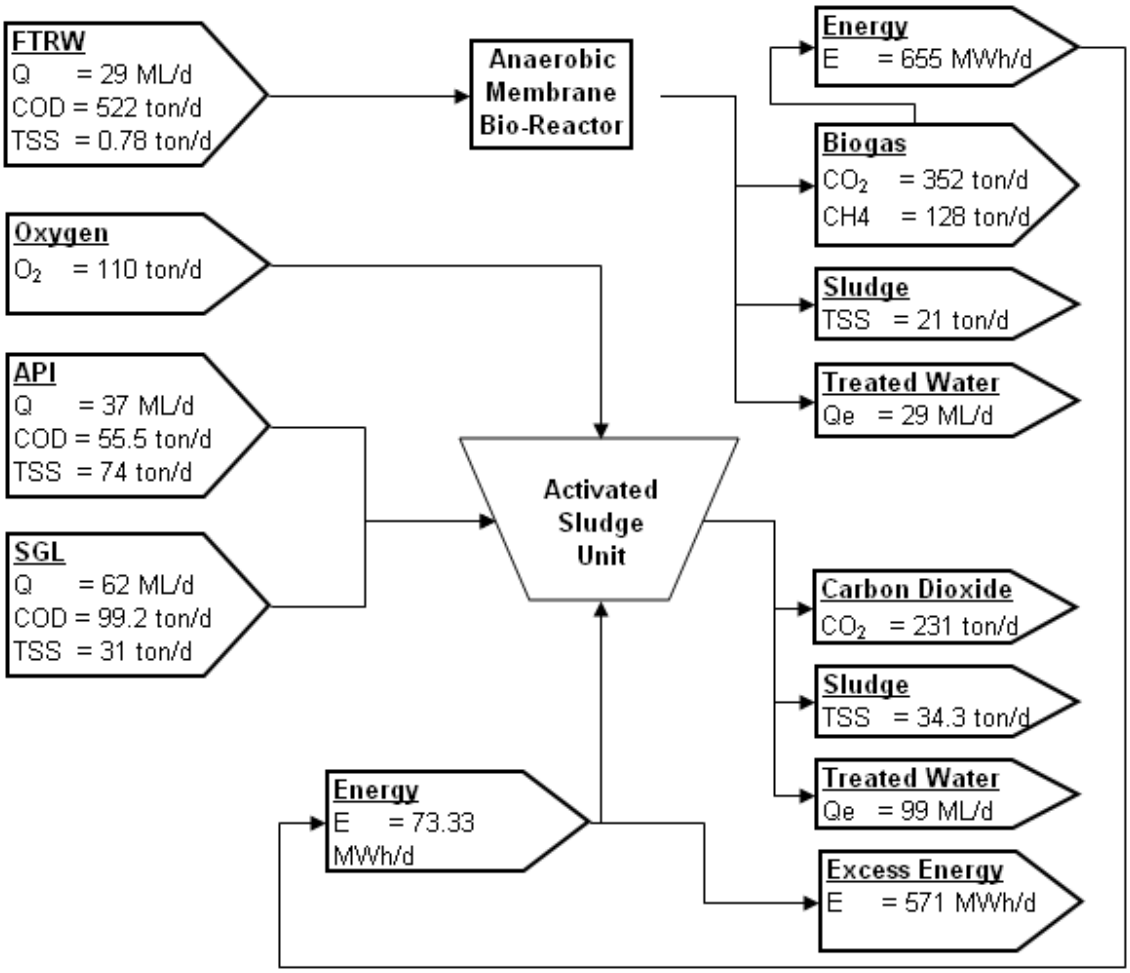

Figure 1.1, Combined Activated Sludge & AnMBR Treatment System

Since sludge incineration and energy requirements for aeration are the major contributors to the overall operating cost of the activated sludge plant, it is estimated that a saving of 60 million Rand/year can be made with the anaerobic digestion of FTRW. Furthermore, if the methane in the biogas is converted to electricity it will exceed the wastewater treatment plant's electricity requirements by approximately 571 MWh/d or 23 MW (at 33% thermal efficiency), enough to power 17 000 average South African house holds (33 kWh/household/d). The carbon footprint of the AS-AnMBR plant will also be 48% less than that of the current waste water treatment system (Appendix 1.1).

Alternatively, the biogas can be blended into the natural gas line before auto-thermal reforming which will then be converted to synthesis gas and polymerized via the FTRW process. It is estimated that if the 127.8 ton/d of methane is converted to diesel, 52 000 L/d can be produced extra, resulting in a further capital gain of ± 65 R million per year (Appendix 1.2).

CHAPTER 2

2. Literature Review

The aim of Chapter 2 is to review the three major topics that form the foundation of this research project, namely; (i) Sasol's Fischer-Tropsch (FT) synthetic fuel synthesis process, (ii) anaerobic digestion and (iii) membrane solid-liquid separation and the Anaerobic Membrane Bio-Reactors (AnMBR).

In the FT process either coal or natural gas is converted to synthetic fuels and other value added polymers. A brief discussion on the basic FT process and on the wastewaters it generates is given. The current methods of FT wastewater treatment will be evaluated and it will be shown that one of the streams, namely Fischer-Tropsch Reaction Water (FTRW) might be amenable to anaerobic digestion. If this is the case, significant savings in oxygen requirements and sludge disposal costs can be expected, as was discussed in Chapter 1. Secondly, if the methane produced in the anaerobic processes can be recycled and blended with the natural gas, it can be used as a feedstock for the FT process and recycle as much as 50% of the carbon in FTRW (62 tonC/d), rather than release it to the atmosphere as CO_2.

Anaerobic digestion forms the second major topic of discussion in this chapter. It will be shown that the stepwise decomposition of organics like the Short Chain Fatty Acids (SCFAs) in FTRW is mediated by 4 major anaerobic trophic micro-organism groups. The focus will then move towards the environmental conditions required for optimal micro-organism growth and organic removal rates. This will then lead to a discussion on the development of the anaerobic bio-reactor and the continual drive in wastewater treatment to improve solids-liquid separation to increase Organic Removal Rates (OLRs), leading to smaller volume high rate reactors. A discussion of the first 3 generations of anaerobic reactors will be given, highlighting the strengths and weaknesses of each. It will then be shown that due to the unique characteristics of FTRW, the anaerobic reactors capable of

treating it, is expected to yield poor effluent quality, high alkalinity requirements and large reactor volumes.

The third part of this chapter entails a discussion on the fourth generation Anaerobic Membrane Bio-Reactor (AnMBR). The various types of membranes and reactor configurations currently available will be discussed. Furthermore it will be shown that even though AnMBR technology is still in its infancy, a significant amount of development has taken place in the water research community in the last 3 years, driven by major benefits expected from application of the AnMBR. The AnMBR might be an elegant solution to solids retention and effluent quality issues around the anaerobic treatment of FTRW, even in the midst of high membrane prices, more complicated reactor designs and process control systems.

2.1 Sasol's Coal to Synthetic Polymer Processes

Sasol leads the world in the conversion of low grade coal to motor fuels and synthetic polymers. In addition to producing more than 40% of South Africa's liquid fuels and more than 200 other value added polymers, the group directly contributes more than 4% of South Africa's gross domestic product. This conversion of coal (and natural gas) into synthetic fuels products is achieved through propriety Fischer-Tropsch (FT) technologies unique to Sasol.

In the first part of the process, 46 Mton/y of coal is converted to synthesis (or producer) gas, a combination of carbon monoxide and hydrogen. This is known as Gasification (Figure 2.1). In the gasifier, the coal is pressurized with steam and oxygen and is converted to crude synthesis feed. The gasification condensates once cooled, yields tars, pitches, oils and most importantly purified synthesis feed gas. Gasification is the first part of the Coal to Liquid (CTL) process. Coal is the most important feedstock. However, to reduce carbon emissions, a second feedstock used is natural gas. In this case, the gas is reformed via a process called auto-thermal reforming to produce a comparatively pure synthesis gas, this is known as the Gas to Liquids (GTL) process.

Even though 70 % of the currently used feedstock is coal, it is this Gas to Liquid (GTL) approach that holds the most future promise for the application of FT technology. The main component of natural gas is methane. The conversion of natural gas to synthesis gas is called methane reforming. For methane reforming, as with gasification, the feedstock usually reacts with steam and oxygen to

produce hydrogen and carbon monoxide. The cleaner nature of the methane feed (compared to coal) is conducive to the use of high-activity catalysts to enhance the conversion process. The purified synthesis feed gas is then available for conversion either through the high temperature Sasol Advanced Synthol (SAS) or the lower temperature Slurry Phase Distillate (SPD) process.

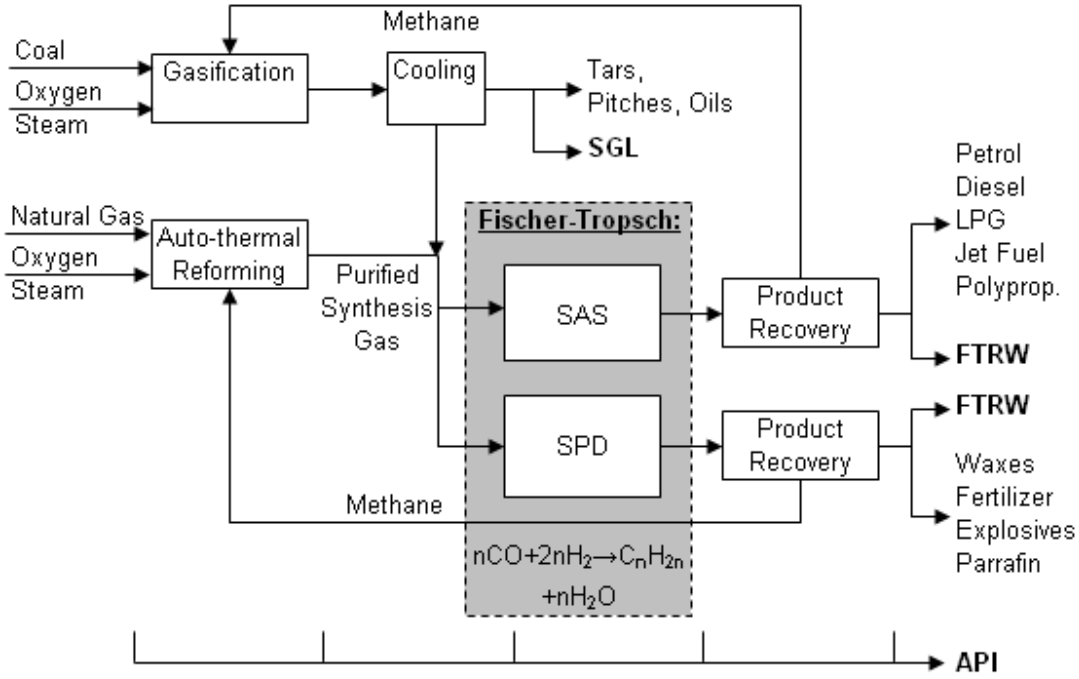

Figure 2.1, Simplified Block Flow Diagram of the Sasol Process

In the SAS process the synthesis gas reacts under pressure, in a fluidized iron based catalyst bed to yield C_1 to C_{20} hydrocarbons. The product stream is cooled successively to yield liquefied products like petrol, diesel and jet fuel and a methane rich gas that is recycled to the reformer to be again converted to synthesis gas. In the lower temperature Slurry Phase Distillate (SPD) process, the synthesis feed is converted to linear chained hydrocarbons, waxes, paraffin and high quality diesel (Sasol Facts, 2005). Irrespective of the reactor configurations, catalyst and hydrocarbon feedstock, the basic Fischer-Tropsch reaction can be described as follows:

$$nCO + 2nH_2 \rightarrow C_nH_{2n} + nH_2O + CH_4 \qquad (2.1)$$

The Fischer-Tropsch process produces more water (on a molar basis) than it does actual product (Eq 2.1). The water produced in this reaction, is known as Fischer-Tropsch Reaction Water (FTRW).

FTRW comprises of C_1 to C_6 Short Chain Fatty Acids (SCFA). The average COD of this stream is in the order of 18 000mg/L (~20 times the concentration of raw sewage) and at Secunda 29 ML/d is produced (Phillips & Du Toit, 2002).

Currently, the FTRW is treated in an activated sludge plant along with two other wastewater streams, namely API (American Petroleum Industries) which is oily sewer water from the plant and Stripped Gas Liquor (SGL) (Figure 2.2). The former originates from plant drainage and the latter is from the Gasification condensate which has undergone physical processing to recover by products. Figure 2.2 gives a graphical presentation of the flows and loads on Sasol's activated sludge treatment system.

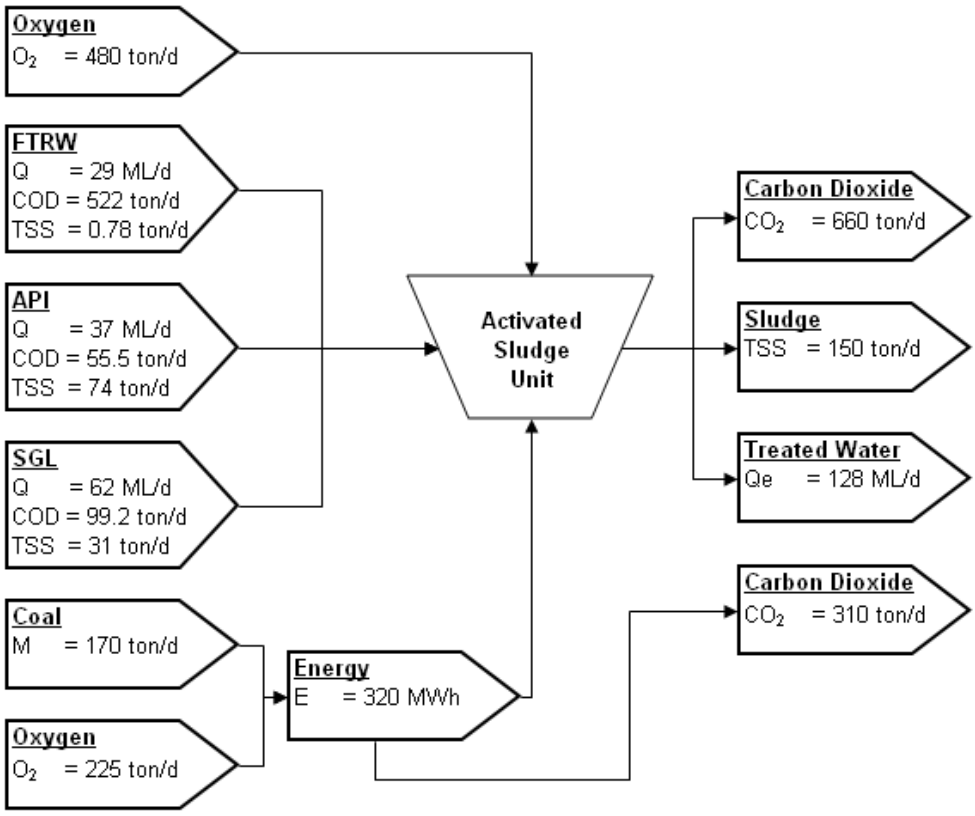

Figure 2.2, Current Organic Effluent Treatment System Used at Sasol

The Secunda fully aerobic activated sludge plant treats 128 ML/d of wastewater with a COD load of 677 ton per day, a 7 million person equivalent organic load. At this organic load, 150 ton (TSS) of sludge is produced and 480 tonO_2/d is required for aeration. A further 225 tonO_2/d and 170 ton/d of coal is required for energy production to supply the 320 MWh of electricity required to run the plant.

77% of the 677 tCOD/d organic load originates from the FT process (Appendix 1.1). The FTRW consists mostly of C_2 to C_6 short chain fatty acids (SCFAs), has a low pH (3.77) and TDS (35 mg/L) and little other contaminants.

Aside from the high oxygen, electricity and sludge treatment costs, aerobic treatment of SCFA streams are problematic because of their tendency to produce biomass that flocculates and settles poorly, thus leading to high solids liquid separation costs and an effluent with a high suspended solids after secondary settling (Ekama, 2004). SCFA streams are readily treatable anaerobically, which would lead to much lower sludge production (0.04 gTSS/gCOD), zero oxygen demand and a methane rich biogas stream (Kalyuznhyi & Davlaytshina, 1997a; Sam-Soon et al., 1989). Since the biomass yields of anaerobic micro-organisms is extremely low, most (>95%) of the 522 tonCOD/d of the FTRW will be converted to methane – which can be recycled and reformed and used as synthesis feed (Table 1.1 and Appendix 1.1). Much lower electricity and sludge treatment costs as well as a significantly reduced carbon footprint are therefore expected with the anaerobic treatment of FTRW.

2.2 Introduction to Anaerobic Digestion

In the absence of terminal electron acceptors like O_2 or SO_4^{2-}, anaerobic conditions prevail. Under these conditions anaerobic micro-organisms proliferate, using biodegradable organics as electron donor (carbon source) and CO_2 as terminal electron acceptor producing methane for growth and energy. Since methane still contains a significant proportion of the energy and electrons of the original organics, very little energy (few electrons) is actually made available to the AD micro-organisms. This result in very slow growth rates compared to aerobic heterotrophic micro-organisms. However, advantages of the slow growth includes: (i) low sludge production and (ii) the energy captured in the methane can be utilized for heating or electricity or fuel production.

Figure 2.3 depicts the "typical' anaerobic digestion process. The complex organics entering the system (or reactor volume), are hydrolysed by extra cellular enzymes secreted by the acid producing (acidogenic) bacteria (Step 1). The products of hydrolysis are typically simple sugars which undergoes acidogenesis (Step 2). The digested products of this group of organisms are mostly acetic acid under low dissolved hydrogen gas ($H_{2(aq)}$) concentration and mostly propionic acid under high dissolved hydrogen gas ($H_{2(aq)}$) concentration, and carbon dioxide and trace amounts of hydrogen.

Acetogenic bacteria utilise the propionate to produce acetic acid (Step 3). However, propionate utilization can only happen under low $H_{2(aq)}$. The acetoclastic methanogens degrade the acetic acid to carbon dioxide and methane (Step 4). Finally, the hydrogen produced by the higher trophic groups is utilised by the hydrogenotrophic methanogens (Step 5) to produce more methane (Sam-Soon et al., 1989).

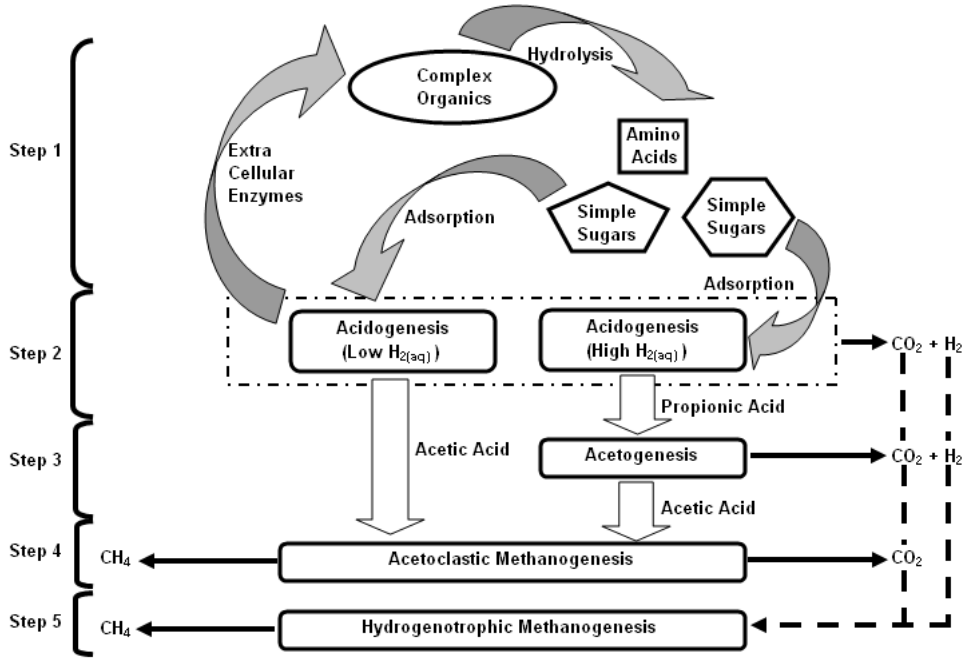

Figure 2.3, Typical Anaerobic Digestion Flow Scheme

Note: The actual values of high and low hydrogen partial pressure (P_{H2}) and dissolved hydrogen gas concentration ($H_{2(aq)}$) will be discussed in Chapter 6.

If one looks at the composition of the FTRW stream, it can be noted that the stream consists largely of short chain fatty acids, most of which is acetic acid (55.4 %) (Appendix 3.5, Table A3.7). To anaerobically convert FTRW to biogas, only the second, third and fourth functional trophic groups of the anaerobic digestion process will be required. Figure 2.4 gives a graphical representation for how this digestion process will progress.

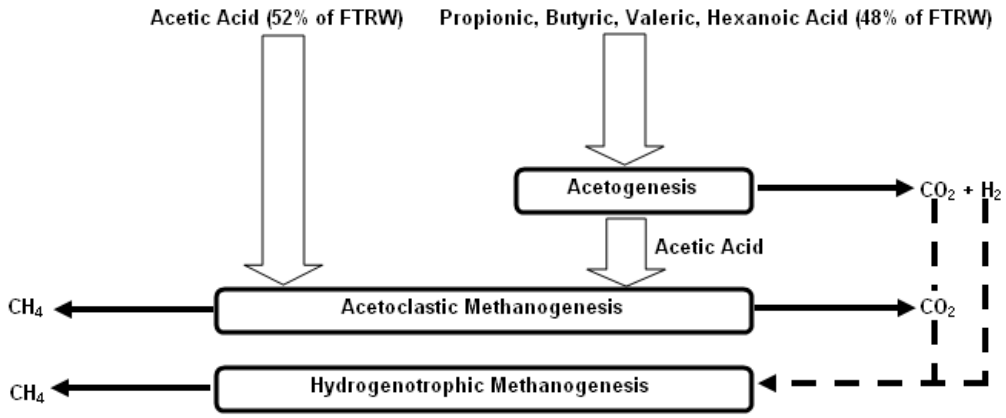

Figure 2.4, FTRW degrading anaerobic consortium

The acidogenic group will also be present, but in a significantly reduced concentration. The only function of this group will be to hydrolyze dead biomass. The most prominent species in the reactor will be the acetoclastic methanogens and acetogenic organisms. These organisms together with the hydrogenotrophic methanogens are also the most pH sensitive and complex to control. A study done by Britz and Nel (1986) on the anaerobic treatment of FTRW found that with the addition of a cocktail of different alkalinities an organic loading rate of 10.4 kgCOD/m^3_{Vr}/day could be achieved in a CSTR-type anaerobic reactor.

2.2.1 Trophic Group Functionality and Characteristics

The anaerobic biodegradation of complex biodegradable organic compounds including carbohydrates, proteins and lipids to methane gas takes place in 5 stages, involving 4 trophic organisms groups: (i) Hydrolysis and acidogenesis, (ii) acetogenesis, (iii) acetoclastic methanogenesis and finally (iv) hydrogenotrophic methanogenesis. From Figures 2.3 and 2.4 it can be noted that the order of the processes and the relative quantity of the organism groups are somewhat reversed for the anaerobic digestion of FTRW, as will be shown below;

- **Acetogenesis**

  Short chain fatty acids with a carbon chain longer than 2 cannot be utilized directly by methanogenic organisms to produce methane. Thus acetogenesis plays a pivotal role in the conversion of fatty acids like Hexanoic (Ha), Valeric (Va), butyric (Bu) and propionic (Pr)

acids that contributes 45 % of the FTRW organic load. The reactions involved in the conversion of these SCFAs can be seen in Appendix 5.1.

The more hydrogen that is produced in the conversion process the more sensitive the process to an increase in hydrogen partial pressure. Under dissolved hydrogen concentrations ($H_{2(aq)}$) in excess of 150 µmol ($P_{H2}=10^{-2.7}$ atm), the forward reaction for both propionic and the longer chain SCFAs breakdown (acetogenesis) is thermodynamically unfavorable so that the propionic and butyric acids remain unaltered in the system. Accumulation of these compounds increases the SCFA concentration which, in turn can lead to inhibitions of other processes like acetoclastic and hydrogenotrophic methanogenesis (Batstone et al., 2002).

- **Acetoclastic Methanogenesis**

Since 55 % of FTRW is acetic acid, acetoclastic methanogens will be the predominant active mass in the anaerobic reactor treating this wastewater, compared to acetogenic biomass, the acetoclastic methanogens are robust and insensitive to hydrogen partial pressure; however they are sensitive to pH fluctuations. This organism group converts acetic acid to methane in the following reaction (Eq 2.2):

$$CH_3COOH \rightarrow CH_4 + CO_2 + Biomass \quad (2.2)$$

Two genera of acetoclastic methanogens utilize acetic acid to produce methane; (i) Methanosarcina dominates above 60 mgAc/L while (ii) Methanosaeta dominates below this level. The latter is (i) more pH sensitive and (ii) has slower growth rates, but (iii) can operate at very low acetic acid concentrations (Batstone et al., 2002)

- **Hydrogenotrophic Methanogenesis**

Degradation of higher organic acids to acetate is an oxidation step, with no internal electron acceptor. Therefore the organisms oxidizing the organic acids are required to utilize an additional electron acceptor such as hydrogen ions to produce hydrogen gas. This metabolic product ($H_{2(aq)}$) must be maintained at a low concentration for the $H_{2(aq)}$-oxidation (via hydrogenotrophic methanogenesis) reaction to be thermodynamically possible. The reaction can be described as follows (Eq 2.3):

$$4H_2 + CO_2 \rightarrow CH_4 + 2H_2O + \text{Biomass} \quad (2.3)$$

- **Hydrolysis**

Parallel to the biomass growth processes, organism death also occurs on a continuous basis in the anaerobic environment. Acidogenic biomass secretes enzymes to degrade the dead cell complex organics extra-cellularly to organic product groups like called soluble biodegradable fermentable organics (S_{bsf}) which is assumed to be glucose, unbiodegradable solubles (S_{us}) and unbiodegradable particulates (S_{up}) in the following reaction:

$$\text{Dead Active Mass} \rightarrow S_{bsf} + S_{us} + S_{up} \quad (2.4)$$

Unlike Acidogenesis, hydrolysis does not appear to be affected by high hydrogen partial pressures.

- **Acidogenesis**

Similar to acetogenesis, acidogenesis is generally defined as an anaerobic acid-producing microbial process with $H_{2(aq)}$ as electron acceptor. Because free energy yields are normally higher, the reactions can occur at high hydrogen partial pressures and at high biomass yields (Batstone et al., 2002). Biodegradables (S_{bsf}) from the hydrolysis process are ingested by acidogenic organisms and fermented intracellularly to short chain fatty acids (SCFA) like acetic and propionic acid, carbon dioxide and hydrogen gas. The biochemical pathways by which the substrate is fermented and the type of SCFA in the end product is dictated by the hydrogen partial pressure and the type of substrate fermented (Batstone et al., 2002). The most important products and their stoichiometric reaction from S_{bsf} (assumed to be glucose) are given in Appendix 5.1. Compared with the organic load from FTRW, the S_{bsf} produced by hydrolysis is extremely small and will have only a negligible effect on biogas production pH and alkalinity. However, the degradation of dead biomass does have a significant effect on the reactor solids concentration (MLSS) and thus needs to be taken into consideration for the AD-FTRW process.

2.2.2 pH and Alkalinity

In the anaerobic digestion of FTRW, the dominating pH buffering system is the carbonate weak acid/base system. The $H_2CO_3^*$ Alkalinity defines the amount of carbonate alkalinity and is commonly used to quantify the amount of buffer capacity present in anaerobic digesters. The minimum concentration of $H_2CO_3^*$ Alkalinity required to maintain the pH within the optimal for anaerobic digestion (6.8 – 7.5) depends on the type of wastewater treated under specified stable conditions.

The type of wastewater will dictate the maximum expected SCFA concentrations in the reactor, which in turn, dictates the reactor pH for a given $H_2CO_3^*$ Alkalinity. The amount of buffer required for operation at a given pH should be determined experimentally (Moosbrugger et al., 1991). However, the Ripley Ratio is a tried and tested means of predicting $H_2CO_3^*$ Alkalinity [mg$CaCO_3$/L] requirements; the system alkalinity should be at least 3 times the maximum expected SCFA concentration in the reactor (Ripley et al., 1986).

Assuming steady state conditions in an anaerobic system treating a particular substrate, one would expect a stable low level of SCFA (< 20% daily fluctuation), a stable pH between 6.8 and 7.5 and a stable methane to CO_2 ratio (< 5% daily fluctuation). With deviant behavior, a rise in SCFA, reduction in methane to CO_2 ratio and a decrease in pH would occur. Changes in (i) pH, (ii) $H_2CO_3^*$ Alkalinity to SCFA ratio and (iii) methane to CO_2 ratio are currently the three major parameters used for assessing the 'health' of an anaerobic system (Moosbrugger et al., 1991). Many components in wastewater that can have an effect on the anaerobic digester pH like the FSA and Sulfate system, however since FTRW is a chemically created water, the only two components that are of sufficiently high concentration to have an effect on pH is the carbonate and SCFA systems. A detail discussion of the parameters affecting pH in the anaerobic digestion of FTRW is presented in Chapter 5.

2.2.3 Inhibitors and Toxicity

Molecular hydrogen (dissolved hydrogen gas – $H_{2(aq)}$) is the single most inhibitory metabolic product produced by the anaerobic bio-processes. It has been widely demonstrated the anaerobic systems subject to inhibition and overloading showed an increase in the liquid phase concentration ($H_{2(aq)}$) and resultant gas phase hydrogen partial pressure (Whitmore & Loyd, 1986; Archer et al., 1986;

Pauss & Guiot, 1993). It would appear that the more hydrogen is produced per mol of substrate utilized – by any anaerobic pathway – the more prone to hydrogen inhibition the reaction will be. The reaction most affected is the conversion (acetogenesis) of propionic acid (3 mol_{H2}/mol_{Pr}) to acetic acid, secondly the acidogenesis of glucose (2 $molH_2/molS_{bsf}$) and thirdly acetogenesis of butyric acid (2 mol_{H2}/mol_{Bu}) (Appendix 5.1). Because of this, propionate in the effluent is regarded as a 'tell-tale sign' of reactor instability.

Since most parameters typically measured on anaerobic reactors like pH, Ripley (SCFA /Alkalinity) ratio, CO_2 to CH_4 ratio of the biogas, are responses to the inhibitory effect of hydrogen, it has been widely stated that the liquid phase hydrogen concentration ($H_{2(aq)}$) or gas phase partial pressure (P_{H2}), it the ideal process control parameter to measure on any anaerobic system (Hickey & Switzerbaum, 1991). However, hydrogen is inhibitory at concentrations as low as 12 µmol/L and only expensive and labor intensive methods were traditionally available to detect it accurately. Fortunately, recent advantages in hydrogen fuel cell technology have also fueled research into more sensitive and cost effective hydrogen measurement systems. On-line measurement of dissolved hydrogen in anaerobic mixed liquor has been used for process control of UASB reactors with a large amount of success (Pauss & Guiot, 1993). The process of hydrogen inhibition is fairly complex and this section is only an introduction to the topic, a detail discussion on this is presented in Chapter 6.

Free SCFA concentrations in the anaerobic mixed liquor can also have an inhibitory effect on the anaerobic bioprocesses. It would appear that the groups mostly affected are the hydrogenotrophic methanogens and acetogenic organisms. This, in turn, leads to an increase in hydrogen in the liquid phase ($H_{2(aq)}$) and a further inhibition of the system. Free (or un-dissociated) SCFA concentration – and its inhibitory effects – is inversely proportional to pH and directly proportional to the total SCFA concentration in the system. An interrelationship exists between pH and SCFA inhibition, this topic is expanded in Chapter 6.

2.4 Development of Anaerobic Bio-Reactors

Assyrian references to using anaerobically generated biogas for water heating dates back as far as 1000 BC. However it was not until 1776 that the relationship between the amount of decaying organic matter and the amount of flammable biogas produced was established. The first anaerobic digestion plant was constructed by a leper colony near Bombay around 1859. The primary goal was

not waste stabilization, but energy recovery from digester gas in the form of heat. The benefits involved in 'fuel from waste' were soon realized and as early as 1895, biogas was already used in Brittan to power street lamps.

The continuous digestion process known as the anaerobic digester was developed by Imolff around 1900, and became the generally accepted treatment method for the stabilization of municipal sewage sludge (Jones, 2006). The focus of this section is to review briefly the development of the anaerobic reactor, from the unmixed or completely mixed dispersed systems developed more than a century ago, to the current state-of-the-art high rate anaerobic reactors.

2.4.1 Dispersed Biomass Reactors

The conventional flow through anaerobic digester is used mostly for the treatment of municipal sewage sludge and also some other concentrated wastewaters. The influent enters the reactor volume where it comes into contact with the anaerobic biomass. The biodegradable organics get converted via the anaerobic processes mentioned above to methane and CO_2, which escapes the liquid phase in the form of biogas, and a small fraction of the organic matter is converted to anaerobic biomass. This conversion of biodegradable organics to methane reduces the influent organics (COD) concentration and stabilizes the wastewater by leaving very low residual biodegradable organics in the effluent. Early designs did not incorporate mixing or heating, however it was discovered early on that mechanical agitation and digester heating significantly increases the organic removal rate of the anaerobic digester (Figure 2.5). The remaining unbiodegradable solids and anaerobic biomass are not removed from the effluent and recycled to the digester, with the result that the sludge age and hydraulic retention time are the same. Because sludge ages need to be long, hydraulic retention times also are long, resulting in large reactor volumes. High organic loading rates (OLR) could only be achieved by feeding concentrated organic influents.

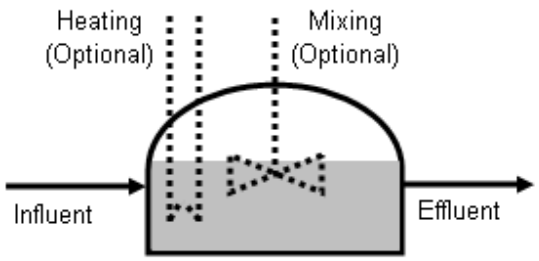

Figure 2.5, Simple Anaerobic Digester

The advantage of this process is its simplicity in design and operation. One of the disadvantages is that long hydraulic retention time is required for high organic removal efficiency and reliability. Secondly, since the hydraulic and solids retention times are the same, a high concentration of suspended solids exits the system in the effluent unless some means of solid-liquid-separation or post treatment is provided (Ross et al., 1992).

The anaerobic contact process was developed to overcome the disadvantages experienced with the conventional flow through anaerobic digester (Figure 2.6A). The effluent from the anaerobic reactor passes through a secondary settling tank where the suspended solids – including the active biomass – are separated and returned to the reactor. This results in a partial uncoupling of the hydraulic and solids retention times, allowing a longer retention of active biomass (sludge age) in the reactor than the hydraulic retention time. This modification permits a significant (~5 times) increase in OLR and also a reduced pollution load in the effluent.

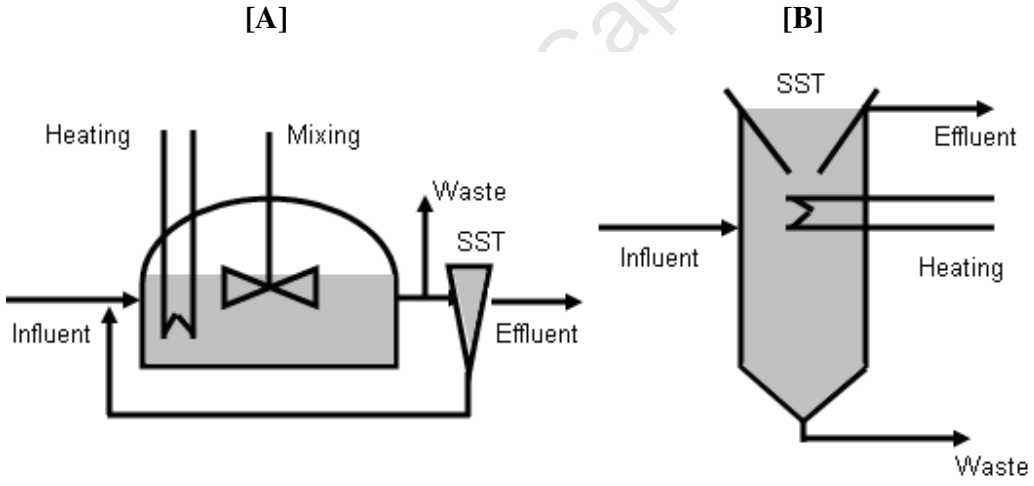

Figure 2.6, Anaerobic Contact Process [A] and Clarigester [B]

However, because of the dispersed nature and poor settleability of anaerobic biomass, a large surface area secondary settling tank (SST) is required for sufficient settling to take place. This large footprint requirement – and resultant large capital cost – forms the main disadvantage of the anaerobic contact process (McCarty, 1974; Metcalf & Eddy, 1991). A modification on the standard anaerobic contact process design is the clarigester. In the clarigester design, the secondary settling tank (SST) is mounted on top of the anaerobic digester (Figure 2.6B). The mixing induced by the influent flow

regime produces enough agitation so that no mechanical mixing is required. Since the clarigester is still regarded as a "dispersed biomass" reactor and solid-liquid separation not very efficient, total suspended solids (TSS) in the effluent is still a major problem. The clarigester is the first of the "tall cylinder" type configurations typically associated with high rate anaerobic reactors.

2.4.2 High Rate Immobilized Biomass Reactors

Apart from energy production from wastewater, the second most economically advantageous attribute of anaerobic biomass is its ability to immobilize - to form fixed biomass on packing media or fast settling biomass pellets - under certain conditions. This immobilization meant that biomass retention inside the reactor (sludge age - R_s) is significantly longer than that of the wastewater to be treated (hydraulic retention time - HRT) resulting in small reactor volumes and high OLRs.

The immobilized anaerobic biomass reactors was developed in response to the difficulties experienced with the treatment of soluble or relatively dilute organic industrial wastes. Maintenance of high treatment rates over extended periods with such wastes using dispersed biomass systems proved problematic. It was found however that when biomass immobilization could be induced, high organic removal rates (> 5 kgCOD/m^3_{Vr}/d) could be maintained continuously (McCarty, 1974).

Major process configurations developed for high rate anaerobic reactors over the last 5 decades include the fixed film systems such as the Anaerobic Packed Bed Reactor (AnPBR) and the Anaerobic Fluidized Bed Reactor (AnFBR). A third generation of reactors that have become popular in the past 3 decades are the granulating anaerobic bioreactors such as the Up-flow Anaerobic Sludge Bed Reactor (UASB), the Extended Granular Sludge Bed Reactor (EGSB) and the Internal Circulation (IC) ultra high rate reactors. The design philosophy of these systems is biomass retention to increase OLR and reduce reactor volume. The biomass retention is accomplished by immobilizing the anaerobic biomass as a biofilm on support media surfaces as in the AnPBR and AnFBR or by granulation, which is the spontaneous aggregation of bacteria to form granular sludge. This granular sludge usually shows a high level of activity and good settling properties as is observed in the UASB, EGSB and IC systems.

Fixed Film Anaerobic Bio-Reactors

Fixed film anaerobic bio-reactors are systems in which biomass is immobilized on a solid material and retained in the reactor volume. They offer distinct advantages such as (i) simplicity of construction, (ii) elimination of mechanical mixing, (iii) elimination of external solid-liquid-separation systems such as SSTs, (iv) better stability at higher loading rates and they are (iii) generally less sensitive to organic shock loads (Kansal et al., 1998)

In the AnPBR – also known as the Anaerobic Filter - biomass immobilizes on some sort of packing media to form a thick biofilm. This biofilm contains the predominant active mass fraction in the reactor (Show & Tay, 1999). The packing is typically a large sized solid support optimized for cell immobilization. In the case of the AnPBR, the packing is situated in a fixed bed, submerged in the reactor liquid volume through which the wastewater passes. Mixing in the AnPBR can be enhanced by including an effluent recycle in the system. This recycle has advantages in situations where (i) alkalinity needs to be recycled to avoid low pH conditions at the entrance of the reactor (McCarty, 1974, Moosbrugger et al., 1991) and (ii) to maintain settlable solids in suspension in the reactor volume (Kansal et al., 1998).

During the initial research conducted on the AnPBR, it was suggested that a staged process, in which the acidogenic (acidification) and methanogenic steps are separated, will enhance the reactor performance (Alves et al., 2000). However, in studies comparing multi-staged to non-staged AnPBRs under laboratory conditions, no conclusive evidence for enhanced performance of the multi-staged system could be found (Kansal et al., 1998).

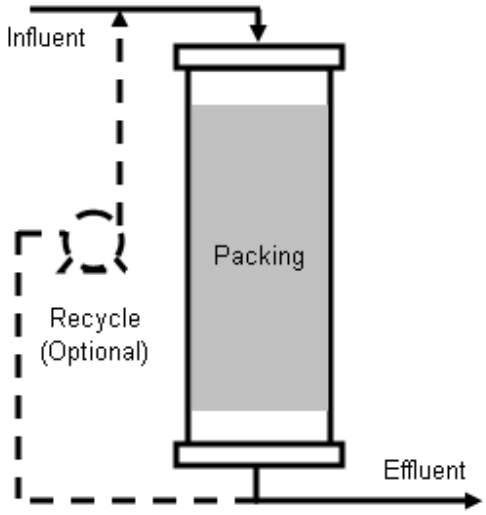

Figure 2.7, Anaerobic Packed Bed Reactor (Anaerobic Filter)

Various configurations of AnPBR systems exist including up and down flow with and without recycle (Figure 2.7). It has been proven extensively that a recycle significantly increases the mixing in the AnPBR and decreases the negative effect of channeling and dead zones in the packed bed. The recycle can also act as a method of backwashing to remove inactive biomass after long periods of operation.

From most studies conducted on AnPBR systems, the ability of the packing media to retain high concentrations of immobilized biomass, dictates the reactor performance. It has been found that the surface properties of the packing material have a significant effect on the rate of biomass immobilization, especially during the start-up stages. However, under steady state operating conditions, media surface area appears to only have only a minor effect on performance. A less than 5% improvement in COD removal performance has been documented with a twofold increase in media surface (Show & Tay, 1998).

In comparative studies involving the anaerobic contact process and the AnPBR under identical conditions, it was found that steady state was reached quicker in the contact process than in the AnPBR. However, the AnPBR proved more stable and the daily methane production and corresponding COD removal was higher. TSS and SCFAs in the effluent also were far lower in the AnPBR (Hamdi & Garcia, 1991).

Effluents treated at full scale with the AnPBR include; pharmaceutical, olive mill (Hamdi & Garcia, 1991), industrial (Perez et al., 1998), potato waste (Parawira et al., 2005) and sewage (Reyes et al., 1999). It has been proven extensively that start-up after a period of starvation is comparatively quick (Kansal et al., 1998). This makes the AnPBR ideal for the treatment of intermittent charges and seasonal operations – such as experienced in the fruit canning industry – where rapid secondary start-ups are required (Van Zyl et al., 2002; Reyes et al., 1999). In addition AnPBRs can tolerate sudden organic shock loads and recover to normal performance within a few days if the alkalinity is sufficient and the pH is maintained above 6.2 (Kansal et al., 1998).

Accumulation of high concentrations of active solids permits the treatment of dilute wastewaters at low temperatures (<35 ^{o}C) with little sludge production and an effluent substantially free of TSS compared to the anaerobic contact process. Removal efficiencies of 90% at 4 kgCOD/m^3/d and 75% at 16 kgCOD/m^3/d are typically observed. It was found that about 55% of the COD removal and resultant methane production was done by the suspended biomass in the AnPBR. Hence system failure at OLRs higher than the maximum (~16 kgCOD/m^3/d) was attributed to un-immobilized (planktonic) micro-organism washout, rather than short circuiting and dead zones (Show & Tay, 1998).

It was shown with tracer tests that mixing can be problematic in the AnPBR. This was verified in comparative studies done on the mixing regimes in the AnPBR and the Anaerobic Fluidized Bed Reactor (AnFBR). The steady state OLR of the AnPBR was only 60% of that of the AnFBR. Insufficient mixing – even with a large recycle – and dead space in the reactor volume due to the accumulation of biomass clogging media porosity are the two major disadvantages of the AnPBR (Show & Tay, 1998).

In response to the performance limiting problems generally experienced with the AnPBR, the AnFBR was developed (Figure 2.8). In this reactor, the water to be treated is pumped through an expanded aggregate of the appropriate medium (typically coal, sand or PVC) on which an anaerobic biofilm has developed. Effluent is recycled to dilute the incoming waste and to provide adequate flow to maintain the bed in the expanded condition.

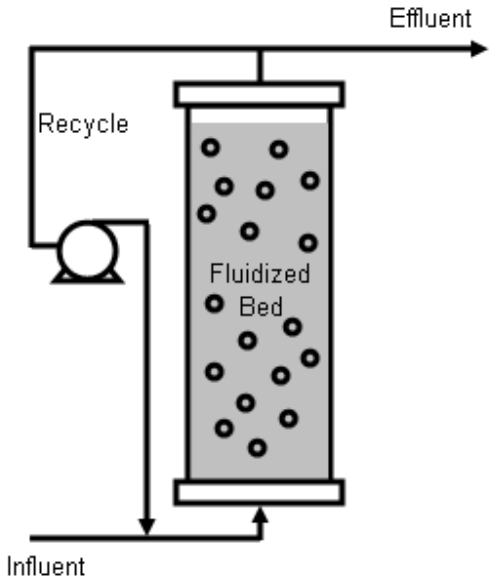

Figure 2.8, Anaerobic Fluidized Bed Reactor

To maintain the sludge bed fluidized in the AnFBR, an up-flow velocity ~ 5 times higher than the AnPBR (~1m/h) is required. Because of the good settling properties of the biomass and media, biomass concentrations in the order of 15 to 40 gTSS/L can be maintained and because of the high organic loading capabilities (8 – 15 kgCOD/m^3/d), the AnFBR can treat municipal sewage – in conjunction with chemical nutrient precipitation – at very short HRTs (Metcalf & Eddy, 1991). Even though the AnFBR addresses the issues around mixing experienced in the AnPBR, the packing material that is used takes up a significant fraction of the reactor volume (up to 40%). This large fraction of 'dead' space in the reactor volume is the primary disadvantage of the AnFBR.

Granulating Anaerobic Bio-Reactors

The development of the third generation, self granulating anaerobic bio-reactors was a direct response to the mixing and dead volume issues that were experienced in the fixed media reactors. The exact start of research into this field is not clear, but it would appear that the UASB concept was developed from the combination of two up-flow systems namely; (i) the reverse flow clarigester and (ii) the up-flow anaerobic filter.

The reverse flow clarigester was developed by Hemes and others in South Africa in the 1960's. The feed point was moved from the normal middle inlet of the clarigester to the bottom of the reactor,

creating an enhanced mixing due to the up-flow regime in the reactor. It was found that the reverse flow clarigester could treat influent strengths of 10 gCOD/L at an organic loading rate of 3 kgCOD/m^3_{Vr}/d. Unknowingly the system was designed to select biomass prone to aggregation and granule formation. Over time the system developed a good settling sludge and granular sludge developed at the bottom of the reactor. No significance was attached to this phenomenon at the time (Ross, 1984)

McCarthy (1974) in the USA investigated various means of separating the solid and liquid retention times in anaerobic digestion so that low strength wastewaters could be treated anaerobically without requiring long HRTs and excessively large reactor volumes or sludge recycling (anaerobic contact process). So the up-flow anaerobic filter (AnPBR) was born. It was found that low strength wastes (1500 – 6000 mg/L) could be treated without solids recycling at OLRs of up to 4 kgCOD/m^3/d. A secondary observation was that flocculated solids were suspended in the voids between the packing along with granules of ±3 mm in diameter. The formation of these granules was attributed to the rolling action induced by rising biogas bubbles (McCarthy, 1967).

The water research group at the University of Wageningen in the Netherlands lead by Lettinga, took cognizance of the experience on the reverse flow clarigester and the up-flow anaerobic filter and developed the Up-flow Anaerobic Sludge Bed Reactor (UASB) as a combination of the two. The UASB consists of a tall cylindrical reactor with the influent entering the reactor at the bottom, where it comes into contact with the granulated anaerobic sludge (Figure 2.9, without recycle). A 3 phase separator at the top of the UASB separates the produced biogas, granulated biomass and the treated effluent.

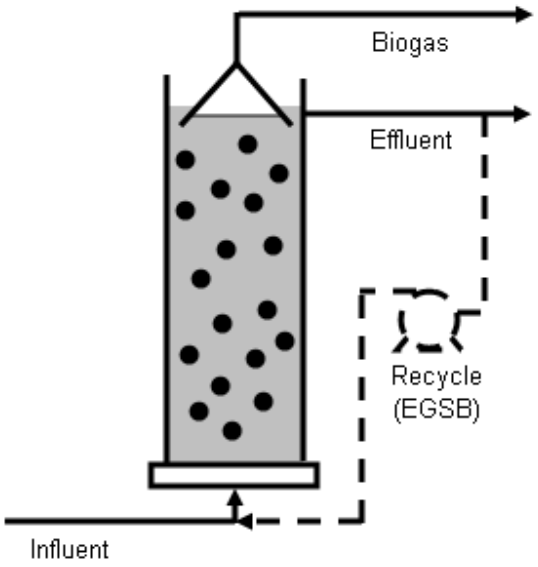

Figure 2.9, Up-flow Anaerobic Sludge Blanket (UASB) and Extended Granular Sludge Bed Reactor (EGSB) (Lim, 2007)

The UASB typically operates at an up-flow liquid velocity of ± 1 m/h and OLRs in the order of 10 kgCOD/m^3/d can be maintained. A further modification to the UASB is the Extended Granular Sludge Bed Reactor (EGSB). In the EGSB an external effluent recycle increases the up-flow velocity of the sludge bed to ~6 m/h, thus significantly increasing the mixing in the reactor. Design loading rates in the order of 20 kgCOD/m^3/d are typical for the EGSB configuration. Such high OLRs are possible due to the very fast settling rate of the anaerobic granules (2-4 mm diameter) (Versprille, 2001).

Apart from effluent recycle, increased up-flow velocities and mixing in granular sludge beds can also be attained with a biogas recycle. This is the case with the Internal Circulation (IC) reactor.

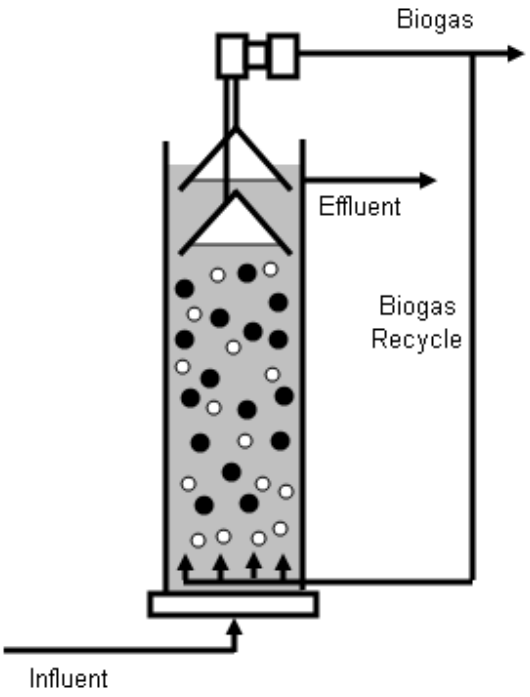

Figure 2.10, Internal Circulation (IC) Reactor (Driesen et al., 2000)

The IC reactor is also tall cylindrical reactor such as the UASB and EGSB systems. The internal biogas recirculation ensures rapid dispersion of the raw wastewater and also ensures optimal mixing conditions for the anaerobic granules and wastewater (Figure 2.10). Optimal biomass retention is provided by a two stage of solid liquid separator. The first stage separates the majority of the biogas from the liquid so that the second stage mainly separates the biomass from the effluent (Driesen et al., 1999).

Currently more than 70% of the world's full scale anaerobic bioreactors are self granulating systems. These reactors are especially suitable for the treatment of sugar, carbohydrate and protein rich wastewaters, provided there is a high level of solubility and biodegradability. However, the granulation process on SCFA streams appears to be slower and more unreliable than if compared to granules cultivated on more complex soluble substrates. It was found that the granules that were cultivated, were weak and filamentous and tended to break apart easily (De Zeew & Lettinga, 1980; Hulshof Pol et al., 1982). This lead to poor settling properties, biomass washout and the eventual failure of UASB-type systems treating pure SCFA streams (Sam-Soon et al., 1989). For FTRW it has been extensively proven (1986 to present) that the start-up of granulating bioreactors on

domestic sludge and FTRW is not economically viable and if these systems are seeded with granules from other UASB-type systems, stable operation cannot be maintained for extended periods of time. (Rossouw & Van Zyl., 2008).

Although a major development over the first and second generation digesters, the UASB-type reactors still have two major disadvantages; (i) granulation papers to be problematic on high SCFA wastewater streams (especially for FTRW) (ii) the total COD particulate concentration in the effluent is typically in the order of 500 mgCOD/L and 200 mgTSS/L respectively, which implies that aerobic post treatment (effluent polishing) is still required. These are the two major issues which led to the development of the fourth generation anaerobic treatment systems; the Anaerobic Membrane Bio-Reactor (AnMBR).

2.5 Anaerobic Membrane Bioreactors

Un-coupling the solids (R_s) and hydraulic retention time (HRT) are key features of virtually all modern wastewater treatment systems, the goal being to retain the biomass in the reactor for much longer times than the wastewater, which increases the organic loading rate (OLR) and reactor biomass concentration. A high biomass concentration is commonly attained by biofilm formation or post reactor separation and recirculation. In anaerobic bioreactors – where biomass growth rates are slow – biomass retention is of utmost importance, since it makes the biomass concentration in the reactor independent of the wastewater throughput. The higher the biomass concentration, the higher the organic removal rate will be which in turn, leads to smaller reactors. Biofilm formation, such as fixed bed and granulating systems, are the most common strategy currently for biomass retention in high rate anaerobic reactors (Jeison & Van Lier, 2007a).

A recent advance in solid liquid separation in biological systems is the use of membranes and during the last two decades the use of membrane separation for biomass retention has received an ever increasing interest. The membrane acts as a positive barrier to rejected components like suspended solids, but still allowing water and aqueous solutes to pass through (Cheryan & Rajagopalan, 1998). Membrane bioreactors have the advantage of total biomass retention. No selection based on settling, flocculation, attachment or granulation exists anymore, enabling the retention of all anaerobic micro-organisms (Jenson & Van Lier, 2007a). Because of the complete retention of biomass, very high mixed liquor concentrations can be achieved (up to 70 gTSS/L) leading to high organic removal

rates as well as an effluent free of settlable solids and pathogens (Hu & Stuckey, 2006). Membranes are regarded as a breakthrough technology in water treatment and that it is no longer new, but vital for the achievement of currently required effluent standards (Lesjean & Rosenberger, 2004). Factors such as; (i) the retention of slow growing or dispersed biomass, (ii) particulate retention and (iii) superior effluent quality, opens a large number of new possibilities for the combination of high rate anaerobic treatment and membrane technology that could previously not be explored due to the failure of biofilm and/or granulating systems.

Over the next few sections a brief overview will be given on the membrane technology currently available for wastewater treatment. The primary focus will be on anaerobic membrane reactor systems, their characteristics, advantages and also their shortcomings. This will include the types of membranes available, membrane fouling, current anaerobic membrane reactor applications, and a comparison between the two configurations currently dominating the market. The discussion will be closed with an economic evaluation and the expected future prospects of the anaerobic membrane reactor.

2.5.1 Membrane Separation

Membranes used in water treatment can be classified into four different categories depending on the pore size. Micro-filtration membranes have the largest pore size and are typically used for settlable solids removal and/or pretreatment of wastewater for finer membrane systems (Table 2.1)

Table 2.1, Membrane Classification (Li et al., 2004)

Process	Pore Size	Typical TMP	Particle Size Cutoff	Typical Materials Retained	Applications
Micro Filtration	10 - 0.5 um	30 - 300 kPa	0.1 - 10 um	SS, Most Bacteria, Some Viruses	Clarification, pretreatment
Ultra Filtration	0.5 um - 2 nm	10-1000 kPa	1000 - 500000 Da	Bacteria, Viruses, Particulates	Concentration, clarification, pretreatment
Nano Filtration	± 2 nm	1000 - 1500 kPa	200 - 300 MW	Divalent Ions, Sugars, Calcium	Softening, Color removal
Reverse Osmosis	< 2 nm	3500 - 10000 kPa	Most > 25 MW	Low MW Organics, Salts, Calcium	Desalination

The finest membranes, namely Nano-filtration and Reverse Osmosis membranes are generally used for softening and desalination of potable water by municipalities. These membrane systems are energy intensive because of the high Trans Membrane Pressure (TMP) requirements. The membrane size most suitable to biological wastewater treatment has proven to be the Ultra-filtration membrane.

Ultra-filtration membranes have a low molecular cutoff (1000 – 500000 Da, Table 2.1) and thus retain particulates, settlable solids, bacteria and most viruses. Energy requirements are considerably lower than for finer membranes, because of the significantly lower TMP requirements. Two major categories of ultra filtration membranes currently dominate the wastewater treatment market. These are the external and submerged polymeric membranes. In the external configuration, a large external recycle passes the pressurized mixed liquor over the membrane. The cross flow velocity of the mixed liquor over the membranes combats membrane fouling.

In the submerged configuration, the membranes are submerged in the reactor volume and effluent is typically extracted under negative pressure out the reactor. To avoid membrane fouling the same aeration that is typically used to aerate the biomass in activated sludge systems, is also used to scour

the hydrophobic membrane surface area. Table 2.2 gives a summary of the most popular ultra-filtration membrane systems.

Table 2.2, Ultra-filtration membrane types and characteristics (Fane & Chang, 2002; Churchouse, 1997; Jenson & Van Lier, 2007a)

Ultra-filtration Membrane Characteristics	External				Submerged	
	Flat Plate	Spiral Wound	Tubular	Hollow Fiber	Flat Panel	Hollow Fiber
Packing Density	Mod.	High	Low	High	Mod.	High
Energy	High	High	High	High	Low	Low
Solids Handling	Mod.	Poor	Good	Good	Good	Mod.
Cleaning	Mod.	Difficult	Good	Good	Excellent	Good
Replacement	Cartridge	Element	Tubes	Element	Panel	Bundle
Flux [L/m^2/h]	70 - 100	70 - 100	70 - 100	70 - 100	15 - 25	20 - 30
MLSS [gTSS/L]	15 - 100	15 - 100	15 - 100	15 - 100	12 - 18	10 - 15
Energy [kWh/m^3]	2 - 10	2 - 10	2 - 10	2 - 10	0.3 - 0.6	0.3 - 0.6

If the external configurations are compared to the submerged, it can be noted that the fluxes and mixed liquor concentrations attainable with the external systems is significantly higher than for the submerged membrane reactors. This implies that reactor volumes can be smaller, organic loading rates higher. However, because of the high TMP and pumping requirements, the energy demand for the external systems is typically higher than that of the submerged membrane bioreactors.

2.5.2 Membrane Fouling

Polymeric membranes suffer form fouling and degradation during use (Cheryan & Rajagopalan, 1998). Membrane fouling can be classified into four different categories (Li et al., 2004), namely:

- Inorganic fouling (Mineral Precipitation)
- Colloidal fouling (Extra Cellular Polymer Deposition)
- Cake layer formation (Organic & Biological Deposition)
- Gel Polarization (Size Excluded Soluble Organics (Hu & Stuckey, 2006))

For biological reactors, it has been shown that the major contributor to filtration resistance in Ultra-filtration membranes is cake layer formation and not internal pore (inorganic) fouling (Elmaleh &

Abdelmoumni, 1997). However, organic matter and EPS also has an effect on the membrane performance and a linear relationship between EPS and TMP is typically observed (Lesjean et al., 2004). Other authors claim that virtually anything that affects the reology of the sludge, in the vein of a decrease in floc size or an increase in long chain hydrocarbons can affect membrane performance adversely (Jeison & Van Lier, 2007c).

Deposition of biological constituents on the membrane surface occurs when the convective transport of particulates to the membrane exceeds the back transport into the mixed liquor due to membrane scour (liquid or gas). It was found that the back transport phenomena is positively related to particle size, thus the reduction of floc size due to mechanical shear has a significant effect on membrane performance (Jeison & Van Lier, 2007b). A direct proportionality between fouling and membrane flux and an inverse proportionality between fouling and scouring is typically observed (Soares et al., 2007). This implies that an optimum exists between MLSS, TMP, flux and membrane cleaning costs.

For ceramic (inorganic) membranes, struvite ($MgNH_4PO_4.6H_2O$) accumulates inside the pore and plays a key role in flux decline. No cake layer formation is observed for these membranes, but rather a gradual fouling over time (Kang et al., 2002). Ceramic membranes can maintain high fluxes with almost no fouling as manifested by an increase in TMP. However, they are currently around an order of magnitude more expensive than polymeric membranes (Judd, 2006).

2.5.3 Membrane Cleaning

Several approaches to enhance the back transport of fouling from the membrane surface to the bulk liquid have been proposed. These include (Cheryan et al., 1998; Li et al., 2004):

- Centrifugal Membrane Devices
- Vibratory Shear Systems (VSEP)
- Increased Membrane Surface Hydrophobicity
- Ultra Sonic Vibrations
- Hydraulic Cleaning
- Mechanical Cleaning
- Chemical Cleaning

- Enhanced Shear at membrane Surface (Gas or Liquid)

In centrifugal and vibratory shear systems, the membranes are rotated or vibrated in the bulk liquid, thus inducing a form of liquid shear over the surface. Increasing the membrane surface hydrophobicity has proven to be very effective against cake layer formation. Ultrasonic fields use cavitating air bubbles and sonic vibrations near membrane surface to generate micro-jets at high velocities that increase the back transport of fouling from the membrane surface. Hydraulic cleaning includes back flushing, back shock treatment, alternate pressurizing and depressurizing by reversing flow direction. Mechanical cleaning includes; sponge ball cleaning of tubular membranes and physical scouring of membranes with a brush or scouring pad.

Of the various membrane cleaning methods, the only membrane cleaning techniques that have seen commercial application are gas and liquid scour and chemical cleaning. In both gas and liquid scour a convective cross-flow is induced to aid the back-transport of concentrated surface solids (fouling) to the bulk liquid. It has been shown that both gas and liquid scour plays an important factor in the control of reversible and irreversible fouling rates that consequently affects TMP, operational flux and chemical cleaning frequencies (Fane & Chang, 2002; Soares et al., 2007).

2.5.4 Membranes and Anaerobic Technology

Various anaerobic processes have been developed with the objective of maintaining biomass inside the reactor while allowing the largest possible wastewater flow to pass through the reactor. Typical examples include the UASB and the up/down flow fixed film systems. However, following the development of 'new generation' less expensive filtration membranes in the 1980's, a new system has emerged in water treatment technology; the Anaerobic Membrane Bioreactor (AnMBR) (Beaubien et al., 1995). Membrane enhanced retention is likely to be of interest under those conditions where granular formation may not proceed well, such as under extreme operating conditions (Jeison & Van Lier, 2007c), long expected start-up's due to a lack of granular seed sludge and situations where the organics in the wastewater are not conducive to granular formation (Sam-Soon et al., 1989). It has already been proven that UASB-type systems shows no or impaired granulation which typically leads to poor long term performance on certain wastewaters. Substrates that appear to inhibit granulation include; fat and oil emulsions, Oleate, benzoic acid, therepthalic acid, SCFA rich wastewaters. (Jeison & Van Lier, 2007c).

AnMBRs have the potential to overcome some of the short-comings of the fixed media and granulating systems. Also long sludge ages can compensate for low temperatures. On the other hand it has also been proven that membrane resistance is significantly lower in thermophillic systems which open the door also to high temperature applications (Beaubien et al., 1995). Further advantages identified from lab-scale studies done on AnMBRs include:

- Low sludge production due to long sludge ages (Elmalesh et al., 2005)
- High effluent quality suitable for reverse osmosis treatment (Soares et al., 2007)
- Significant reduction in Soluble Microbial Product toxicity in effluent
- High energy recovery from methane (Hu & Stuckey, 2007)
- Heavy metal accumulation in biomass
- Can treat dilute wastewater streams (short HRTs)
- Small reactor volumes due to high mixed liquor concentrations (Oh et al, 2004)

Current AnMBR applications under evaluation include; herbicide degradation (Yuzir et al, 2007), hydrogen production at short HRTs (Oh et al., 2004), aerobic nitrification/de-nitrification combined with methanogenesis (Zhang et al., 2005) and phosphate recovery (Subramanim et al., 1992). AnMBRs are also combined with R/O systems for energy and nutrient recovery from municipal wastewater (Hellstrom et al., 2007) and have proven to be especially effective in treating high strength biodegradable particulate streams (Jeison & Van Lier, 2006).

2.5.5 Anaerobic Membrane Bio-reactor Designs

As stated earlier, many AnMBR designs are currently under evaluation at laboratory scale (Section 2.5.3). However, only two systems appear to be economically viable for scale-up at this stage. These are the submerged panel membrane system with biogas scour and the external cross flow type systems.

- **Cross-flow membrane System**

  In the cross-flow (or external loop) design, the mixed liquor is circulated from the bio-reactor to the membrane module and back (Figure 2.11). The recycle pump induces a TMP over the membrane module and permeate passes through the membranes. Two pumps are required for the design to function properly, the first is the pressure pump that induces TMP for permeate

extraction and the second is the cross-flow pump to maintain the desired hydrostatic shear over the membranes (Jeison & Van Lier, 2007c).

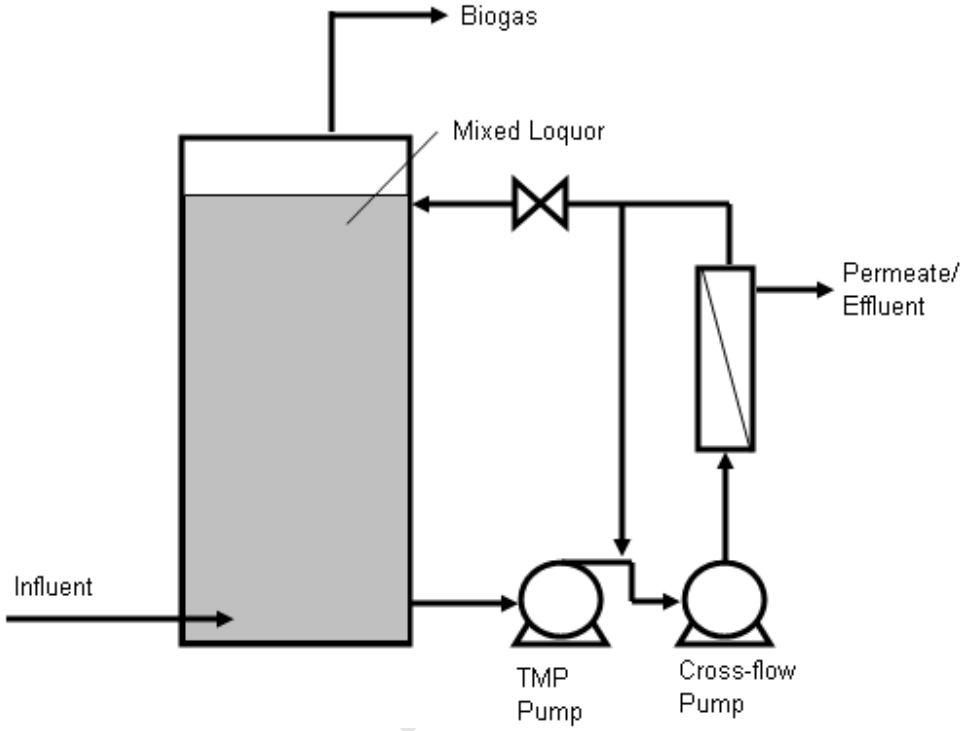

Figure 2.11, Cross-flow AnMBR

The cross-flow systems can produce much higher shear rates than other configurations; this implies that the membrane surface area in the cross-flow is significantly lower than in other configurations (Lesjean et al., 2004). However, this saving comes at a cost, (i) energy and equipment requirements are high for the cross flow and (ii) the high shear can lead to floc breakage and a decrease in performance of the anaerobic biomass (Jeison & Van Lier, 2007c).

- **Submerged Membranes**

In 1989 the Japanese government charged many of its large corporations – including Kubota – to invest time and money in new water treatment technologies that had a small footprint and produced a high quality final effluent with reuse capabilities. The Kubota flat sheet submerged membrane arose from this initiative (Churchouse & Wildgoose, 1999). The Kubota flat sheet membrane was also the first membrane technology to see commercial application and the first commercial aerobic Kubota plant came into operation in 1991

(Churchouse, 1997). In immersed systems, gas is introduced through a coarse bubble diffuser situated below the membranes to (i) aerate - in activated sludge systems - and mix biomass and (ii) to reduce fouling and promote cleaning by scour of the submerged membranes (Howell, 2003) (Figure 2.12).

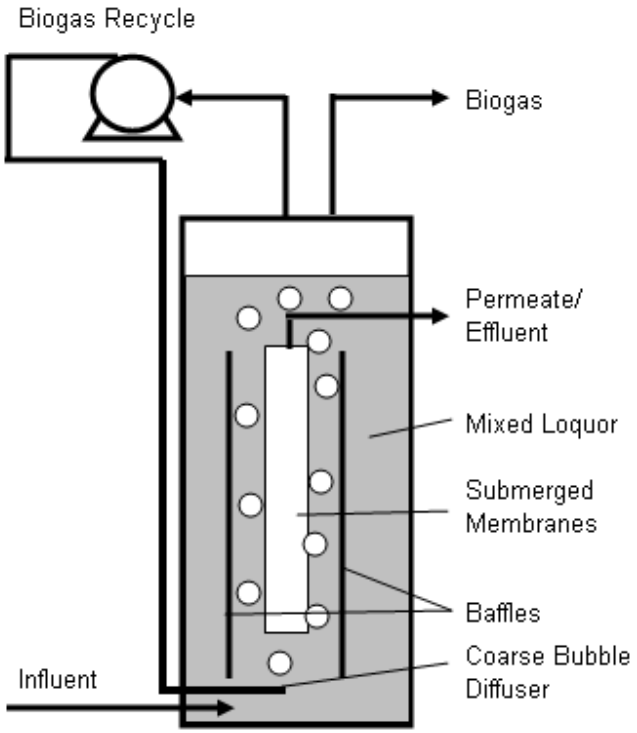

Figure 2.12, Submerged AnMBR

For biological reactors (both aerobic and anaerobic) with the submerged membrane configuration, the membranes are located in the mixed liquor tank. Gas scouring is applied to produce surface shear and keep the cake layer formation to a minimum. A coarse bubble diffuser is situated below the membranes. The gas bubbles (air – aerobic, biogas – anaerobic) force the sludge to rise up between the panels and causes recirculation of sludge within the reactor volume. Each membrane panel is connected to a permeate collection manifold and treated effluent is removed by low pressure suction or a hydrostatic head. The number of membranes required is dependant on the influent flow rate and achievable flux through the membranes.

The absence of primary/secondary settling stages allows the use of high biomass concentrations (10 - 20 gTSS/L) in low volume reactors and directly provides an excess sludge concentration of 2% in thickness (Churchouse, 1997). The application of submerged AnMBRs might overcome problems frequently observed with cross-flow systems such as (Jeison & Van Lier, 2007a):

- Loss of activity due to floc breakage
- High shear
- High TMPs
- High energy requirements due to pumping costs

2.5.6 Critical Flux

Two definitions of the critical flux exist. The first one refers to the 'strong' definition of the critical flux, which represents the flux below which the membrane resistance is the same as that observed in clear water. The second or 'weak' definition of the critical flux, this definition describes an area where TMP and flux is directly proportional and an area where further increase in TMP does not result in an increase in flux. The transition between the two is known as the critical flux (weak definition). Throughout this thesis the critical flux will refer to the 'weak definition' of the term. The critical flux is generally determined by the formation of cake layers on the membrane surface. Cake formation is one of the most important causes of flux decline in MBRs (Jeison & Van Lier, 2006b).

Several studies performed on aerobic and anaerobic MBRs have pointed out the existence of a certain gas (air – aerobic, biogas – anaerobic) scour flow rate over which no further improvement in fouling control can be achieved (Jeison & Van Lier, 2006b). When operating at a controlled flux it is possible, in principle, to operate without particle deposition on the membrane. The flux at which particle deposition begins is known as the critical flux (Fane & Chang, 2002).

On short term basis, cake layer formation in AnMBRs is mostly reversible. However cake layer formation plays a major role in long term operation and proceeds fast once the critical flux has been exceeded. This restricts the operational flux to the range below the critical (Jeison & Van Lier, 2007a).

Under mesophillic conditions, biomass concentration strongly affects the critical flux. Biogas recycling levels also exerts a significant influence (up to a point). An increase in the biomass concentration will increase the convective flow of solids towards the membrane surface. On the other hand, an increase in gas flow will increase the shear rate, increasing the back transport of solids from the membrane proximity. Therefore an increase in mixed liquor concentration and decrease in scouring rate will decrease the critical flux (Jeison & Van Lier, 2006a). However, an upper limit for TMP and scouring rate also exists above which no significant increase in filtration performance is observed (Jeison & Van Lier, 2007b). The effect of biomass concentration is three times greater than that of gas flow rate on critical flux.

If the AnMBR is operated at sub critical flux conditions, cake layer formation can be minimized and the membrane fouling that does occur can mainly be attributed to membrane pore blocking (Jiang et al., 2005). Compared to cake layer formation, the rate of membrane pore blocking (irreversible fouling) has been stated as 'strikingly low' irrespective of reactor configuration, temperature or substrate composition. It was found that the relationship between TMP and flux gives an adequate representation of the membrane performance and that these two parameters can be used to quantify membrane fouling. Therefore, dynamic TMP and flux assessment is a prerequisite for stable AnMBR operation (Jeison & Van Lier, 2006b).

2.5.7 Economic Considerations

Notwithstanding the constraints imposed by fouling, the commercial applications of aerobic MBRs are extensive. The submerged configuration in particular has achieved a significant market penetration. It is evident therefore that the technical advances offered by MBRs more than compensate for the perceived higher costs and more rigorous process control demanded (Judd, 2004). At present aerobic MBRs are broadly applied and there are more than 2000 full scale installations already in operation around the world (Soares et al., 2007). However aerobic MBRs are very energy intensive with a typical energy requirement of 1 kWh/m^3 wastewater treated. This is 2 to 3 times higher than other advanced treatment systems available, depending on the organic strength of the wastewater. Anaerobic MBRs provides a means to recover some of this energy cost though methane production (Jiang et al., 2005).

So far there was no direct need for the development of MBR technology for anaerobic digestion due to the market availability of high rate sludge bed systems. It is expected that investment and operational cost related to anaerobic MBR technology will be higher than granular sludge based reactors due to the higher energy costs and membrane acquisition and replacement. Considering the low growth rates of anaerobic micro-organisms, AnMBR technology is likely to be feasible if these systems can be operated at high biomass concentrations enabling high organic loading rates (Jeison & Van Lier, 2007c), in particular where the influent organics are not conducive to flocculation, settling, attachment or granulation. The economic viability of membranes are restricted by the achievable permeate flux, the cleaning frequency and the lifetime of the membrane modules. The benefit-cost performance of membranes depends on different factors including (Lesjean et al., 2004):

- Membrane hydrophbicity
- Robustness
- Cost
- Ease of fabrication

In aerobic MBRs the selection between submerged and side stream configurations is somewhat settled. Most applications are based on the submerged configurations for various local and site specific reasons. However, since AnMBR technology is still in its infancy, and various factors including membrane life span in the anaerobic environment and serviceability of membrane modules has not yet been established. Because of this both submerged and cross-flow systems are still under evaluation for the AnMBR (Jeison & Van Lier, 2007b).

Submerged membrane technologies involve lower energy costs than side stream configurations. However lower applied surface shear usually involves higher membrane surface requirements and in so doing increasing the capital cost of the submerged systems Furthermore cross-flow systems can also operate at higher MLSS, in so doing decreasing the required reactor volume and capital cost. The cost of hollow fiber submerged membranes are more competitive that flat sheet but more equipment is required to operate the former due to back flushing requirements (Lesjean et al., 2004).

Since the permeate from AnMBRs is free of organisms, settlable solids and all particulate biodegradables, water would require less post treatment steps, if re-use or recycle is of interest. Calculations for a full scale AnMBR-R/O plant – for energy and nutrient recovery from sewage – showed a total energy requirement of 2 kWh/m^3, with the produced biogas corresponding to 1.3 kWh/m^3. If struvite is precipitated from the R/O brine it can be sold as fertilizer for approximately R 500 / ton to further decrease the plant operating cost. Thus the net energy requirement of such a system – 0.7 kWh/m^3 – corresponds quite well with that of other advanced treatment systems. It is expected that future applications of AnMBR-R/O systems will increase with a decrease in membrane production costs and an increase in water supply cost (Hellstrom et al., 2007).

2.5.8 Future Prospects of AnMBRs

Although macro and ultra filtration were only laboratory curiosities a few decades ago, they are now attractive techniques in practical industrial processes for solid liquid separation (Kang et al., 2002). From Figure 2.13, it can be noted that even though membrane prices have experienced a dramatic decrease during the past decade, it still represents a much more important economic factor than energy. Energy requirement for gas scouring makes up less than 10% (50 $US/$m^2_{\text{membrane area}}$ vs. 5 $US/$m^3_{\text{treated effluent}}$) of the overall treatment cost.

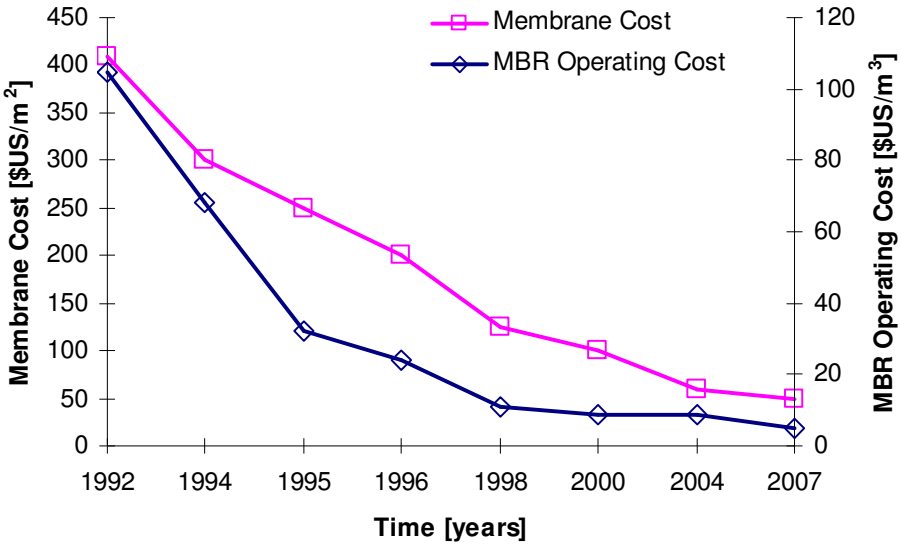

Figure 2.13, Membrane Cost & Overall Operating Cost of a 2000m^3/d Municipal Treatment Plant (Jeison & Van Lier, 2007b)

Membrane bioreactors will continue to penetrate the wastewater treatment market, with the primary drivers being a need for:

- compact plants
- existing wastewater treatment plant retrofitting (upgrading capacity on the same site)
- high quality of effluent for reuse
- value of recycling

In a review done on the state of the art of the application and world wide research currently conducted in this field, Yang et al. (2006) found that after the middle 1990's there was a linear increase in research outputs for aerobic MBRs (Figure 2.14A). This indicates that researchers trained in the early and mid 1990's are now making MBR research part of their research program and focusing consistent attention to the area. It is expected that this will also result in wider acceptance of MBR technology as a mainstream alternative for water and wastewater treatment by both the scientific community and end users (Elmaleh et al., 1997). The same was done specifically for anaerobic MBRs (AnMBRs) and two scientific databases were chosen for the project namely Science Direct and Scholar Google. Figure 2.14B displays the chorological distribution of peer reviewed journal articles specifically on AnMBRs for the past two decades:

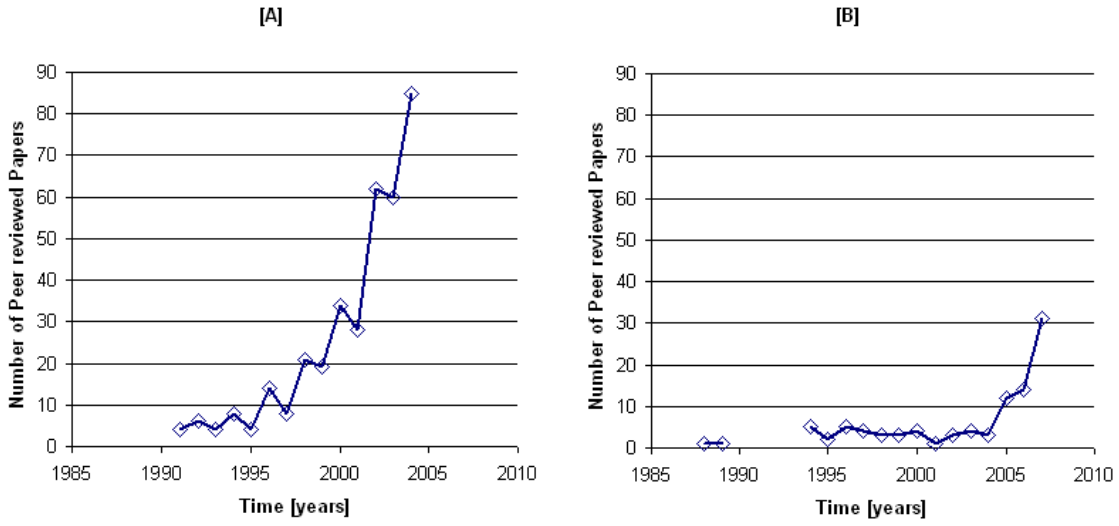

Figure 2.14, Chorological Distribution of Worldwide Peer Reviewed Journal Articles Involving Studies on [A] Aerobic MBRs and [B] AnMBRs

For the first 15 years of AnMBR research the number of peer reviewed papers was virtually constant each year. During this period only cross-flow type systems were evaluated. However in 2005 the first papers on submerged AnMBRs were published and in 2006 the first papers on flat panel submerged AnMBRs were presented. In 2007, more than 60% of the papers published were on flat panel submerged AnMBRs. This current trend in AnMBR research outputs corresponds quite well with the observations made by Yang et al. (2006) on aerobic MBRs.

This 10 fold increase in AnMBR publications in only four years might also point towards a global recognition of AnMBRs as a possible solution to some of the most challenging wastewaters and effluent standards. It is further expected that energy recovery from produced methane and the ever tightening of effluent standards and water reuse will be the primary driving factors in the development of AnMBRs.

2.6 Closure

Fischer-Tropsch technologies form the basis of the CTL and GTL processes of Sasol. In these processes, coal and natural gas (mostly methane) is converted to synthetic fuels and other value added polymers. Irrespective of the feedstock and catalysts used, the FT process produces three major effluent streams, namely API, SGL and FTRW. At the Secunda plant situated in South Africa, the three streams have a combined flow and organic load of 128 ML/d and 677 tonCOD/d respectively. The combined wastewater stream is currently treated in a fully aerobic activated sludge plant, requiring 600 tonsO_2/d and producing in the order of 150 tonTSS/d of dry solids. FTRW contributes 77% of the organic load and consists mostly of C_2 to C_6 SCFAs. The aerobic treatment of SCFA streams are problematic because of the tendency to produce biomass with poor settling properties, leading to high aeration demands, high sludge production as well as poor effluent quality and high solid liquid separation costs.

If the FTRW stream is kept separated and treated anaerobically, an estimated 77 % decrease in oxygen demand and 62 % decrease in sludge disposal costs will be achieved. Secondly, the SCFA in FTRW is highly biodegradable under anaerobic conditions, which implies high OLRs and compact, high rate anaerobic reactor designs. Apart from the compact reactors, there will be no oxygen requirements and low sludge production, >95% of the COD in FTRW will be converted to biogas (carbon dioxide and methane) which can be recycled to the beginning of the FT process and blended with natural gas and used as a feedstock for fuel and polymer production. This carbon recycling will make a significant reduction in the CO_2 emissions from Sasol's plants.

Analogous to aerobic digestion, SCFAs also produce a dispersed un-flocculated anaerobic biomass with poor settling properties. This hampers the applicability of high rate anaerobic bio-reactors that uses bio-granulation for solids-liquid separation since granulation on high concentration SCFA streams (especially FTRW) cannot be guarenteed. This well documented phenomenon of impaired anaerobic granulation with SCFA rich wastewaters, leads to biomass washout and poor effluent quality. Fixed bed anaerobic technologies appear more feasible but require large reactor volumes due to lower design OLRs and effluent quality is such that a significant amount of post treatment is still required.

The fourth generation anaerobic bio-reactor - the AnMBR – appears to address issues around the application of anaerobic systems to the SCFA rich FTRW stream viz. (i) AnMBR performance is not dependant on biomass immobilization or granulation, (ii) membranes give a 100% solids-liquid separation resulting in superior effluent quality and (iii) high MLSS can be maintained leading to high OLRs and compact reactor design.

Membranes provide a positive solid-liquid separation barrier, retaining biomass in the reactor while effluent can pass through. Currently, ultra-filtration membranes are the most popular membrane pore size in wastewater treatment since it operates under economic TMPs, and retains bacteria and viruses while allowing soluble constituents to pass through. AnMBR research is currently dominated by two reactor configurations; the first is the cross-flow system, in which an external membrane module is mounted on a completely mixed anaerobic reactor. In the second configuration, the membranes are submerged in the mixed liquor and uses recycled biogas for membrane scour. The submerged configuration has gained significant popularity in research in the past few years. The AnMBR technology is still in its infancy, however a 10 fold increase in research outputs has occurred in the past 3 years in this field, proving that major wastewater research groups around the world are considering the AnMBR as a viable treatment method for applying at full scale, despite currently high (but decreasing) membrane costs and the more complicated reactor designs and control schemes required to operate these systems.

CHAPTER 3

3. Materials and Methods

Design, methods of data capture and operation of the anaerobic reactors developed to treat FTRW is the primary focus of Chapter 3. The first section entails a discussion on the design of the Submerged Anaerobic Membrane Bio-Reactor (AnMBR). This design is based on the following; (i) developing a environment suitable for anaerobic biomass to digest Fischer-Tropsch Reaction Water (FTRW) and (ii) to devise a state-of-the-art means of solid-liquid-separation by using flat panel membranes submerged in the mixed liquor. The second part of Chapter 3 discusses the design of the control reactor used as baseline for the evaluation of the AnMBR performance.

The control reactor in this study was a laboratory-scale version of a pilot plant fixed media anaerobic reactor for treating FTRW. The main design approach for the lab-scale unit was to try and mimic as close as possible the liquid flow rates and conditions around the packing media in the pilot plant. Both the AnMBR and Anaerobic Packed Bed Reactor (AnPBR) systems were evaluated on various parameters including OLR, COD removal and alkalinity and nutrient requirements.

Description of the experimental procedures applied to measure the abovementioned parameters is the third main part of Chapter 3. Apart from being the means of comparison between the two technologies, the data collected is also required for mass balance checks for steady state and dynamic simulation models developed for the Anaerobic Digestion of Fischer-Tropsch Reaction Water (AD-FTRW) (Chapter 5 and 6). The final section will describe feedstock preparation and the daily operation of the two anaerobic reactors.

3.1 AnMBR: Design

The AnMBR design is based on laboratory-scale aerobic submerged membrane activated sludge reactors by Aquator®. For both system types, flat panel Kubota® membranes, cased in a membrane rack, are submerged in the mixed liquor. Effluent flows through the membranes and out the reactor under hydrostatic pressure. In aerobic systems, compressed air enters the reactor through a coarse bubble diffuser situated below the membrane rack. In the activated sludge reactor, the function of the air is three fold; (i) to transfer oxygen to the aerobic biomass, (ii) to ensure that the reactor is completely mixed (CSTR) and (iii) to scour the membranes and in so doing significantly reduce membrane fouling.

A gas flow is also required for mixing and membrane scour in the AnMBR. Because air cannot be used for this, biogas was re-circulated. The biogas produced by the anaerobic bio processes was extracted from the biogas headspace via a compressor and reintroduced through a coarse bubble diffuser situated below the membrane rack. Hence, the biogas recirculation fulfilled the functions of mixing and scour.

3.1.1 Flat Panel Kubota Membranes

The AnMBR was developed around 200x300 mm flat panel type Kubota® membranes specifically designed for laboratory-scale reactors (Figure 3.1). These membranes are constructed of a non-woven hydrophobic polymer, with pore size in the 0.1 – 0.5 µm range and have a molecular mass cut off of ± 1000 to 500 000 Da, and hence most bacteria and viruses will be retained. However, unlike reverse osmosis (or nano-filtration) constituents that can pass through the membrane include; ions, soluble organics, alkalinity, dissolved gas –especially CO_2 and of course water. Therefore, membranes provide a state-of-the-art means of solids-liquid-separation between the reactor MLSS and the effluent. While affecting membrane fluxes, membrane solid-liquid-separation efficiency (% solids removal) is unaffected by factors such as a poor sludge flocculation and settleability, high MLSS concentrations and high effluent flow rate.

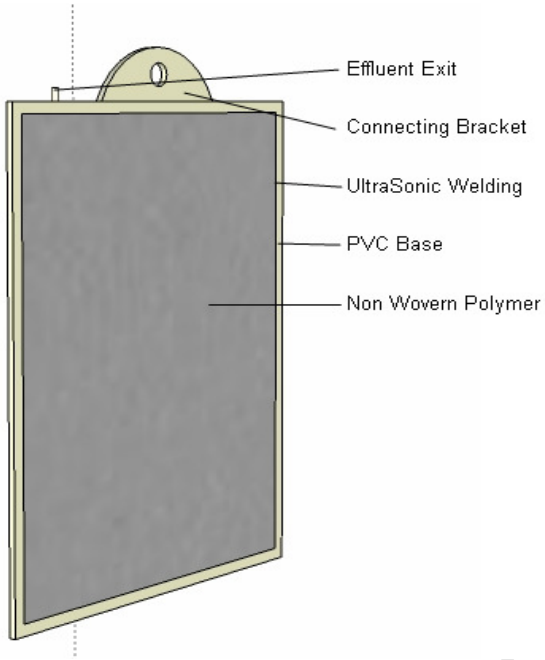

Figure 3.1, A4-Size Flat Panel Kubota® Membrane

For the flat panel Kubota® membranes, optimum fluxes are typically obtained with a MLSS of between 12 and 18 gTSS/L in aerobic systems. Manufacturers of the membranes state then for full scale operation the maximum short term flux is 40 L/m^2/h and the maximum sustained flux is 30 L/m^2/h. To maintain these fluxes, a scouring rate of 750 L/m^2/h is required yielding an up-flow gas velocity of 0.5 m/s over the membrane surface. For the three lab-scale membrane panels that were used a gas flow rate of 225 L/h was required. Three 200x300 mm membrane panels are installed in the AnMBR giving a membrane surface area of 0.11772 x 3 = 0.3516 m^2. The membranes were taken from a parallel lab-scale activated sludge unit, and had been in operation for 18 months. The membranes were chemically cleaned (5% hypochlorite solution) before installation in the AnMBR

3.1.2 Reactor Shell and Membrane Housing

Originally it was expected that foaming might be a problem in the AnMBR, and thus to aid foam and liquid level observation, the chosen material of construction was Perspex. Apart from transparency, a further advantage of using Perspex includes, better insulation from temperature fluctuations than would be expected for metal reactors. The reactor design is illustrated in Figure 3.2. The reactor shell comprises three sections; (i) the top section comprise the foam accumulation and biogas headspace biogas from which biogas is recycled. (ii) The middle section of the reactor shell houses

the effluent collection manifold. The membranes are connected via silicon tubing to the effluent manifold through which the effluent exits the reactor. (iii) The bottom section encases the membrane housing and also contains the anaerobic mixed liquor.

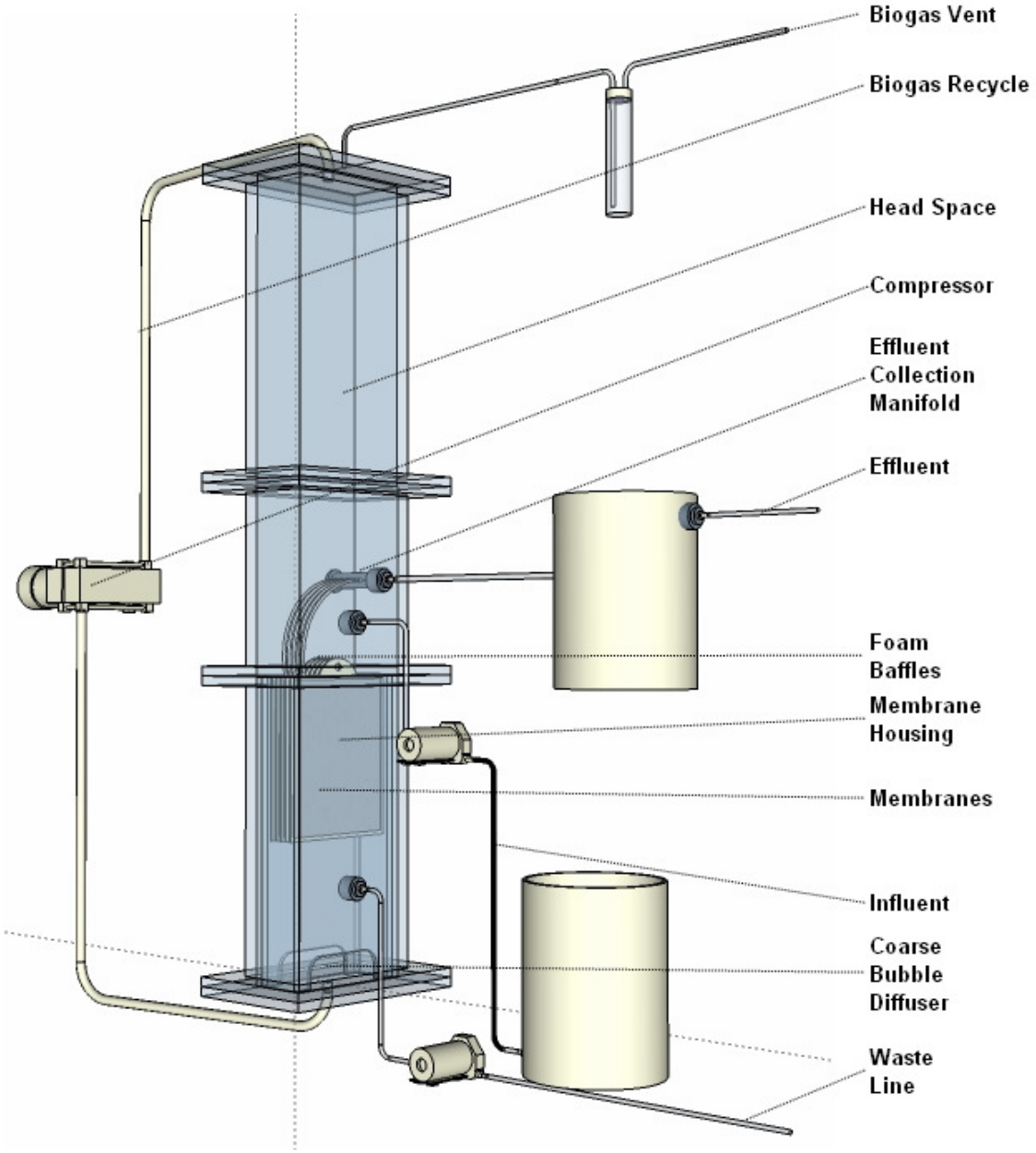

Figure 3.2, Detail sketch of AnMBR

A coarse bubble diffuser is mounted on the reactor base below membrane housing. The membranes are fixed in this housing. To reduce the effects of foaming, foam baffles were later mounted on top of the membrane housing. The mixed liquor level in the reactor is maintained such that there is a continuous flow of mixed liquor over the foam baffles, which induces a 'mixing' of the foam back

into the liquid phase. Ideally, the AnMBR liquid volume is set at 23±0.5 L with a 35 L headspace volume above it. The headspace was constructed large so that a significant foam head could develop without the risk of drawing foam into the gas recirculation intake. Figure 3.2 highlights the positions of the influent line, waste line, membrane housing, foam baffles and also the position of the effluent collection manifold.

3.1.3 Biogas: Recycling & Trans Membrane Pressure Control

Biogas gets extracted from the top of the headspace via a compressor and reintroduced via the coarse bubble diffuser situated on the reactor base directly below the membranes (Figure 3.3). The membrane housing forces the gas to rise vertically upwards and between the membrane panels. Since the gas bubbles are more hydrophobic than the biomass itself, it continuously 'scrapes' the biomass from the hydrophobic membrane surface area. This ensures that the membranes do not block and effluent can pass through at the required rate. Secondly the biogas recycling ensures the AnMBR stays completely mixed. The upward flow of gas in the membrane housing exits at the top near the mixed liquor surface and causes a down-flow to the bottom of the reactor outside the membrane housing. Biogas is constantly produced by the anaerobic bio-processes; hence the biogas that is not recycled needs to be vented to avoid pressure build-up.

The biogas venting system designed for the AnMBR is depicted in Figure 3.3. The biogas escapes the reactor headspace through a gas line the end of which is submerged in water to a desired level. If biogas accumulates in the system the pressure will eventually exceed that of the water level (H_3) in the pressure release valve and the excess biogas will be vented. The vented biogas first passes through a biogas counter and then escapes to the atmosphere. This pressure release valve system has two main advantages; (i) there is always a net positive pressure inside the reactor, which eliminates possible air leaks into the reactor. And (ii) by controlling the water level (H_3) the Trans Membrane Pressure (TMP), membrane flux and the reactor volume can be controlled.

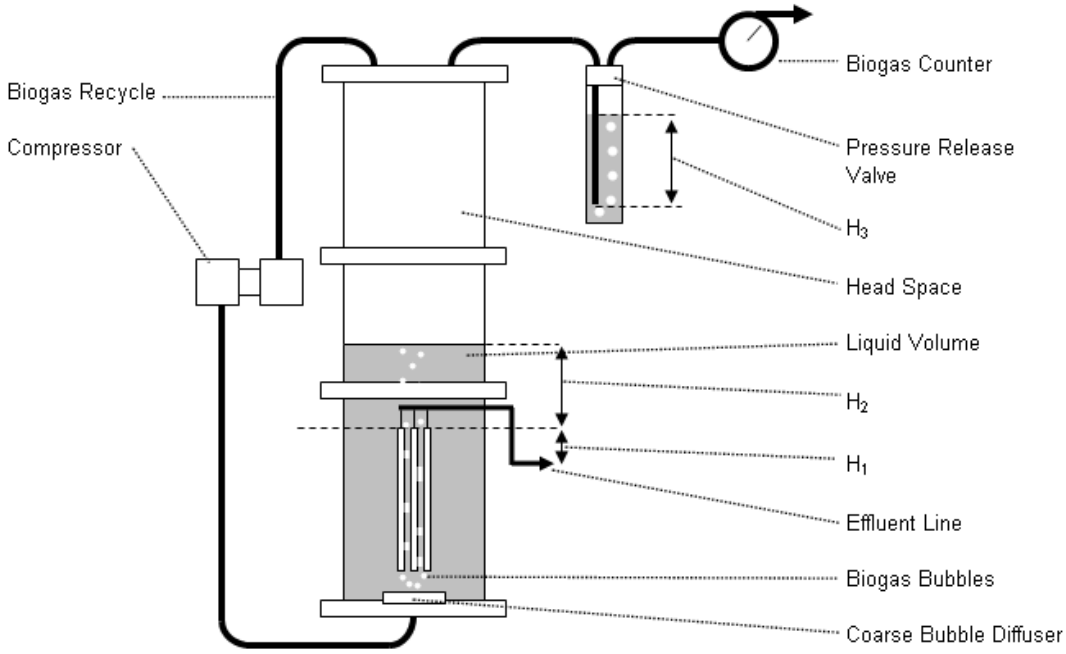

Figure 3.3, Biogas Recycle, Venting & TMP Control System

The flux is governed by the pressure difference (TMP) across the membranes. The higher the TMP the higher the flux of effluent will be through the membranes. Since the influent flow rate is constant, the reactor volume will vary with variation in TMP and resultant effluent flow rate. From Figure 3.3 it can be noted that three factors affect the TMP. The first is the level of the opening of the effluent line (H_1) below the top of the membranes. The second is the liquid volume height above the membranes (H_2) and the third is the gas pressure in the reactor head space (H_3).

The higher the TMP ($H_1 + H_2 + H_3$), the faster effluent flow will be out the reactor. If the effluent line is kept at a constant level and a constant reactor volume is required, the only parameter that can be easily manipulated is the biogas headspace pressure (H_3). This is done by increasing/decreasing the liquid level height (H_3) in the pressure release valve and in so doing controlling the reactor volume and effluent flow rate. A Piping and Instrumentation Diagram of the AnMBR design and layout and a detailed explanation of it presented in Appendix 3.1.

3.1.4 AnMBR On-line Control System

At relatively short hydraulic retention times (< 20h), it was found the AnMBR became sensitive to overloading. The cause of the overload is the high acidity of FTRW (11 000 mgAc/L), which means that a feed load increase of less than 10% can increase the reactor SCFA concentration from 50 to 1000 mgAc/L within hours. Originally, the pH in the reactor is controlled above 7 by NaOH dosing. The objective here is not to neutralize the acid feed, which is not necessary because the anaerobic biomass utilizes the SCFAs in their acid form, but to provide some pH buffering. The dosed NaOH reacts with dissolved CO_2 to form HCO_3^-. However, when the reactor pH variations become large due to significant load variations (resulting in high SCFA concentrations), a large mass of NaOH will be dosed, which would lead to inhibition of the biological processes through high SCFAs and high Na^+ concentrations. The result would be a snowball effect introducing reactor instability (SCFA/Alkalinity >0.3) within hours. SCFA and Na^+ concentrations as high as 4000 mgHAc/L and 6000 mgNa/L has been observed in such overloading conditions. Resulting in compete system failure (Mignone, 1995).

It was therefore decided to devise an on-line control system to increase the robustness of the AnMBR. The control system design criteria were to (i) act as an override system if an influent overload is not detected soon enough by the operator, secondly (ii) observe an easily measurable parameter continuously as a control measure and (iii) if this parameter starts deviating, intervene and rectify the situation within a short period of time (< 5h). Finally the (iv) development cost should also be as low as possible.

The system developed was based on the observation that a decrease in reactor pH was invariably linked to an increase in reactor SCFA concentration. If the pH in the reactor (measured on-line) continued to decrease below a low set point (7.1) while NaOH was dosed, an influent overload is assumed and the influent feed is stopped. Figure 3.4 gives a graphical representation of how the control system responds to a possible SCFA over load:

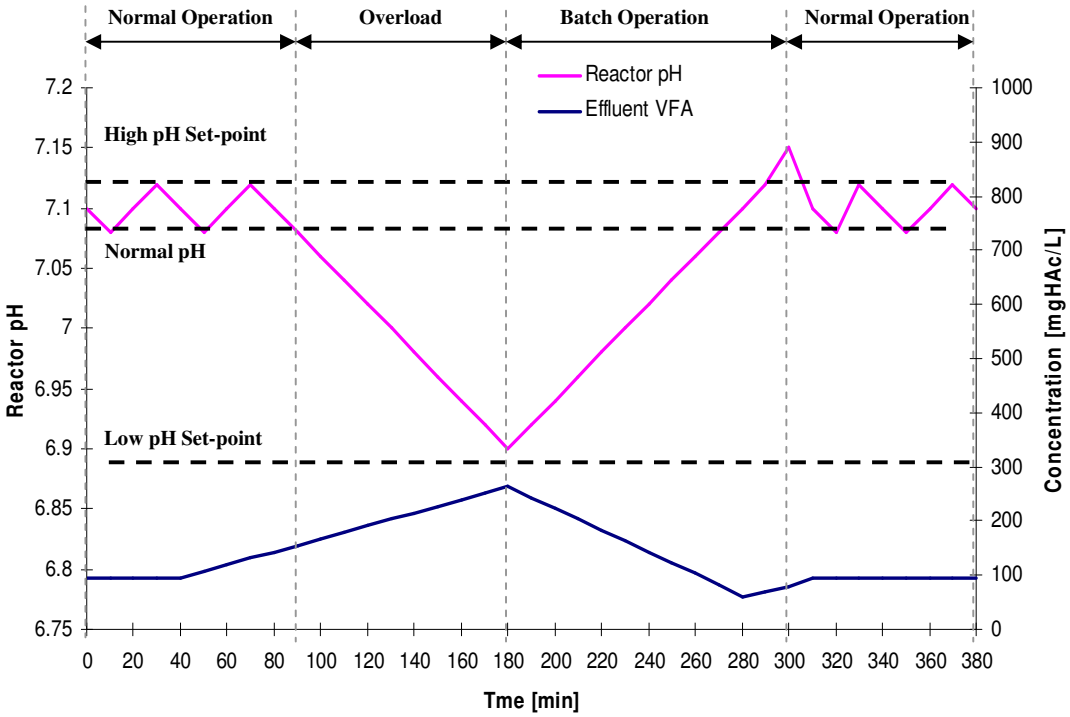

Figure 3.4, Online Control System Response to SCFA Overload

The on-line control system functions as follows:

- Only enough alkalinity is dosed to neutralize a reactor residual SCFA <100 mgAc/L (Normal Operation, Figure 3.4)
- If a system overload occurs and the reactor SCFA increases >100 mgAc/L, the system acidity would increase, resulting in a decrease in pH (Overload, Figure 3.4)
- If the SCFA overload continues to increase the pH will drop below a minimum level (pH = 6.9) and the controller automatically switches off the feed and alkalinity pumps and closes the effluent line.
- The AnMBR now operates in batch mode, consuming the SCFAs and increasing the pH (Batch Operation, Figure 3.4).
- As the SCFAs are consumed, the pH will continue to increase until a high set-point is reached (pH = 7.15).
- Both the feed and alkalinity pumps are switched back on and the effluent valve is opened and normal operation is continued.

In this way the anaerobic biomass is protected from high SCFA and Na^+ concentrations. A detailed discussion on the design and workings of the on-line control system is presented in Appendix 3.2. The on-line control system was only incorporated in the last quarter of the study, during the first three quarters of the experimental period; the system was manually controlled by controlling the OLR. After the on-line control system was installed, the OLR was still manually controlled; the control system only intervened if a drop in pH (due to SCFA increase) was observed.

3.2 Anaerobic Packed Bed Reactor (AnPBR): Design

Apart from membranes, another means of achieving a high degree of solid-liquid-separation in the AD-FTRW environment has been identified as fixed film anaerobic technologies. Therefore anaerobic packed bed technology is currently being evaluated at pilot-scale by Sasol. To get a direct comparison between the performance of the membrane and packed bed technologies for AD-FTRW, a laboratory-scale replica of the AnPBR pilot plant was designed and constructed to serve as control reactor for the performance evaluation of the AnMBR. Factors including temperature and feed composition fluctuations negatively affect accuracy of comparisons between lab-scale and pilot-plant anaerobic systems. So the constructed lab-scale AnPBR system was operated at the exact same laboratory conditions as the AnMBR and fed the same feed and nutrient mix as the AnMBR. A detail discussion on the pilot-scale down-flow packed bed reactor and the basis for the scale-down design of the lab-scale AnPBR is presented in Appendix 3.3.

The final scaled down AnPBR had a 23 L volume (similar to the AnMBR) with a diameter of 0.19 m and a height of 0.81 m (Figure 3.5). As with the AnMBR the material of construction was Perspex. The down flow velocity in the lab-scale unit was kept the same as the pilot plant at 0.884 m/h requiring a recycle flow of 20.05 L/h. The same packing material (Flocor Rings) as was used in the pilot plant was used in the lab scale unit. Since the diameter of the lab-scale system was selected so that the down flow velocity and the packing densities are the same as in the pilot plant, the hydrodynamics experienced by the micro-organisms inside the lab scale unit should be similar to that of the pilot plant. This was the primary design requirement of the AnPBR.

The literature review indicated that one of the most challenging areas in Packed Bed Reactor (PBR) design is to ensure sufficient mixing and plug flow conditions. Also in PBR's of small diameter, the effects of wall flow also contribute to inefficiencies in the mixing in the packed bed since channeling

becomes a significant problem (Fogler et al., 1999). Because of this, influent disperser tubes and perforated plates and wall baffles were mounted on the inside of the reactor shell. The reactor volume is sealed from the environment with bottom and top lids on which the reactor inlets and outlets are mounted. The packing (grey in Figure 3.5) is randomly distributed (as opposed to structured packing) inside the reactor and is kept in place by the upper and lower disperser plates.

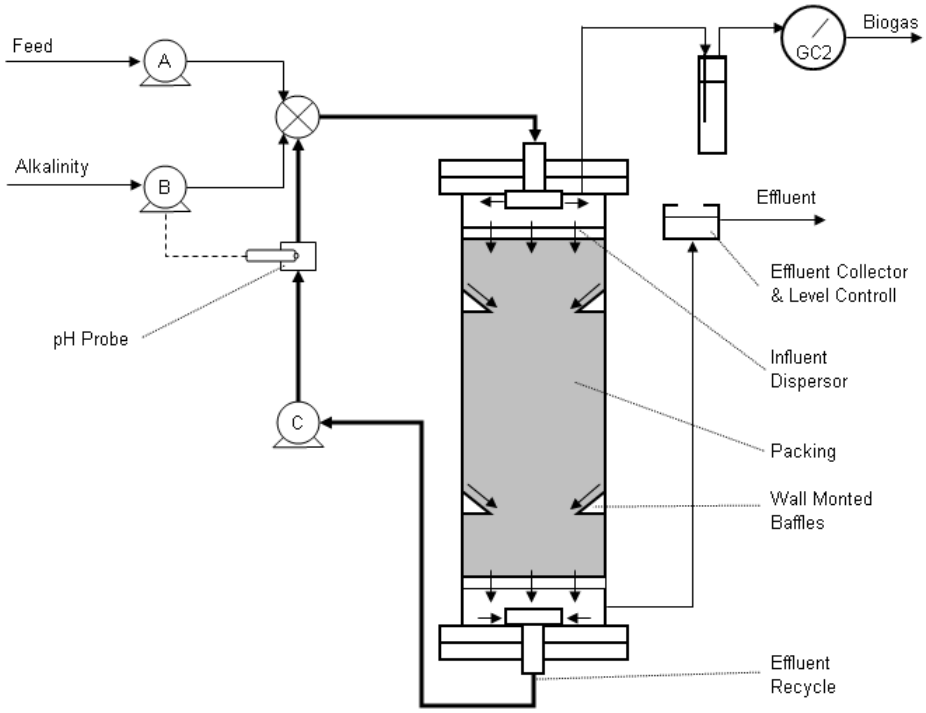

Figure 3.5, AnPBR Design

Figure 3.5 gives a basic flow diagram of the lab-scale AnPBR system. Liquid flows downwards through the reactor and gets recycled by the recycle pump (C) and reintroduced in the top. The relatively large recycle serves four functions: (i) to recycle alkalinity produced by the anaerobic process for influent SCFA neutralization, (ii) to dilute the influent COD to a level manageable by the fixed film anaerobic microbial population, (iii) to ensure the optimal down flow velocity is maintained through the packed bed and (iv) provide mixing.

The system pH is measured in the recycle line. The pH is controlled via a dosing system (B) which maintains the pH at the desired level. The feed pump (A) introduces the feed via the recycle line where it is diluted before it comes into contact with the biomass. Level control in the AnPBR is

controlled by the height at which the effluent line is open to the atmosphere (Figure 3.5), if the liquid volume in the reactor rises above this point, the effluent will flow out the reactor, thus controlling the volume. In this way the liquid volume in the reactor can be maintained such that efficient wetting by submergence of all the packing is ensured. Biogas is vented from the top of the headspace and escapes the system through a pressure release valve and out via a biogas counter.

3.3 Experimental Methods

The following entails a discussion on the methods used for data capture. Analysis includes COD, Nitrogen (FSA & TKN), Settlable Solids and Methane in biogas. These measurements enable mass balance checks around the system to be made ensure that the data collected is of sufficient quality for model development and calibration. The discussion will also give a brief overview of the format in which the data will be recorded.

- **COD** is defined as the Chemical Oxygen Demand or amount of electrons that can be donated by a given organic molecule, mix of organics or waste water ($8gCOD/mol_{electrons}$). These electrons can then be utilized by micro-organisms, along with the carbon, nitrogen, oxygen and hydrogen to either form biomass or in the case of anaerobic digestion, biogas. The COD test forms the backbone of the mass balance over the anaerobic system and is done on a daily basis on the influent, effluent and mixed liquor (of the AnMBR). In instances where there are particulates in the sample, such as the AnPBR effluent, both the filtered and un-filtered COD is analyzed for the sample. The technique used for analysis is a wet chemistry titration using ferrous ammonium sulfate (FAS), dichromate and sulfuric acid and is discussed in detail in Standard Methods 1985. The COD test shows a standard deviation of ± 5 % but is strongly related to the accuracy of the pipettes and dilution methods used. Table A3.2 in Appendix 3.4 gives a break down of how a sample's COD can be classified into its various fractions by measuring its filtered and unfiltered COD i.e. biodegradable soluble organics (S_{bs}), unbiodegradable soluble organics (S_{us}), biodegradable particulate organics (S_{bp}) and unbiodegradable particulate organics (S_{up}). Once the COD fractions have been identified, a number of parameters that quantify reactor performance can be calculated (Appendix 3.4, Table A3.3). These can be used as a comparison between various anaerobic systems

treating the same substrate (like FTRW). The volumetric Organic Loading Rate OLR is a useful parameter, because lab-scale, pilot plant and even full scale reactor performance can be compared directly. By comparing the OLR on a day to day basis, it also gives information about the health and performance of any given anaerobic system.

$$OLR = \frac{S_{ti}..Q_i.24}{V_r * 1000} \qquad [kgCOD/m^3{}_{Vr}/d] \qquad (3.1)$$

Where

S_{ti} = unfiltered influent COD [mgCOD/L]

Q_i = influent flow rate [L/d]

V_r = reactor volume [L]

- **Alkalinity and Short Chain Fatty Acids** are measured with the 5-pt titration method (Moosbrugger et al., 1992). This method gives a quick (< 1h) indication of the three most important operational parameters of the AD-FTRW system, namely; (i) pH, (ii) $H_2CO_3^*$Alkalinity and (iii) SCFA concentration. If the measured SCFA is too high (>100 mgAc/L) the feed flow - and resultant OLR - is decreased and vice versa. As discussed in Chapter 2, the buffer capacity or alkalinity is defined as the resistance of a system to pH change. According to Ripley et al., (1986) the alkalinity should be at least 3 times higher than the SCFA concentration to shield the anaerobic system from pH fluctuations. Both the $H_2CO_3^*$ Alkalinity and SCFA are measured in the 5-point titration and is recorded in [mg$CaCO_3$/L] and [mgAc/L] respectively, as discussed in Loewenthal & Lahav, (2000). Individual SCFA concentrations were also measured with a HPLC as will be discussed in detail in Chapter 6.

- **The Mixed Liquor Suspended Solids** are one of the most important design parameters in biological water treatment, which is used in conjunction with the OLR to predict reactor volumes (Chapter 5). The MLSS is defined as the dry mass of solids in one liter of mixed liquor from any given biological reactor. The MLSS is obtained by means of the Total Settlable Solids (TSS) test, which is the mass of solids obtained from a sample after drying at 105 ºC. In conjunction with this, the Volatile Settlable Solids (VSS) test is done, in which the

dried sample is combusted at 520 ºC for > 20 minutes. The remaining non-combusted mass is known as the Inorganic Suspended Solids (ISS). The VSS is the difference between the TSS and ISS (Standard Methods, 1985). The VSS gives the measure of how much organic mass. For the FTRW system, the measured VSS comprises only active biomass and endogenous residue because there are no particulates organics in the feed.

- **Sludge Age** (Mean Cell Residence Time/Solids Retention Time) originated in sewage treatment plants where the sludge age was required to be longer than a certain minimum number of days to ensure the slowest growing micro-organisms (usually the nitrifiers) are not washed out of the system. The sludge age (R_s) defines the mass of biomass that is harvested from the reactor as a fraction of the total mass of sludge in the system. If a sludge age of 10 days is required, then $1/10^{th}$ of the mass of sludge is wasted per day thus

$$R_s = \frac{M_{SludgeTotal}}{M_{SludgeWasted}} \quad [d] \qquad (3.2a)$$

Where

$M_{SludgeTotal}$ = Total mass of sludge in the system [gTSS]

$M_{SludgeWasted}$ = Mass of sludge wasted per day [gTSS/d]

If the sludge is wasted directly from the reactor then

$$R_s = \frac{X_t.V_r}{X_t.Q_w} = \frac{V_r}{Q_w} \quad [d] \qquad (3.2b)$$

Where

V_r = Reactor Volume [L]

X_t = MLSS concentration in the reactor [gTSS/L]

Q_w = Waste flow rate directly from the reactor [L/d]

Harvesting sludge from the system whether directly from the reactor or from the secondary settling tank underflow to control the reactor solids concentration is not sludge age control,

but sludge mass in system control. When controlling the reactor concentration, if the organic load on the system increases, the sludge age decreases. Sludge age control is equivalent only if the long term organic load on the system remains constant. Conversely, with sludge age control, the reactor MLSS is directly proportional to OLR, with reactor mass control, daily wastage volume is directly proportional to OLR.

For the AnMBR, sludge age is likely to be extremely long due to high reactor MLSS concentration required (12-18 gTSS/L) for membrane scour, and the very low net yield of anaerobic biomass (the combined effect from yield of growth and loss from endogenous respiration). Also sludge can be wasted only from the reactor so sludge age is established by wasting a proportion of the reactor volume.

- **pH** is one of the most important continuously measured parameters in the AD-FTRW system. This is because the anaerobic micro-organisms only operate optimally in a very narrow pH range around 7. So from an operational point of view, it is desirable to maintain the 6.8-7.5 pH in this range. Also from a modeling perspective, pH is normally the final and most important predicted output, since it is affected by the performance of the entire system. For these reasons, influent and effluent pH is checked on a daily basis and the reactor pH is measured continuously on-line. The pH electrodes that are used on both reactors are designed to measure pH on-line and can be submerged in mixed liquor for long periods of time.

- **The Biogas volume and composition** is required to close the COD and C a mass balances over any anaerobic system. Since the biogas production from either of the two systems can vary between 10 and 500 L/d, available laboratory gas measuring systems did not have adequate capacity. Therefore Ritter drum type wet gas flow meters with a accuracy of 0.02% and a capacity of 2-120 L/h were chosen for this application and the gas flow rate (Q_g) was recorded in L/d. Since most of the COD (>95%) exits the anaerobic process in the form of methane, the composition of the biogas is also required. 5 L biogas bags is connected to the biogas vent of each reactor and filled with biogas, to give an average biogas composition over the capturing period. The biogas samples are then analyzed with a gas chromatograph (GC1, Appendix 3.6) to give the fraction of methane, carbon dioxide and nitrogen (residual

air constituent) in the biogas sample. The percentage methane is given as $\%CH_4$ and the COD in the methane (S_{me}) as:

$$S_{me} = \frac{\left(Q_g.\%CH_4.64000\right)P_{atm}}{8314.T_k} \quad \text{[mgCOD/d]} \quad (3.3)$$

Where

P_{atm} = Atmospheric pressure [Pa]

T_k = Temperature [Kelvin]

Ideally, the hydrogen partial pressure in the gas phase P_{H2} should also have been measured to quantify the concentration of H_2 in the gas and liquid phase ($H_{2(aq)}$) in the system ($H_{2(aq)} = K_{H2}.P_{H2}$). However, the systems available for biogas analysis were not sensitive enough to measure the low P_{H2} in the gas phase and electrodes capable of measuring the dissolved H_2 concentration were regarded as too costly for this exercise.

- **Alkalinity Requirements** is the largest contributor to operating costs for the AD-FTRW system. FTRW is mostly un-dissociated SCFAs and it is very acidic, which makes the anaerobic process alkalinity deficient. However the FTRW does not need to be neutralized before it is digested because the anaerobic biomass utilizes undissociated SCFAs. Alkalinity only needs to be dosed to add sufficient buffer capacity for pH control. NaOH was chosen for pH control for economic reasons. The hydroxide converts weak acids existing in the system into weak bases ($H_2CO_3 + OH^- \rightarrow HCO_3^- + H_20$), thus even though NaOH cannot increase the system alkalinity by itself, the resultant effect of adding NaOH is an increase in alkalinity. Throughout this thesis, adding alkalinity implies adding NaOH. Because of its effect on operating cost, NaOH dosing needs to be optimized as far as possible. NaOH dosing is recorded in two ways; (i) as an equivalent concentration in the effluent:

$$NaOH_e = \frac{\left(Q_d.C_{NaOH}\right)}{Q_e} \quad \text{[mgNaOH/L]} \quad (3.4)$$

and (ii) as Specific Caustic Utilization (SCU), or mass of NaOH utilized per mass of COD loaded.

$$SCU = \frac{(Q_d . C_{NaOH})}{OLR} \qquad [\text{mgNaOH/mgCOD}_{\text{removed}}] \qquad (3.5)$$

Where

Q_d = the volume of buffer dosed per day [L/d]

Q_e = the effluent flow rate [L/d]

C_{NaOH} = concentration of the buffer solution. [L/d]

- **Nitrogen** (N) is the main nutrient required in the anaerobic process and is usually dosed in Free and Saline Ammonia (FSA) form (NH_4Cl) or as Urea ($(NH_2)_2CO$) the latter of which hydrolyses to HCO_3^- and $2NH_4^+$. FSA is required for protein synthesis and is therefore required at fairly high concentrations compared to the concentration of other nutrients such as phosphorous and trace metals (Section 3.5). The TKN, OrgN and FSA concentrations of the influent, effluent and mixed liquor is required to complete the nitrogen mass balance around the system. The FSA is analyzed by steam stripping NH_3 at high pH, which is turn, is condensed in boric acid and titrated against a standard acid. The TKN test includes a digestion step before steam distillation and so included the OrgN. The method is described in detail in Standard Methods (1985). The TKN/FSA test is fairly crude and can show a standard deviation of ± 10 %. Table A3.4, Appendix 3.4 gives a breakdown of how the various nitrogen fractions are obtained and characterized.

- **Phosphate** (P) is the second most abundant nutrient required by the anaerobic micro-organisms. However, since the ratio of N to P is kept constant in the nutrient mix, P is only analyzed as a cross reference to check the nutrient levels. Ortho and Total P is analyzed and recorded as mgP/L. The methods of analysis are given in detail in Standard Methods (1985).

- **Trace Metals** required for the optimal AD-FTRW can be seen in Table 3.1. Some of these needs to be present as macro nutrients (ppm range) and others are required only as micro

nutrients (ppb range). The analysis of metals in the effluent was done as required to ensure that all metallic compounds are present in the required amounts and not over or under dosed. Also, the trace metal analysis was done on the sludge mass to evaluate the C:H:O:N:P:S:Fe ratio of the sludge.

Details on the equipment required for analysis and data capture is presented in Appendix 3.6.

3.4 Operation

The following discussion focuses on the daily operation of the AnMBR and AnPBR. Unless specifically stated otherwise, the discussion applies to both the reactors. Both systems have visual 'health indicators' incorporated into the design which gives the experienced operator a quick indication of how the system is performing. This combined with analytical tests are used to judge the overall performance and health of the system.

The first of the visual health indicators (VHIs) is the bubbling of biogas that is vented through the pressure release valve. This gives a quick indicator of the activity and overall activity of the biomass. The gas bubbles through the water in the pressure release valve at a relatively constant rate (example; 100 bubbles/minute), if this bubbling rate slows down (<50 bubbles/minute), it is normally an early sign of problems. The reading on the biogas counter is then logged to quantify the volume of biogas produced each day. The methane fraction of the biogas is also checked on a weekly basis.

In both systems, the reactor pH is controlled with automated buffer dosing to near neutral pH. However, small fluctuations (±0.05 pH units) do still occur. The pH is also measured manually to act as a cross reference and check on the live pH output. An effluent sample is then drawn and a 5-point titration is done to give the alkalinity and SCFA concentration of the sample. If the effluent SCFA concentration is above a desired level (100 mgAc/L – AnMBR and 850 mgAc/L – AnPBR) the feed flow rate and resultant OLR is decreased. If the reactor SCFA decreases below the required level of 100 mgAc/L, the organic loading is again increased. In this way the reactor SCFA concentration dictates the OLR. This manual OLR control was done in parallel with the on-line control system. After the 5-pt titration test, 3 drops of 0.05 M $HgCl_2$ is then added to the sample after which it is refrigerated for COD, FSA, OrthoP and Suspended Solids (AnPBR) tests.

Unlike the AnPBR the membrane rector is a variable volume system. This is due to the interactions between TMP and membrane flux which governs the flow out the reactor. Hence the first VHIs that are logged on the membrane reactor are the mixed liquor and foam volume. This gives a good indication of membrane and biomass performance. If the membrane flux decreases due to foulants, less liquid will exit the reactor than enters it. This causes an accumulation and the liquid volume in the AnMBR will rise.

It was experimentally observed that a foam head on the mixed liquor would appear the moment NaOH dosing and membrane scour was started. Under stable operating conditions, the foam volume is about 10 % of the mixed liquor volume (in the current design), but if more NaOH is dosed than normal (due to high SCFAs) the foam level rises (experimental observation). Other factors that also increases foaming is biomass stress, for example under high hydrogen partial pressure.

Table A3.5 and A3.6 in Appendix 3.5 gives a representation of all the quantitative analysis done on the AnMBR and AnPBR respectively.

3.5 Feedstock

The primary feedstock fed to the AnMBR and AnPBR in this project is Synthetic Fischer-Tropsch Reaction Water (FTRW). However, to make FTRW amenable to anaerobic digestion, two secondary feedstock's are also required namely; (i) macro and micro nutrients for biological growth and (ii) alkalinity to maintain pH neutrality.

- **Synthetic FTRW's** composition is based on a 'worst-case-scenario' composition of actual FTRW. The assumption is that if an anaerobic system can be adapted to treat this synthetic FTRW with a certain level of stability, if would definitely be able to treat the normal plant runoff. Only species that contribute more than 1% of the real FTRW make-up was included in the recipe. The synthetic FTRW is made up in a stock solution (Table A3.7, Appendix 3.5) and in turn is diluted to18 gCOD/L. Since the mix consists mostly of $C_2 – C_6$ SCFAs, the pH is low (pH ~ 2.5) and alkalinity (1.4 g$NaHCO_3$/L) needs to be added to increase the pH of the synthetic FTRW to that of real FTRW (pH = 3.77).

- **Nutrients** required for optimal growth is the second part of the feedstock. It is based on that suggested by Du Preez et al. (1987), as can be seen in Table 3.1. The most prominent nutrients are Nitrogen (N), Phosphate (P), Sulfide (S), Iron (Fe), Magnesium (Mg) and Calcium (Ca), these are also known as macro-nutrients

Table 3.1, Original Un-optimized Nutrient Mix for FTRW

Species	Element	Concentration of Element [mg/L]
FTRW (COD)	COD	18000
Urea	N	250
KH_2PO_4	P	60
	K	130
$MgCL_2.6H_2O$	Mg	13
Na_2SO_4	S	23
$CaCl_2.2H_2O$	Ca	3
$FeSO_4.7H_2O$	Fe	11
Yeast Ext.		54
$MnSO_4.5H_2O$	Mn	0.2
$ZnSO_4.7H_2O$	Zn	0.33
$NiCl_2.6H_2O$	Ni	0.1
$CuSO_4.5H_2O$	Cu	0.15
$CoCl_2.6H_2O$	Co	0.02
$Na_2MoO_4.2H_2O$	Mo	0.007
H_2BO_3	B	0.009
KI	K	0.001

Micro nutrients include Copper (Cu), Zink (Zn), Manganese (Mn), Nickel (Ni), Cobalt (Co), Boron (B) and Molyboleneum (Mo). These nutrients are only required at ppb (µg/L) levels but are still of importance. Most of the metals in the macro and micro nutrients are added as salts of sulfate and thus the pH of the mixture needs to be lowered below 3 for these salts to dissolve. This is done with HCl. From the stock nutrient solution, 360 mL is added to 100 L

of feed to give adequate nutrient concentrations. Because of the high SCFA concentrations and low pH there is no growth in the feed container and influent pipes. It can therefore be kept at room temperature for days without decomposition. So the feed is made up in 200 L tanks and continuously stirred to ensure that the nutrients remain in solution. Both reactors are then fed from the same feed tank to ensure the exact same feed conditions.

- **The Alkalinity** required for pH control is NaOH, since this is what will be dosed at full-scale. The NaOH is made up to a concentration of 100 gNaOH/L in distilled water and dosed via a dosing pump to control the reactor pH to the desired set point (Section 3.1.4).

3.6 Closure

Two reactor systems were designed and constructed for the anaerobic treatment of Fischer-Tropsch Reaction Water, each in their own way an attempt to optimize both the (i) anaerobic environment and also (ii) solid liquid separation, to separate the biomass from the effluent. The first is a completely mixed anaerobic membrane reactor (AnMBR). This system is fitted with 3 200x300mm-size flat panel Kubota® membranes acting as a very fine filter (0.45 µm) to retain the biomass in the reactor but allowing the effluent to exit. The AnMBR uses a biogas recycle system in combination with a coarse bubble diffuser to induce mixing and membrane scour.

The second system is a down flow packed bed reactor (AnPBR). Plastic packing media provides surface area inside the reactor on which biomass adheres thereby retaining the biomass in the reactor, while treated effluent exits. Effluent is extracted from the bottom of the reactor. By means of a recirculation pump, some of the effluent is mixed with fresh influent and reintroduced at the top of the reactor. This has two main functions (i) to recycle alkalinity to the top of the reactor and in so doing protecting the biomass in the upper region from low pH and alkalinity conditions and (ii) to introduce a high down flow velocity of ~ 0.9 m/h for optimal mixing and reduction of media clogging.

The performance of the two systems will be compared on the basis of various parameters including COD removal and nutrient and alkalinity requirements, biogas production, biomass retention and most importantly effluent quality. The abovementioned parameters will be measured on a daily basis

over the test period. To make the results obtained from the system as comparable as possible, environmental conditions such as temperature were kept the same in both systems with temperature controllers (37 ^{o}C) and both systems were fed the same feed and nutrient mixture because they were fed from the same source. The feed is a synthetic FTRW and is made up from mixture of C_2 to C_6 short chain fatty acids and some methanol and ethanol. Synthetic FTRW is a highly acidic substrate (11 000 mgAc/L) and thus alkalinity deficient. To maintain the pH in the desired range for anaerobic digestion (6.8-7.5), alkalinity (NaOH) needs to be dosed from an external source. A nutrient mix is also added to the synthetic FTRW because FTRW is nutrient deficient. The nutrient mix consists of two parts; (i) micro nutrients required in the ppm range such as N, P, Fe, S & Ca and (ii) micro nutrients required only in the ppb range like Ni, Co, B, Mo etc.

CHAPTER 4

4. Results & Discussion

The results obtained in the feasibility study and performance evaluation of the laboratory-scale AnMBR are presented in this chapter. These results are separated into five sections namely; (i) commissioning and seeding, (ii) start-up, (iii) membrane performance, (iv) mixed liquor characteristics and (v) steady state performance evaluation and comparison to a control Anaerobic Packed Bed Reactor (AnPBR). The major focus of the commissioning was addressing 'teething problems' akin to; oxygen leaks, heating, foaming control and alkalinity dosing optimization. After this, the reactor was seeded with biomass obtained from a municipal anaerobic digester and start-up was commenced. The adaptation of the municipal anaerobic biomass to FTRW and its duration were observed.

During the first 100 days of start-up, virtually no biomass growth was observed; nutrient deficiency was braced to be the cause. This problem initiated a nutrient optimization investigation, in which the effects of various nutrients – and their optimal concentrations – were evaluated for the Anaerobic Digestion of Fischer-Tropsch Reaction Water (AD-FTRW). This was identified as one of the main research outcomes of the AnMBR performance evaluation.

Next was the performance evaluation of the flat panel membranes in the AD-FTRW environment. At the beginning of this study, virtually no literature could be found on AnMBR membrane performance and no estimations could be made as to how the membranes would respond to the AD-FTRW environment. Membrane performance and preliminary design guidelines in the AD-FTRW environment were identified as the second main outcome of the AnMBR study. Because of the lack of information the membrane surface area in the AnMBR was significantly oversized, 10 times greater than that required for an Aerobic MBR treating the same flow rate. Membrane performance factors that were evaluated include; (i) membrane fouling, (ii) chemical cleaning intervals, (iii)

membrane life span and most importantly; (iv) the Trans Membrane Pressure (TMP) - operational flux relationship for flat panel membranes in the AD-FTRW environment.

The third main research outcome is the performance evaluation of the steady state operation of the AnMBR. This was done by comparing the AnMBR with an existing AD-FTRW treatment technology for which there is some experience already, i.e. the down-flow Anaerobic Packed Bed Reactor (AnPBR). Both systems had similar operational volumes, environmental (laboratory) conditions and were fed the same FTRW to ensure that the results obtained from the systems were comparable. Performance criteria that were evaluated include effluent quality, sludge production, nutrient & alkalinity requirements and shock loading responses.

The total evaluation of the AnMBR performance was 685 days. The first 100 days was commissioning and also initiated the nutrient optimization study. The next 150 days was the first start-up. For 385 days after start-up, the membrane performance evaluation and the nutrient optimization was continued. Finally the steady state comparison was done during the last 50 days of the study.

4.1 Commissioning & Start-up

4.1.1 Inoculum & Seeding

The choice of inoculum for any anaerobic reactor has a significant effect on length of the start-up period. Choosing biomass with a high MLSS (> 5 gTSS/L), near neutral pH and low SCFAs (< 10 mgAc/L) normally ensures that the required anaerobic trophic groups are all present and active. The anaerobic biomass was obtained from a municipal anaerobic digester at a local treatment works in Cape Town (South Africa). This digester treated Primary Sludge (PS) and Waste Activated Sludge (WAS) originating at the municipal treatment works.

The sludge had an alkalinity of 900 mg$CaCO_3$/L, SCFA < 5 mgAc/L and a pH of 7.02, thus pointing towards a stable anaerobic biomass ideal for seeding of the AnMBR. The biomass was heated to 37 - ^{o}C and allowed to settle for 24 hours. The supernatant was then decanted and the AnMBR was then seeded with the settled biomass. The result was a start-up concentration of ~17 mgTSS/L (75% VSS). The high start-up biomass concentration was dictated by the design criteria of the flat panel

membranes. These membranes require an operational MLSS of 12 to 18 gTSS/L (based on the design criteria of activated sludge systems, Section 3.1.1).

4.1.2 Start-up Problems

A considerable amount of time (100 days) was spent on the mechanical optimization of the AnMBR before start-up could be commenced. This was done between the seeding and the actual start-up, but minor changes continued well into the evaluation period. The following section gives a breakdown of the major issues that were encountered:

- **Air leaks** into the AnMBR posed a significant problem because of the inhibitory effect of oxygen on the anaerobic biomass. Replacing the centrifugal-type compressor required for biogas recycle with a diaphragm-type compressor partially alleviated this problem. The second strategy was to seal all the connections on the recycle line and biogas venting system with a combination of silicon and hose clamps. Thirdly, a pressure release valve was incorporated into the biogas venting system to ensure the reactor operates at a slight positive gas pressure (20 – 200 mmH_2O) at all times. This would further ensure that if a gas leak does occur on the system, it would be from the reactor to the atmosphere and not vice versa. The result of these alterations was that the biomass in the AnMBR was completely protected from oxygen inhibition.

- **Heating** of the AnMBR to 37 ^oC is required to ensure optimal growth rates of the anaerobic biomass. Various systems were evaluated including; feed stream heating and heating coils around the reactor volume, but finally a 200 W fish-tank type heater with a on/off control system was accepted as best. The result was a reliable and easily operated heating system which controlled the reactor temperature stably at 37±1 ºC

- **Foaming** posed a major problem whenever the biomass underwent a stress conditions. These include; start-up, high reactor SCFA and Na^+ concentrations and temperature fluctuations. In extreme cases, the headspace volume would fill up with foam, enter the biogas recycle line and end up in the moisture trap before the biogas recirculation pimp. This had a deteriorating effect on reactor performance which added to the stress situation. The problem was overcome by (i) installing foam baffles above the membrane housing, (ii) increasing the biogas recycle

rate by 25% for 4 hours and (iii) avoiding known stress conditions. The result was a significant decrease in foaming problems from a foam volume of ~20 L above the liquid volume in the head space to ~2 L after the alterations.

- **Alkalinity** optimization also posed a major issue at the beginning of the project. Initially only $NaHCO_3$ was dosed to control reactor pH. However this proved problematic because a large amount of $NaHCO_3$ was required to maintain a neutral pH, since HCO_3^- is a weak base. This raised the Na^+ concentration in the reactor to such an extent that it became inhibitory to the anaerobic biomass (>3500 $mgNa^+/L$). After experimenting with combinations of $NaHCO_3$, $KHCO_3$, KOH and NaOH, it was found that a combination of $NaHCO_3$ and NaOH gave the best results. 1.46 $gNaHCO_3/L$ was added to the feed to up the pH (3.77) and alkalinity (800 $mgCaCO_3/L$) to that of actual FTRW. pH control was done via the dosing pump with a NaOH solution of 100 gNaOH/L. The result of the $NaHCO_3$-NaOH combination was a stable reactor pH with only minor variance (±0.05 pH-units) around the pH controller's set points (7 – 7.2).

4.2 AnMBR Start-up

The main question to be answered by the start-up investigation was: Can municipal anaerobic digester sludge acclimatize to (i) the AnMBR environment, (ii) FTRW and if so (iii) how long will this start-up period take? The start-up period was defined as the time from the last major alteration to the point where the OLR reached 15 $kgCOD/m^3_{Vr}/d$. Start-up was achieved after the commissioning stage and the initial nutrient requirement problems were eliminated. To acclimatize the anaerobic biomass to FTRW, initially a mix of 70% glucose and 30% acetic acid was fed, first at a low concentration and then gradually increasing up to 18 gCOD/L. Reaching 18 gCOD/L, the glucose and acetic acid was gradually replaced with FTRW. Thereafter the Organic Loading Rate (OLR) [$kgCOD/m^3_{Vr}/d$] of FTRW was increased by increasing the flow through the reactor, with the governing factor being an effluent SCFA < 150 mgAc/L. Figure 4.1 represents the first 300 days of operation.

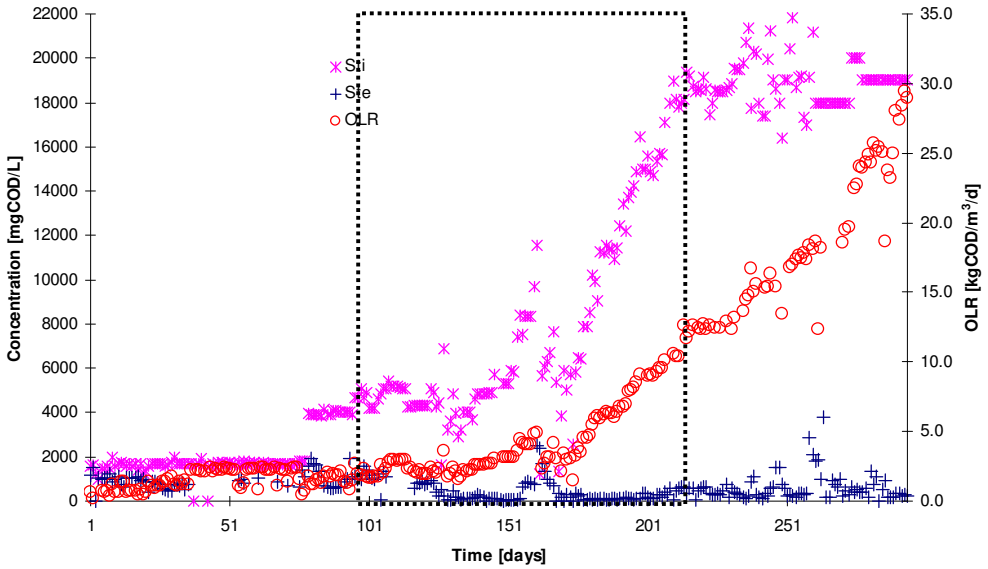

Figure 4.1, AnMBR Start-up: Influent (S_{ti})-, Effluent COD (S_{te}) and Organic Loading Rate (OLR) vs. Time

The last significant change made to the AnMBR was switching to the nutrient mix suggested by Du Preez et al. (1987) on day 121 of the experimental period. Before this change, no significant increase in the OLR was ever observed. However after the abovementioned change, a rapid increase was observed and the target OLR of 15 kgCOD/m^3_{Vr}/d was reached within 110 days. The time between the final nutrient change and the system reaching an OLR of 15 kgCOD/m^3_{Vr}/d is represented in the square in Figure 4.1 and is regarded as the actual start-up period. The OLR increase was continued and it was proven that the AnMBR can operate at OLRs of up to 30 kgCOD/m^3_{Vr}/d, if adequately controlled.

From this evaluation it was proven that municipal anaerobic digester sludge can adapt to the AnMBR and FTRW environment. This adaptation was so extensive that OLRs and Removal Efficiencies (RE) comparable to state-of-the-art anaerobic reactors such as EGSB and IC systems were observed. The start-up period was unnecessarily extended because of nutrient deficiencies and commissioning problems, but once these were solved, the system started up in less than 4 months. At a later stage of the project, the AnMBR was restarted with a biomass well adapted to FTRW and then a start-up time of only 25 days were observed (Appendix 4.1)

4.3 Nutrient Optimization

FTRW is a chemically created industrial wastewater with virtually no naturally occurring nutrients. For this reason the nutrients required for optimal biomass growth in the AnMBR had to be identified and added - and since nutrients are a significant contributor to operating cost – their individual concentrations had to be optimized. Initially only N and P were dosed (days 1 to 90, Figure 4.1), this was later supplemented by a nutrient mix optimized for biological phosphate removal (Wentzel et al., 1988). However it was not until the incorporation of macro and micro nutrients as suggested by Du Preez (1987) for the anaerobic digestion of acetic acid, that a significant increase in system performance was observed (day 120, Figure 4.1). This nutrient mix proved sufficient; however a significant concentration of N and P was measured in the effluent, which gave rise to questions on the further optimization of the Du Preez nutrient mix. This commenced the second phase of the nutrient optimization study, i.e. finding optimal concentrations of the various species in the nutrient mix.

These optimal concentrations were identified by varying the individual nutrient concentrations over extended periods of time (>30 days) to observe the effect on the system OLR. As discussed in Chapter 3, the OLR is a direct response of the reactor performance; if the effluent SCFA was high (> 150 mgAc/L; poor/deteriorating reactor performance) the OLR is decreased and if the effluent SCFA is low (< 150 mgAc/L; increasing/high reactor performance) the OLR is increased. The extraction of the effects of the individual nutrients on the OLR proved complicated. After much consideration the following approach was adopted: Since there are a large number of parameters that can have an effect on the OLR a high/low OLR at a high nutrient concentration does not give any valuable information. However, if the OLR remains low for an extended period of time - if a nutrient concentration is low - then the probability of this nutrient having an effect on the OLR is high. The effect of the low nutrient concentration was then confirmed by increasing it and observing its effect on OLR recovery. The individual nutrient concentrations vs. OLR are plotted for the entire 685 day dataset, as presented in Figure 4.2 for Sulfate (as S).

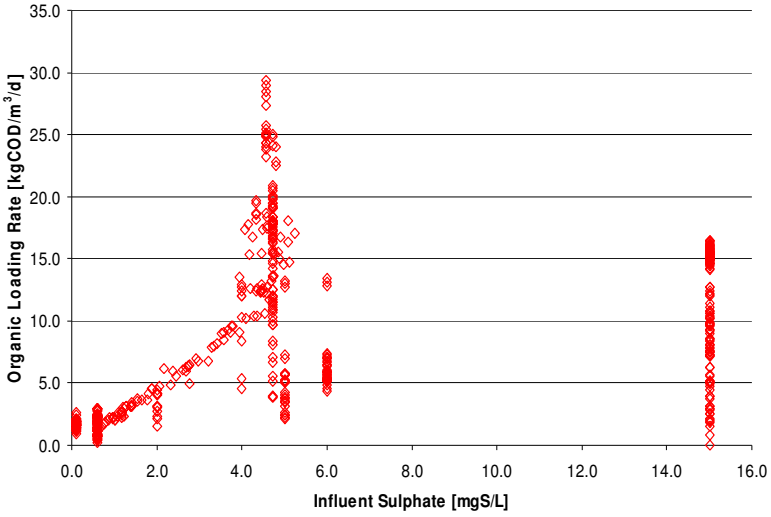

Figure 4.2, Influent Sulfate (S) vs. Organic Loading Rate (OLR)

For sulfate (as S), high OLR and a low (<4 mgS/L) influent S concentration were never simultaneously observed. However when a threshold value of 4 mgSO_4^{2-}-S/L was reached, the reactor performance increased rapidly.

Nutrients are required for biological growth, which means that the nutrients consumed forms part of the cell mass and MLSS of the reactor. However it was found that the actual concentrations of macro nutrients like Phosphates (P), Sulfide (S) and Iron (Fe) are so low in the MLSS that the nutrient requirements are virtually independent of sludge age. This further validates the individual-nutrient-concentration vs. OLR technique for nutrient optimization.

This optimization study was done for all the macro nutrients and also for yeast extract and the micro nutrient Nickel. The OLR-nutrient-concentration scatter plot for each of these species can be seen in Appendix 4.2. The results of this study are presented in Table 4.1. In contrast to other nutrients, anaerobic biomass does contain a significant amount (~10 %) of Nitrogen (N) and sludge age has a significant effect on the AD-FTRW system's N requirements. The relationship between influent nitrogen (N_{ti}) and sludge age can be expressed as:

$$N_{ti} = N_s + N_b = \frac{V_r.X_t.f_n}{R_s.Q_i} + N_b \quad (4.1)$$

Where

N_{ti}	= Influent Nitrogen Concentration	[mgN/$L_{influent}$]
N_s	= Influent N concentration that has become bound in the biomass harvested from the system per day	[mgN/$L_{influent}$]
N_b	= Minimum background liquid N concentration for uninhibited growth	[mgN/$L_{influent}$]
V_r	= Reactor Volume	[L]
X_t	= MLSS Concentration	[mgTSS/L]
R_s	= Sludge Age	[d]
Q_i	= Influent Flow Rate	[L/d]
f_n	= Nitrogen Fraction in Biomass	[mgN/mgTSS]

N_b is the minimum "back ground" concentration for uninhibited N uptake by the anaerobic biomass. Unfortunately, nitrogen was always dosed in excess to the AnMBR, so the N_b concentration could not be quantified. However, from earlier research done on the pilot-plant AnPBR it would appear that a N_b = 25 mgN/L is required (Table 4.1). Correspondingly, for a 23 L reactor volume, 25 gTSS/L solids concentration, 300 day sludge age and an influent flow of 23 L, the influent nitrogen (N_{ti}) should be ~50 mgN/L.

Table 4.1, Optimized Nutrient Concentrations for the AD-FTRW

Influent Nutrient	Abbre-viation	Du Preez Nutrients' Concentration [mg/L]	Optimized Concentration [mg/L]
Nitrogen	N_{ti}	252	$[V_r.X_t.f_n]/[R_s.Q_i] + N_b$
Phosphate	P_{ti}	57	10.0
Sulfate	SO_4-S_{ti}	23	4.0
Calcium	Ca_{ti}	3	<1
Magnesium	Mg_{ti}	13	<1
Yeast Extract		54	<1
Iron	Fe_{ti}	11	1.0
Nickel	Ni_{ti}	0.002	<0.001

If the 'Du Preez nutrients' is compared to the nutrient requirements optimized for the ADMBR is compared, it is can be noted that the optimized nutrients are significantly lower in all of the cases. A possible reason for this is very long sludge ages (>100 days) and resultant low sludge wastage on the ADMBR, this will be discussed in detail in Chapters 5 and 6. The nutrients N, P, S and Fe are of primary importance for the AD-FTRW and should be dosed as macro nutrients. In contrast, the study has shown that Ca, Mg, and Yeast extract are not required as macro nutrients. Even at µg/L levels, Nickel (Ni) does not seem to have any effect on the reactor performance.

4.4 Mixed Liquor: Operational Concentrations and Characteristics

In aerobic membrane reactors, the upper limit of the mixed liquor concentration (up to18 gTSS/L) is governed by the alpha values of oxygen transfer i.e. the ratio of the mass oxygen transfer rate (kgO_2/h) in the activated sludge reactor vs. that of clean water (Ramphao et al., 2004). In anaerobic reactors, where oxygen transfer is not required, because the upper limit of the Mixed Liquor Suspended Solids (MLSS) and the factors that govern this limit is not yet defined.

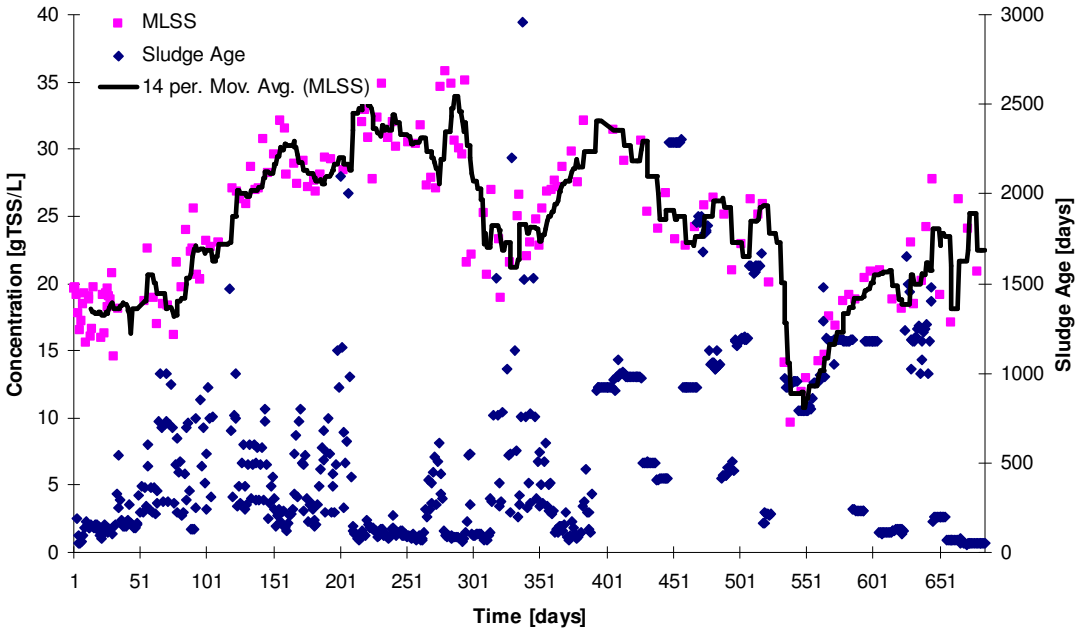

Figure 4.3, MLSS & Sludge Age vs. Time

In the AnMBR, the MLSS concentration was allowed to increase gradually up to 30 gTSS/L; the system was allowed to operate at this concentration for approximately 100 days with no adverse effects on membrane performance (Figure 4.3). The MLSS was then increased to a maximum of 36 gTSS/L. The MLSS was typically 91% VSS. The long sludge age is due to the very low net biomass yield of the acetoclastic methanogens, the most abundant trophic group in the system. The sludge settleability in terms of the Dilute Sludge Volume Index (DSVI) of the sludge mass was around 3000 mL/g. The DSVI is defined as the volume that 1g of sludge occupy after 30 min of settling in a 1 L measuring cylinder (Marais and Ekama., 1984) At the MLSS concentration of ~30 gTSS/L, it does not settle at all

One of the major questions on the AnMBR performance that required addressing was how the membrane flux and TMP relationship responded to a change in MLSS concentration. Figure 4.4 depicts this relationship.

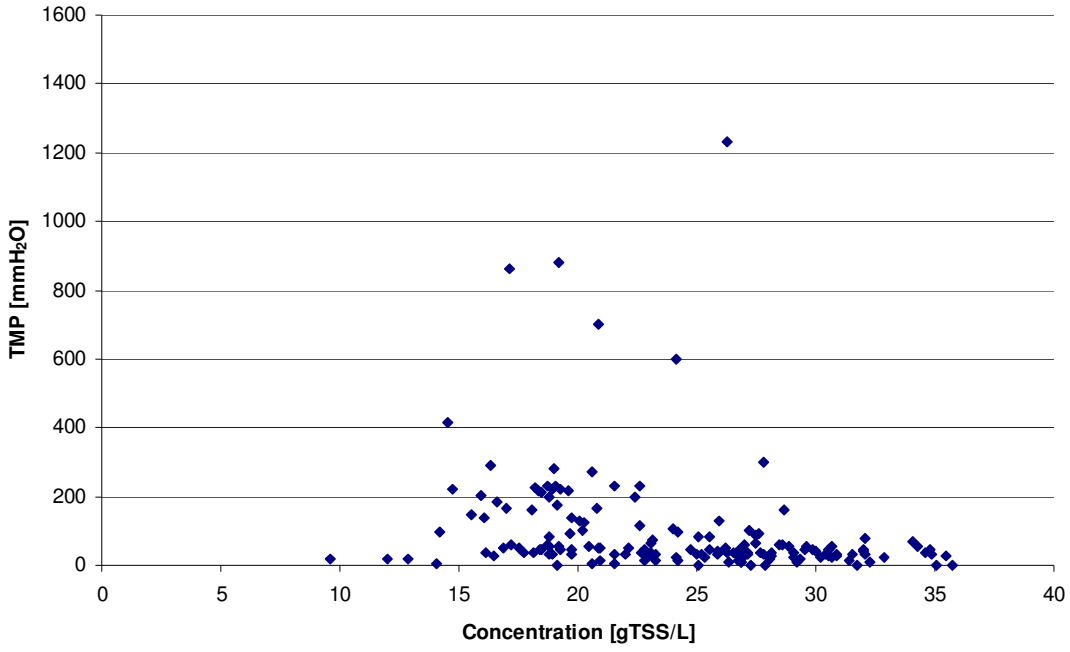

Figure 4.4: Trans Membrane Pressure vs. MLSS

No correlation between TMP and mixed liquor concentration can be found, even for MLSS's of as high as 35 gTSS/L.

4.5 Membrane Performance

The evaluation of the flat panel membranes in the AD-FTRW environment with biogas recycle for membrane scour is one of the primary objectives of this research project. Since membranes are a major contributor to capital costs, design criteria are needed for; (i) optimal operational flux, (ii) membrane fouling causes and affects (iii) intervals between chemical cleaning and (iv) membrane life span. The membrane performance was evaluated throughout the 685 day test period.

4.5.1 Membrane Fouling

Membrane performance was primarily evaluated on the Trans Membrane Pressure (TMP) required to maintain a desired flux (Section 2.5.6). If the TMP increased significantly for a constant flux, the possibility of membrane fouling was investigated. Figure 4.5 gives the membrane flux vs. TMP for the observational period.

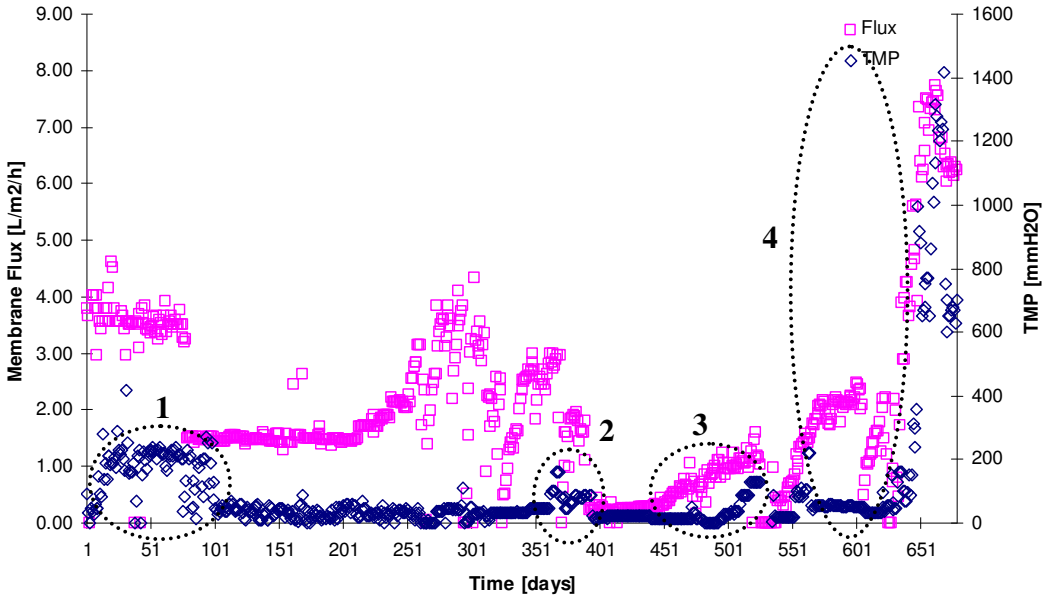

Figure 4.5, Membrane TMP & Flux vs. Time

Four possible instances of membrane fouling were identified. The first (Figure 4.5, 1) was observed for the first 100 days, the problem was gas bubbles trapped in the effluent collector. These bubbles

obstructed the effluent flow out the AnMBR thus increasing the TMP. The problem was rectified by modifying the effluent collection system so that the gas bubbles and effluent can exit the reactor without obstruction. No chemical clean was done on the membranes to restore the TMP to < 50 mmH_2O.

The second fouling instance (Figure 4.5, 2) occurred between day 363 and 395. The problem was an inorganic foulant in the form of rust. The rust entered the system via the feed, because a mild steel mechanical stirrer shaft in the feed tank was corroded by the FTRW. A 90% decrease in membrane performance was experienced in less than 48 hours. The biomass was drained and the membranes rinsed with tap water, their recovery was full. No chemical clean was done. Fortunately, only rust resistant materials are used on full-scale to convey FTRW, therefore this will not pose a major problem on full scale. However, coalescers and primary clarifiers will be incorporated into the full scale design to avoid membrane fouling by oils, greases and precipitates.

Because no sensible means of separating the particulate rust and the organics could be found, the AnMBR was reseeded with municipal digester sludge and restarted (day 400). During the second start-up, full strength FTRW was fed, resulting in a very low flux through the membranes for a significant period of time (50 days). When the flux started to increase with an increased OLR a sharp increase in TMP was observed (Figure 4.5, 3). When the problem was investigated, nearly the entire internal surface area of the 3 membranes was covered in a biological growth. The biomass was drained from the AnMBR and the membranes were cleaned with a 5% hypochlorite solution.

4.5.2 Critical Flux

The fourth instance of membrane fouling was at the end of the test period (day 625 – 685), where the Flux-TMP relationship was investigated in greater depth (Figure 4.5, 4). Up to this stage of the investigation, there were 3 membrane panels in the reactor. This resulted in low fluxes, because the solids liquid separation behavior of the biomass was not known. To increase the flux, two of the three membranes were blocked off to observe the TMP vs. flux relationships at higher flow rates. This relationship is depicted in Figure 4.6, which is a scatter plot of the TMP vs. flux data for the entire evaluation period, including the period with only 1 membrane panel in operation.

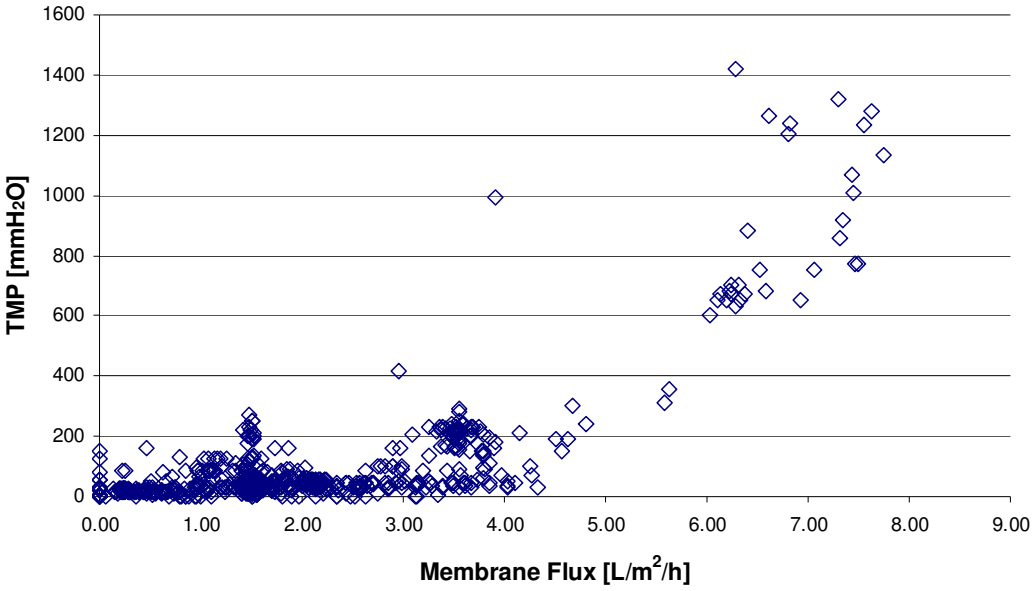

Figure 4.6, Membrane Flux vs. Trans Membrane Pressure (TMP)

For fluxes below 4.3 L/m^2/h no correlation can be found between TMP and flux. However, when the flux increased over 4.3 L/m^2/h (0.1 m/d), a sharp increase in the TMP was observed. Increasing (+100%; 500 L/h) or decreasing (-50%; 125 L/h) the scouring rate over the membranes had no notable effect on this increase in flux. The only means of recovering TMP was to lower the flux below the 4.3 L/m^2/h value. If this was done, the TMP would drop to normal (20 – 150 mmH_2O) within 24 hours.

4.5.3 Membrane Life Span & Permanent Fouling

Nonpermanent membrane fouling can be removed by rinsing/back-flushing or chemical cleaning of the membranes. The second process of membrane fouling is known as permanent fouling. In this case, precipitates block the membranes to such an extent that it is chemically bound to the membrane surface. This permanently reduces the flow through the membranes. The permanent fouling rate dictates the life span of the membrane, the slower this permanent fouling the longer the period of time before the membranes needs replacing and vice versa.

The permanent fouling rates were measured by (i) draining the AnMBR biomass and filling the reactor with clean tap water and (ii) doing a chemical clean on the membranes to ensure all

nonpermanent fouling was removed. (iii) The biogas recycle is set to 750 $L/m^2_{membrane\ surface}/h$ as suggested by Kubota® for aerobic systems to induce gas up-flow velocity of 0.5 m/s. Then (iv) tap water fluxes were measured at various TMPs. The (v) slope of this TMP vs. flux relationship was then compared to that of earlier tap water TMP vs. flux tests. The closer this slope is to 1, the lower the TMP required for a given flux and the better the membrane performance. This test is severely disruptive to the biomass activity in the AnMBR, since the reactor has to be drained completely, so it was only done twice during the 685 day investigation.

The first permanent fouling test was done before commissioning the AnMBR. The aim was to form a basis for comparison of membrane performance and deterioration over the evaluation period. It was found that the TMP vs. flux correlation for tap water was directly correlated and the initial tap water flux test is given by line 1 on Figure 4.8.

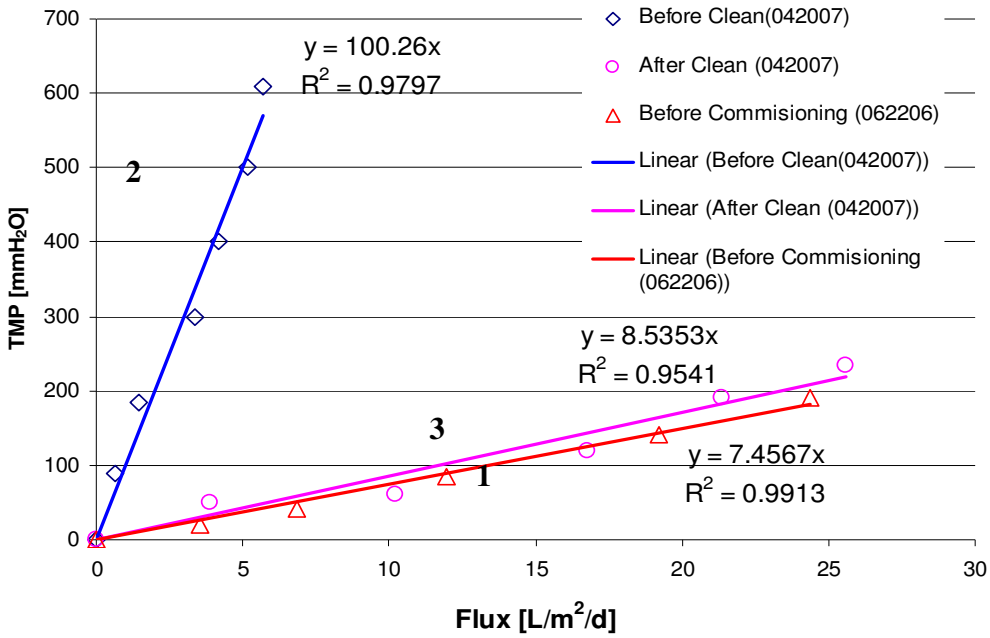

Figure 4.7, Tap Water Flux Tests

The second permanent fouling test was done on day 530 when biological fouling was observed on the membranes (Figure 4.5, 3). The AnMBR was drained and filled with tap water, a TMP vs. flux tests was done before (Figure 4.8, 2) and after (Figure 4.8, 3) a chemical clean. The difference in the

slope of line 2 and 3 on Figure 4.8 gives an indication of how effective the hypochlorite chemical clean is.

Comparing line 1 and 3, it can be seen that the change in flux through the clean membranes changed very little over the 530 days between the two chemical cleans. From the data in Figure 4.8, at a flux of 15 L/m^2/h (0.35 m/h), the TMP increased from 15/0.1336 = 112 mmH_2O to 15/0.1152 = 130 mmH_2O in 530 days. This is 18/530 = 0.034 mmH_2O/day permanent fouling. In the activated sludge (AS), this permanent fouling rate at an operating flux of 10-15 L/m^2/h was around 0.1 mmH_2O/d (Ramphao et al. 2004). Based on this observation it would appear that the permanent fouling rate of activated sludge is at least twice that of the AnMBR; however the operating flux of the AnMBR at 4.3 L/m^2/h was significantly below that of the AS system (10 – 15 L/m^2/h). If a 50 % decrease in flux is allowable before membrane replacement this data points to a membrane life span in the AD-FTRW environment of at least 7 years (Appendix 4.3). However, it should be emphasized that this prediction is an extrapolation from a small dataset (2 tap water flux tests) and relatively short period of investigation. The investigation of permanent fouling of flat panel membranes in the AD-FTRW environment probably merits as significantly larger dataset and evaluation period to yield a concrete prediction of membrane life span. Note; because lines 1 and 3 lies close to each other, a t-test was done to verify if these lines are in fact statistically deferent, which the case was indeed.

4.6 AnMBR Steady State Performance Evaluation

To get a quantitative measure of the AnMBR's performance it was compared to a control reactor treating the same feed under the same laboratory conditions. The control reactor was a down-flow Anaerobic Packed Bed Reactor (AnPBR). Both systems were allowed to reach steady state after which a dataset of 35 days each were captured. The complete steady state datasets can be seen in Appendix 4.4. The sections below present the results obtained.

4.6.1 Effluent Quality

The comparison of the AnMBR effluent quality with that of other AD-FTRW treatment systems is one of the primary outcomes of this research project. The effluent quality produced by the first step of a water treatment system dictates the size – and thus capital and operating costs – of the downstream processes. The effluent quality comparison was done by evaluating the average and variance of the effluent concentrations of the two systems over the 35 day steady state period. The

effluent evaluation criteria was total COD (S_{te}), particulate COD (S_{pe}), dissolved COD (S_{se}), Total Settlable Solids (X_{te}), Short Chain Fatty Acids ($SCFA_e$) and Total Nitrogen (N_{te}). Daily samples were taken for both the AnMBR and AnPBR with the average values and 95% confidence intervals (CI95%) represented in Table 4.2. The 95% confidence interval is that range of variance around the mean in which 95% of the data points are distributed.

Table 4.2, AnMBR & AnPBR Steady State Comparison

Parameter	AnMBR		AnPBR		Units
	Avg	CI95%	Avg	CI95%	
Reactor OLR	15.3±0.15		15.2±0.28		kgCOD/m^3/d
Reactor Volume	23±-		23±-		L
Reactor Temperature	37±1		37±1		^oC
Reactor pH	7.08±0.05		7.11±0.05		
Reactor MLSS	20.2±0.37				gTSS/L
Reactor MLVSS	15.4±0.28				gVSS/L
Sludge Age	61±3.6				d
Influent COD	18500±-		18500±-		mgCOD/L
Influent Alkalinity	875±-		875±-		mg$CaCO_3$/L
Influent N	84±-		84±-		mgN/L
Effluent Total COD	35.1±6		1749±91		mgCOD/L
Effluent Particulate COD	0.0±-		768±80		mgCOD/L
Effluent TSS	0.0±-		512±266		mgTSS/L
Effluent Alkalinity	2213±29		3031±107		mg$CaCO_3$/L
Effluent N	37.6±3.2		35.7±30		mgN/L
Effluent SCFA	10.41±4.8		775±30		mgAc/L
Effluent Na	1441±188		1997±289		mgNa/L
Specific NaOH Consumption	0.067±0.01		0.11±0.02		kgNaOH/$kgCOD_{removed}$
COD Removal Efficiency [%]	99.81		90.55		[$kgCOD_{in}$*100/$kgCOD_{out}$]
Biomass Production	7.57		10.60		gTSS/d
N Consumption	0.003		0.0029		kgN/$kgCOD_{removed}$

For virtually identical influent concentrations and reactor loading and environmental conditions, the AnMBR effluent COD (S_{te}) is more than an order of magnitude lower than that of the AnPBR. If the particulates (S_{pe} and X_{te}) are compared, the AnMBR yields virtually zero value, where this is a significant contribution (43 %) to the COD in the AnPBR effluent. Because of the low effluent

COD, the Removal Efficiency (RE) of the AnMBR is significantly higher (by 9 %) than that of the AnPBR. Biomass production and nitrogen consumption are both 30 % lower in the AnMBR than in the AnPBR.

4.6.2 Alkalinity Requirements

FTRW is an acidic, alkalinity deficient industrial effluent. To provide buffer capacity for anaerobic digestion at neutral pH, a significant amount of alkalinity is required. This alkalinity requirement is the main operating cost of any AD-FTRW treatment system. For this reason, the steady state alkalinity consumption of the AnMBR and AnPBR was evaluated. Figure 4.9 displays the Specific NaOH consumption for the 35 day steady state evaluation period.

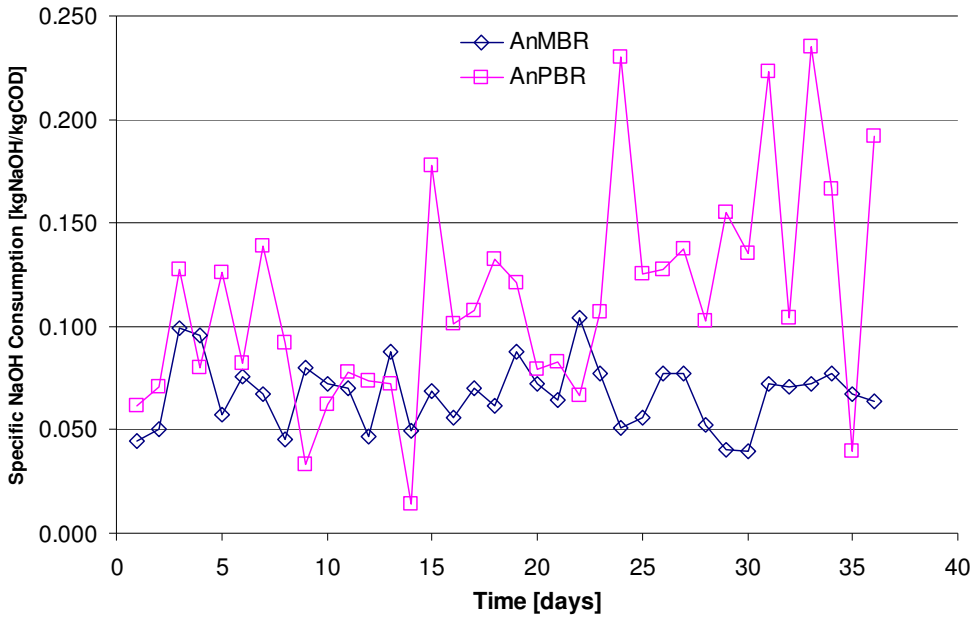

Figure 4.8, AnMBR & AnPBR Specific Alkalinity Consumption vs. Time

From Figure 4.9 it can be noted that the Specific NaOH consumption which reacts with CO_2 to from HCO_3^- of the AnMBR is consistently lower than that of the AnPBR. The average for the AnMBR over the evaluation period is 0.067 kgNaOH/kg$COD_{removed}$ (Table 4.2), which is nearly 30% lower than that observed in the AnPBR. The effluent NaOH concentration was also proven to be in the order of 25 % lower in the AnMBR.

4.6.3 Shock Loading Responses

When a biological water treatment system undergoes a period of stress due to a shock load, the biological activity can decrease, particularly with the acidic FTRW which can depress reactor pH and cause acetoclastic methanogen inhibition. When this happens, the system needs to be operated at reduced OLR until the biomass activity recovers and a low effluent SCFA (< 150 mgAc/L) concentration is again achieved. During this 'down-time' the wastewater that cannot be treated needs to be stored or treated by another means, both having significant cost implications. Shock loading responses of the AnMBR and AnPBR were therefore observed and compared.

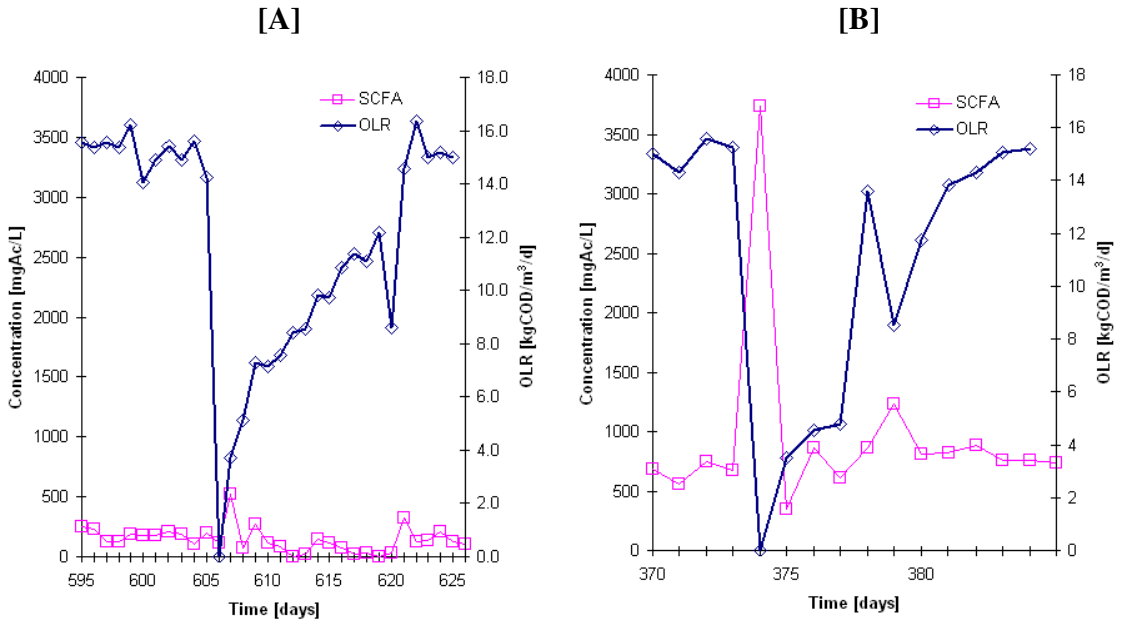

Figure 4.9: AnMBR [A] and AnPBR [B] shock loading responses.

Shock loads were imposed on both systems after a period of steady state operation. Note the on-line control system was deactivated for this part of the study. The shock loads were introduced by increasing the feed flow rate to the reactor. In this overloaded state there is not enough active biomass to remove the SCFAs introduced by the FTRW in the feed. Thus an accumulation of SCFAs occurs in the reactor. If the SCFAs go above a maximum value - 800 mgAc/L in the AnMBR and 1600 mgAc/L in the AnPBR – the pH decreases below 6.8 which has an inhibitory effect on the anaerobic biomass resulting in a reduction in activity. If this happens the flow rate to the reactor needs to be decreased or stopped completely, depending on the severity of the overload. This allows

time for the biomass to utilize the excess SCFAs which in turn increases the pH (and alkalinity). If after 24 hours, if the effluent SCFA is below the required minimum (150 mgAc/L), the OLR can be increased; if higher, it must be decreased. This procedure allows the system to recover from shock loads. Figures 4.10A & B show the shock loading responses of the AnMBR and AnPBR respectively.

In both reactors the OLR overload was ~15 % of the steady state value, in the case of the AnMBR (day 604 to 605), a sharp increase in SCFAs was observed within the first 24 hours and the feed was stopped (Day 606). In the AnPBR (day 372 to day 374) the overload only became apparent after 48 hours and the feed was immediately stopped (Day 374). The SCFA increase in the AnMBR was significantly (60%) smaller than that of the AnPBR system and the recovery time of the AnMBR was 15 days compared to only 10 days for the AnPBR.

4.7 Closure

Commissioning and nutrient problems caused an unnecessary initial lag in the start-up of the AnMBR. However, after the correct nutrients were added the OLR increased from 2 to the desired steady state value of 15 kgCOD/m^3_{Vr}/d in less than 4 months. This gave an indication of the start-up period of an un-adapted municipal anaerobic biomass to treat the very specific FTRW.

From the nutrient optimization done after start-up it was found that N, P, S and Fe is of primary importance in the AD-FTRW system and should be dosed as macro nutrients. Yeast extract, Ca and Mg is of secondary importance and can be dosed as micro nutrients along with other micro nutrients as suggested by Du Preez (1987).

In the membrane performance evaluation it was found that inorganic foulants can be removed by merely rinsing and back-flushing the membranes. However, for biological foulants, a chemical clean is required. Membrane life span was estimated at longer than 7 years, but conclusive results will require an investigation period significantly longer than the 680 days of this investigation. A critical flux of 4.3 L/m^2/h was identified. At fluxes higher than the critical, biological cake layer formation cannot be controlled by biogas scour and excessively high TMPs (>1000 mmH_2O) are required to maintain flux. The low critical flux observed in the AnMBR is probably due to the accumulation of extra cellular polymers and/or endogenous biomass in the MLSS due to the very long sludge ages (> 500 d). However, conclusive evidence that supports this could not be found and thus requires further investigation.

The AnMBR effluent is free of particulates and TSS compared with the AnPBR where 43 % of the effluent COD is in particulate form. Furthermore the total COD of the AnMBR is only 2% of the total effluent COD of the AnPBR at an OLR of 15 kgCOD/m^3/d. This result would be a significantly reduced operating and capital cost for the downstream processing system of the AnMBR. The membranes act as a positive barrier retaining biomass in the AnMBR. Because of this and the long sludge age, the dead biomass in the reactor gets hydrolyzed and is reintroduced as substrate to be utilized by the anaerobic biomass (Chapter 5 and 6). This re-utilization of biomass results in a 30% lower sludge production - and hence sludge incineration cost - compared with the AnPBR.

The main operating cost in anaerobic systems treating acidic wastewater is the alkalinity dosing cost. Because of the high effluent SCFA and slightly higher reactor pH of the AnPBR, the alkalinity consumption of this system was 25% higher than that of the AnMBR under the same operating conditions. The AnPBR can handle significantly greater shock loads of the AnMBR (3 times higher) and also shows a 30% shorter recovery period before complete recovery (low effluent SCFA concentration). From an operational point of view it was also found that the AnPBR was far easier to operate and control than the AnMBR. Thus to avoid system upsets and loss of productivity an inline control system will be required to operate the AnMBR.

The AnMBR study has indicates that a steady state design loading rate of 25 kgCOD/m^3/d can be maintained, compared with 8 kgCOD/m^3/d for the AnPBR. This implies a 3 times smaller reactor volume than required with the AnPBR for the same organic loading. This and the significant savings capital and main operating costs namely; alkalinity (25%), sludge incineration (30 %) and downstream processing (± 95%), indicates that the AnMBR might be a financially competitive treatment option for FTRW. This statement appears to be true, even in the light of high ultra filtration membrane costs and more complex control strategies.

CHAPTER 5

5. Steady State Modeling

"The making of a mass balance is essential in the design of biological treatment systems in order to establish the necessary quantity of material inputs into systems, such as nutrients and oxygen, and to evaluate the resulting quantity of material outputs, such as waste biological sludge, carbon dioxide and methane. One of the easiest and most direct ways to begin a mass balance is to write a balanced stoichiometric equation for the overall reaction occurring in the system."

– **Perry L. McCarty, 1974**

The aim of Chapter 5 is to develop a full conversion stoichiometric model for Anaerobic Digestion of Fischer-Tropsch Reaction Water (AD-FTRW). This full conversion stoichiometric AD-FTRW model will be calibrated on steady state data. The model, hereon forth referred to as the 'steady state model' will be generally applicable, in that it will be able to predict the process products formed from the anaerobic digestion of any biodegradable substrate of known composition. In this case, the biodegradable substrate will be FTRW, a highly acidic, low alkalinity, nutrient deficient petrochemical waste water. The use of this model will be reactor design for *inter alia* the prediction of (i) mixed liquor organic concentration (MLVSS) or reactor volume, (ii) reactor operational pH or alkalinity requirements, (iii) nutrient requirements and (iv) biogas production and composition.

These model outputs are dependant on the reactor sludge age (R_s), organic loading rate (OLR, kgCOD/m^3_{Vr}/d), influent pH and the composition of the biodegradable organics (x, y and z in $C_xH_yO_z$) in the wastewater. The steady state AD-FTRW model is different from its steady state Anaerobic Digestion of Primary Sludge or Waste Activated Sludge (AD-PS/WAS) predecessors in a number of respects: (i) separation of sludge age and hydraulic retention time allowing solids

retention, (ii) influent comprising mostly SCFA with a (iii) low pH requiring alkalinity dosing to maintain a reactor pH >7.0, (iv) nutrients (N & P) required from an external source.

Anaerobic digestion of organics requires a consortium of four organism groups, viz. (i) acidogens (Z_{ad}), which convert complex organics to glucose and then to acetic (Ac) and propionic acid (Pr), carbon dioxide (CO_2) and hydrogen (H_2), (ii) acetogens (Z_{ac}), which convert propionic- to acetic acid and H_2, (ii) acetoclastic methanogens (Z_{am}), which convert acetic acid to CO_2 and methane (CH_4) and (iv) hydrogenotrophic methanogens (Z_{hm}), which convert H_2 and CO_2 to CH_4 and water (Mosey, 1983; Massé and Droste, 2000; Batstone et al., 2002; Sötemann et al., 2005). A more detailed discussion on this stepwise decomposition of complex organics is presented in Appendix 5.1.

The two methanogenic groups are very sensitive to pH and so the acetogens and acetoclastic methanogens must utilize the Ac and Pr respectively as soon as they are produced to maintain a near neutral pH for optimal operation. The hydrolysis/acidogenesis process mediated by the acidogens ((i) above), is the slowest process in the system, so for sewage sludge high SCFA concentrations and therefore low pH, arise only under unstable and digester upset operating conditions caused by a shock load in organics, a rapid temperature fluctuation or an accumulation of an inhibitory metabolic intermediate such as dissolved hydrogen gas ($H_{2(aq)}$). A steady state AD-PS/WAS model, therefore need only consider the kinetics of this process (Vavilin et al., 2001) - the processes following hydrolysis/acidogenesis, being much more rapid (usually), can be accepted to reach completion. This implies that in stable sewage sludge anaerobic systems the intermediate products of the processes following after hydrolysis/acidogenesis such as SCFAs and H_2, do not build up in the system and their concentrations are sufficiently low to be considered negligible.

Consequently, in the full conversion stoichiometric anaerobic digestion model, the products of hydrolysis/acidogenesis can be dealt with stiochiometrically and converted to digester end products. In effect, it can be assumed that the hydrolysis/acidogenesis process generates directly the digester end-products biomass, CH_4, CO_2 and water (Appendix 5.2). In conformity with this, the steady state AD-PS/WAS model of Sötemann et al. (2005) comprises three sequential parts: (i) a COD based kinetic part from which the influent COD concentration hydrolyzed, methane gas COD, biomass COD production and the effluent COD concentrations are determined for a given sludge age, (ii) a

C, H, O, N, charge and COD mass balance based stoichiometry part from which the gas production and composition (or partial pressure of CO_2), ammonia released and alkalinity generated are calculated from the COD concentration hydrolyzed and its x, y, z and a composition in $C_xH_yO_zN_a$ of the biodegradable organics, and (iii) a carbonate system weak/acid base chemistry part from which the pH of the digester is obtained from the partial pressure of CO_2 and alkalinity generated.

By assigning an average composition to the most prominent biodegradable organics in the feed ($C_xH_yO_zN$), the metabolic end products including CO_2, CH_4 and biomass can be predicted (McCarty 1974, Rodríguez et al., 2005, Sötemann et al., 2005). Unlike dynamic simulation anaerobic digestion models, steady state models cannot predict; inhibition, response to organic over-loading and digester failure, but steady state results correlate well with dynamic model predictions under steady flow, organic load and sludge age conditions. Steady state models are (i) more practical for design, because they allow reactor sizes to be simply calculated from specified system performance criteria in a spreadsheet and (ii) provide a basis for crosschecking for simulation model outputs and (iii) can generate consistent initial predictions for dynamic simulation models, such as biomass concentrations and reactor volumes (Brink et al., 2007).

The steady state AD-FTRW model developed in this chapter is an extension of its predecessors to account for the high acidity, and alkalinity and nutrient deficiencies of the wastewater under study (FTRW). The model will be calibrated on a 35-day steady state experimental data set obtained from the lab-scale Anaerobic Membrane Reactor (AnMBR) treating synthetic Fischer-Tropsch Reaction Water (FTRW) as discussed in Chapter 4. Ideally the steady state AD-FTRW model should have been validated against a second steady state experimental dataset collected on the AnMBR, but due to the extremely long sludge ages required to maintain a high enough MLSS for membrane performance, complete steady state was virtually impossible to achieve, as will be seen later. Because of this, the calibrated model's outputs will be validated against two 200-day dynamic flow and load datasets, one from the AnMBR and the other from an Anaerobic Packed Bed Reactor (AnPBR). The aim of evaluating the steady state AD-FTRW model's predictions against "non-steady" experimental data is to highlight the strengths and possible shortcomings of the model. Both AnMBR and AnPBR systems treated the same feed (synthetic FTRW) under mesophillic (37^oC) conditions (Section 3.5).

5.1 Steady State Model Development

The steady state AD-FTRW model will be developed in 3 parts: (i) a kinetic part in which the fraction of the organics entering the system that ends up as biomass (E) is estimated by means of a COD mass balance over the system; (ii) a stoichiometric part which links the E value calculated in the kinetic part to the catabolic and anabolic pathways followed in anaerobic digestion and (iii) a Weak Acid/Base Aqueous Chemistry (WABC) part based on the carbonate system to calculate reactor pH.

5.1.1 Kinetic Part

In steady state models the organism growth process is governed by the slowest step in the sequence. For sewage sludge digestion, this was the hydrolysis/acidogenesis step. With FTRW, all the influent organics are readily biodegradable and do not require hydrolysis. The rate of utilization is therefore very fast, especially at long sludge ages, which will be required to provide bio-process stability and capacity to absorb small variations in Organic Loading Rates (OLR). The rapid rate of utilization will result in virtually complete consumption of influent organics, which was in fact observed to be the case in the experimental AnMBR (99.8% COD removal) (Section 4.6.1). It can therefore be assumed that all the influent organics are completely utilized by three groups of anaerobic organisms, acetogens (Z_{ac}), acetoclastic methanogens (Z_{am}), and hydrogenotrophic methanogens (Z_{hm}), with the result that kinetics of the growth processes are not required in the steady state model – they can be assumed to be instantaneous. The effluent COD concentration (S_{be}) will be assumed zero for this steady state AD-FTRW model.

The three groups of organisms undergo endogenous respiration in the reactor. This endogenous process generates biodegradable particulate organics (S_{bp}) which will undergo hydrolysis/ acidogenesis (Z_{ad}) to produce acetic acid and hydrogen. So while no acidogens grow from the influent organics, they will nevertheless be part of the biocenosis, and undergo endogenous respiration themselves also. Because the endogenous process is very slow ~0.04/d for all four organism groups, the acidogens will be a small proportion of the total biomass. Even though the rate of hydrolysis of biomass complex organics is slow compared with the growth rate, the generation rate of these organics by endogenous respiration is much slower than hydrolysis, i.e. the endogenous

respiration rate (b) is the rate limiting step in endogenous-hydrolysis process sequence. Therefore, only the endogenous respiration rate (b) needs to be considered in the steady state model.

In the interests of keeping the steady state model simple, only a single anaerobic organism will be modeled representing all four organism groups. The yield coefficient of this representative organism (Y_{AR}) will be close to the yield of the acetoclastic methanogens (0.04 $gCOD_{biomass}/gCOD_{utilized}$), which will dominate the biocenosis due to the high proportion of acetic acid in the influent (~50%) and relative to the acetoclastic methanogens, the hydrogenotrophic methanogens have a low yield value and the acidogens have a high yield value. Starting from Y_{AR} = 0.04 $gCOD_{biomass}/gCOD_{utilized}$, this value will be calibrated against the steady state experimental data

With sewage sludge digestion, the effluent COD concentration is mostly particulate unbiodegradable organics (~35% of influent COD) and biomass. Endogenous residue generation, which is negligible compared with the particulate unbiodegradable organics, could therefore be ignored by Sötemann et al. (2005). However, for completely biodegradable organics and the long sludge age at which the AnMBR operates, endogenous residue generation becomes significant and no longer can be regarded a negligible part of the reactor VSS concentration, particularly with low growth yield values of the anaerobic biomass. Thus, endogenous residue accumulation needs to be included in the AnMBR model to predict the sludge production accurately. The endogenous respiration rates of the four anaerobic organisms are quite similar (~0.04/d) so an average value of 0.0377/d (b_{AR}) will be used for the representative anaerobic organism in the steady state model (Sötemann et al., 2005). The unbiodegradable fraction of the biomass (f_{AR}) was taken as 0.08 from activated sludge models (Dold et al., 1980).

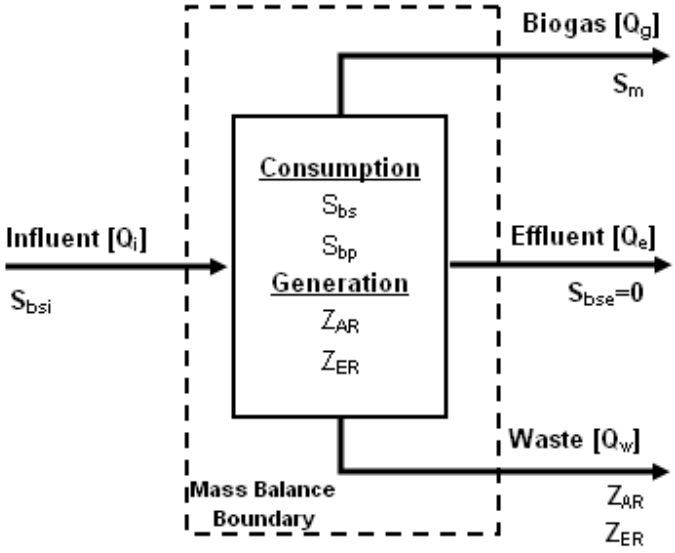

Figure 5.1, AnMBR Steady State Mass Balance

Applying the above considerations in a COD balance over the AnMBR (Appendix 5.3) at a defined sludge age (R_S), established hydraulically by a waste flow rate ($Q_W = V_r/R_S$) directly from the reactor (Figure 5.1), the following kinetic model equations are obtained:

$$Z_{AR} = \frac{Y_{AR}\left(S_{bi} - S_{be}\right)R_s}{\left(1 + b_{AR}R_s\left(1 - Y_{AR}\left(1 - f_{AR}\right)\right)\right)R_h} \tag{5.1}$$

$$Z_{ER} = f_{AR}b_{AR}R_sZ_{AR} \tag{5.2}$$

$$Z_{VSS} = Z_{AR} + Z_{ER} = \frac{Y_{AR}\left(S_{bi} - S_{be}\right)R_s(1 + f_{AR}b_{AR}R_s)}{\left(1 + b_{AR}R_s\left(1 - Y_{AR}\left(1 - f_{AR}\right)\right)\right)R_h} \tag{5.3}$$

$$S_m = \frac{\left(1 - Y_{AR}\right)\left(1 + b_{AR}R_s\right)}{\left(1 + b_{AR}R_s\left(1 - Y_{AR}\left(1 - f_{AR}\right)\right)\right)} \tag{5.4}$$

Where

Z_{AR} = representative active organism concentration [$gCOD/L_{reactor}$]

Y_{AR}	= yield coefficient of the active organism concentration = 0.04 (provisionally)	[$gCOD_{biomass}/gCOD_{utilized}$]
b_{AR}	= representative active organism endogenous respiration rate = 0.038	[1/d]
f_{AR}	= unbiodegradable fraction of representative active organism = 0.08	
Z_{ER}	= endogenous residue concentration	[$gCOD/L_{reactor}$]
S_{bi}	= influent COD concentration	[$gCOD/L_{influent}$]
S_{be}	= effluent COD concentration =0	[$gCOD/L_{effluent}$]
R_S	= sludge age (=V_r/Q_w)	[d]
R_h	= hydraulic retention time (=V_r/Q_i)	[d]
V_r	= reactor volume	[L]
Z_{VSS}	= reactor organic suspended solids concentration	[$gCOD/L_{reactor}$]
S_m	= methane production	[$gCOD/L_{influent}$]

The reactor suspended solids COD concentration (Z_{VSS}, gCOD/L Eq 5.3) and the methane gas Eq 5.4 and sludge (Eq 5.3*Q_w) production as a % of the influent COD (S_{bi}) are plotted versus sludge age for an OLR (= Q_i S_{bi}/V_r) of 15kgCOD/m^3/d in Figure 5.2, where Q_i is the influent flow rate and V_r the volume of the membrane reactor. It can be seen that (i) a very high proportion of influent COD is converted to methane (>98% for sludge age > 40d), (ii) this percentage increases with sludge age (due to endogenous respiration of biomass) and is 99% at 80d sludge age with the result that (iii) the sludge production is very low, i.e. 100-99 = 1% of influent COD mass at 80d sludge age and (iv) the reactor solids COD concentration increases with sludge age and >12 gTSS/L required for membrane scour for sludge ages longer than 60d. If the OLR is increased to 25 kgCOD/m^3/d, the reactor concentration exceeds 15gCOD/L for >50d sludge age. Long sludge ages, high reactor solids concentration for membrane scour and high % influent COD conversion to methane work together in the AnMBR system.

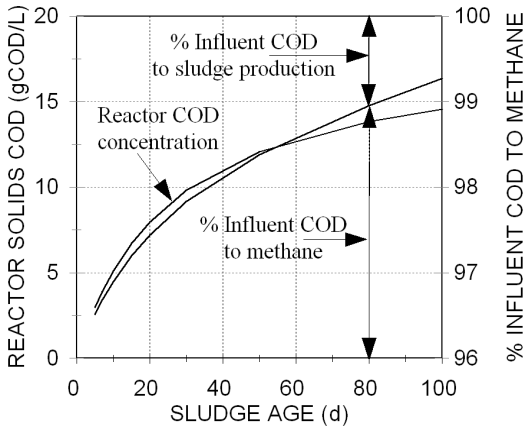

Figure 5.2: Reactor solids COD concentration and % influent COD converted to methane (1-E) versus sludge for the AnMBR system.

The net proportion (E) of the influent biodegradable organics load [Q_i (S_{bi}-S_{be})] that remains as sludge mass and is harvested daily from the reactor to maintain the sludge age [Q_w (Z_{AR}+Z_{ER})] can be calculated from Eq 5.3. From Figure 5.2, it can be seen that this E value decreases as sludge age increases. From Eq 5.3,

$$E = \frac{Q_w\left(Z_{AR}+Z_{ER}\right)}{Q_i\left(S_{bi}-S_{be}\right)} = \frac{Y_{AR}\left(1+f_{AR}.b_{AR}.R_s\right)}{\left(1+b_{AR}.R_s.\left(1-Y_{AR}\left(1-f_{AR}\right)\right)\right)} \tag{5.5}$$

The link between the reactor MLSS (kgTSS/m^3 or gTSS/L), reactor volume (V_r, m^3), sludge age (R_s, d) and influent flow and load is given by combining Eqs 5.3 and Eq 5.5, viz.

$$MLSS = \frac{\left(Z_{AR}+Z_{ER}\right)}{f_{cv}.f_i} = \frac{Q_i.\left(S_{bi}-S_{be}\right).E.R_s}{V_r.f_{cv}.f_i} = \frac{OLR.E.R_s}{f_{cv}.f_i} \quad \text{[gTSS/L]} \tag{5.6}$$

where

f_{cv}	= COD/VSS ratio of the sludge in the reactor and	[gCOD/gVSS]
f_i	= VSS/TSS ratio of the sludge in the reactor	[gVSS/gTSS]
OLR	= Organic Loading Rate	[kgCOD/m^3_{Vr}/d]

Both COD/VSS and VSS/TSS ratios were measured on the experimental AnMBR system and were f_{cv} = 1.53 and f_i = 0.78. While the former (f_{cv}) is close to the value accepted for activated sludge (1.48), the latter (f_i) seems unexpectedly low for a purely biodegradable organic feed – f_i values for activated sludge fed pure organic substrates are around 0.90. Possibly the low f_i value is due to the municipal anaerobic digester sludge used for seeding of the experimental AnMBR, which had a fairly large ISS component. Thus because of the large initial ISS concentration, which combined

with the extremely long sludge ages in the AnMBR, resulted that the ISS was not fully harvested from the AnMBR by the time the steady state experimental investigation was commenced.

The nitrogen for sludge production (growth) can also be determined from Eq 5.3. With the N content of the VSS in the reactor (f_n) known from measurement (0.11 gN/gVSS – also close to 0.10 measured on activated sludge), the minimum N concentration in the influent required for sludge production (N_s) [mgN/L] is given by

$$N_s = f_n \frac{V_r Z_{VSS}}{f_{cv} R_s Q_i} = \frac{f_n}{f_{cv}} \left(S_{bi} - S_{be} \right) \quad \text{[mgN/L]} \quad (5.7)$$

Where f_n = TKN/VSS ratio of the sludge [gN/gVSS]. However, usually a back ground (non-utilized) ammonia concentration (N_b) is required so the ammonia dosed $N_d = N_s + N_b$ [mgN/L], Eq 4.1 as discussed in Section 4.3.

5.1.2 Stoichiometry

The stoichiometry of anaerobic digestion is a combination of the anabolic and catabolic pathways and a mass and charge balance on the various cations and anions entering and exiting the system. The influent substrate, generically defined as $C_xH_yO_z$ for undissociated FTRW organics and $C_xH_{y-1}O_z^-$ for dissociated organics are converted to methane and carbon dioxide (both dissolved, HCO_3^- and gaseous, CO_2) and biomass with a general composition of $C_kH_lO_mN_n$. Because sludge production is so low, the precise values of k, l, m and n for the biomass are not required so the commonly accepted ones are applied, viz. $C_5H_7O_2N$. A more detailed explanation on how the steady state model was developed is presented in Appendix 5.4. The C, H, O, N, COD mass and charge balanced relationship between a completely biodegradable substrate with urea as nitrogen source and OH^- dosing for pH control and the metabolic end products of anaerobic digestion is:

$$
\begin{aligned}
&(1-F).C_xH_yO_z + F.C_xH_{(y-1)}O_z^- + b.CO(NH_2)_2 + d.OH^- \\
&+\left(2.x+3b+F-z-\frac{E.D_s}{D_b}(2k-m+n)-\frac{(1-E)D_s}{4}\right).H_2O \rightarrow \\
&\left(x-b-F-d-\frac{E.D_s}{D_b}(k-n)-\frac{(1-E)D_s}{8}\right).CO_{2AD}+\frac{(1-E)D_s}{8}.CH_{4AD} \\
&+\left(2b+F+d-\frac{n.E.D_s}{D_b}\right).HCO_3^-{}_{AD}+\left(2b-\frac{nED_s}{D_b}\right).NH_4^+ + \frac{ED_s}{D_b}C_kH_lO_mN_n
\end{aligned}
\tag{5.8}
$$

Where

D_s = $4x + y - 2z$ = electron donating capacity of the influent organics $C_xH_yO_z$ [$e^-/mol_{substrate}$]

D_b = 4k+l-2m-3n electron donating capacity of the biomass $C_kH_lO_mN_n$ [$e^-/mol_{biomass}$]

b = moles urea dosed for nitrogen requirements [mol/L]

d = moles OH^- dosed for pH control, i.e. alkalinity [HCO_3^-] increase. [mol/L]

F = proportion of influent SCFAs in dissociated (ionized) form. [-]

From Eq 5.8 it can be noted that the proportion dissociated SCFAs (F), the urea dose (b) and of course the hydroxide dose (d) all generate alkalinity (HCO_3^-), which help to control the pH of the reactor. The F value is governed by the pH of the influent FTRW and the dissociation constant of the SCFAs (pK_{ax}), viz.,

$$
F=\frac{C_xH_{(y-1)}O_z^-}{C_xH_yO_z+C_xH_{(y-1)}O_z^-}=\frac{1}{\left(1+\frac{K_{ax}}{(H^+)_{feed}}\right)}=\frac{1}{\left(1+\frac{10^{-pKax'}}{10^{-pH_{feed}}}\right)} \tag{5.9}
$$

From Eqs 5.3 and 5.8 the reactor COD solids concentration and methane production can be calculated and should be very closely equal. Also from Eqs 5.7 and 5.8, the nitrogen requirements for sludge production (the b value to keep a positive ammonia concentration in the effluent) can be calculated and should be closely similar to N_s, provided the b value in Eq 5.8 is set to give a zero

effluent ammonia concentration. Usually a background ammonia concentration (N_b) is required in the reactor for non-limited growth – this need to be added to the N_S of Eq 5.7. In Eq 5.8, the b value is selected to give the required background ammonia concentration because of its affect on alkalinity generation. Based on the assumption that the phosphate (as P) requirements is 20% of the nitrogen requirements (McCarty 1975), the P requirements also can be estimated. However, to calculate the operational pH and alkalinity requirements, the weak acid base chemistry of the P system need not be considered because its influence is negligible compared with the organic carbon system

5.1.3 Weak Acid Base Aqueous Chemistry

The weak acid base chemistry for the AnMBR is more complex than for anaerobic digestion of sewage sludge described in previous models because a base (NaOH) needs to be dosed externally to keep the reactor pH >7.0. The optimum pH for anaerobic digestion is between 6.5 and 8 (Capri and Marais, 1974) but the lower the pH, the lower the alkalinity, the closer to failure and the shorter the time for corrective action. The calculation of the base dose (NaOH) for pH control in alkalinity deficient systems is very important because base dosing is one of the main operating costs. The pH calculation is based on the inorganic carbon weak acid base system, taking into account the alkalinity (HCO_3^-) and partial pressure of CO_2 in the reactor head space (P_{CO2}, and so also in the liquid), generated by the stoichiometry of the anaerobic process (Eqs 5.8 and 5.9). The reactor pH can be calculated by doing an inorganic carbon mass balance over the system. In the pH range optimal for anaerobic digestion (6.8-7.5), 90% of the inorganic carbon (C_t) is in the HCO_3^- form and since the pH calculation is fairly insensitive to the inorganic carbon calculation:

$$C_t \approx [HCO_3^-]_{Total} = [HCO_3^-]_{AD} - [HCO_3^-]_{SCFA} \quad \text{[mol/L]} \quad (5.10)$$

Where

$[HCO_3^-]_{AD}$ = bicarbonate produced in (i) the anaerobic digestion of the dissociated SCFAs ($F.C_xH_{(y-1)}O_z$, Eq 5.8, $HCO_3^-{}_{Inf}$), the (ii) hydrolysis of urea ($b.CO(NH_2)_2$, Eq 5.8, $HCO_3^-{}_{Urea}$) to NH_4^+ and (iii) hydroxide dosing ($d.OH^-$, Eq 5.8, $HCO_3^-{}_{Alk}$) [mol/L]

At pH < 8.3 $H_2CO_3 + OH^- \rightarrow HCO_3^- + H_2O$ (5.11)

$[HCO_3^-]_{SCFA}$ = alkalinity consumed by the undigested (effluent) SCFAs i.e. [mol/L]

At pH > 6.5 $CH_3COOH + HCO_3^-{}_{SCFA} \rightarrow CH_3COO^- + H_2O + CO_{2SCFA}$ (5.12)

The unutilized SCFA concentration in the effluent is not given by the steady state model. The dosing required to neutralize this concentration is an operation control issue, because this concentration can vary hour by hour depending on the operational conditions at the time. The unutilized SCFA concentration in the effluent from the laboratory AnMBR, which was operated as close as possible to constant flow and load conditions, was 156±19 mgAc/L.

The carbon dioxide partial pressure (P_{CO2}) in atmospheres in the reactor head space and therefore also the liquid, is the moles of CO_2 in the biogas (Eqs 5.8 & 5.12) as a fraction of the total moles of biogas (CH_4+CO_2) produced:

$$P_{CO2} = \frac{CO_{2(g)}}{CO_{2(g)} + CH_{4(g)}} = \frac{(CO_{2AD} + CO_{2SCFA})}{(CO_{2AD} + CO_{2SCFA} + CH_{4AD})} \quad (5.13)$$

Where

CO_{2AD} = Gaseous carbon dioxide produced by anaerobic digestion (Eq 5.8) [mol/L]

CO_{2SCFA} = Gaseous carbon dioxide produced by SCFA dissociation (Eq 5.12) [mol/L]

CH_{4AD} = Methane produced by anaerobic digestion (Eq 5.8) [mol/L]

With C_t (i.e. $[HCO_3^-]_{Total}$ in moles/L) and P_{CO2} known (in atm), the reactor pH can be calculated from the inorganic carbon weak acid base system, and is given by:

$$pH_{reactor} = -\log_{10}\left(\frac{K'_h + \left(K'^{2}_h - 8.\left(\frac{\left[HCO_3^-\right]_{Total}}{K'_{c1}.P_{CO2}} - 1\right).K'_{c2}\right)^{\frac{1}{2}}}{2\left(\frac{\left[HCO_3^-\right]_{Total}}{K'_{c1}.P_{CO2}} - 1\right)}\right) \quad (5.14)$$

Where

K'_{c1}	= H_2CO_2/HCO_3^- carbonate dissociation constant (10^{-pKc1})	
K'_{c2}	= HCO_3^-/CO_3^{2-} carbonate dissociation constant (10^{-pKc2})	
K'_h	= Henry's law constant	
$[HCO_3^-]_{Total}$	= total inorganic carbon (Eq 5.10)	[mol/L]
P_{CO2}	= carbon dioxide partial pressure	[atm]
$pH_{reactor}$	= predicted reactor pH	[-]

Note the dissociation constants for the carbonate system and Henry's law (K_{c1}', K_{c2}' and K_h') have been adjusted for ionic activity as described by (Loewnethal et al., 1987). A detail discussion on the derivation of Eq 5.14 is presented in Appendix 5.5.

5.1.4 Statistical Methods

To evaluate how well the model predicts the experimental data, some statistical method of comparison was required. The first method considered was comparing the average and 95% confidence interval of the experimental and model predicted data. The observed data (for both the model and the experimental) is distributed around a mean, the 95% confidence interval (CI95%) is that interval which encloses 95% of the variance in the data (squares in Figure 5.3 A, B and C).

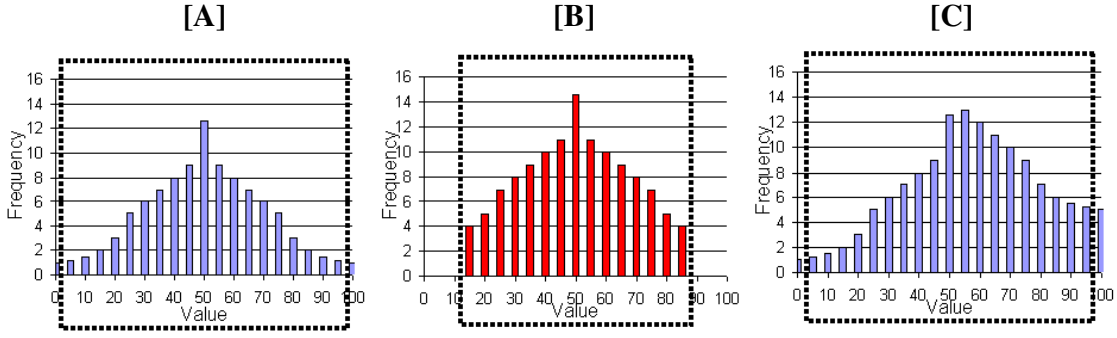

Figure 5.3, Average and CI95% of 'Measured [A]', 'Predicted[B]' and 'Time Skewed Data[C]'

The average and CI95% of the Figure 5.3 A, B and C is 50±47, 50±37 and 70±?? respectively. From this imaginary predicted and time skewed experimental data sets it can be seen that the method only gives an sufficient description of the model fit if the data is normally distributed and does not show variance with time (time skewed data). Because of the nature of the data to which the model will be fitted to i.e. time varied (example start-up) data, the CI95% method is probably not the ideal method of comparison.

The second statistical method that was evaluated is the traditional coefficient of determination (R^2) method (Wadsworth, 1998). This was calculated in the traditional method ($R^2=SS_{er}/(SS_{er}+SS_{reg})$ from the regression sum of squares (SS_{reg}) and the sum of squared errors (SS_{er}). However, when this technique was applied to the data very low (<0.5) R^2 values were typically obtained, even when there was a visibly good fit, if the predicted and experimental values were compared graphically. The reason for this was found in the definition of the coefficient of determination method, which evaluates the amount of variance in the experimental data that is described by the model. This makes the R^2 method very sensitive to random scatter (noise) in experimental data. Because of the fairly large errors in the experimental methods (COD ±5%, VFA-5pt ±5%, TSS/VSS ±10% and TKN/FSA ±10%) it was thus decided that the coefficient of determination was probably not the best method to validate the model fit.

The following method was found to best present the model's correlation to the experimental measurements. Firstly, the absolute error between the experimental (y_j) and the model (f_j) predications were expressed as a percentage of the experimental observation (Eq 5.15), viz.

$$\%Err_j = \frac{\left(\sqrt{\left(f_j - y_j\right)^2}\right)100}{y_j} \qquad (5.15)$$

This then yields an array of relative errors independent of time varied data. To eliminate outliers (possibly due to experimental error), the 90 and 50 percentile values will be used to describe the model fit to the experimental values. It should be emphasized that this method is still sensitive to the accuracy of the experimental methods, but appears far less sensitive to random scatter (noise) than the R^2 method, due to the scatter being proportional to the magnitude of the parameter being measured. To give the reader a tangible method of comparison, the experimental average, model

predicted average and the 90 percentile (P_{90}) and 50 percentile (P_{50}) of the *%Err* value will be presented. Note if the dataset is time skewed, the average will be presented with a superscript S (example; Avg Alkalinity = 2400^{S} mg$CaCO_3$/L).

5.2 Model Calibration

The stoichiometric model developed for the anaerobic digestion of FTRW was calibrated against data measured on the AnMBR. The dataset spanned from day 572 to 606 of the experimental period. Over this period the AnMBR was operated at an OLR of ± 15 kgCOD/m^3_{Vr}/d, with three membranes and operational fluxes below critical (i.e. normal operating conditions). Because of the extremely long sludge ages at which the AnMBR operates(> 100 days) and the large amount of parameters that have an effect on the system performance, a true steady state (constant OLR for > 3 sludge ages) could never be attained. However, the average sludge age over the 300 day period before the steady state investigation was estimated from the measured daily waste flow rate (Q_w) and reactor volume (V_r), which varied somewhat with the flux through the membranes, at ~ 200 days. 10 days before day 572 the sludge age was specifically controlled to this value (200 days) for the constant OLR (15 kgCOD/m^3_{Vr}/d). Thus it will be assumed that the system was at virtual steady state.

Although one of the underlying assumptions of this steady state anaerobic digestion model is that the biodegradable substrate is all utilized (S_{be} = 0), in order to calibrate the representative organism mass yield value (Y_{AR}) correctly, the effluent COD concentration will be subtracted to give the COD utilized in the system. Thus for model calibration S_{be} was used as an input parameter obtained from the experimental data obtained from the AnMBR, viz.

$$S_{b(utilized)} = S_{bi} - S_{be} \tag{5.16}$$

The model was calibrated by changing the yield value (Y_{AR}) of the representative anaerobic organism until an optimal fit to the measured data was obtained. A COD, N and C balance could be done on the system because the COD entering the system and the COD exiting is known (assuming sludge is $C_5H_7O_2N$), likewise the N and C. If these balances do not close (not 100%), then the margin of error in the calibration will be greater. Table 5.1 shows the COD, C and N mass balance

that was done on the experimental dataset. It can be noted that the COD and N balance was fairly low (83% and 88%) and calibration on this data would probably yield unreliable model parameters. However, the C balance was very good (99%).

Table 5.1, Average COD, C & N Mass Balance Day 572-606

	Influent	Biogas	Waste	Effluent	Mass Balance [%]
COD [mgCOD/L]	344.4	278.2	2.8	3.5	82.6
C [mol/L]	9.4	8.3	0.087	0.89	98.9
N [mol/L]	0.082	0.000	0.017	0.055	87.9

The F, x, y and z values for the synthetic FTRW were 0.091, 2.76, 5.61 and 1.97 respectively. A possible reason for the low COD balance is preferential escape of methane through the membranes. Being a smaller molecule than CO_2, it is possible that methane gas selectively passes through the membranes. The escape of some gas bubbles via the effluent manifold was observed on the AnMBR. However to account for the COD shortfall (60 gCOD/d), some 21 L_{CH4}/d is required to have escaped, which would reduce the carbon balance by 0.9 mol carbon or ~10%. This is too high in relation to the good C balance which was very close to 100% (98.9). Secondly, dissolved methane escaping in the effluent could also not account for the loss in COD since the saturation point is ~100 $mgCH_4/L$, this would amount to less than 2 gCOD/d. The third option might be high COD-low carbon EPS in the biomass, but this would have been detected in the COD tests done on the waste sludge which was conducted on a regular basis. It was therefore concluded that the low COD balance, but accurate carbon balance was due to the methane fraction in the biogas measured too low by the gas chromatograph (GC1) on which it was analyzed.

Because the C balance was close to 100%, it was decided to calibrate the steady state AD-FTRW model against the carbon instead of the COD data. The method used to observe the model's fit to the experimental data was done in much the same manner as discussed in Section 5.1.4. This was done by observing how the % Error between the predicted and experimental (i) biogas, (ii) biomass and (iii) effluent carbon compared with change in Y_{AR}.

$$\%Err = \frac{\left(\sqrt{\left(x_{Exp} - x_{SS}\right)^2}\right)100}{x_{Exp}} \quad (5.17)$$

Where

x_{Exp} = Actual experimental measurement

x_{SS} = Corresponding steady state model prediction varying with a variation in Y_{AR}

The average sludge age and OLR of the 35 day steady state period was 195 days and 15 kgCOD/m^3_{Vr}/d respectively, these values were used as input for the steady state AD-FTRW model. The Y_{AR} was then varied and the predicted carbon exiting the system as (i) biogas, (ii) biomass and (iii) bicarbonate (HCO_3^-) in the effluent in relation to the actual measured carbon exiting the experimental system and was compared via Eq 5.17 (Figure 5.4 A, Figure 5.4 B being a magnification of the square in Figure A).

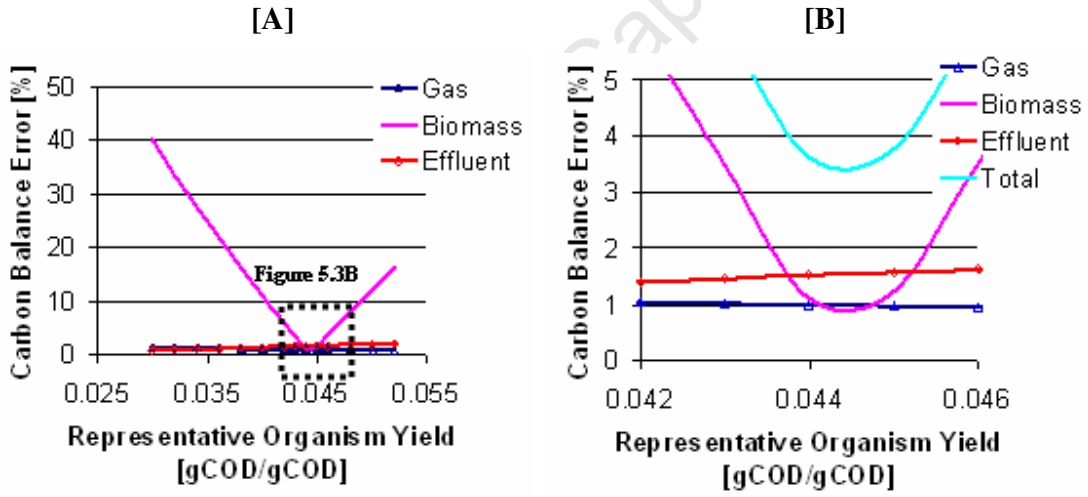

Figure 5.4, % Squared Error for Predicted & Actual Carbon vs. Yield

It was found that the initial yield of 0.04 [gCOD/gCOD] (acetoclastic methanogenesis) had to be increased by 10% to 0.044 [gCOD/gCOD] to give a best fit to the experimental data. This was indicated by the minimum in the Total Error in Figure 5.4B which is the sum of the errors between the experimental and predicted values for (i) biogas, (ii) biomass and (iii) effluent carbon. This technique ensures that one parameter, like biogas prediction, is not preferentially calibrated which might negatively affect the estimations of effluent and biomass

carbon predictions. The death rates for most anaerobic organisms are quite similar so this value was kept constant at b_{AR} = 0.0377 [/d]. Furthermore, it was assumed that the un-biodegradable particulate fraction of the representative organism mass is the same as that of activated sludge; f = 0.08 (Dold et al., 1980). A graphical presentation of the calibrated predictions and measured data is given in Figure 5.5 to 5.9.

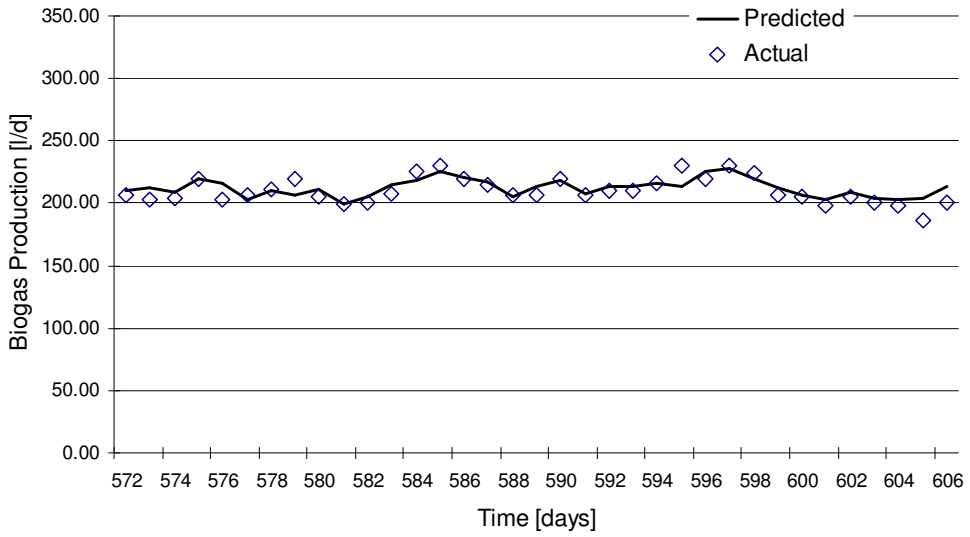

Figure 5.5, Predicted & Actual Biogas vs. Time

A good correlation between the predicted and actual biogas production was observed for the entire steady state test period (Figure 5.5). The measured and predicted averages were 210 L/d and 212 L/d respectively with 90% of the model predictions showing less than 6% variance form the experimental measurements (P_{90} = 6%) and 50% of the model predictions showing less than 1.7% variance from the experimental (P_{50} = 1.7 %). The coefficient of determination for this dataset was calculated at R^2 = 0.54, implying that the model does not fit the experimental very well (ideally R^2 > 0.85). On the other hand, visually and there are a relatively good fit and low P_{90} and P_{50} also implying a good fit. This highlights the problems with using the coefficient of determination to evaluate the model performance compared to visual and the error percentile method. If the biogas composition predicted by the model is compared to biogas samples analyzed with the gas chromatograph (GC1) it can be noted that the model predictions are consistently higher than the measured by about 10% (Figure 5.6):

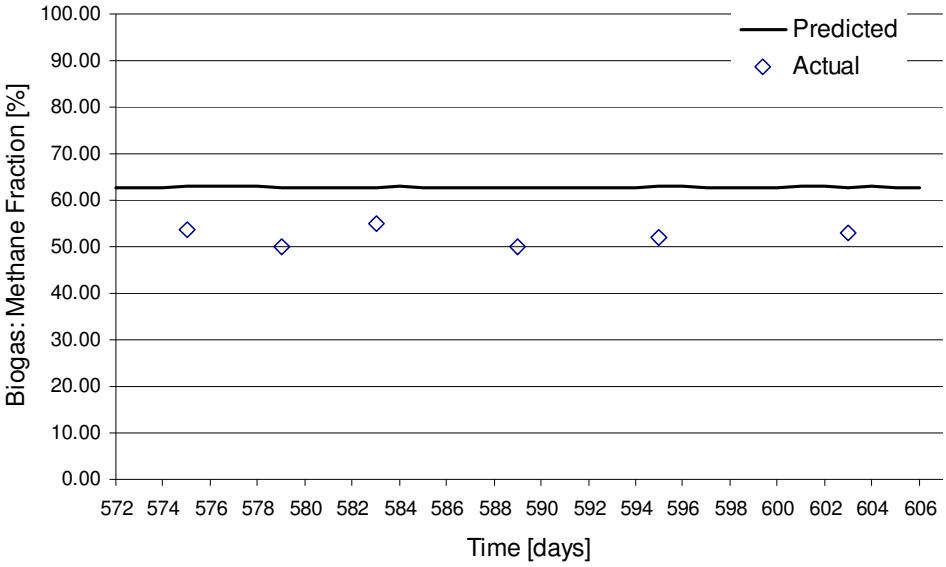

Figure 5.6: Predicted and Actual Biogas Methane Fraction vs. Time

The average measured and predicted methane fractions were 52.3 and 63 respectively with P_{90} = 26% and P_{50} = 20%. Thus the experimental analysis was consistently low by 10% (Figure 5.6). This difference in the predicted and actual methane fraction of the biogas adds weight to the argument of low GC results.

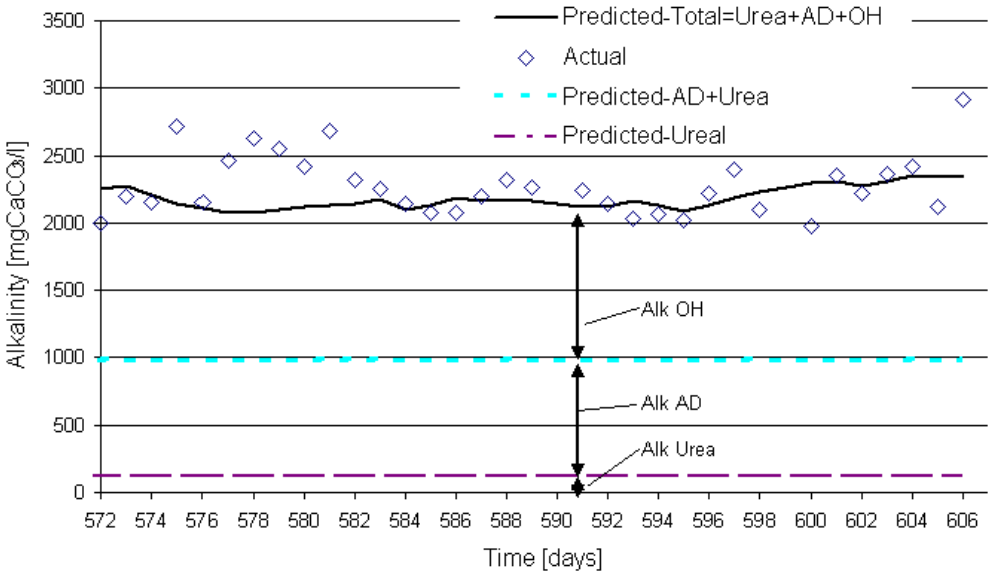

Figure 5.7: Predicted & Actual Alkalinity vs. Time

The predicted and measured (H_2CO_3*) Alkalinity is shown in Figure 5.7. The model predicts the measured data quite well, the average measured and predicted alkalinities are 2288 mg$CaCO_3$/L and 2198 mg$CaCO_3$/L (P_{90} = 18% & P_{50} = 5%). If no biological utilization of the organics in the FTRW stream took place ~10 000 mg$CaCO_3$/L alkalinity or ~6.7 gNaOH/L would have been required for neutralization to a pH of 7. The alkalinity dosed (~1000 mg/L as $CaCO_3$) is therefore only about 10% of the FTRW neutralization demand because the anaerobic biomass utilize the acid (undissociated) form of the SCFAs.

The contributors to the alkalinity in the AnMBR are (i) hydroxide dosed, (ii) urea dosed and (iii) FTRW influent alkalinity (Section 5.1.3). These contribute 57%, 38% and 5% to the total alkalinity respectively. It can be seen that the OH dose is the largest contributor (Figure 5.7 Alk-OH), but the influent alkalinity (Alk-AD) despite the pH being 3.77, is not insignificant and cannot be ignored to predict the reactor pH correctly. The increase in OH dosing from day 596 onwards shows how sensitive the system is to the amount of hydroxide dosed. Since the influent alkalinity and the amount of urea in the feed remains virtually constant, it is the OH dosing that is the most sensitive contributor to reactor alkalinity. Interestingly urea decomposition to form NH_4^+ also adds a significant amount of alkalinity (~120 mg$CaCO_3$/L) and thus cannot be ignored, hence the inclusion of urea decomposition in Eq 5.8.

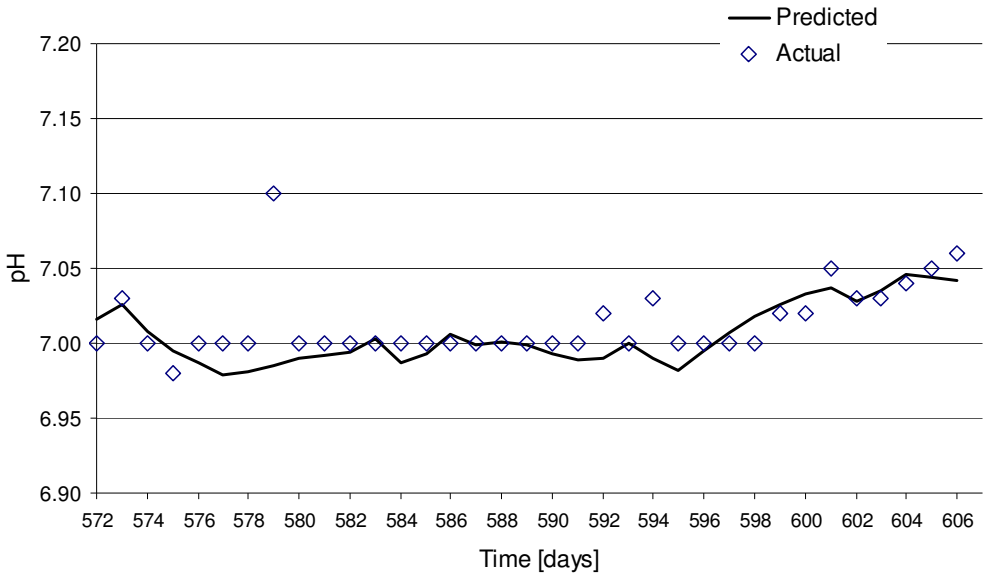

Figure 5.8, Predicted & Actual pH vs. Time

Because of the slight under-prediction of the alkalinity, the predicted pH is also slightly lower than the actual (Figure 5.8). The measured and predicted averages are 7.01 and 6.99 respectively with P_{90} = 0.3% and P_{50} = 0.1%. If the alkalinity measured in the 5-pt titration and the CO_2 partial pressure measured on the gas chromatograph is used in Eq 5.14, the pH is predicted consistently low at 6.89. However if the experimental P_{CO2} is substituted for the P_{CO2} calculated from the COD balance (Eq 5.13), the model predicts the pH accurately. This further ads weight to the questionable gas chromatograph measurements as discussed in earlier in Section 5.2.

The sludge age (Figure 5.9A) was calculated from the measured volume of biomass wasted per day from the AnMBR divided into the actual operational volume of that day ($R_s = V_r/Q_w$), as was discussed in detail in Section 3.3.

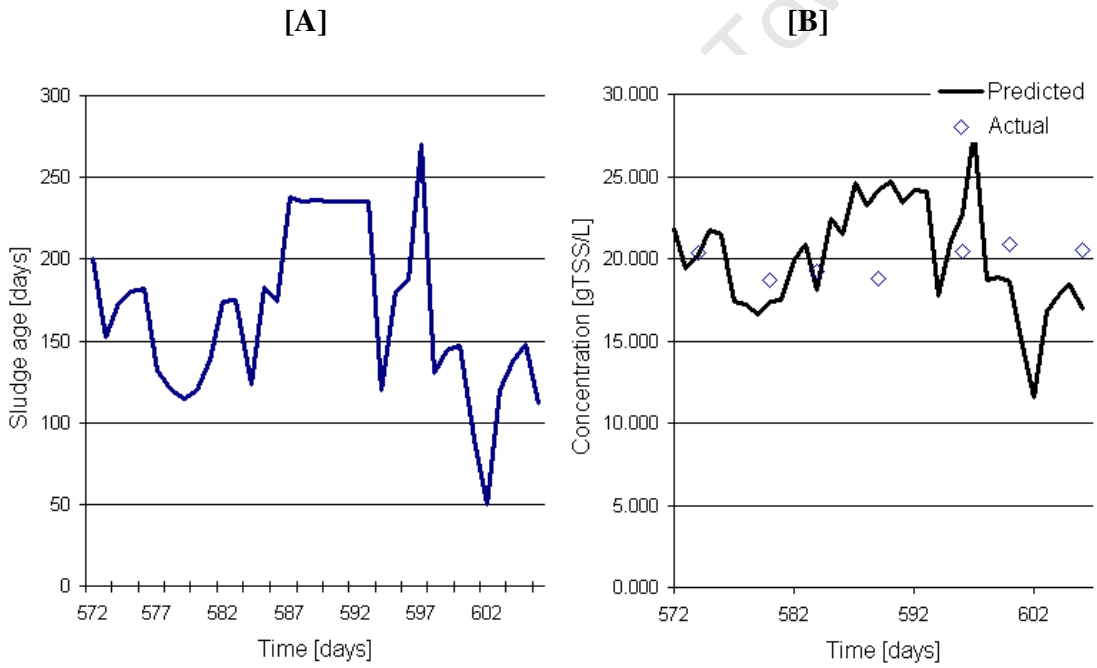

Figure 5.9, AnMBR Sludge Age [A] and Predicted and Actual MLSS [B] vs. Time

The predicted and measured reactor TSS is shown in Figure 5.9B. The predicted reactor TSS concentration show significantly more variance that those measured. The predicted and measured averages are 20gTSS/L and 19.84 gTSS/L with P_{90} = 22% and P_{50} = 11%, implying a large amount of variance in the data even though the averages are statistically similar. Because of the long sludge age and its significant variation over a wide range, resulting from controlling reactor concentration at ~20 gTSS/L and not sludge age, the MLSS concentration is not strongly dependant on the chosen

yield and death rates. Thus it appears that the generic $C_5H_7O_2N$ biomass composition correlates to within the margin of experimental error. If Figure 5.9A and B are compared it can be seen that – for a constant OLR (in this case 15 kgCOD/m^3_{Vr}/d) – the reactor MLSS is directly proportional to the sludge age. Table 5.2 gives a summary of the results obtained in the model calibration:

Table 5.2, Stoichiometric Model Calibration

Comparison	Predicted Average	Actual Average	P_{90} [%]
COD Balance		93	
COD/VSS		1.53	
VSS/TSS		0.78	
TKN/VSS		0.11	
Sludge Age [days]	195*	195	
Nitrogen Requirements [mgN/L]	17	16.6	40
Biogas Production [L/d]	212	210	6.0
CH_4 Fraction [%]	63	52	26
Alkalinity [mg$CaCO_3$/L	2125	2288	18
pH	6.99	7.01	0.30
MLSS [gTSS/L]	20	19.8	22.0

*** Per definition same as measured**

Note: since the steady state AD-FTRW over-predicts the sludge production (slightly by ~1%) there is a corresponding over-prediction in the nitrogen requirements for biomass growth.

5.3 Model Sensitivity Analysis

The next step in the development of the steady state AD-FTRW model is to investigate how sensitive the model predictions are in relation to input parameters. The two parameters chosen for this investigation was the sludge age (R_s) and the representative organism yield (Y_{AR}). Output parameters; (i) CO_2 partial pressure (P_{CO2}), (ii) biogas production (Q_g), (iii) alkalinity, (iv) pH and also the (v) daily biomass production will be evaluated. How these output parameters vary with a 10% increase or decrease in the sludge age or yield will also be investigated.

5.3.1 Sludge Age Sensitivity

For the sludge age sensitivity analysis the yield was kept constant (Y_{AR} = 0.044, Section 5.2) and the sludge age was varied from 50 days to 400 days for a constant (i) OLR = 15 kgCOD/m^3_{Vr}/d, (ii) urea dosage (180 mg/L) and (iii) NaOH dosage (1127 mg/L). Figure 5.10A and B show the difference in P_{CO2} and gas production if the sludge age were 10% longer or 10% shorter than the indicated sludge age.

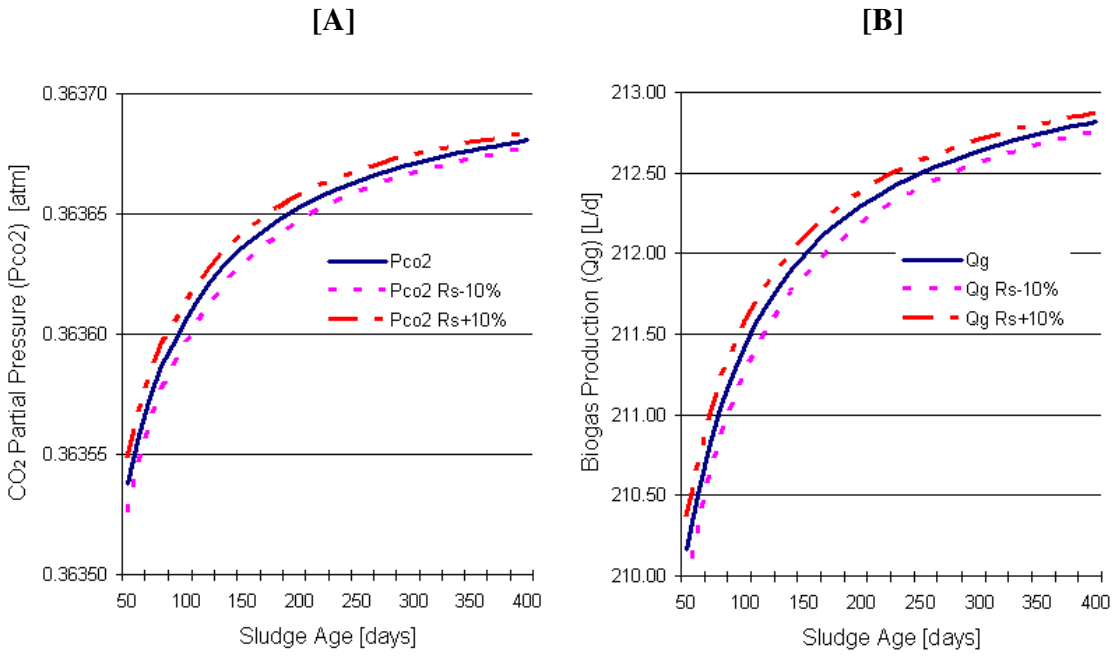

Figure 5.10, Model Sensitivity to Variation in Sludge Age for P_{CO2} [A] and Gas Production [B]

Figure 5.10A shows that there is a slight increase in the CO_2 partial pressure as the sludge age increases and a 10% error in the sludge age makes a negligible difference to the P_{CO2} value. Similar results are obtained for biogas production, since the longer the sludge age the more complete the hydrolysis process will be, resulting in an increased biogas production (Figure 5.10B). A ±10% change in sludge age results in less than 0.1% change in both the gas production and CO_2 partial pressure, emphasizing the insensitivity of these parameters to small errors in sludge age. Error in sludge age is therefore not a cause for model predictions deviating from the measured results for P_{CO2} and gas production.

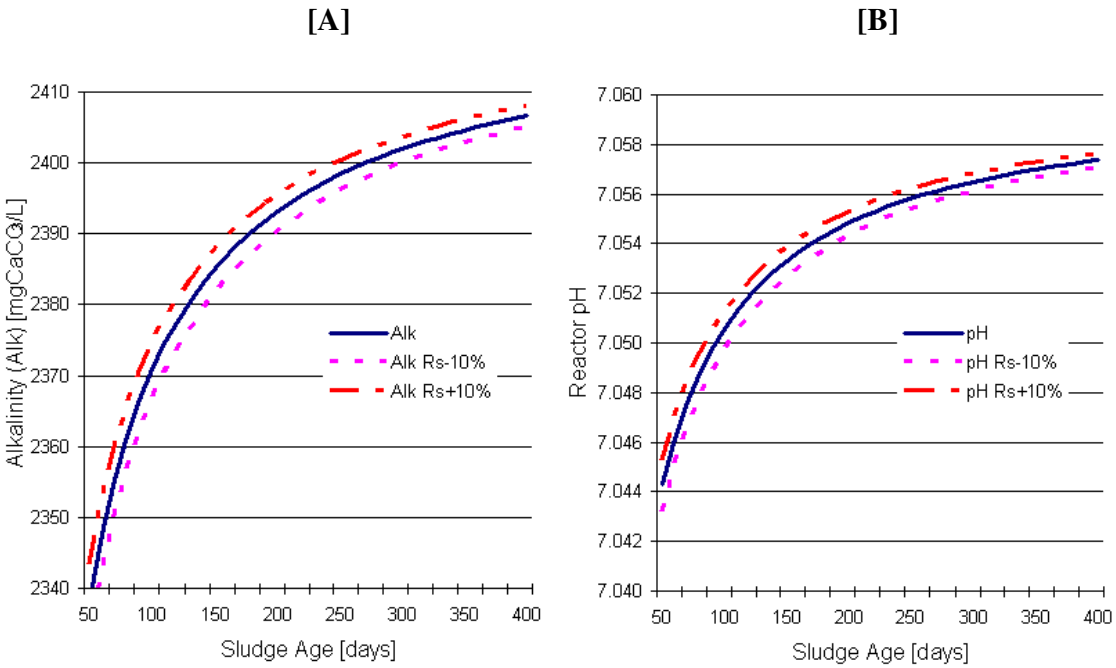

Figure 5.11, Model Sensitivity to Variation in Sludge Age for Alkalinity [A] & Reactor pH [B]

Figure 5.11A shows as the sludge age increases the alkalinity production in the system also increases and that an error of ±10% on sludge age makes a negligible difference to the alkalinity and reactor pH. Over the observational range (50-400 days) small (3%) increase in alkalinity was observed with sludge age varied from 50 to 400 days. Similarly a slight increase in the pH was also observed (Figure 5.11B). Again a 10% increase or decrease of the sludge age has a small (<0.1%) effect on the alkalinity and pH predictions. Again, error in sludge age is not a cause for model predictions deviating from the measured results for alkalinity and reactor pH.

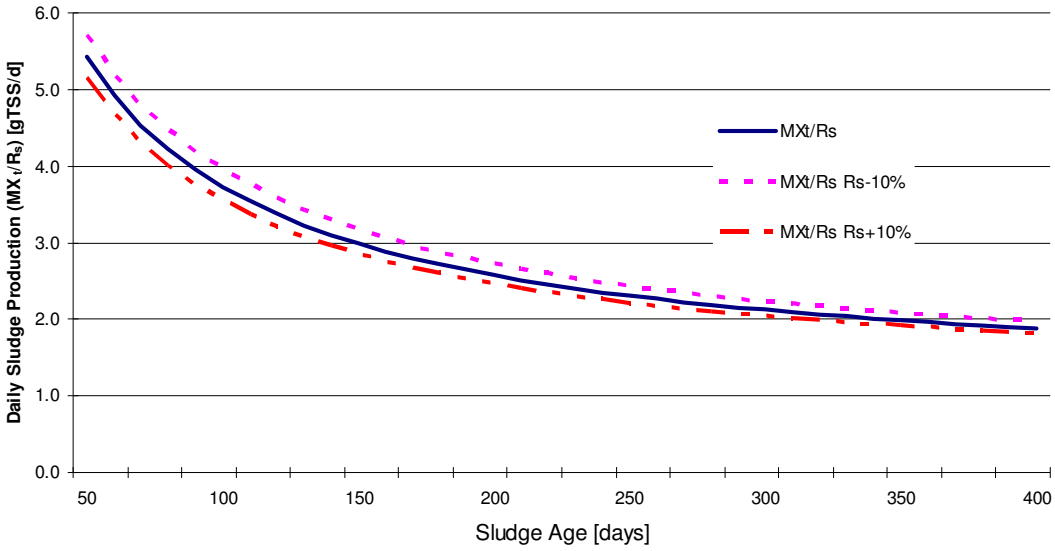

Figure 5.12, Model Sensitivity to Variation in Sludge Age for Sludge Production

Figure 5.12 shows the daily sludge production as a function of sludge age as well as the difference for a ±10% error in the sludge age. The daily sludge production is calculated by dividing the mass of biomass in the system (MX_t) by the sludge age (R_s). The daily sludge production decreases with an increase in sludge age. This is to be expected because the endogenous process results in increased biomass digestion as sludge age increases. Thus the increased utilization of biomass particulates results in a decrease in the total particulate mass (MX_t) in the system. The daily sludge production shows a large change with change in sludge age, on average a 5% over/under estimation was observed for a ±10 % change in sludge age. Although the change is dampened to half the change in sludge age, the change is 50 times higher than for the P_{CO2}, gas production, alkalinity and pH considered above. Error in sludge age therefore is a cause for model predictions deviating from the measured results for sludge production and by direct link also the MLSS concentration.

From Section 5.2 and 3 it can be concluded that the output predicted least accurately by the steady state AD-FTRW model is the reactor MLSS and correspondingly system nitrogen requirements. Possible reasons for this include:

- Since the AnMBR is a variable volume system, daily readings of the reactor volume (V_r) and wastage (Q_w) was taken. This was then used to calculate the sludge age ($R_s = V_r/Q_w$). The

reactor volume could only be estimated accurately to 1 litre, which implies that errors as large as 1/23 ~ 5% were not completely unlikely in sludge age estimations.

- Secondly the AnMBR was operated by controlling the MLSS concentration for optimal membrane performance (i.e. wasting to control concentration) and sludge age was merely a response to this. This implied that the sludge age varied significantly over short periods of time under normal operating conditions, which is not ideal for model calibration.

- Thirdly, the experimental MLSS measurements show a large variance (noise) of ± 10%. Thus even if the steady state model were 100% accurate, MLSS measurements would still show a ±10% variance.

- Finally, only ~ 1% of the daily COD load adds to the MLSS. Traditionally the calibration of bioreactor models on such a small parameter has proven cumbersome (example AS models calibrated on effluent COD where $S_{te}/S_{ti} < 5\%$)

From the abovementioned it can be concluded that the variance observed in the predicted and actual MLSS (and N requirements) is a response to a range of errors which have an accumulating effect, resulting in a poorer accuracy in the prediction of MLSS if compared to other parameters predicted by the model.

5.3.2 Representative Organism Yield (Y_{AR}) Sensitivity

The second parameter to be investigated for sensitivity is the representative organism yield (Y_{AR}). This parameter was varied over a range (0.022-0.066) around the optimal (0.44) found in Section 5.2. For the yield sensitivity analysis the following was kept constant (i) sludge age (R_s = 200 days), (ii) OLR = 15 kgCOD/m^3_{Vr}/d, (iii) urea dosage (180 mg/L) and (iv) NaOH dosage (1127 mg/L).

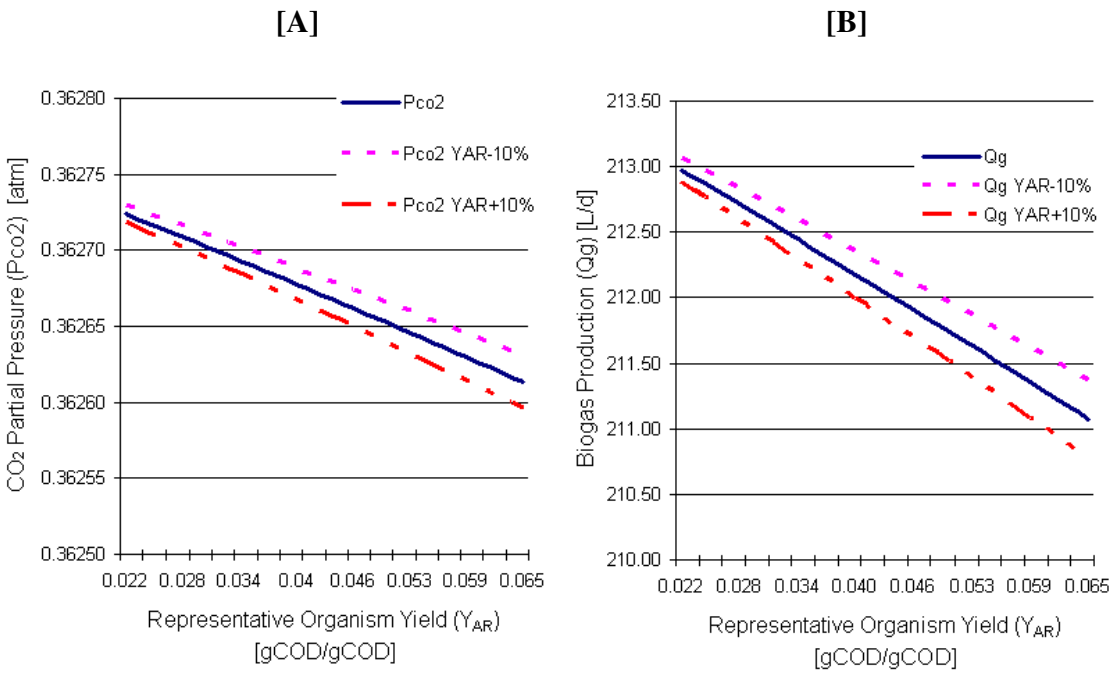

Figure 5.13, Model Sensitivity to Variation in Yield (Y_{AR}) for P_{CO2} [A] and Gas Production [B]

Figure 5.13 A and B shows that as the Y_{AR} increases, the CO_2 partial pressure and the biogas production decreases, because the higher the yield the more COD ends up as biomass at a constant OLR and sludge age. On average the variance in CO_2 partial pressure and gas production is less than 0.1% with a ±10% variance in Y_{AR}, showing that these model output parameters are fairly insensitive to yield variations.

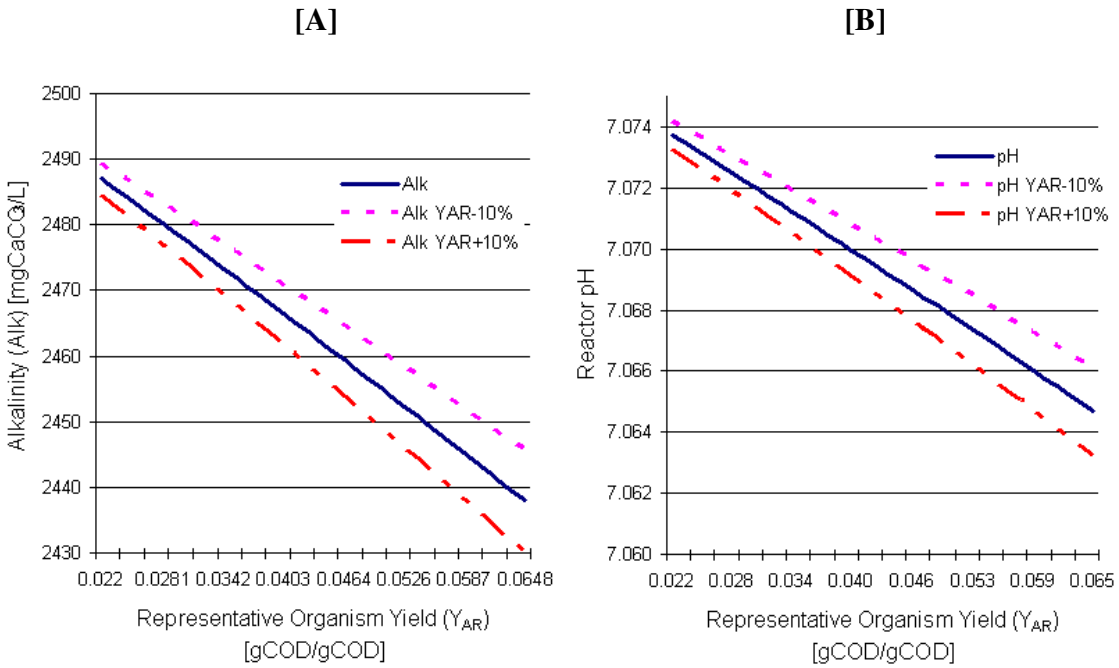

Figure 5.14, Model Sensitivity to Variation in Yield (Y_{AR}) for Alkalinity [A] & Reactor pH [B]

From Figure 5.14 A and B a slight decrease in alkalinity and pH with an increase in Y_{AR} is evident, because as the yield increases so does the amount of biomass produced and more NH_4^+ is converted to NH_3 for cellular synthesis resulting in the production of protons (Eq 5.8). Protons in turn react with HCO_3^- to form H_2O and CO_2 and in so doing decrease the system alkalinity. Both parameters are insensitive to changes in Y_{AR}, showing a less than 0.35% variance with a ± 10% variance in Y_{AR}. Errors in P_{CO2}, biogas production, alkalinity and pH therefore have a very small effect on the determination of Y_{AR}.

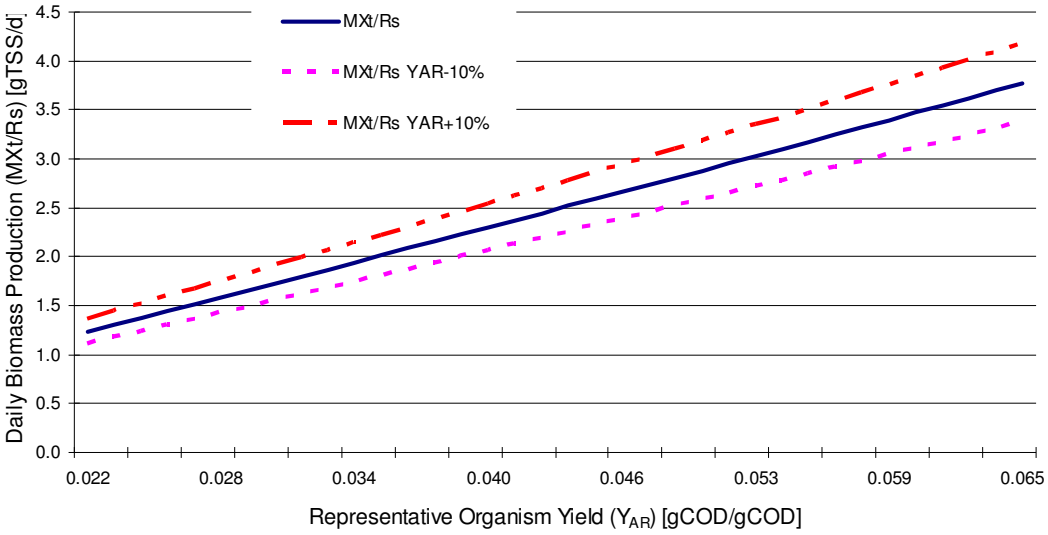

Figure 5.15, Model Sensitivity to Variation in Yield (Y_{AR}) for Sludge Production

As expected, the daily biomass production is directly proportional to Y_{AR} and a 300% increase in Y_{AR} (from 0.022 to 0.066) results in a 300% increase in the daily sludge production (from 1.2 to 3.6 gTSS/d) (Figure 5.15). The sludge production is therefore the model output parameter that is most sensitive to variance in the yield; a 10% increase/decrease is observed for a ±10% variance in the representative organism yield.

5.4 Model Validation

Ideally, a second steady state dataset would be used for the calibration of the steady sate AD-FTRW model. Unfortunately, the data collected in the experimental phase was not aimed towards model development, but more to add to the 'proof of concept' of the AnMBR. After it was proven experimentally that the AnMBR is a viable treatment option for FTRW and the experimental phase completed, it was attempted to develop models predicting the systems performance. Because of the long sludge age requirements to maintain a high enough MLSS concentration for membrane operation, true steady state (R_s*3 = ~300*3 = 900 days) was impossible to reach in the 700 days of data collection. Secondly, the only 'pseudo steady state' dataset that was collected was used for model calibration (Section 5.2). However, rather than abandoning model validation completely because of the lack of data, it was decided to evaluate the steady state AD-FTRW models

performance against a set of variable flow and load (non steady state) data for both the AnMBR and AnPBR to see how the model measures up.

The steady state AD-FTRW model was validated against 200 days of variable flow and load AnMBR (day 175 – 375) and AnPBR (day 167 – 367) data. The average OLR of the AnMBR and AnPBR was 15.94^{S} kgCOD/m$^{3}_{Vr}$/d and 14.82^{S} kgCOD/m$^{3}_{Vr}$/d respectively. Table 5.3 compared the averages of the predicted and measured data for both reactors:

Table 5.3, Compared Averages of the Predicted and Measured Data for the AnMBR and AnPBR

Comparison	AnMBR			AnPBR		
	Predicted Avg^{S}	Measured Avg^{S}	P_{90} [%]	Predicted Avg^{S}	Measured Avg^{S}	P_{90} [%]
Mass Balance COD [%]	100	95		100	91	
Mass Balance C [%]	100	111		100	106	
Mass Balance N [%]	100	103		100	106	
Sludge Age [days]	366*	366		32	**	
Nitrogen [mgN/L]	15	25.6	42.0	65	54	22.00
Biogas Production [L/d]	233	263	11.3	196	213	8.00
CH_4 Fraction [%]	62	52	20.0	65	54	23.00
Alkalinity [mg$CaCO_3$/L	2929	3017	3.00	3305	2916	15.00
pH	7.12	7.05	1.50	7.17	7.18	0.160
MLSS [gTSS/L]	21	27	22.0	25	**	

*** Per definition the same as the actual AnMBR sludge age**

**** Measurement not possible from experimental system**

- **Sludge Age** of the AnMBR was on average 366 days. The sludge age was calculated by dividing by daily wastage from the reactor (Q_w) into the reactor volume (V_r), thus giving an estimation of the sludge age. However Q_w and V_r varied daily resulting in a large variance in sludge age as discussed in Section 5.3.1. However the 90% of the model predictions showed less variance than 22% from the measured value (P_{90} = 22%).

  Because the biomass is immobilized on the fixed bed in the AnPBR, the sludge age cannot be measured directly. However, the sludge age can be estimated from Eq 5.3 and Eq 5.6 from

the system's E value i.e. the ratio of the exiting sludge mass per day via the effluent and mass of COD fed per day (or Eq A5.16, Appendix 5.3). From these predictions it was found that the AnPBR sludge age is around 32 days and an order of magnitude smaller than that predicted for the AnMBR.

- **Nitrogen requirements** predicted for the AnMBR is 41% lower than the actual requirements. In the case of the AnPBR, a slight over-prediction (20%) can be observed. If the AnMBR and AnPBR nitrogen requirements are directly compared, the steady state AD-FTRW model predicts that the AnMBR requires over 50% less nitrogen than the AnPBR. The same will be true for phosphate requirements. Since the AnMBR was not at steady state, a large variation (-22 %) in the predicted vs. actual MLSS was observed, so correspondingly the model also under predicted the reactor nitrogen requirements.

- **Biogas Production** was measured slightly higher than the model predicted for both the systems. However predictions are still close to the 10% error margin. It should again be emphasized that the validation dataset was under daily variable flow and load conditions and thus larger errors are to be expected.

- **Methane Fraction** was predicted high (+10%) for both systems. Again adding weight to the argument of consistently low (-10%) gas chromatograph results.

- **Alkalinity** is slightly under-predicted for both the AnMBR and AnPBR systems, the P_{90} of the AnMBR = 3%, showing a strong correlation between the predicted and the actual values. For the AnPBR, 90% of model predictions showed less than 15% error from the predicted value.

- **pH Predictions** on the AnPBR shows a strong correlation to the measured values. However, some deviation (-0.07 pH unit) is observed for the AnMBR. In this case both the AnMBR and AnPBR shows a strong correlation to the experimentally measured pH values ($P_{90AnMBR}$ = 1.5% and $P_{90AnPBR}$ = 0.16%). This can probably be attributed to the high degree of accuracy typically associated with pH measurements.

- **MLSS** concentrations of the AnMBR was predicted at 21^{S} gTSS/L whereas the actual measurements were 22% higher (on average), the probable cause for this has been discussed in Section 5.3.1. The MLSS of the AnPBR cannot be measured directly, but the model predicted a theoretical $MLSS_{AnPBR}$ at ~ 25 gTSS/L. This correlates closely to a MLSS expected for the AnMBR operating at a similar OLR and sludge age.

5.5 Closure

A full conversion stoichiometric model was developed for the anaerobic conversion of an alkalinity and nutrient deficient low pH soluble biodegradable substrate (including weak organic acids/bases) to biomass, carbon dioxide and methane. The primary use of this model is reactor design, i.e. the calculation of (i) mixed liquor concentration (MLSS), (ii) reactor volume, (iii) reactor operational pH, (iv) alkalinity, (v) nutrient requirements and (vi) biogas production and composition at steady state.

This model comprises three parts (i) a COD based kinetic part from which the methane gas and biomass COD production are determined for a given sludge age, (ii) a C, H, O, N, charge and COD mass balance based stoichiometry part from which the gas composition (or partial pressure of CO_2) and alkalinity generated are calculated from the COD concentration utilized and its x, y, z and a composition in $C_xH_yO_z$ of the biodegradable organics and urea dosed for nitrogen requirements and (iii) a carbonate weak/acid base chemistry part from which the pH of the digester is obtained from the partial pressure of CO_2 and alkalinity generated. The model takes into account alkalinity dosing to maintain a reactor pH at 7.0 and the dissociation (K_a) of the acidic substrate, since it was found that the protonation of a substrate (eg. Short Chain Fatty Acids) have a significant effect reactor pH. One of the underlying assumptions of all steady state anaerobic digestion models is that the biodegradable substrate is utilized to completion ($S_{be} = 0$). Thus for model calibration S_{be} was used as an input parameter obtained from the experimental data obtained from the AnMBR. The model was calibrated on steady state experimental data of an Anaerobic Membrane Bioreactor (AnMBR) treating Fischer-Tropsch Reaction Water (FTRW). Then a sensitivity analysis was performed to evaluate the sensitivity of model outputs to sludge age and the yield value chosen for the representative organism mass. The model was also validated against 'non-steady' datasets of 200 days each from the AnMBR and an Anaerobic Packed Bed Reactor (AnPBR) both treating the same FTRW to observe how well the model can predict under these conditions.

It was found that parameters including (i) CO_2 partial pressure, (ii) biogas production, (iii) alkalinity and (iv) pH was virtually unaffected by an ±10% variation in either the representative organism yield or the sludge age. Contrary to this, the daily biomass production was much more sensitive to a ±10% variation in the yield or the sludge age. A variation in the daily biomass production of ±10%

and ±5% was observed for a ±10% variation in the yield and sludge age respectively. Since ~99% of the COD (and C) exits the system as biogas and a mere ~1% exits the system as biomass, a -1 % error in the biogas can lead to a ~100% over prediction. Because of this the 'Minimum Total Error' method as discussed in Section 5.2 was used to ensure that one model output was not preferentially calibrated at the expense of the predictive capabilities of the other model outputs.

Biogas and pH are predicted to well within 5% of the actual measured values. The mixed liquor concentration predictions can vary as much as 25%, but yields results typically within 15% of the actual under normal operating conditions. The steady state model is so robust; it can be applied to judge the health of the system, even under non-steady conditions. If parameters – such as biogas production and pH – deviates from the predicted values, it is usually an early sign of equipment malfunction or bioprocess failure. It was found that experimental sludge age and MLSS concentrations play a pivotal role in the model performance. Rather than varying sludge age to control MLSS, a system sludge age should be chosen, allowing MLSS to vary with time. This combined with true steady state reactor operation will yield data much more useful for model calibration.

The steady state AD-FTRW model is based on a 100% mass, COD and charge balance and exactly the same substrate were fed to both systems, and thus the same kinetic constants (Y_{AR} & b_{AR}) could be accepted for both the AnMBR and AnPBR. This assumption was then applied to calculate the 'theoretical MLSS' and 'theoretical sludge age' for the AnPBR. From this it was found that the AnMBR operates at a theoretical MLSS of ~25 gTSS/L and a sludge age of ~32 days – a order of magnitude shorter than the AnMBR for the same OLR (~15 kgCOD/m^3_{Vr}/d). Since nutrients tend to accumulate in the biomass, the short sludge age might explain the 50% higher nutrient requirements for the AnPBR. Steady state models are (i) more practical for design, because they allow reactor sizes to be simply calculated in a spreadsheet and (ii) provide a basis for crosschecking for simulation model outputs (Brink et al., 2007) and (iii) can predict initial values for dynamic simulation models, like biomass concentrations and reactor volumes. However, steady state models cannot predict effluent biodegradable COD concentration (S_{be}), the effect of effluent SCFA on the system pH, inhibition, response to organic over-loading or digester failure conditions. For this, the time dependant metabolic intermediate production by the individual organism groups is required. This will be addressed in the final part of this thesis; Chapter 6 – Dynamic Modeling.

CHAPTER 6

6. Dynamic Modeling

In this chapter a dynamic model for the Anaerobic Digestion of Fischer-Tropsch Reaction Water (AD-FTRW) is developed. In the steady state AD-FTRW model it was assumed that a single representative organism mass consumes a single biodegradable substrate to completion ($S_{be} = 0$). In the dynamic model, a unique Functional Organism Group (FOG) is assigned to each biodegradable fraction of the feed (Figure 6.1). Each of the FOGs has unique growth and death rates and substrate utilization capabilities, thus responding differently to substrate concentrations and environmental conditions. Secondly, the dynamic model is time dependant, thus it can predict individual biomass responses to influent and system changes with time. The dynamic AD-FTRW model is developed to complement the steady state model developed in Chapter 5, since it can predict parameters that cannot be predicted by the steady sate model, these include:

- Effluent Quality
- The effect of effluent SCFA concentration on reactor pH
- System response to dynamic flow and load variations
- Inhibitory effects of pH, temperature and metabolic products
- System responses to different control strategies

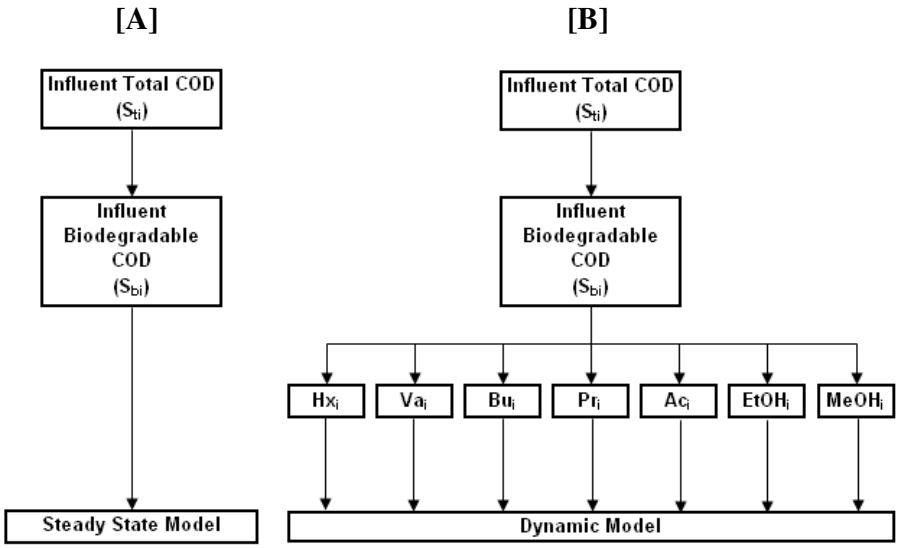

Figure 6.1, Influent Characterization for Steady State [A] and Dynamic [B] AD-FTRW Models

FTRW has Short Chain Fatty Acid (SCFA) concentrations 3 orders of magnitude larger than are typically observed in the Anaerobic Digestion of Primary Sludge and Waste Activated Sludge (AD-PS/WAS) (compare to Sötemann et al., 2005). Because of this, and the wide range of SCFAs in FTRW, proton fluxes are also 3 orders of magnitude larger than is observed in dynamic AD-PS/WAS models. If the background Weak Acid/Base Chemistry (WABC) relationships are applied as was described in Mosvoto et al. (1997), the result is a matrix with process rates ranging between 2 and 10^{-14} days. This, combined with the high proton fluxes observed in the dynamic AD-FTRW model, results in a 'stiff' Petersen Matrix (PM) which cannot be solved by conventional means. A system is labeled 'stiff' if the range of time constraints is large, which implies that some processes occur very rapidly while others happen very slowly.

A specialized stiff Ordinary Differential Equation (ODE) solver, known as a stiff solver, is required to solve the resultant stiff PM. These solvers have an inherent inability to deal with variations in influent flow and load as observed under dynamic flow and load conditions (Rosen et al., 2006). Secondly, FTRW has a substrate composition distinctly different from that typical to municipal waste water. This made it impractical to modify existing dynamic AD-PS/WAS models to treat FTRW; a completely new model had to be derived.

The model development technique that will be applied is similar to that described by Siegrist et al. (2002) i.e. the model is (i) developed based on the metabolic pathways of anaerobic digestion, then (ii) it is verified (checked for material consistencies such as mass balances) then (iii) it is calibrated and finally (iv) validated on actual dynamic flow and load experimental data. The first step in the development of the dynamic AD-FTRW model is to assign an individual organism mass to each of the biodegradable fractions in the substrate that mediates the substrate utilization (Figure 6.1B). The biomass will be classified into the traditional 4 trophic groups in anaerobic digestion namely Acetogenesis (Z_{ac}), Acetoclastic Methanogenesis (Z_{am}), Hydrogenotrophic Methanogenesis (Z_{hm}) and Acidogenesis (Z_{ad}) (Figure 2.3, Chapter 2). However, to compensate for the wide range of SCFAs, Ethanol (EtOH) and Methanol (MeOH) in the feed, a further subdivision is required. The reason for the high degree of sub-classification of the biomass is that each biodegradable fraction requires a unique biomass and produces a unique ratio of metabolic products.

After model development, the system will firstly be checked for a COD, C, O, H, N and charge balance. Secondly it will be calibrated under steady state conditions against the steady state model developed in Chapter 5, this calibration will be conducted to find the optimum values for the stoichiometric yield (Y) for each of the individual biomass species. Thirdly, the maximum specific growth rates of the different FOGs will be obtained from literature and fourthly, the individual half saturation constants of the SCFA degrading FOGs will be determined from anaerobic batch tests conducted on sludge harvested from the AnMBR reactor. The remainder of the stoichiometric and kinetic constants will be obtained from literature. The dynamic AD-FTRW model will then be validated against 55 days of actual experimental data recoded on the AnMBR under dynamic flow and load conditions.

In the experimental phase of the project it was found that inhibition by metabolic intermediates, high SCFA concentrations, pH and temperature played a significant role in the high rate AD-FTRW reactor. Since the study of inhibition did not form part of the experimental phase, a literature survey was done to identify inhibition functions that could characterize the system. Chapter 6 is concluded with an estimation of reactor failure conditions. System responses to different control strategies were not explored with the model – this will be taken up when the AnMBR finds application at pilot scale at Sasol.

6.1 Model Development

The dynamic AD-FTRW model comprises of three parts. Firstly there is the stoichiometry, this section deals with the conversion of the different biodegradable organics by each of the FOGs to a unique set of metabolic end products. The corresponding WABC relationships will be incorporated into the stoichiometry of each organism group, since it was found that this reduces the stiffness of the Petersen Matrix and so significantly reduces computation time. This is possible because the embedded aqueous WABC relationships are much faster than the biological processes. The second part of the model comprises the kinetics of the process rates i.e. the speed at which the stoichiometric reactions occur. These include organism growth and death rates and some WABC process relationships. The final part of the dynamic AD-FTRW model is the external calculations of the parameters defined by composite components; these include reactor solids concentration (MLSS [gTSS/L]), effluent Short Chain Fatty Acid concentration ($SCFA_e$ [mgAc/L]), effluent COD (S_{be} [mgCOD/L]) and the reactor pH calculation.

6.1.1 Stoichiometry

One of the main differences between the steady state and dynamic AD-FTRW model is that in the dynamic model the metabolic intermediates produced are taken into consideration. Every biodegradable fraction – once utilized by its corresponding FOG – produces a different combination of metabolic products (Figure 6.2).

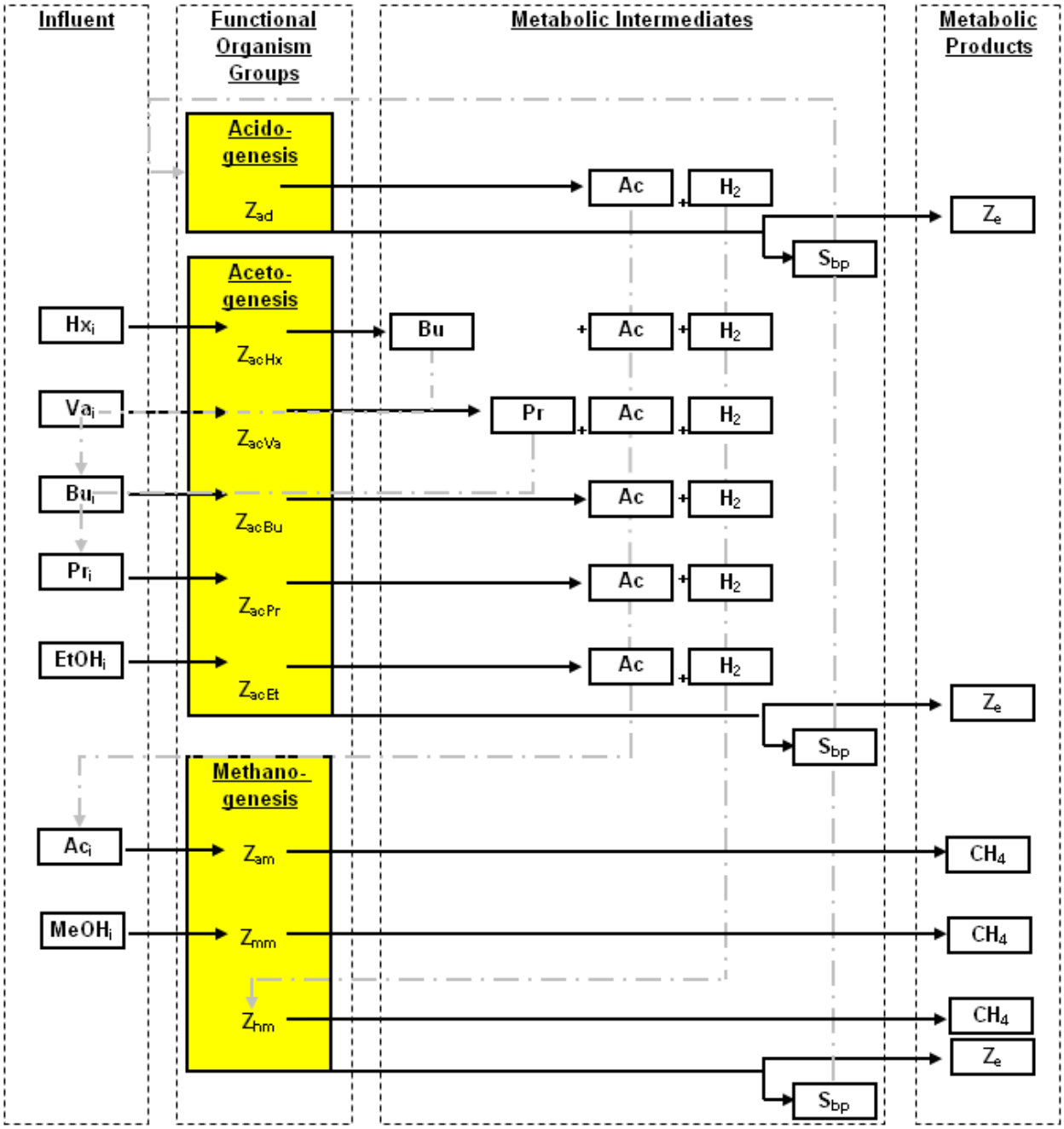

Figure 6.2, Dynamic Model Metabolic Pathways & Functional Organism Groups

The acetogenesis of $>C_2$ SCFAs produces metabolic products that include Acetic (Ac), Propionic (Pr) and Butyric Acid (Bu) (eg Hx → Bu + Ac + H_2), these metabolic products add to the bulk concentration of these SCFAs (Figure 6.2 and Appendix 6.3). Therefore, a unique stoichiometric equation will be derived for each of the biodegradable fractions in FTRW. This will again be done

by combining the catabolic and anabolic pathways of substrate utilization as described in Chapter 5 (and Appendix 5.1). The dynamic AD-FTRW model is based on the following:

1) A literature survey, which was done to obtain the catabolic pathways of the individual SCFAs, MeOH, EtOH and the slowly biodegradable organics from anaerobic biomass death and hydrolysis (S_{bp}) (Kalyuznhyi, 1997b; McCarty, 1975; Batstone et al., 2002; Sötemann et al., 2005)

2) Assuming that all the FOGs have a generic composition of $C_5H_7O_2N$ (McCarty 1975), the standard anabolic equation can be described as

$$C_xH_yO_z + \left(\frac{5.D_s}{20} - x\right).CO_2 + \frac{D_s}{20}.NH_3 \rightarrow \left(\frac{8.D_s}{20} - (2x - z)\right).H_2O + \frac{D_s}{20}.C_5H_7O_2N \quad (6.1)$$

Where

$D_s = (4x+y-2z)$ = Substrate electron donating capacity [e^-equivalents/mol] (6.2)

3) All CO_2 produced will be in soluble form (H_2CO_3) thus:

$$CO_{2\,\mathrm{Produced}} + H_2O \rightarrow H_2CO_3 \quad (6.3)$$

4) Analogous to the steady state model, the carbonate system (HCO_3^-/H_2CO_3) acts as the proton source/sink for all of the WABC reactions. Secondly, the contribution of CO_3^{2-} will be regarded as negligible in the anaerobic digestion pH range.

5) Only the protonated (non-ionic) form of any SCFA can be metabolized, thus un-protonated (ionic) SCFAs need to pick up a proton from the carbonate system before metabolism:

$$C_xH_{y-1}O_2^- + H_2CO_3 \rightarrow C_xH_yO_2 + HCO_3^- \quad (6.4)$$

6) Since the fraction of the SCFA in the un-protonated form is again governed by the influent pH (compare Section 5.1.2), this gets taken into consideration via the F value, as was the case

in the steady state model. However, in the case of the dynamic model, each of the SCFAs have an individual pK_a value, thus Eq 5.9 can be rewritten as:

$$F_{C_x} = \frac{C_x H_{2x-1} O_2^-}{\left(C_x H_{2x-1} O_2^- + C_x H_{2x} O_2\right)} = \frac{1}{\left(1 + \frac{\left[H^+\right]_{feed}}{K_{ax}}\right)} \tag{6.5}$$

Where

x = 1 to 6 and

K_{ax} = 10^{-pKax} of the SCFA with carbon chain length x.

$[H^+]_{feed}$= Feed proton activity = $10^{-pHfeed}$

Thus if $C_{xTotal} = C_xH_{2x-1}O_2^- + C_xH_{2x}O_2$ then:

$$C_{xTotal} + F_x.H_2CO_3 \rightarrow C_x H_{2.x} O_2 + F_x.HCO_3^- \tag{6.6}$$

7) The relationship between the soluble (H_2CO_3) and gaseous CO_2 is described by the following:

$$H_2CO_3 \xleftrightarrow{r_h} H_2O + CO_{2(g)} \tag{6.7}$$

With r_h being the combined association/dissociation rate of carbon dioxide dependant on Henry's Law (Appendix 6.1, Section 6.1.3)

8) Urea is the sole nitrogen source for AD-FTRW. In the operational pH range (6.5-7.5) >99% of the ammonia will be in saline (NH_4^+) form, thus upon entering the reactor urea decomposes as follows:

$$(NH_2)_2CO + 2H_2CO_3 + H_2O \xrightarrow{r_{Urea}} CO_2 + 2NH_4^+ + 2HCO_3^- \tag{6.8}$$

9) Similarly it is assumed that the NaOH dosed for pH control is converted to $H_2CO_3^*$ Alkalinity upon entering the system:

$$NaOH + H_2CO_3 \rightarrow Na^+ + H_2O + HCO_3^- \quad (6.9)$$

Under normal operating conditions, the carbonate system concentration is significantly (10 times) larger than any other weak acid/base concentration; it will be assumed that this will be the primary proton source/sink.

10) The saline ammonia (NH_4^+) produced from urea decomposition needs to be de-protonated before it can be utilized by the FOGs:

$$NH_4^+ + HCO_3^- \rightarrow NH_3 + H_2CO_3 \quad (6.10)$$

Both assumptions 8 and 9 were proven experimentally. The assumptions made above will be applied in conjunction with the metabolic pathways to derive the dynamic AD-FTRW model stoichiometry.

Metabolic Pathways

In the steady state AD-FTRW model, the anabolic and catabolic pathways are linked through the E value since the yield and death rates are modeled in a single stoichiometric equation. Because the growth and death processes are modeled separately in the dynamic AD-FTRW model, the catabolic and anabolic rate equations are linked through the true organism yield, Y [$mgCOD_{Biomass}/mgCOD_{Utilized}$]. However, in the case of the dynamic model, an individual yield is assigned to each of the functional organism groups. From Figure 6.2 it can be noted that acetogenesis is subdivided into a further 5 functional organism groups to model the utilization of the wide range of SCFAs. Since the weak acid/base chemistry reactions happen significantly faster than the biological processes it was decided to incorporate these into the biological process steps, rather than using separate algebraic equations to solve them. This is one of the primary distinctions of the dynamic AD-FTRW model if compared to its predecessors. The derivation of the acetogenic biological processes in the dynamic AD-FTRW model is represented in Appendix 6.3; the remainder (acetoclastic methanogenesis, acidogenesis and hydrogenotrophic methanogenesis) is derived in much the same manner as presented in Appendix 5.3. The biological growth processes in the dynamic AD-FTRW model can be summarized as follows;

- **Acetogenesis of Hexanoic Acid (AcHx)**

$$\frac{5(1-F_{Hx})}{8.Y_{AcHx}}C_6H_{12}O_2+\frac{5F_{Hx}}{8.Y_{AcHx}}C_6H_{11}O_2^-+\frac{(10-34.Y_{AcHx})}{8.Y_{AcHx}}H_2O$$
$$+\frac{(5.F_{Hx}+2.Y_{AcHx})}{8.Y_{AcHx}}H_2CO_3+NH_4^+\xrightarrow{r_{acHx}}\frac{(5-5.Y_{AcHx})}{8.Y_{AcHx}}C_4H_8O_2 \quad (6.11)$$
$$+\frac{(5-5.Y_{AcHx})}{8.Y_{AcHx}}C_2H_4O_2+\frac{(10-10.Y_{AcHx})}{8.Y_{AcHx}}H_2+\frac{(5.F_{Hx}-8.Y_{AcHx})}{8.Y_{AcHx}}HCO_3^-+C_5H_7O_2N$$

- **Acetogenesis of Valeric Acid (AcVa)**

$$\frac{10(1-F_{Va})}{13.Y_{AcVa}}C_5H_{10}O_2+\frac{10F_{Va}}{13.Y_{AcVa}}C_5H_9O_2^-+\frac{(20-59.Y_{AcVa})}{13.Y_{AcVa}}H_2O$$
$$+\frac{(10.F_{Va}+2.Y_{AcVa})}{13.Y_{AcVa}}H_2CO_3+NH_4^+\xrightarrow{r_{acVa}}\frac{10.(1-Y_{AcVa})}{13.Y_{AcVa}}C_3H_6O_2 \quad (6.12)$$
$$+\frac{10(1-Y_{AcVa})}{13.Y_{AcVa}}C_2H_4O_2+\frac{20(1-Y_{AcVa})}{13.Y_{AcVa}}H_2+\frac{(10.F_{Va}-13.Y_{AcVa})}{13.Y_{AcVa}}HCO_3^-+C_5H_7O_2N$$

- **Acetogenesis of Butyric Acid (AcBu)**

$$\frac{(1-F_{Bu})}{Y_{AcBu}}C_4H_8O_2+\frac{F_{Bu}}{Y_{AcBu}}C_4H_7O_2^-+\frac{(2-5.Y_{AcBu})}{Y_{AcBu}}H_2O+\frac{F_{Bu}}{Y_{AcBu}}H_2CO_3+NH_4^+$$
$$\xrightarrow{r_{AcBu}}\frac{2(1-Y_{AcBu})}{Y_{AcBu}}C_2H_4O_2+\frac{2(1-Y_{AcBu})}{Y_{AcBu}}H_2+\frac{(F_{Bu}-Y_{AcBu})}{Y_{AcBu}}HCO_3^-+C_5H_7O_2N \quad (6.13)$$

- **Acetogenesis of Propionic Acid (AcPr)**

$$\frac{10(1-F_{\mathrm{Pr}})}{7.Y_{Ac\,\mathrm{Pr}}}C_3H_6O_2+\frac{10F_{\mathrm{Pr}}}{7.Y_{Ac\,\mathrm{Pr}}}C_3H_5O_2^-+\frac{(30-51.Y_{Ac\,\mathrm{Pr}})}{7.Y_{Ac\,\mathrm{Pr}}}H_2O+NH_4^+\xrightarrow{r_{Ac\,\mathrm{Pr}}}$$
$$\frac{10(1-Y_{Ac\,\mathrm{Pr}})}{7.Y_{Ac\,\mathrm{Pr}}}C_2H_4O_2+\frac{30(1-Y_{Ac\,\mathrm{Pr}})}{7Y_{Ac\,\mathrm{Pr}}}H_2+\frac{(10-8.Y_{Ac\,\mathrm{Pr}}-10.F_{\mathrm{Pr}})}{7.Y_{Ac\,\mathrm{Pr}}}H_2CO_3 \qquad (6.14)$$
$$+\frac{(10.F_{\mathrm{Pr}}-7.Y_{Ac\,\mathrm{Pr}})}{7.Y_{Ac\,\mathrm{Pr}}}HCO_3^-+C_5H_7O_2N$$

- **Acetogenesis of Ethanol (AcEtOH)**

$$\frac{5}{3.Y_{AcEt}}CH_3CH_2OH+\frac{(15-19.Y_{AcEt})}{3.Y_{AcEt}}H_2O+NH_4^++HCO_3^-+\frac{3}{2}H_2CO_3\xrightarrow{r_{AcEtOH}}$$
$$\frac{5(1-Y_{AcEt})}{3.Y_{AcEt}}C_2H_4O_2+\frac{10(1-Y_{acEt})}{3.Y_{AcEt}}H_2+C_5H_7O_2N \qquad (6.15)$$

Unlike longer chain SCFAs, acetic acid is metabolized directly to CH_4 and CO_2. Acetoclastic methanogenesis can be described as follows:

- **Acetoclastic Methanogenesis (Am)**

$$\frac{5(1-F_{Ac})}{2.Y_{Am}}C_2H_4O_2+\frac{5F_{Ac}}{2.Y_{Am}}C_2H_3O_2^-+NH_4^++\frac{(5-11Y_{Am})}{2.Y_{Am}}H_2O\xrightarrow{r_{AcEt}}$$
$$\frac{(5-5Y_{Am})}{2Y_{Am}}CH_4+\frac{(5-3.Y_{Am}-5F_{Ac})}{2.Y_{Am}}H_2CO_3+\frac{(5-2Y_{Am})}{2Y_{Am}}+C_5H_7O_2N \qquad (6.16)$$

Another biodegradable fraction in the feed that directly undergoes methanogenesis is Methanol. This substrate is directly converted to methane as follows:

- **Methanogenesis of Methanol (Mm)**

$$\frac{10}{3.Y_{Mm}}CH_3OH + NH_4^+ + HCO_3^- \xrightarrow{r_{AcEt}} \frac{30(1-Y_{Am})}{12Y_{Am}}CH_4 + \frac{(5-9.Y_{Mm})}{6.Y_{Mm}}H_2CO_3 + \frac{(5+33.Y_{Mm})}{6.Y_{Mm}}H_2O + C_5H_7O_2N \quad (6.17)$$

Hydrogen gas produced by acetogenesis and acidogenesis is the single most inhibitory metabolic product produced in the anaerobic process. Apart from the negligible fraction of the dissolved hydrogen gas that escapes to the gas phase, the only means of reducing the dissolved hydrogen concentration is via the following:

- **Hydrogenotrophic Methanogenesis (Hm)**

$$\frac{10}{7.Y_{Hm}}H_2 + NH_4^+ + HCO_3^- + \frac{10(5-3.Y_{Hm})}{20.Y_{Hm}}H_2CO_3 \xrightarrow{r_{AcEt}} \frac{10(1-Y_{Am})}{4Y_{Am}}CH_4 + \frac{10(15+11.Y_{Am})}{20.Y_{Am}}H_2O + Z_{Hm} \quad (6.18)$$

Parallel to microbial growth, endogenous respiration (organism death) occurs. The biodegradable fraction of the dead organism mass is known as biodegradable particulate COD (S_{bp}). S_{bp} is first hydrolyzed and then forms the substrate for the last of the FOGs, namely acidogenesis. Traditionally hydrolysis and acidogenesis are modeled as two separate processes in anaerobic digestion (Batstone et al., 2002 & Sötemann et al., 2005). However in AD-FTRW, the only biodegradable particulates (S_{bp}) that enter the system are those produced from dead organism mass. Thus it will be assumed that S_{bp} has the same composition as that of active biomass i.e. $C_5H_7O_2N$. The contribution of this organism group is so small that it was decided to model both hydrolysis and acidification in a single step:

- **Hydrolysis and Acidogenesis (AD)**

$$\frac{1}{Y_{ad}}C_5H_zO_2N^* + \frac{5(1-Y_{ad})}{Y_{ad}}H_2O \xrightarrow{r_{Ad}} \frac{2(1-Y_{ad})}{Y_{ad}}C_2H_4O_2 + \frac{2(1+Y_{ad})}{Y_{ad}}H_2 + \frac{(1-Y_{ad})}{Y_{ad}}HCO_3^- + \frac{(1-Y_{ad})}{Y_{ad}}NH_4^+ + C_5H_zO_2N^{**} \quad (6.19)$$

Where

$C_5H_7O_2N^*$ = Biodegradable particulates (S_{bp}) of dead organism mass

$C_5H_7O_2N^{**}$ = Active acidogenic biomass (Z_{Ad}) produced from S_{bp} utilization

Organism Death

Organism death is described by the theory of endogenous respiration (Dold et al., 1980). This theory states that parallel to organism growth, a fraction of the biomass dies at a continuous rate. A fraction (f) of this 'dead biomass' is regarded as unbiodegradable and is known as endogenous residue (Z_e). The remainder (1-f) of the dead biomass is biodegradable particulate (S_{bp}) and is hydrolyzed to form substrate for acidogenesis (Eq 6.20). The death process can be described as follows:

$$Z_{Aj} \xrightarrow{r_{dj}} (1-f).S_{bp} + f.Z_e \quad (6.20)$$

Where

Z_{Aj} = The active mass of the jth FOG [mol/L]

r_{dj} = Rate of organism death of the jth FOG. [mol/L.d]

6.1.2 Process Rates

Biochemical experiments carried out over more than half a century, with pure culture as well as mixed cultures have indicated that the organism growth rate (μ_i) is influenced by many physico-chemical and biological environmental factors. These factors include; substrate concentration (S_j), active mass concentration (Z_{Aj}), pH, temperature and the concentration of inhibitory substances that might have an effect on the rate of microbial growth (Dochain & Vanrolleghem, 2001).

Specific Growth Rate

The specific growth rate (μ_j) forms part of the reaction rate ($r_j = \mu_j.Z_{Aj}$) which describes the rate of metabolism of substrate to biomass and additional metabolic products (including SCFAs, CH_4, CO_2, H_2, ect.). The most widely applied specific growth rate model is the empirical 'Michaelis-Menten Law' also known as the Monod kinetic rate equation for microbial growth (Fogler, 1999):

$$\mu_j = \frac{\mu_{\max j}.S_j}{\left(K_{sj} + S_j\right)} \tag{6.21}$$

Where

μ_{maxj}	= Maximum Specific Growth Rate	[1/d]
K_{sj}	= Half Saturation Constant	[mol/L]
S_j	= Biodegradable substrate concentration	[mol/L]

The Monod process rates are dictated by two kinetic constants namely the maximum specific growth rate (μ_{maxj}) and the half saturation constant (K_{sj}) (Figure 6.3).

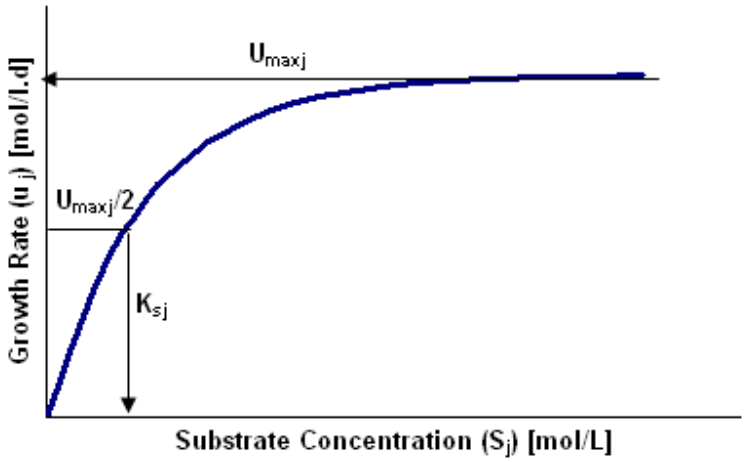

Figure 6.3, Typical Growth Rate Change vs. Substrate Concentration

The K_{sj} dictates the minimum concentration of a substrate at which a specific biomass (Z_{aj}) fraction can be maintained. The μ_{maxj} value in turn dictates the highest possible rate of substrate (S_j) removal by the j^{th} FOG (Figure 6.3). From the Monod functions (Section 6.1.2) it can be noted there exists a high degree of interdependency between the μ_{max} and K_s values, i.e. various combinations of μ_{max}

and K_s values will amount to the same model output. Unlike with the stoichiometric constants, there is a large variation in K_s-values quoted in the literature.

Note that the K_{sj} value corresponds to the substrate concentration for which μ_j is half of its maximum value (μ_{maxj}). This original expression was purposed by Michaelis and Menten in 1913 to express the reaction rate of enzyme catalyzed reactions with a single substrate. In 1942 it was extended by Monod and applied to microbial growth (Monod, 1942):

$$r_j = \mu_j . Z_{Aj} = \frac{\mu_{\max j} . S_j . Z_{Aj}}{\left(K_{sj} + S_j\right)} \tag{6.22}$$

Where

r_j = Rate of process j [mol/L.d]

S_j = Biodegradable substrate j concentration [mol/L]

Z_{Aj} = Active Mass Concentration of FOG_j [mol/L]

The Monod rate expression remains without physical validation, but is the most widely applied form of rate expression in waste water treatment modeling (Dochain & Vanrolleghem, 2001). Two different forms of the Monod expression will be applied in the dynamic AD-FTRW model. The first will only include the inhibitory effects of pH and temperature. This rate expression will be applied to the methanogenesis bioprocesses (including Acetoclastic, Methanol and Hydrogenotrophic Methanogenesis):

$$r_j = \frac{\mu_{\max j} . S_j . Z_{Aj}}{\left(K_{sj} + S_j\right)} . I_{pH_j} . I_{T_j} \tag{6.23}$$

Where

I_{pHj} = pH inhibition for FOG_j [-]

I_{Tj} = Temperature inhibition constant for FOG_j [-]

The second form of the Monod rate expression will be for the hydrogen producing organisms, namely the acidogenic and acetogenic organism groups (Appendix 5.1 and 6.3). Because the

concentration of dissolved hydrogen gas in the liquid phase has proven to have a dramatic effect on the growth rates of the acidogenic and acetogenic organisms, a third inhibition term, describing hydrogen inhibition is included:

$$r_j = \frac{\mu_{\max}.S_j.Z_{Aj}}{\left(K_{s_j} + S_j\right)}.I_{pH_j}.I_{T_j}.I_{H_{2j}} \qquad (6.24)$$

Where

I_{H2j} = $H_{2(aq)}$ inhibition constant for FOG_j [-]

Endogenous Respiration Rates

Predation does not appear to have a significant effect under anaerobic conditions (Batstone et al., 2002). Accordingly organism death consists only of endogenous respiration. Each functional organism group death rate is thus modeled by first order kinetics:

$$r_{dj} = b_j.Z_{Aj} \qquad (6.25)$$

Where

r_{dj} = Death rate of FOG_j [mol/L.d]

b_j = Endogenous mass loss rate for the FOG_j [1/d]

The biodegradable fraction of this dead organism mass adds to the biodegradable particulate organics (S_{bp}) in the system and gets hydrolyzed/acidified by the acidogenic biomass (Z_{AD}, Eq 6.19). The unbiodegradable fraction forms part of the endogenous mass (Z_e) which contributes to the sludge mass (MLSS) in the system.

Carbon Dioxide Expulsion/Dissolution Rate

Musvoto et al. (1997) described the expulsion and dissolution rate of gaseous carbon dioxide by two separate equations;

$$H_2CO_3^* \xrightarrow{r_{fCO2}} CO_{2(g)} + H_2O \quad (6.26)$$

$$CO_{2(g)} + H_2O \xrightarrow{r_{rCO2}} H_2CO_3^* \quad (6.27)$$

Where

r_{fCO2} = K_{fCO2} [$H_2CO_3^*$] = CO_2 Expulsion Rate [mol/L.d]

r_{rCO2} = K_{rCO2}[$CO_{2(g)}$] = CO_2 Dissolution Rate [mol/L.d]

Various authors (including Rosen et al., 2006) suggested that the forward and reverse reaction can be described by a single 'pseudo equilibrium' reaction or;

$$H_2CO_3^* \xrightarrow{r_{eqCO2}} CO_{2(g)} + H_2O \quad (6.28)$$

Where

$$r_{eqCO2} = r_{fCO2} - r_{rCO2} = K_{fCO2}[H_2CO_3^*] - K_{rCO2}[CO_{2(g)}] \quad (6.29)$$

or

$$r_{eqCO2} = K_{fCO2}\left([H_2CO_3] - K_{eqCO2}\left[CO_{2(g)}\right]\right) \quad (6.30)$$

Where

$K_{eqCO2} = \frac{K_{rCO2}}{K_{fCO2}} = \frac{1}{K_h.R.T_k}$ = CO_2 Equilibrium Constant [1/d]

K_h = Henry's Law Constant [1/d]

R = Ideal Gas Law Constant [J/mol.Kelvin]

T_k = Temperature [Kelvin]

6.1.3 Microbial Inhibition

Microbial inhibition was not initially intended as a part of the study, since it was not expected to have such a dramatic effect on the process. However, microbial inhibition was observed at various instances in the experimental phase of the project. It was thus decided to include inhibition functions into the dynamic AD-FTRW model. The functions and their corresponding inhibition constants were obtained from literature. At this point it should be stated that the modeling of process inhibitions in the AD-FTRW environment merits an extensive experimental study. However, due to time constraints on this project, this will be regarded as future research.

Microbial growth can only survive and proliferate in a narrow band of environmental conditions. For anaerobic digestion, pH and temperature is probably the two most important environmental factors. The influence of temperature is most often modeled by an Arrhenius-type law. However, these temperature functions are one sided (Figure 6.4), which implies that it can only describe inhibition as a function of temperature from a minimum to a maximum (typically 37^{o}C) after which the model deviates from the actual observations. This poses two problems for the dynamic AD-FTRW model. Firstly, since the actual FTRW stream undergoes cooling before it enters the biological treatment plant, a scenario where the cooling systems fails is quite plausible, so a temperature increase above the optimum for mesophillic anaerobic digestion as well as the traditional temperature decrease below the optimum needs to be considered. Secondly, mesophillic anaerobic digestion shows a bell shaped activity function around the optimum (37 ^{o}C) (Ross et al., 1992). At the time of the literature survey on inhibition functions, a 'double sided' temperature function that described mesophillic anaerobic digestion could not be found. Thus, the temperature inhibition function chosen to fit the requirements as close as possible is as follows.

$$I_T = sin\left(\frac{\left(\left(T_k - 273.15\right) - 22\right)\pi}{30}\right) \tag{6.31}$$

Where

I_T = Temperature Inhibition Function for All FOGs [-]

T_k = Reactor Temperature [Kelvin]

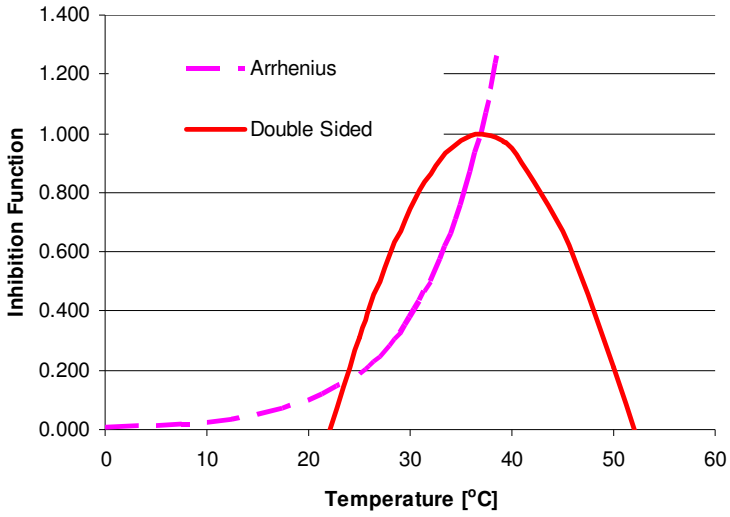

Figure 6.4, Inhibition of Mesophillic Anaerobic Digestion as a Function of Temperature with Arrhenius Law and "Double Sided" Inhibition function.

From Figure 6.4, it can be noted that for temperatures >37 ^{o}C, the Arrhenius law predicts a inhibition > 1, which shows this function is not suitable for the prediction of mesophillic anaerobic digestion's response to high temperature. Thus a double sided sine function was chosen for the dynamic AD-FTRW model. It should be emphasized that this is nothing more than a crude approximation for the system's response to temperature and requires further investigation. Since no literature could be found on how the individual trophic groups of anaerobic digestion responds to temperature, all the groups were modeled with one temperature inhibition function.

Unlike temperature, the modeling of pH inhibition is well studied and fairly well understood. pH often inhibits the biological activity due to non-dissociated acids and bases in the mixed liquor (Dochain & Vanrolleghem, 2001). Free acid and base inhibition has been defined as the disruption of homeostasis by changes in pH, caused by the passive transport of the free acid/base over the cell membrane and subsequent dissociation. However the actual proton activity in the bulk liquid also appears to contribute to the inhibitory nature of this environmental parameter. Batstone et al. (2002) suggested the following pH inhibition function for anaerobic digestion:

$$I_{pHZj} = \frac{1+10^{K_{pHj}(pH_{LLZj}-pH_{ULZj})}}{1+10^{(pH_r-pH_{ULZj})}+10^{(pH_{LLZj}-pH_r)}} \quad (6.32)$$

Where

I_{pHZj} = pH inhibition function of FOG_i [-]

pH_{ULZj} = Upper pH level of 50% inhibition of FOG_i [-]

pH_{LLZj} = Lower pH level of 50% inhibition of FOG_i [-]

pH_r = Reactor pH [-]

K_{pHj} = pH inhibition constant [-]

Because of the high acidity of FTRW and the fact that a strong base (NaOH) is dosed for pH control, it was experimentally observed that the on-line pH control system (Section 3.4.1) can easily over/undershoot the desired pH level. Thus, similar to temperature, a double sided pH inhibition function was selected. Eq 6.32 yields a bell shaped curve around a specified mean ((pH_{UL}+pH_{LL})/2). Figure 6.5 represents the pH inhibition curves for the various FOGs.

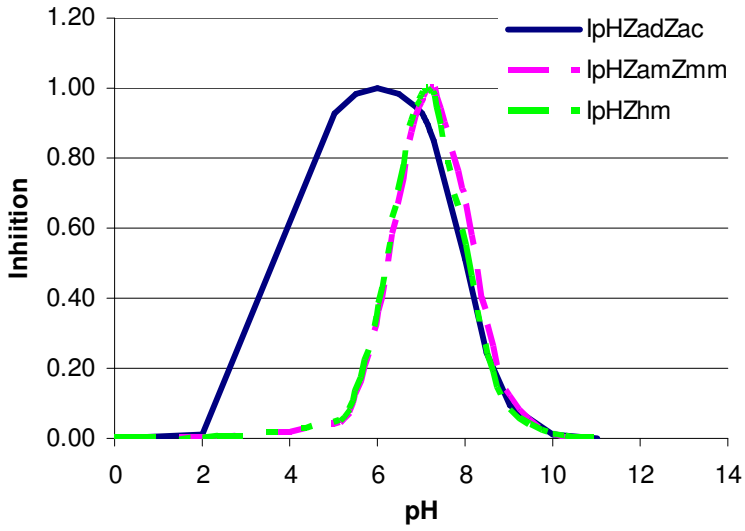

Figure 6.5, pH Inhibition Functions for Dynamic AD-FTRW

From Figure 6.5 it can be noted that three pH inhibition functions describe all of the FOGs in the dynamic model. It was found from literature that acetogenesis and acidogenesis has very similar responses to pH, thus one function describes all the FOGs in these two trophic groups ($I_{pHZadZac}$). No

information was found in the literature about the response of methanol utilizing methanogens to pH, thus it was assumed that these organisms had the same response to pH as the acetoclastic methanogens ($I_{pHZamZmm}$) (Batstone etal., 2002).

Note the acidogenic (Z_{ad}) and acetogenic (Z_{ac}) trophic groups have the widest activity range with variation in pH. This implies that as the pH goes out of bounds, the acetic acid and $H_{2(gas)}$ concentrations will increase in the effluent and correspondingly, the methane fraction in the biogas will decrease. Both SCFA and $H_{2(gas)}$ increases can have adverse effects on anaerobic digestion. The first of which is hydrogen inhibition.

The most inhibitory metabolic intermediate produced in anaerobic digestion is dissolved hydrogen gas ($H_{2(aq)}$). This compound has a detrimental effect on the activity of the H_2 producing organisms even at a micro-mol concentration. FOGs adversely affected by $H_{2(aq)}$ is Acidogenesis (Z_{am}), Acetogenesis (Z_{ac}) and most importantly the propionate reducing Acetogens (Z_{acPr}). Sötemann et al. (2005) suggests the following inhibition function for acidogenesis (Z_{ad}) (Eq 6.33):

$$I_{H_2Zad} = 1 - \frac{[H_{2(aq)}]}{k_{IH_2Zad} + [H_{2(aq)}]} \tag{6.33}$$

Where

I_{H2Zad} = The inhibition of acidogenesis (Z_{ad}) by $H_{2(aq)}$ [-]

$H_{2(aq)}$ = Dissolved hydrogen gas concentration [mol/L]

k_{IH2Zad} = Hydrogen inhibition constant. [mol/L]

Batstone et al. (2002) suggested the following inhibition functions for acetogenesis (Z_{ac}) (Eq 6.34):

$$I_{H_2Zacj} = \frac{1}{\left(1 + \frac{[H_{2(aq)}]}{k_{IH_2Zacj}}\right)} \tag{6.34}$$

Where

I_{H2Zacj} = The inhibition of the j^{th} acetogenic (Z_{ac}) group by $H_{2(aq)}$ [-]

$k_{IH2Zacj}$ = The inhibition constant for the jth Z_{ac} by $H_{2(aq)}$ [mol/L]

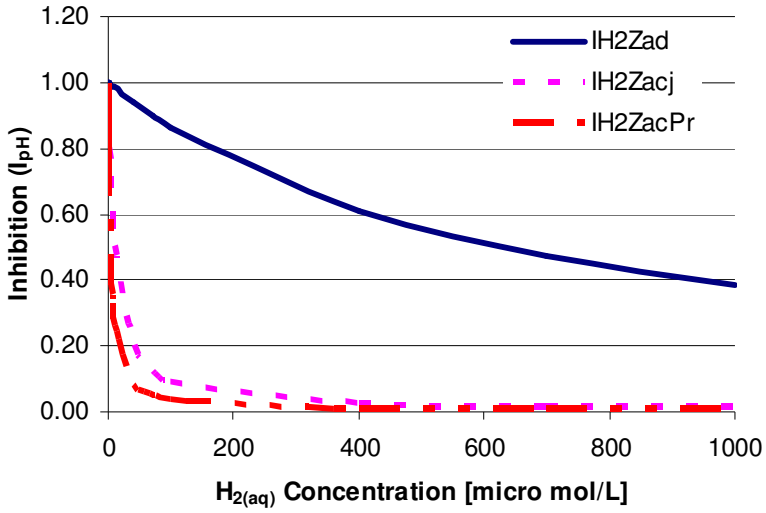

Figure 6.6, $H_{2(aq)}$ Inhibition of Z_{ad} and Z_{ac}

From Figure 6.6 it can be noted that the same $H_{2(aq)}$ inhibition function is used to describe all of the acetogenic (Z_{ac}) FOGs except for propionate reducing acetogenesis (Z_{acPr}). This group is so adversely affected by $H_{2(aq)}$ that it requires its own inhibition constant in Eq 6.34. The effect of $H_{2(aq)}$ inhibition on the methanogenic groups appears to be negligible compared to the that of acidogenesis (Z_{ad}) and acetogenesis (Z_{ac}).

The final inhibitory compound to be modeled is the total SCFA concentration ($SCFA_e$). $SCFA_e$ has an inhibitory effect on both acetoclastic methanogenesis Z_{am} and the propionate reducing acetogens (Z_{acPr}). The SCFA inhibition functions can be described as follows:

$$I_{A_i Z_{am}} = \frac{1}{\left(1 + \frac{[SCFA_e]}{k_{IA_i Z_{am}}}\right)} \tag{6.35}$$

And

$$I_{A_i Z_{ac\,Pr}} = \frac{1}{\left(1 + \frac{[SCFA_e]}{k_{IA_i Z_{ac\,Pr}}}\right)} \tag{6.36}$$

Where

$I_{AtZam}/I_{AtZacPr}$ = Inhibition of Z_{am} & Z_{acPr} by $SCFA_e$ [-]

$SCFA_e$ = Total SCFA concentration [mol/L]

k_{IAtZam} & $k_{IAtZacPr}$ = Inhibition constants [mol/L]

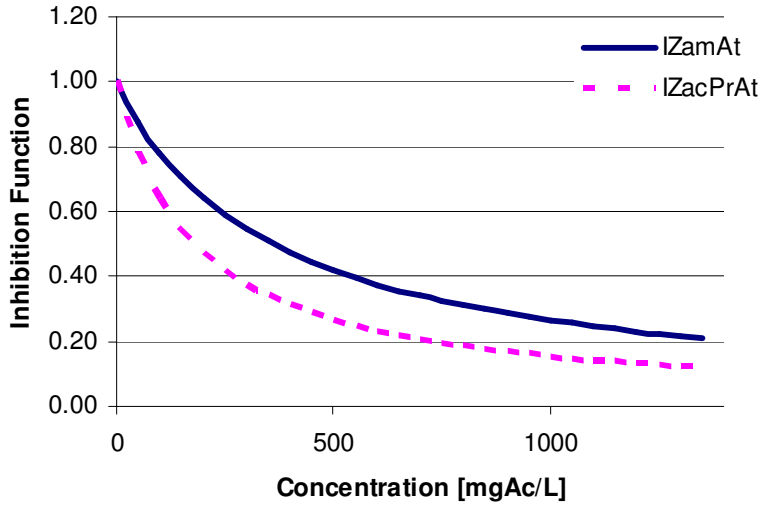

Figure 6.7, Z_{am} & Z_{acPr} Inhibition as a Function of $SCFA_e$

Figure 6.7 shows that the inhibition of both acetoclastic methanogenesis (Z_{am}) and propionate reducing acetogens (Z_{acPr}) is almost linear with an increase in Effluent Short Chain Fatty Acids ($SCFA_e$). However, Z_{acPr} is much more strongly affected by an SCFA increase than Z_{am}, with a 50% decrease in activity occurring at a concentration of 0.0175 mol/L or 1050 mgAc/L (as compared to 0.6 mol/L for Z_{am}).

6.1.4 Assembling the dynamic AD-FTRW model

A Petersen Matrix representing the dynamic AD-FTRW model is presented in Appendix 6.4 with the model components in the columns across the top and the model processes in the rows. The growth processes are shown in the uneven row numbers 1 to 17, with the death rates presented by the even

numbered processes 2 to 18. The complete derivation of the (i) metabolic processes (catabolic and anabolic stoichiometry), (ii) dissociation of the SCFAs and the (iii) weak acid base chemistry combined with the acetogenic growth processes is presented in Appendix 6.3. The remainder of the growth processes (acidogenesis and methanogenesis) is derived in much the same manner as presented in Appendix 5.3. The components 10 to 15 are the total concentrations (dissociated and un-dissociated) of each of the biodegradable fractions in FTRW.

The only weak acid/base chemistry relationships not included in the metabolic processes are the conversion of hydroxide (OH^-) to bicarbonate (HCO_3^-) and the expulsion/dissolution of carbon dioxide, represented by processes 19 and 20 respectively. The final process (21) describes the hydrolysis of urea (component 17) to saline ammonia (component 8).

pH is calculated externally exactly as discussed in Chapter 5 (Section 5.3.1 and Appendix 5.5), using three components i.e. 3 (CH_4), 5 (CO_2) and 7 (HCO_3^-). Further external calculations include effluent COD (S_{be}), effluent SCFA ($SCFA_e$), reactor solids concentration (MLSS), $H_2CO_3^*$Alkalinity and effluent nitrogen (N_{te}) as presented in Appendix 6.4.

6.2 Model Verification and Calibration

As was the case in the steady state model, the stoichiometry of each FOG in the dynamic AD-FTRW model is dependant on two constants, namely the yield (Y_j) and the endogenous decay rate (b_j). Since the dynamic model is time dependant, a second set of kinetic constants is required namely; the maximum specific growth rate (u_{maxj}) and the half saturation constant (K_{sj}). The latter two parameters are required to characterize the process rate equations. In the model calibration, the ideal values for the stoichiometric and kinetic parameters will be identified by a combination of literature survey and an automated parameter optimization done with water treatment simulation software package named West®. The constants required for the inhibition functions of pH, temperature, SCFA and dissolved $H_{2(gas)}$ will also be presented.

Since the variation on both the u_{max} and b values for anaerobic digestion is minimal (within 1 order of magnitude), these were chosen from literature. Next West® was programmed to auto-calibrate the Y-values for the various FOGs. This was done by simulating the AD-FRTW reactor subjected to steady state flow and load conditions for more than three sludge ages until the steady state model

outputs (VSS, gas production and composition) matched the steady state model results. The reactor volume was chosen such that the effluent concentration (S_{be}) ~ 0 and the temperature and pH kept at 37 ^{o}C and 7.1 respectively. Because of this, the effects of K_s and inhibition were assumed to be negligible. Based on these results, the internal consistency of the model was checked by checking the COD, C, H, O, N mass balances. The outcome is listed in Table 6.1 and it can be seen that all the influent fluxes (mass/d) are accounted for in the exiting masses. The model therefore conforms to mass balance and continuity principles and can be further calibrated to represent the AnMBR.

Table 6.1, Dynamic AD-FTRW Model Mass Balance (OLR = 15 kg/m$^3_{VR}$/d & R_s = 300 days)

	Entering	Exiting			
Parameter	**Influent**	**Effluent**	**Waste Flow**	**Biogas**	**% Balance**
COD [gCOD/d]	460.6	5.473	0.017	455.3	100.00
C [mol/d]	12.73	1.463	0.004	11.25	100.00
H [mol/d]	2767	2758	8.502	0.028	100.00
O [mol/d]	2767	2758	8.502	0.008	100.00
N [mol/d]	6.073E-05	6.044E-05	2.909E-07	0	100.00

After model verification the yield (Y) and death (b) values of the different FOGs was applied to attain an estimate of the mass fractions of the individual FOGs as fractions of the calculated VSS. These fractions were assumed to apply to the measured VSS of the AnMBR. The mass fractions of the different organism groups are shown in Figure 6.8.

To get an estimation of the K_s-values for the individual FOGs, batch test experiments were conducted on biomass harvested from the AnMBR system and the utilization of the individual SCFAs were observed with time. This data, along with the Y, b and u_{max} values for each FOG was then used to auto-calibrate the K_s-values in West®. The steady state and batch test calibration is discussed in detail below.

6.2.1 Steady State Calibration

For a constant flow and load bio-reactor with sludge age control, steady state is typically reached after three sludge ages. If this constant flow and load state is applied for longer than 3 sludge ages, then the dynamic and steady state models should yield virtually identical outputs for the same set of input parameters.

Provided the above criteria are met, the steady state model results can be used to calibrate some of the stoichiometric constants required in the dynamic model. However, since the number of parameters required is more than the number of stoichiometric relationships, only ratios between parameters can be explicitly identified. Thus prior knowledge about some parameters is required to identify of each individual parameters.

Under steady state conditions with effluent COD concentration (S_{be}) = 0 i.e. eliminating process rates and reducing the model to stoichiometry on the basis that the observed yield (Y_{obs}) = $Y_{metabolic}/(1+b.R_s)$, the influent biodegradable COD (S_{bi}) can only exit the system in the form of biogas (S_m) or biomass (Z_{VSS}). The ratio between the COD exiting as biogas vs. the COD entering the system is governed by the net yield (Y_{obs}), which is a fraction of the metabolic yield ($Y_{metabolic}$) and the endogenous respiration rate (b_i) for a fixed unbiodegradable biomass residue f = 0.08 and sludge age (R_s). Since the endogenous respiration rates of the anaerobic organism groups are fairly similar, a literature survey was done to obtain the b_j values. Thus the steady state parameter optimization was only done on the stoichiometric yield ($Y_{metabolic}$) values for each of the FOGs.

The parameters optimization in West® requires lower- and upper-bound values for each of the parameters to be optimized. These ($Y_{metabolic}$) values were obtained from literature and the lowest and highest quoted values for each of the organism yield values were taken as the upper and lower-bound values respectively. To avoid the issues around using a 'Simplex' optimizer to fins the optimim Yield values, a constrained 'Praxis' optimizer with a covariance and perturbation factor set to 1E-6 was used for a high degree of accuracy. Table 6.2 displays the upper and lower-bound and the optimized Y value for each of the functional organism groups as optimized for a sludge age of 300 days:

Table 6.2, Steady State Metabolic Yield ($mol_{Biomass}/mol_{substrate}$) Optimization

Metabolic Yield	Lower-Bound	Upper-Bound	Optimized Value
Y_{ad}	0.03 [4]	0.15 [3]	0.1074
Y_{acHx}	0.03 [1]	0.1027 [1]	0.0474
Y_{acVa}	0.0338 [3]	0.1027 [3]	0.0496
Y_{acBu}	0.02875 [1]	0.125 [1]	0.0558
Y_{acPr}	0.0278 [2]	0.0632 [3]	0.0376
Y_{acEt}	0.0125 [1]	0.125 [1]	0.0832
Y_{am}	0.0056 [3]	0.0304 [3]	0.0157
Y_{mm}	0.0056 [1]	0.0304 [1]	0.0127
Y_{hm}	0.0014 [3]	0.0183 [3]	0.004

1. **Kalyuznhyi, 1997b**
2. **Sötemann et al., 2005**
3. **Batstone et al., 2002**
4. **Sam-Soon et al., 1989**

Table 6.2 shows that optimized yield values for all of the functional groups could be found between the lower and upper bounds indicating that none of the $Y_{metabolic}$ values found compensated for another one constrained by the upper and lower bounds. After the yield optimization the dynamic model was compared to the steady state model for a constant load of 346 gCOD/d (i.e 19.23 L/d at 18 000 mgCOD/L) for a 23 L reactor volume for a sludge age of 100, 300 and 500 days (Table 6.3):

Table 6.3, Steady State and Dynamic AD-FTRW Model Comparison for a constant influent flow rate of 19.23 L/d and a reactor volume of 23 L

Sludge Age	R_s = 100 days			R_s = 300 days			R_s = 500 days		
Parameter	**SS**	**Dyn**	**% Error**	**SS**	**Dyn**	**% Error**	**SS**	**Dyn**	**% Error**
S_{ti} [mgCOD/L]	18000	18000		18000	18000		18000	18000	
S_{te} [mgCOD/L]	0	9.60		0	7.83		0	7.50	
CH_4 [L/d]	135.0	134.8	0.1	135.8	135.7	0.0	135.9	136.0	-0.1
CO_2 [L/d]	75.5	78.4	-3.8	76.0	79.0	-3.9	76.1	79.2	-4.1
Alk [mg$CaCO_3$/L]	2642	2593	1.9	2674	2644	1.1	2681	2660	0.8
MLVSS [mgVSS/L]	12.48	13.28	-6.3	21.17	21.17	0.0	28.80	23.40	18.8
pH	7.1	7.09	0.1	7.1	7.1	0.0	7.1	7.1	0.0
N_{ti} [mgN/L]	85.3	85.3	0.0	85.3	85.3	0.0	85.3	85.3	0.0
N_{te} [mgN/L]	70.4	69.4	1.3	76.9	76.9	0.0	78.4	79.7	-1.6
$COD_{Methane}/COD_{Influent}$ [%]	98.7	98.6	0.1	99.3	99.2	0.0	99.4	99.5	-0.1
$COD_{Biomass}/COD_{Influent}$ [%]	1.3	1.4	-10.6	0.7	0.8	-6.2	0.6	0.5	11.6
COD	100.0	100.0	0.0	100.0	100.0	0.0	100.0	100.0	0.0
C	100.0	100.0	0.0	100.0	100.0	0.0	100.0	100.0	0.0
H	100.0	100.0	0.0	100.0	100.0	0.0	100.0	100.0	0.0
O	100.0	100.0	0.0	100.0	100.0	0.0	100.0	100.0	0.0
N	100.0	100.0	0.0	100.0	100.0	0.0	100.0	100.0	0.0
Charge	100.0	100.0	0.0	100.0	100.0	0.0	100.0	100.0	0.0

Note: Since the gas temperature was assumed to be 37 °C, the molar volume of the biogas was taken as 25.285 L/mol

Table 6.3 shows that all the masses again balanced and after optimization a large degree of correlation (< 4 % error) exists between the steady state and dynamic AD-FTRW model on most of the parameters evaluated. However, the dynamic model tends to under-predict reactor MLVSS by as much as 19% as the sludge age increases from 300 to 500 days and under predicted the MLSS by 6% by decreasing the sludge age to 100 days. The resultant effect is also an over (or under) - prediction of the effluent N concentration (N_{te}). However, to place this error into interest, the % of the influent COD exiting as MLVSS is ~1% and of methane is ~99%. The 19% error on the reactor VSS concentration estimate results in a 0.04 % error on the mass of VSS wasted per day (i.e. 19%/500 = 0.04%). This is because the mass of VSS wasted per day is 1/500th of the mass of VSS in

the reactor at a 500 d sludge age. Clearly this error is acceptable from a sludge production point of view. Figure 6.8 gives a presentation of how the VSS is distributed between the various FOGs and also endogenous mass.

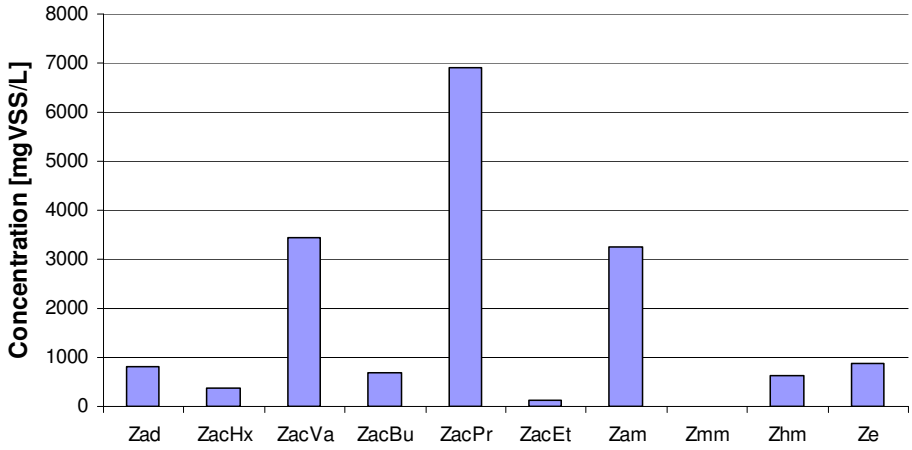

Figure 6.8, FOG and Z_e Mass Distribution (OLR = 15 kgCOD/m^3/d & R_s = 300 days)

From Figure 6.8 it can be noted that the major part of the VSS consists of acetogenic biomass with especially the propionate (Z_{acPr}) and valeric acid (Z_{acVa}) reducers contributing a significant amount to the total VSS due to their high yields. As expected the acetoclastic methanogens (Z_{am}) are also a major contributor to the reactor VSS. Interestingly, even at a sludge age of 300 days the endogenous mass fraction (Z_e) is only ~5% of the total VSS.

6.2.1 Batch Test Calibration

Analogous to the death rates (b_j), the quoted maximum specific growth rates (u_{maxj}) in the literature does not differ significantly for the individual FOGs, thus the required u_{max} values were obtained from literature. Contrary to this, a wide range of values is quoted in literature for the half saturation constants (K_{sj}) for each of the FOGs. Thus, batch test experimental data were used to calibrate the K_s-values.

Batch tests were done using mixed liquor harvested from the AnMBR and synthetic FTRW feed. The mixed liquor was diluted and placed in a 1 L batch reactor with environmental conditions (alkalinity, pH and temperature) similar to that of the AnMBR. A known amount of FTRW was introduced and samples were taken at regular intervals. Analysis done on the samples was the

following; Filtered COD, Total SCFAs (VFA-5pt), pH and the individual SCFAs were also analyzed with an HPLC. For a detail discussion on the experimental setup, experimental methods and data reconciliation techniques for the batch tests, refer to Appendix 6.2.

The parameter optimization was started with the longest chain length SCFAs namely hexanoic acid (Hx) and valeric Acid (Va), since these can only be degraded and not produced by the acetogenesis process (Figure 6.8).

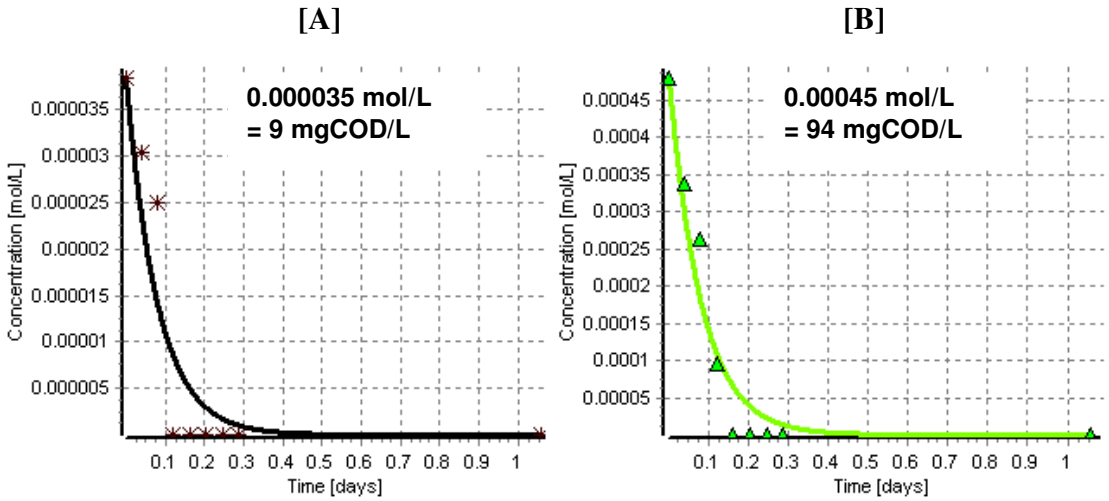

Figure 6.9, Hexanoic – [A] and Valeric Acid [B] Degradation vs. Time

Figure 6.9 shows a fairly good fit of the dynamic model to the experimental data for hexanoic- (Hx) and valeric acid (Va). Very low hexanoic (Hx) and valeric acid (Va) concentrations were measured earlier in the batch test than predicted, which indicates a lower half saturation constant (K_s) would provide a better fit to these low concentrations. However, because 0.000005 mol/L is extremely low (~0.5 mgCOD/L) and the higher concentrations are given more emphasis, the estimated K_s-values were accepted. Butyric acid (Bu) enters the system via the feed and is also produced in the degradation of Hx. From Figure 6.10A it can be noted that the model prediction for butyric acid (Bu) removal also fits the experimental data quite well, but also shows higher predicted values than measured at the low concentration.

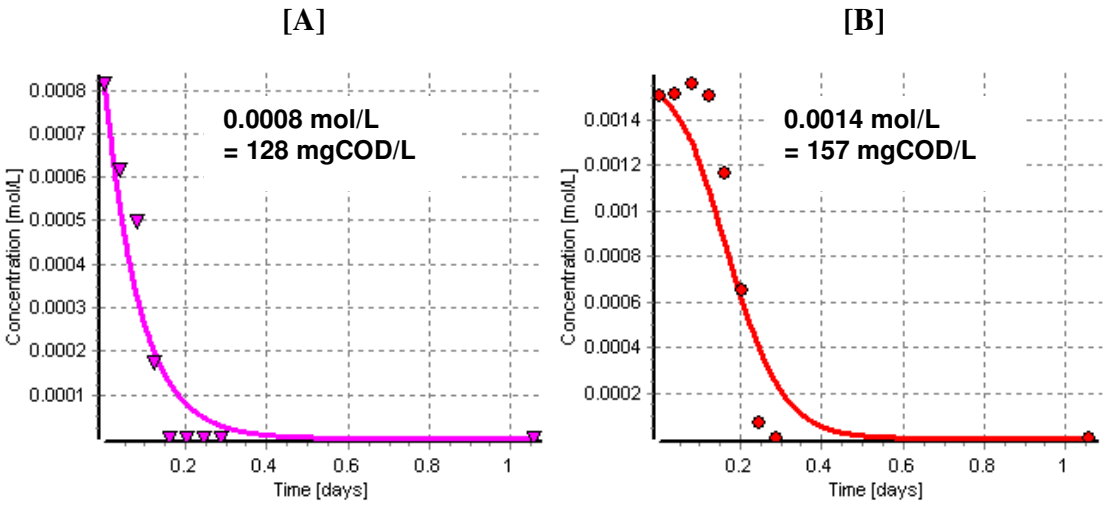

Figure 6.10, Butyric – [A] and Propionic Acid [B] Degradation vs. Time

Propionic acid enters the system via the feed but is also produced by valeric acid (Va) degradation (Figure 6.10B). A significant amount of propionic acid is produced by valeric acid degradation, so much so that the propionic acid peaks around 0.1 d (2.4 h) after the injection time ($t_{injection}$) (Appendix 6.2). From Figure 6.10B it can be noted that the dynamic model does not predict the propionic peak as pronounced as observed in the experimental data. This would seem to indicate that the growth rate of the acetogenic organisms is too fast. However, it cannot be reduced because then the predicted decrease in concentration takes far too long. It therefore appears that the Monod equation is not the best model to represent the acetogenesis kinetics. However it was retained because it predicted the decreasing concentration reasonably well and therefore was assumed sufficient for this first version of the dynamic AD-FTRW model. The HPLC analyzer was only calibrated to a concentration of 0.00025 mol/L for the SCFAs evaluated (Method Detection Limit = 0.00025 mol/L) and data below this value would probably be recorded as zero. This might have an effect on the calibration of the K_s-values, but at the time of the investigation, this was the most sensitive SCFA analyzer available.

Similarly, the acetic acid (Ac) concentration peaks well after $t_{injection}$. This is because acetic acid is produced in the oxidation of all of the higher SCFAs. Figure 6.11 shows how the Ac concentration increases without any removal ($\mu_{maxAm} = 0$) as well as how Ac is removed by the acetoclastic methanogen functional group.

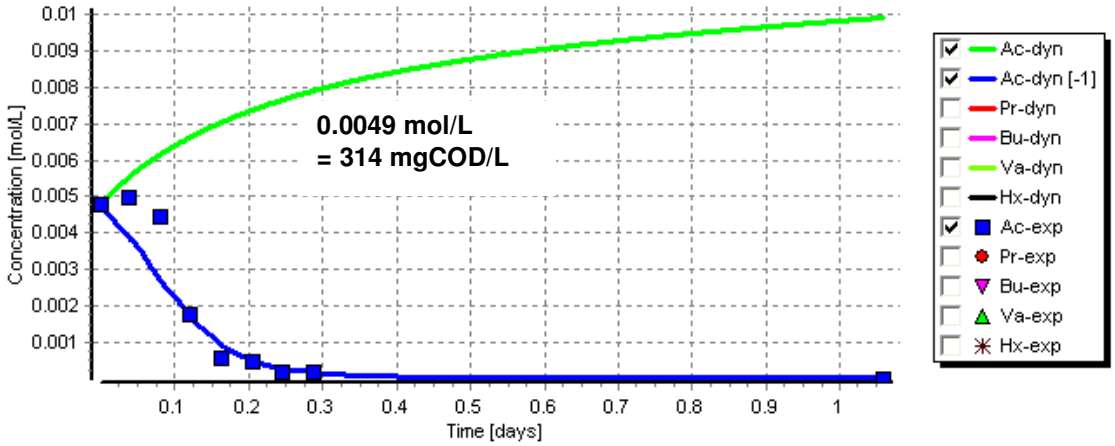

Figure 6.11, Acetic Acid Accumulation (Ac-dyn) & Removal (Ac-dyn[-1]) vs. Experimental Data (Ac-exp)

From Figure 6.11 it can be noted that there is a significant addition of acetic acid after $t_{injection}$. The reason for this is the all of the higher SCFAs are converted to Ac and other metabolic products. If the model prediction is compared to the experimental results, it can be noted that the model predicts relatively well the low concentrations. However the two measured concentrations between 0.05 and 0.1 days are under predicted by as much as 50%.

The analysis for the remaining soluble biodegradable fractions in the system (EtOH, MeOH) was regarded as impractical; because they are very low in the FTRW (< 2%) so will not affect the effluent COD concentration. Also utilization of biomass slowly biodegradable organics (S_{bp}) was not calibrated kinetically, since these particulate organics remain in the AnMBR for the duration of the sludge age (which was very long > 100 days) and so are virtually completely degraded also. The kinetic constants for the digestion of these compounds were obtained from literature (Sötemann et al., 2005).

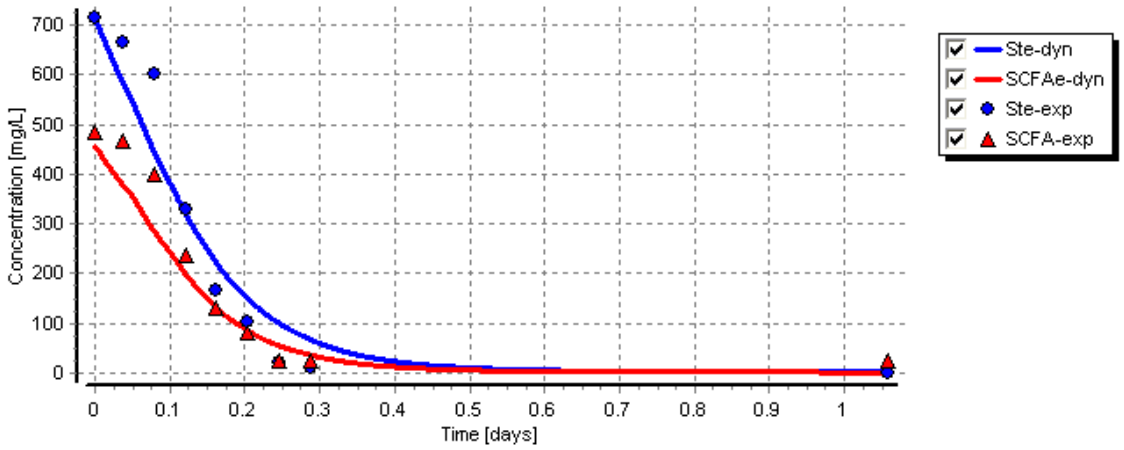

Figure 6.12, Total Filtered COD [mgCOD/L] & Total SCFA [mgAc/L] vs. Time

Both the total filtered COD (S_{te}) and total SCFA predictions correlate well with the measured values in the high and low ranges (Figure 6.12). For the higher concentrations (>300 mgCOD/L) concentrations deviations as large is 25% is observed. It should be emphasized that the both the 5-point titration method and the COD tests showed large variations (± 15%). Note; the total filtered COD in the batch test was used to simulate the membrane filtered effluent of the AnMBR. Table 6.4 displays the upper and lower bounds and also the K_s and μ_{max} values from the batch test simulation and parameter estimation.

Table 6.4, Kinetic Constant Parameter Optimization

Functional Group	Kinetic Constant	Lower-Bound	Upper-Bound	Selected Value	Optimized K_s [mgCOD/L]
Z_{acHx}	$U_{maxAcHx}$	16 [3]	0.041 [3]	1.18	
	K_{sAcHx}	1.14E-4 [3]	0.0066 [3]	2.10E-04	53.8
Z_{acVa}	$U_{maxAcVa}$	1.4 [4]	0.69 [3]	1.53	
	K_{sAcVa}	3.23E-4 [3]	0.00186 [3]	0.0009	187
Z_{acBu}	$U_{maxAcBu}$	0.24 [1]	2 [1]	2.27	
	K_{sAcBu}	8E-6 [1]	3.125E-3 [1]	5.00E-03	800
Z_{acPr}	$U_{maxAcPr}$	0.02 [3]	2.7 [3]	1.1	
	K_{sAcPr}	8.9E-5 [2]	0.01023 [3]	2.00E-03	224
Z_{acEt}	$U_{maxAcEt}$	6.72 [1]	10 [1]	1.15	
	K_{sAcEt}	3E-6 [1]	1.28E-4 [1]	1.00E-03	96.0
Z_{am}	U_{maxAm}	0.02 [3]	4.4 [2]	1.15 [2]	
	K_{sAm}	1.7E-4 [3]	0.0145 [3]	5.00E-04	32.0
Z_{mm}	U_{maxMm}	0.02 [3]	4.4 [2]	1.15	
	K_{sMm}	1.7E-4 [3]	0.0145 [3]	1.00E-03	48.0
Z_{hm}	U_{maxHm}	0.02 [3]	8 [3]	1.2 [2]	
	K_{sMm}	1E-6 [3]	6E-4 [3]	1.00E-03	2.45
Z_{ad}	U_{maxAd}	0.41 [3]	43 [1]	0.8 [2]	
	K_{sAd}	4.2E-5 [1]	6.66E-3 [3]	1.00E-03	140

μ_{max} [1/d]

K_s [mol/L]

1. Kalyuznhyi, 1997b
2. Sötemann et al., 2005
3. Batstone et al., 2002
4. Sam-Soon et al., 1989

From Table 6.4 the growth rates of all of the functional groups considered are fairly similar, as expected. However, the K_s values differ considerably. This implies that even though most of the functional groups grow at the similar rates, some groups such as acetoclastic methanogenesis (K_{sAm} = 0.034 mol/L) can only function at high substrate concentrations while others can function at low substrate concentrations (hydrogenotrophic methanogenesis, K_{sHm} = 0.000156mol/L). FOGs with high K_s-values cannot remove their substrate down to very low values and these would then be the

reactor hydraulic retention time governing groups. However, because the sludge age of the reactor is so very long, to maintain the required TSS for membrane operation, even the bioprocesses with high K_s-values will virtually reach completion and associated effluent substrate concentrations (S_{be}) will be very low. Once the model has been validated, the predicted S_{be} versus sludge age (R_s) will be explored. The possible overlap of the system sludge age requirements for membrane scour (high MLSS) and for bioprocess kinetics - effluent SCFA and COD is discussed in Section 6.4 below.

6.3 Model Validation

To validate the dynamic AD-FTRW model, an extract (day 550 to 605) of the 700 day AnMBR experimental dataset was chosen where the system was subjected to dynamic flow and load conditions, but no nutrient deficiencies or membrane fouling problems occurred – since these can as yet not be modeled.

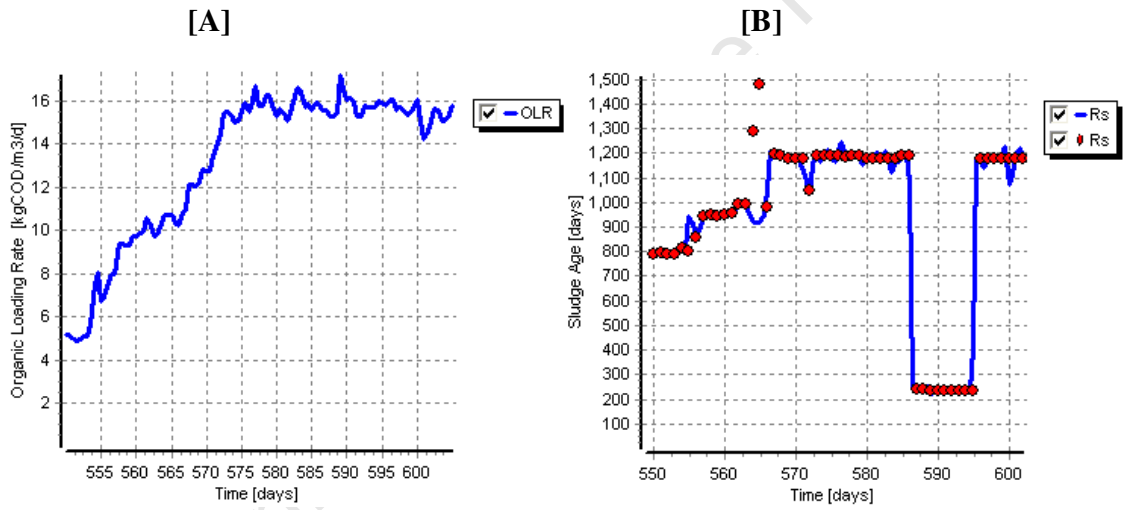

Figure 6.13, A and B: AnMBR Experimental OLR & Sludge Age

Figures 6.13A and B show that the experimental data applied to validate the dynamic AD-FTRW model were actual plant data with large changes in (i) flow, (ii) organic load and (iii) sludge age which was calculated from the volume of mixed liquor wasted from the system daily ($R_s = V_r/Q_w$). In Figure 6.13A it can be noted that in the first part of the period observed the OLR was increased by increasing the flow through the reactor, the second part of the period (> day 575) the OLR was kept constant around ~ 16 kgCOD/m^3_{Vr}/d. The on-line control system was relaxed during this period. The sludge age was also varied considerably in an attempt to control the MLSS of the AnMBR. The experimentally measured and model predicted alkalinity, reactor pH, biogas production, biogas

partial pressure of CO_2, effluent COD and SCFA concentrations and reactor MLSS are given in Figures 6.14 to 6.17.

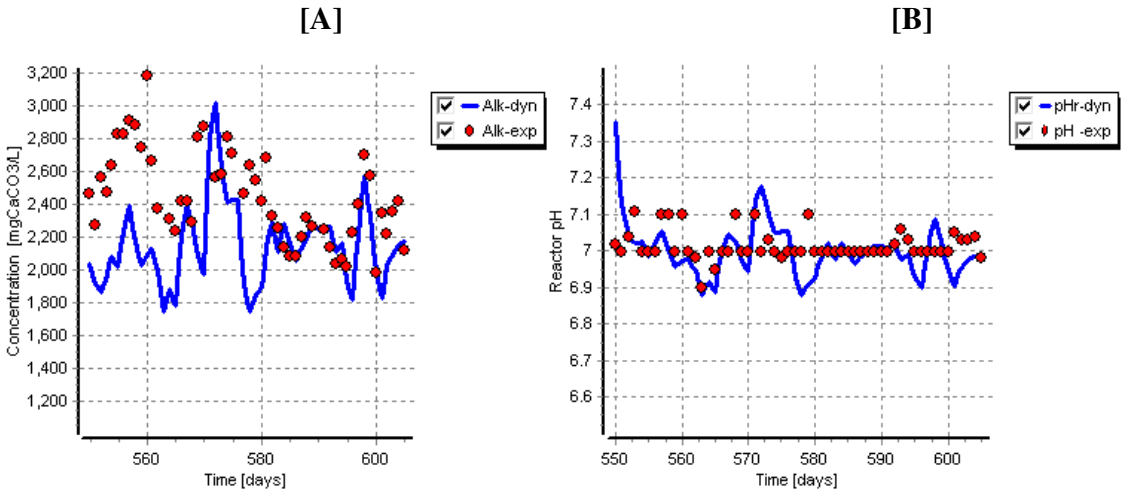

Figure 6.14 [A] and [B]: pH and Alkalinity; Experimental vs. Dynamic Model

For a detail discussion on the various parameters (OH^-, Urea and Dissociated SCFAs) contributing to the total alkalinity, refer to Section 5.2. In both cases the experimentally observed pH and alkalinity shows far less variability than the model. This is due to the input file for the simulation. The data in this file is daily averages over the experimental period, thus the dynamic model will yield "averaged" daily outputs. Contrary to this, the experimentally measured outputs measured on the AnMBR are mostly grab samples, thus showing a large variability. The dynamic AD-FTRW model's pH predictions yields a P_{90} = 4% which points towards a strong correlation with the measured pH data. For alkalinity a P_{90} = 25% and a P_{50} = 14% is obtained if compared to the actual measurements. In contrast to this, the dynamic model shows a very good correlation with the measured daily biogas production (Figure 6.15A).

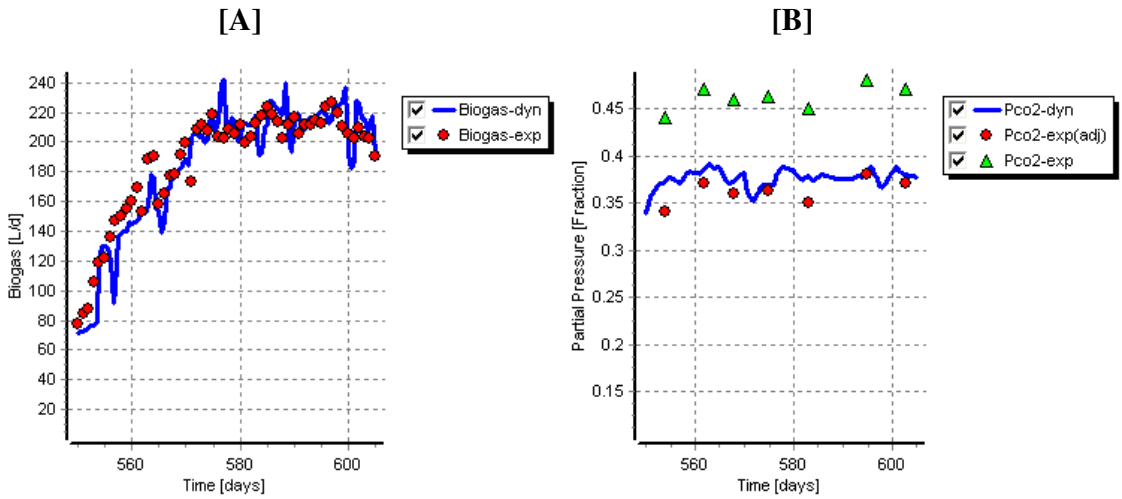

Figure 6.15, [A] and [B]: Biogas and P_{CO2}; Experimental vs. Dynamic Model

For the CO_2 partial pressure the dynamic model (P_{CO2}-dyn) also correlates well with the experimentally observed values (P90 = 7%), provided the CO_2 partial pressure data (P_{CO2}-exp) are corrected (P_{CO2}-exp(adj)) to fix the COD balance as discussed in Chapter 5 (Figure 6.15B). This was done by forcing a 100% COD mass balance on the experimental data by decreasing the P_{co2} values, which were typically 0.10 higher (~0.45) than required for a COD balance (~0.37).

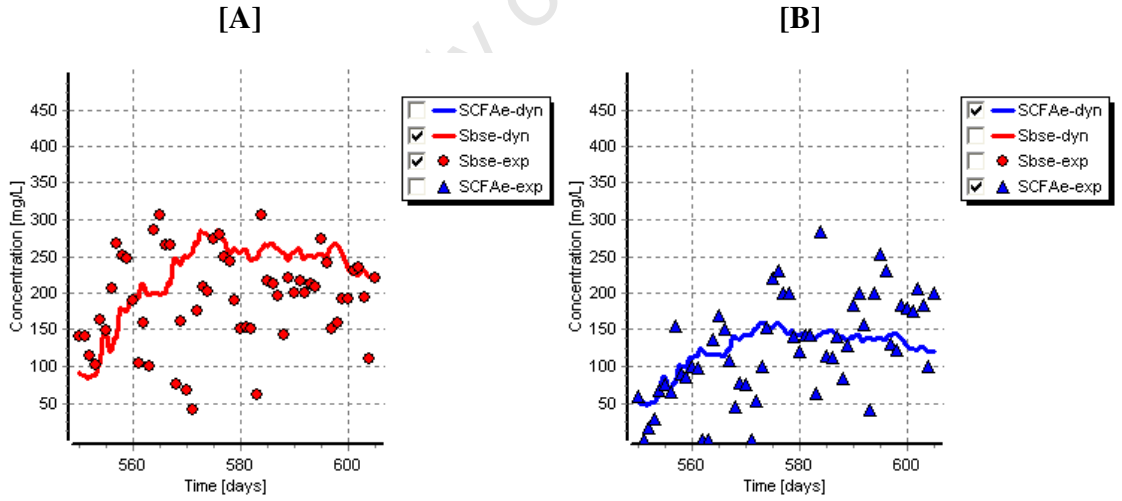

Figure 6.16 A & B: Effluent COD ($SCFA_e$) and $SCFA_e$; Experimental vs. Dynamic

In the dynamic model, far less variance is observed in the effluent COD and SCFA concentrations than in the experimental data (Figure 6.16). A possible explanation for this is that the dynamic model gives the effluent daily average concentration, because the influent COD concentrations are constant

over 24 hour periods. Whereas both the effluent COD (S_{be}) and Effluent Short Chain Fatty Acids ($SCFA_e$) experimental data are grab samples taken from the AnMBR. The experimental vs. predicted outputs for S_{be} and $SCFA_e$ are 190^S vs. 224^S mgCOD/L (P_{90} = 65%) and 134^S vs. 112^S mgAc/L (P_{90} = 75%) respectively. The dynamic model predicts the reactor MLSS with a large degree of accuracy, with a 16.9^S predicted average compared to a 17.4^S (P_{90} = 14%) measured average for the dataset (Figure 6.17). Note: This variance was also significantly less than was observed for the experimental data in Chapter 5 (Section 5.2). The comparatively large degree of variance in the model predicted MLSS is possibly due to variations in LOR and sludge age.

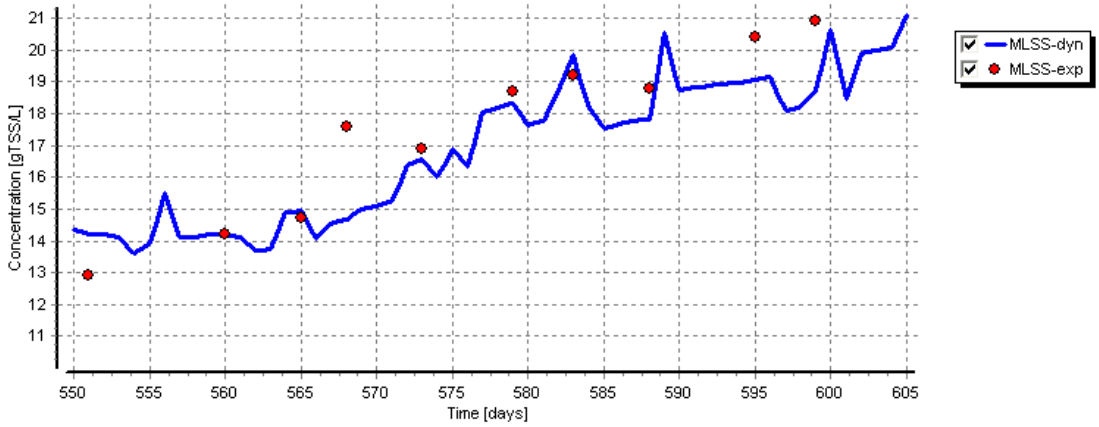

Figure 6.17, MLSS; Experimental vs. Dynamic

Figure 6.18 displays the composition of the effluent COD (S_{be}) as predicted by the dynamic AD-FTRW model. It can be seen that most (~53 %) of the COD that escapes in the effluent is acetic acid (Ac). This is expected because more then 50% of FTRW consists of acetic acid (Ac) and secondly the acetoclastic methanogens have a fairly high half saturation constant (K_{sAc}, Table 6.4)

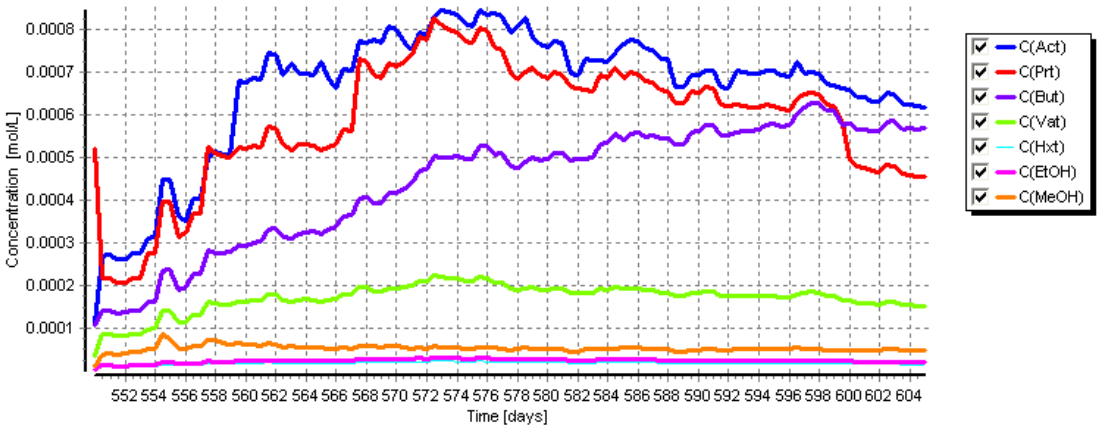

Figure 6.18: AnMBR Treated Effluent Composition

Secondly, Propionate and Butyric Acid makes up the 2nd and 3rd largest fractions with the remainder being the longer chain SCFAs and the least concentration is the dissolved H_2 gas (not shown). The effluent substrate was also plotted as a breakdown of the total effluent COD in Figure 6.19.

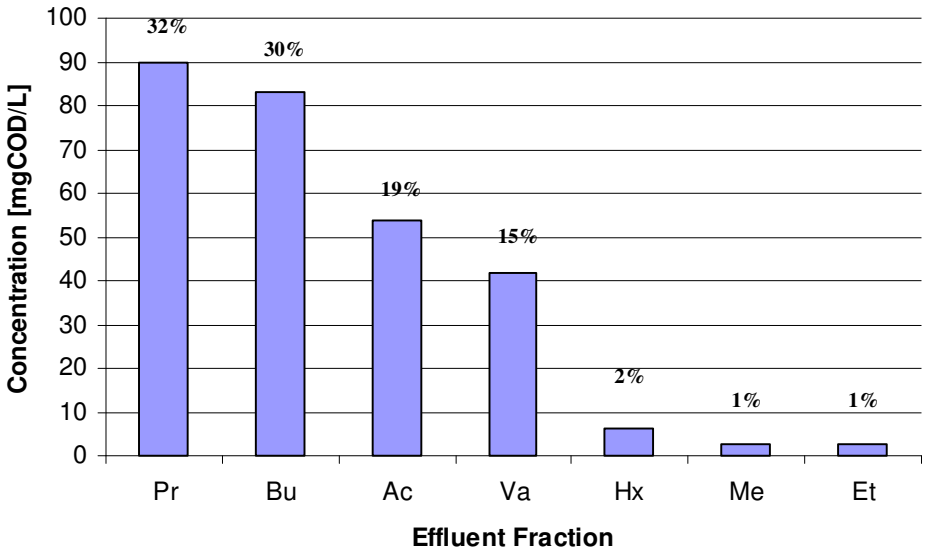

Figure 6.19, Effluent Biodegradable Fractions (Day 576)

Day 576 was chosen since the effluent COD was at its highest on this day and the OLR constant at 16 kgCOD/m^3.d (Figure 6.19). From the COD breakdown it can be noted that mostly propionate (32%) exits the system. From the predicted VSS composition (Figure 6.20), it can be noted that even at long sludge ages (>500 days) most (>80%) of the biomass is active. This is because the

endogenous respiration rates of the organisms are all very low (~ 0.04 /d) and the unbiodegradable fraction of the biomass also low (f = 0.08) (Figure 6.20).

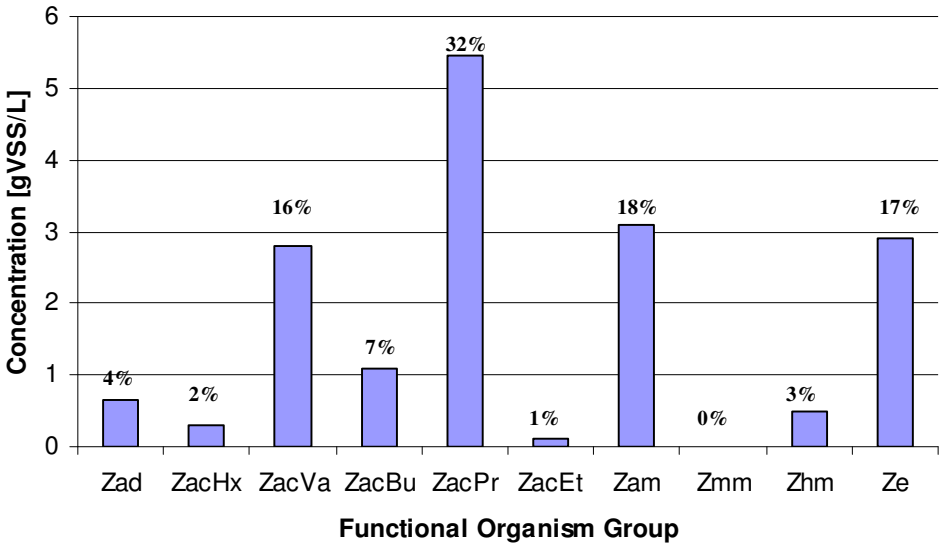

Figure 6.20, Predicted VSS Composition

Secondly it can be noted that the FOGs contributing the most to the VSS is the propionate reducing acetogens (Z_{acPr}) followed by the acetoclastic methanogens (Z_{am}). As expected the acidogens (Z_{ad}) contributes only a small fraction (<4%) of the total VSS because the endogenous respiration rate is so low. Of the total biogas production, 3.8% is due to biomass biodegradable organics (S_{bp}) digestion, which is significant because with only 1% of the influent COD becoming biomass wasted, the observed yield (Y_{obs} = nett sludge production) is only about a quarter of the metabolic sludge production.

6.4 Modeling Reactor Failure

In this section, the inhibition functions that was chosen from literature to best represent the AD-FTRW environment, will be applied to predict the AnMBR response to fluctuations in pH, Temperature, $H_{2(aq)}$ and reactor SCFA concentrations. Factors including (i) pH and (ii) temperature fluctuations and (iii) OLR overload situations will be evaluated. $H_{2(aq)}$ inhibition will not be evaluated explicitly, but the effects of the various parameters on the $H_{2(aq)}$ concentration will be

presented. Since FTRW is nitrogen deficient and urea is only dosed as a nutrient, its concentration and resultant effect on pH and inhibitions will be assumed negligible compared with other compounds under evaluation. To model reactor failure, the sludge age was set to 300 days and the OLR to 20 kgCOD/m^3/d.

6.41 Reactor Failure Due to OH^- Dosing

The first scenario investigated was that of a failure of the NaOH dosing system required for pH control. This can happen due to the NaOH storage tank running empty or a dosing pump malfunction. In the first simulation (Figure 6.21 - OHin[-1] and Figure 6.22) a pH decrease from the normal 7.1 to 6.8 was evaluated. The NaOH dosing was decreased from its normal 0.8 molOH/d (1285 mgNaOH/L) to 0.24 mol/d (385 mgNaOH/L). This caused the system to acidify, resulting in the desired pH decrease to 6.8. After 72 hours, the OH^- dosing was reset to the original level (Figure 6.21 – OHin[-1]) and the pH in the reactor recovered back to 7.1.

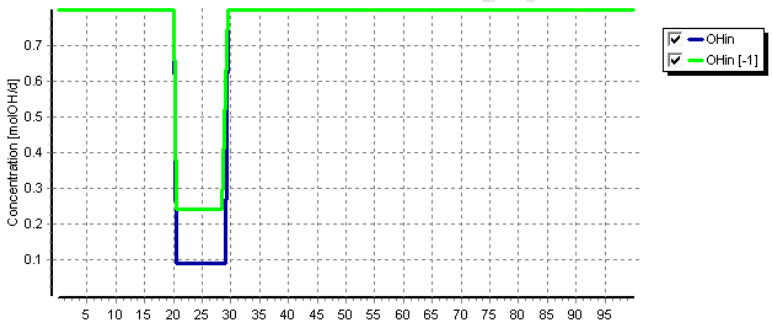

Figure 6.21, OH^- dosing for pH control

Therefore based on the pH inhibitions as included in the model, if the pH is lowered to a level of 6.8 due to a dosing malfunction, the AnMBR can recover completely if this is not continued for longer than 4 days (Figure 6.22). If this period is exceeded, the system fails catastrophically (similar to Figure 6.23).

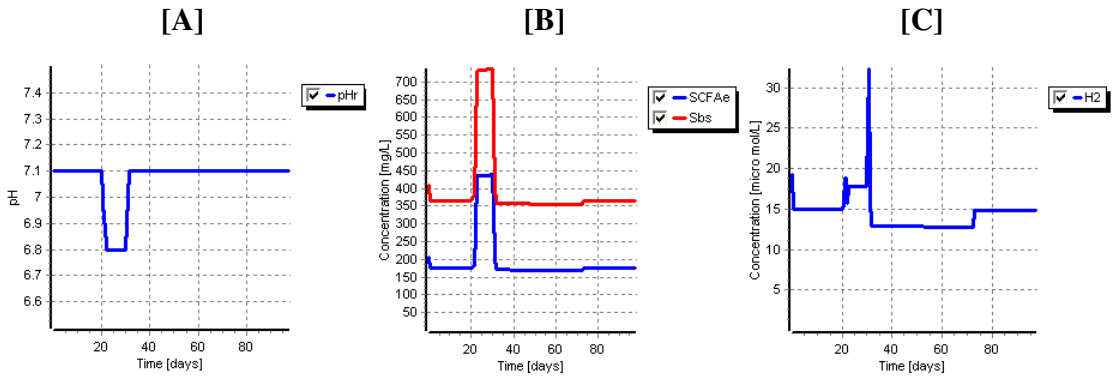

Figure 6.22, Maximum Time at Decreased pH = 6.8 for Full Recovery

Since the peak $H_{2(aq)}$ and SCFA concentration was still fairly low for the pH<6.8 scenario, no excessive OH^- dosing was not required for full system recovery – NaOH dosing only needed to be recovered to normal and the $SCFA_e$ concentration recovered shortly afterwards.

In the next simulation the goal was to decrease the reactor pH to 6.7 (Figure 6.21 – OHin). In this simulation the NaOH dosing was decreased to 0.095 molOH/d (160 mgNaOH/L) to observe the pH decrease (Figure 6.23).

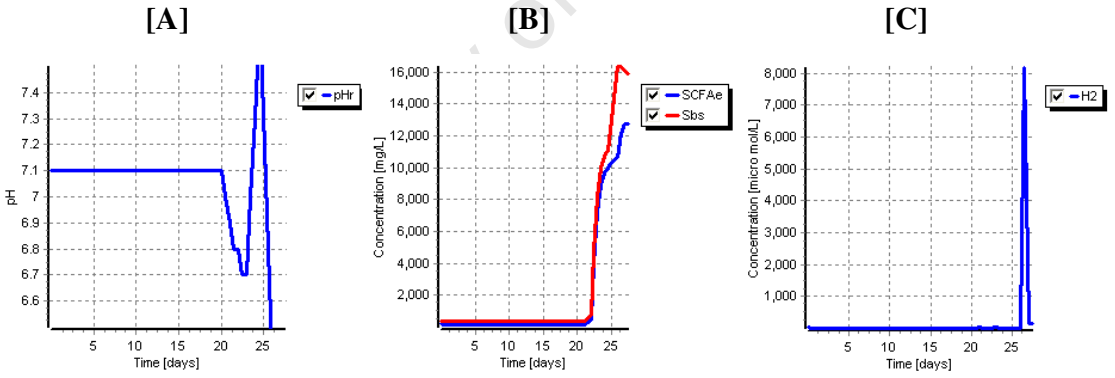

Figure 6.23, Minimum Time at Decreased pH = 6.7 for Reactor Failure

After approximately 36 hours, the system failed catastrophically. The investigation of the effect to pH fluctuation on the AD-FTRW system could not be continued since the system shows immediate failure for pH values below ~6.68. Similar results were obtained for decreasing the system pH above the optimal (> 7.4), which can happen in a NaOH overdose-situation.

6.4.2 System Failure Due to Temperature Fluctuation

The next inhibitory effect that was investigated was that of temperature fluctuations (Figure 6.24). The actual FTRW stream is cooled from 100 ^{o}C to 37 ^{o}C before it enters the full-scale wastewater treatment plant (Section 2.1). Thus a scenario of temperature increase above the optimal is quite plausible if the cooling system fails. Secondly, a temperature decrease is also plausible if the ambient temperature decreases or if the reactor's backup internal heating system fails.

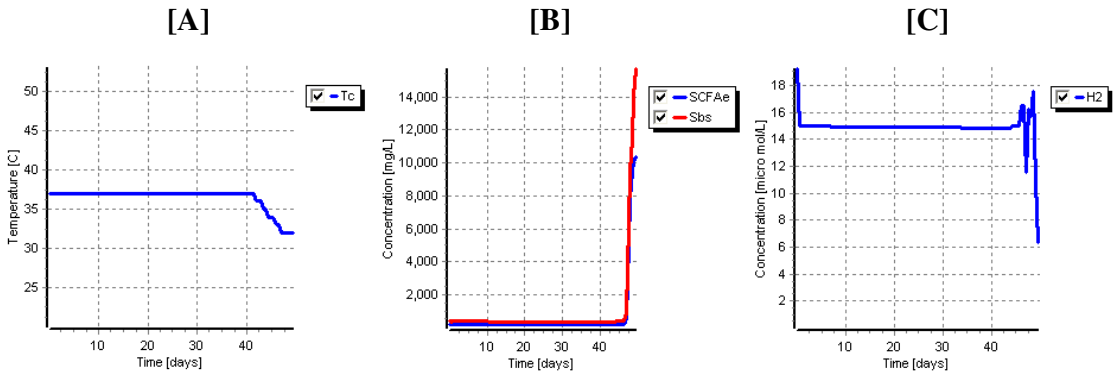

Figure 6.24, Minimum Time at Decreased Temp (305 K) for Reactor Failure

Unlike pH, temperature is a control parameter in the dynamic AD-FTRW model i.e. it can be varied directly (Figure 6.24A). The model predicts very high temperature sensitivity. Even a gradual 5 ^{o}C temperature decrease (over 4 days) still leads to catastrophic failure of the biomass (Figure 6.24). Similar results were obtained for increasing the temperature above 37 ^{o}C. The effects of both temperature and pH appeared to be described quite well when compared with experimental observations during the investigation, but this aspect of the model was not formally validated.

6.4.3 System Failure Due to Overloading

The effect of an increase in $SCFA_e$ an $H_{2(aq)}$ is interlinked and the one usually happens in response to the other. To simulate the effect on an increase in these two parameters, an organic overload is applied to the AnMBR. An OLR overload is the most common type of inhibition observed in the AnMBR. This is especially prevalent in the start-up phase (Section 4.2) when the OLR is increased on a daily basis. In the next two presented simulations, the smallest OLR increase (for 24 hours) which leads to a catastrophic system failure were investigated (Figures 6.25 & 6.26). For the first simulation, the influent flow rate was increased by 15% (24.9 L/d to 28.635 L/d) for 24 hours and

then it was reset to the initial flow rate. Correspondingly, the OLR also increased with 15% since OLR = $Q_i.S_{ti}/V_r$ and the influent COD (S_{ti}) and the reactor volume (V_r) is constant at 18 500 mgCOD/L and 23 L respectively.

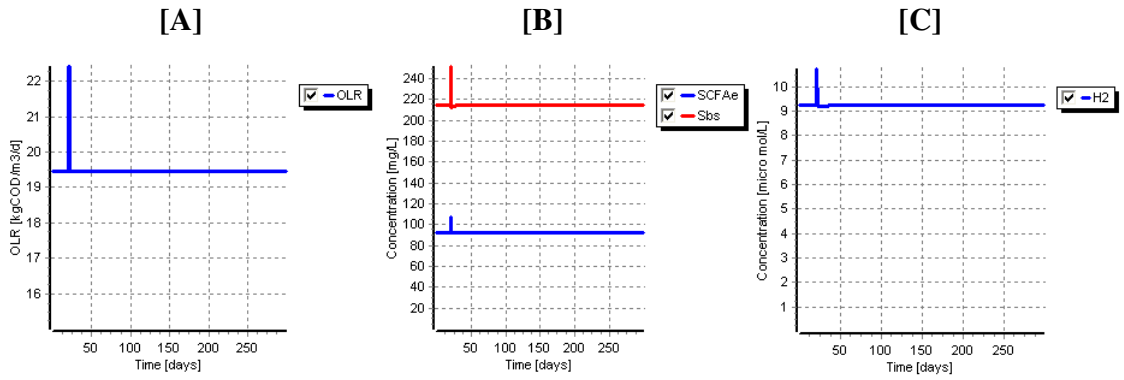

Figure 6.25, Minimum 24 Hour OLR increase for Reactor Recovery

For an OLR increase of 15% the model predicts a full system recovery (Figure 6.25). A small spike in the $SCFA_e$ and $H_{2(aq)}$ is observable, but once the influent flow (and OLR) is reset to normal, the system recovers completely. However, a 17% OLR increase, corresponding to a 17% influent flow rate increase, leads to a catastrophic failure (Figure 6.26). The reason for the failure is that inhibitory compounds ($SCFA_e$ and $H_{2(aq)}$) accumulate in the reactor because it cannot be removed at a high enough rate by the active biomass. This leads to inhibitory conditions that shut down the bio-processes. Experimentally, this value was observed as slightly lower. The laboratory scale AnMBR could handle an OLR increase of ~12%, but a 24 hour increase of 15% would lead to complete system failure.

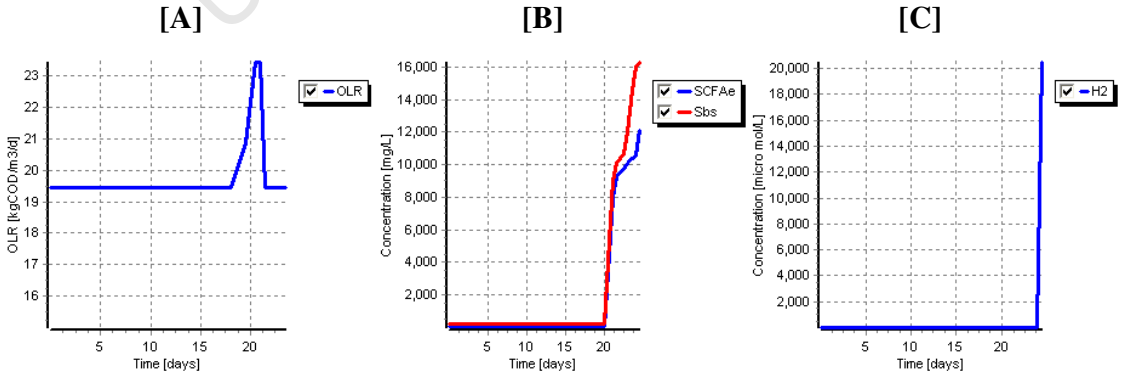

Figure 6.26, Minimum 24 Hour OLR increase for Reactor Recovery

6.4.4 System Failure from Too Low Sludge Age

Next the minimum sludge age for a given OLR was investigated. This simulation was done by allowing the system to reach steady state at a long sludge age (~300 days) for a given OLR. Then the sludge age was decreased to ~100 days and the simulation was allowed to run to steady state (> 3 sludge ages). If the system reached steady state, the sludge age was again decreased to ~95 days and the process was then restarted at a lower sludge age. This procedure was then continued until the minimum sludge age was identified where the system was still able to reach steady state for the chosen OLR. In other words, if the sludge age was decreased any more the biomass in the system would not be able to grow fast enough to remove all of the SCFA. This would lead to a SCFA overload and catastrophic system failure. Figure 6.27 presents the 'failure sludge age'(R_{Sfail}) vs. OLR and also the corresponding reactor solids concentration (MLSS). As a matter of interest the steady state MLSS as predicted by the steady state model was also plotted for the given OLR and sludge age. A good correlation exists between the steady state and dynamic model predictions and is typically within 10% of one another (Figure 6.27 & Table 6.3).

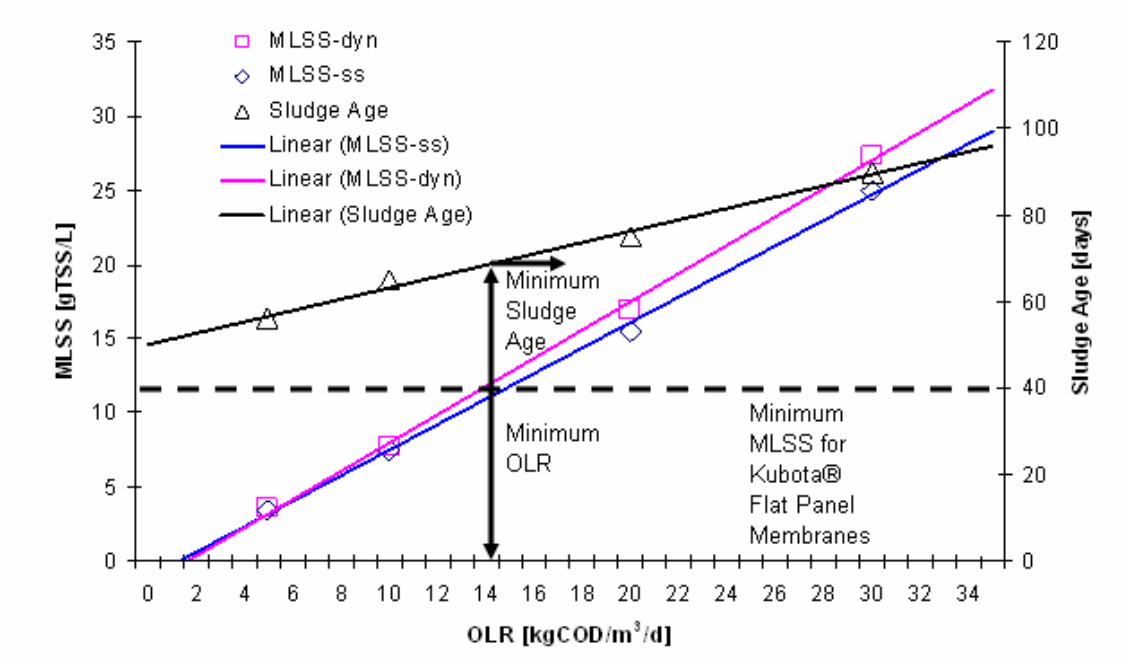

Figure 6.27, Predicted Minimum Stable Sludge Age & Corresponding MLSS vs. OLR

From Figure 6.27, as the OLR increases, so does $R_{Sfail.}$ Furthermore it can be seen that the minimum MLSS of 12 gTSS/L for the membranes to function properly (Section 3.1.1), a minimum sludge age

of 70 days and a minimum OLR of 13.5 kgCOD/m^3/d will be required. To observe how effluent quality and MLSS changes with sludge age at a constant OLR, Figure 6.28 was constructed.

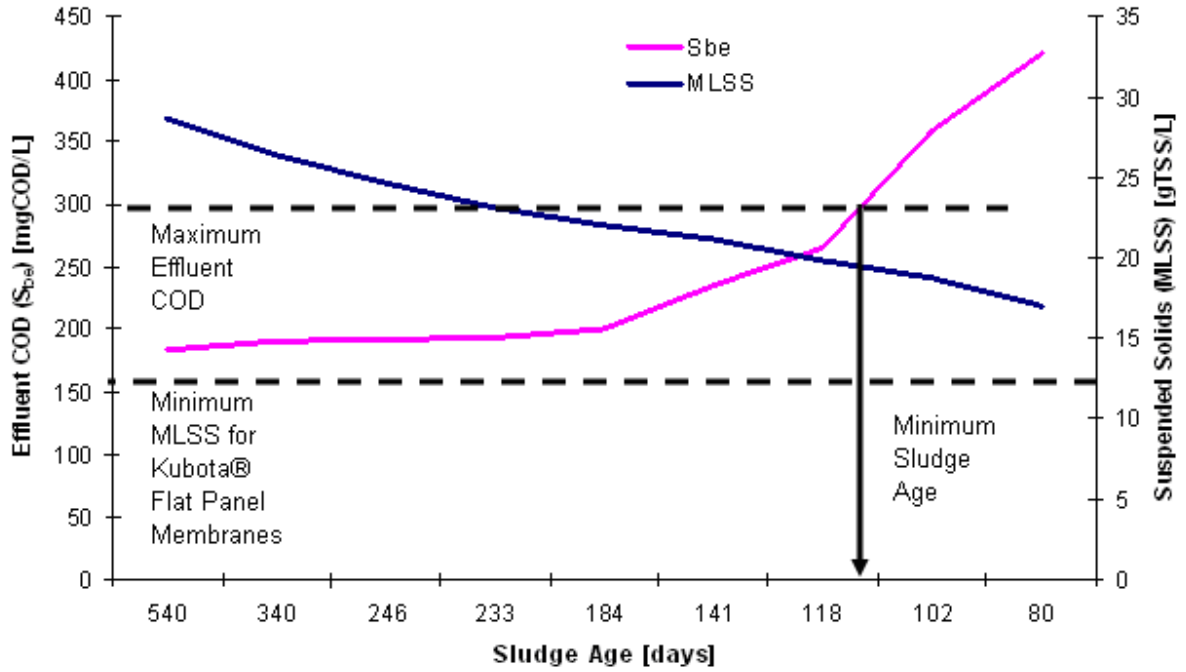

Figure 6.28, Effluent COD and Reactor MLSS vs. Sludge Age at OLR = 15 kgCOD/m$^3_{Vr}$/d

Ideally, the effluent COD (S_{be}) should be maintained below 300 mgCOD/L, this not only ensures a high quality effluent, but also avoids SCFA inhibition which could lead to system failure and high OH^- dosages to neutralize the unutilized SCFAs accumulating in the reactor. To maintain a S_{be} < 300 mgCOD/L the system should be operated at a sludge age > 110 days (for OLR = 15 kgCOD/m^3/d). If these criteria are met, sufficient solids (MLSS > 12 gTSS/L) should be generated for membrane scour (Figure 6.27).

6.5 Closure

The dynamic AD-FTRW model was developed from mass balanced stoichiometric reactions describing the anaerobic metabolism of each biodegradable fraction of the FTRW by its corresponding functional organism group (FOG). This was then combined with WABC relationships derived and simplified from Mosvoto et al. (1997). pH predictions was derived from an inorganic carbon balance similar to that of the steady state model (Appendix 6.4). The yield values of the individual FOGs were calibrated against the steady state model with an automated parameter optimization using the water treatment simulation package West®. Similarly, the half saturation constants for the individual FOGs were calibrated with West® against batch test experimental data from an experiment specifically designed for this purpose. The outcome was a dynamic AD-FTRW model able to predict all of the measured parameters – including effluent COD (S_{be}), effluent SCFA ($SCFA_e$) and reactor mixed liquor concentration (MLSS) – typically to within 10%.

After calibration, the dynamic AD-FTRW was validated against dynamic flow and load experimental data. The model shows less variability in the predicted outputs than the experimental data. The reason for this is that the model only calculates daily averages, whereas the experimental data are grab samples obtained form the experimental system every few days. Nevertheless parameters (i) alkalinity, (ii) pH, (iii) biogas production and (iv) composition and (v) MLSS are predicted to typically within the ± 10 % error margin. The largest variability in experimental data is observed in the effluent SCFA and COD (S_{be}). The experimental vs. predicted outputs for S_{be} and $SCFA_e$ are 190^S vs. 224^S mgCOD/L (P_{90} = 65%) and 134^S vs. 112^S mgAc/L (P_{90} = 75%) respectively. Thus it can be concluded that the dynamic AD-FTRW model slightly over predicts the effluent COD (18%) and SCFA (20%). This slight over prediction is advantageous, since it will result in a more conservative design of downstream processes.

Even at very long sludge ages (~300 days), the endogenous (inactive) fraction of the biomass does not dominate the MLSS. Indeed it appears that at a sludge age > 1000 days ~80% of the biomass is still active. This is due to the high influent COD of FTRW (18 000 mgCOD/L) and its high degree of biodegradability and low endogenous decay rates (b) and unbiodegradable fraction of the biomass (f).

During the experimental part of the project it was discovered that the AnMBR is prone to inhibition which can lead to system failure. Inhibitory parameters include pH, T, high SCFA concentrations and $H_{2(aq)}$ inhibition. Since these were not specifically investigated in the experimental part of the project, a literature survey was conducted to find the required inhibition functions for mesophillic anaerobic digestion. It was found that a temperature and pH variation of ± 4 ^{o}C and ± 0.3 pH units respectively over a period of 3 to 4 days can lead to a catastrophic system failure. Secondly a rapid (1 day) OLR increase of 17% also leads to a catastrophic failure, although not formally validated, these findings correlated with observations on the experimental AnMBR system. It should however be emphasized that the inhibition functions obtained from literature were applied 'as is' and should be validated experimentally if the AnMBR finds application at pilot scale.

The dynamic AD-FTRW model predicts that, irrespective of the inhibition type (pH, T, SCFA or OLR increase) the $H_{2(aq)}$ always shows a fluctuation before the system fails catastrophically. It can also be noted that, if the $H_{2(aq)}$ recovers, the system also recovers from the inhibition of a shock load. Secondly the $H_{2(aq)}$ also recovers far quicker than other parameters like $SCFA_e$ or S_{be}. Thus the $H_{2(aq)}$ concentration appears to the ideal pre-emptive parameter for predicting (i) inhibitions, (ii) imminent reactor failure and also (iii) reactor recovery. Traditionally, the $H_{2(aq)}$ and the gas phase hydrogen partial pressure could not be measured economically due to its low concentrations. However, due to recent advances in hydrogen fuel cell technology inexpensive $H_{2(aq)}$-probes that can measure $H_{2(aq)}$ concentrations as low as 90 nano-mols are currently available. It has also been proven that these probes can survive long term use in anaerobic digestion mixed liquor (Pauss & Guiot, 1993).

CHAPTER 7

7. Conclusions & Recommendations

The aim of Chapter 7 is to summarize the main conclusions drawn from the body of work represented in this thesis. It will be in chronological order i.e. will start with conclusions drawn on the combination of membrane technologies, anaerobic digestion and the treatment of a high strength acidic organic stream including Fischer-Tropsch Reaction Water (FTRW). This will be followed by the conclusions drawn from the feasibility study of the AnMBR and will discuss issues like start-up optimization, nutrient requirements, maximum attained OLRs, optimal pH control methods and sludge age. The third set of conclusions will be on the performance evaluation of the AnMBR, in this section the performance of the AnMBR was compared to the control-reactor (AnPBR). (i) Nutrient and (ii) alkalinity requirements, (iii) sludge production, (iv) effluent quality and (v) shock loading responses will be used as means of comparison for the performance evaluation.

A large fraction of the research project also entailed modeling of the AnMBR, both at steady state (time independent) and under dynamic (time dependant) conditions. Both the steady state and dynamic AD-FTRW models were calibrated and validated against data collected in the experimental phase of the project, conclusions will be drawn on model accuracy, model versatility and model weaknesses/short comings.

This research project will close off with recommendations that arose from the literature survey, feasibility study, performance evaluation and modeling. The recommendations will focus on the up-scaling of the AnMBR to pilot plant size (> 1000 L reactor volume), possible design alterations to increase performance on lab-scale.

7.1 Conclusions

7.1.1 Literature Review

The literature considered (i) the Sasol process, (ii) anaerobic digestion, (iii) anaerobic bio-reactors, (iv) membrane technologies and (v) Anaerobic Membrane Bio-reactors (AnMBRs). From the literature review, the following conclusions were identified:

- In the anaerobic (and aerobic) treatment of SCFA rich waste waters – such as FTRW – biomass settleability poses a major issue. This leads to biomass washout and large required reactor volumes. In a response to this, fixed bed anaerobic technologies were developed. The anaerobic treatment of FTRW has the added benefit that > 90% of the biodegradable organics that enter the system is converted to methane, which can be used for energy generation. However the fixed bed anaerobic systems produces a effluent with high TSS and SCFA concentrations and required an aerobic polishing step as post treatment. This further increases the operating cost to prepare the treated wastewater for reverse osmosis and recycling into the Sasol process (Section 2.2).

- Anaerobic systems relying on granulation such as the USAB, EGSB and IC reactors show poor process performance in the long term treatment of SCFA streams. This problem is overcome by the 100% solids-liquid separation imposed by the membranes in the AnMBR (Section 2.4.2).

- The capital cost of membranes has traditionally been one of the main factors hampering the full-scale implementation of MBRs. However, from the early 90's to the present, membrane costs have shown a >95% decrease. The same has also been observed for the operating cost of MBR plants. If these trends continue the competitiveness of membranes over conventional solid-liquid separation systems will continue to increase into the next decade (Section 2.5.8).

- In the early 90's there was a significant increase in the number of research outputs generated by research facilities investigating the aerobic MBR. In response to these research outputs

and skills developments, full-scale aerobic MBR plants rapidly increased in number in the past decade. For the AnMBR, a 10 fold increase in publications has been observed over the past 4 years. It is thus anticipated that the AnMBR will similarly find increasing full-scale application over the next decade (Section 2.5.8).

7.1.2 Feasibility Study

After the design and construction of a novel AnMBR system (Section 3.1) for the treatment of FTRW the feasibility study was commenced. This part of the research project comprised an investigation into (i) the response of the anaerobic biomass to the FTRW, (ii) the effect of the dispersed anaerobic biomass on the trans membrane pressure and flux through the membranes and (iii) overall process performance characteristics of the AD-FTRW process. The following conclusions were drawn:

- The AnMBR can treat Fischer-Tropsch Reaction Water at organic loading rates (OLR) of up to 30 kgCOD/m^3/d within 5 months from start-up. The system yields an effluent with a total COD < 400 mgCOD/L, an effluent SCFA < 250 mgAc/L and no particulates > 0.45 µm (Section 4.2).

- Since FTRW is chemically created water, it has no natural nutrients and very little alkalinity (~800 mg$CaCO_3$/L). Nutrients have a significant effect on the growth rates of the anaerobic micro-organisms and as a result also on the OLR. From the nutrient optimization done after start-up it was shown that N, P, S and Fe is of primary importance in the AD-FTRW system and should be dosed as macro nutrients (~ 80, 10, 4, 1 mg/L_{feed} respectively for 18 000 mgCOD/L FTRW). Yeast extract, Ca and Mg is of secondary importance and can be dosed as micro nutrients (< 1 mg/L_{feed}) along with other micro nutrients normally required for anaerobic digestion (Section 4.3).

- Because of the 100% solid-liquid separation imposed, and long sludge ages (> 100 days) required to increase the MLSS into the optimal range for membrane scour (> 12 gTSS/L), the membranes trap all the particulate COD and endogenous biomass inside the AnMBR, where it can be hydrolyzed almost to completion. This induces an abnormally high nutrient recycle

within the biomass. It was found that the system can operate with a COD:N:P ratio of 2000:10:1 without nutrient deficiency. This is more than three times higher than the typical COD:N:P ratio of 650:10:1 used for anaerobic systems treating acidic substrates. An operational effluent Ammonia (FSA) < 50 mgN/L can be maintained (Section 4.3).

- Provided the system is operated below the critical flux (<4.3 L/m^2/h), MLSS concentrations > 30 gTSS/L were maintained without deterioration of membrane fluxes, even though the DSVI (3000 ml/g) indicates that the sludge cannot be settled by traditional methods. The AnMBR system produced 1/10^{th} of the sludge mass traditionally observed in aerobic systems(0.0215 $gTSS/gCOD_{removed}$ vs. 0.22 $gTSS/gCOD_{removed}$) and has zero oxygen requirements (Section 4.6.1)

- More than 98% of the COD entering the AnMBR is converted to methane (Section 4.6.1). This energy rich biogas can be used for digester heating, electricity generation or even recycled for fuel production. It is estimated that if the biogas produced from the anaerobic digestion of the entire Secunda-FTRW stream (29 ML/d at 18 gCOD/L) is converted to electricity, it will exceed the wastewater treatment plant's electricity requirements by approximately 23 MW (571 MWh/d) (at 33% thermal efficiency), enough to power 17000 average South African house holds (33 kWh/household/d). The carbon footprint of the AS-AnMBR plant will also be 48% less than that of the current waste water treatment system (Appendix 1.1).Alternatively, the biogas can be blended into the natural gas line before auto-thermal reforming which will then be converted to synthesis gas and polymerized via the FTRW process. It is estimated that if the 128 ton/d of methane is converted to diesel, 52 000 L/d can be produced extra, resulting in a further capital gain of ~65 R million per year (Chapter 1).

- The Specific NaOH Utilization of the AnMBR is affected by three parameters, (i) the feed flow rate through the reactor, (ii) the reactor pH and the (iii) effluent SCFA concentration. It was found that the NaOH requirement of the AnMBR was on average 0.067 kgNaOH/kgCOD at a reactor alkalinity and pH of 2200 $mgCaCO_3$/L and 7.05 respectively (Section 3.5 & Section 4.6.1).

- In the design of the AnMBR, the membrane surface area was significantly oversized, since there was no way of predicting how the membrane performance would be affected by the anaerobic biomass. For the first 650 days of the study membranes were operated at 1 to 10 % of their capacity. The recirculation of biogas for reactor mixing and membrane scour was successful. No noticeable deterioration of membrane performance was observed over the test period. However, inorganics including rust or precipitates can cause a reversible fouling that has a detrimental effect on membrane performance, but once removed, membranes recover completely (Section 4.5.1).

- In the last 50 days of the experimental phase, an effluent recycle was incorporated into the AnMBR design to simulate the effects of an increased flux over the membranes. For fluxes below 4.3 L/m^2/h no correlation could be found between TMP and flux. However, when the flux increased over 4.3 L/m^2/h, a sharp increase in the TMP was observed. Under the conditions imposed, the flat panel membranes appear to have a critical flux of ~4.3 L/m^2/h. At fluxes of higher than this critical value, biological cake layer formation cannot be controlled by biogas scour, even at increased scour gas flow rates up to 150% (Section 4.5.2). The normal scouring rate was 750 L/m^3/h as recommended by Kubota®.

- The first irreversible fouling test was done before commissioning the AnMBR, the second was done 530 days later. The change in flux through the clean membranes changed very little over the 530 days between the two chemical cleans. If a 50 % decrease in flux is allowable before membrane replacement this data points to a membrane life span on the AD-FTRW environment of at least 7 years. However, it should be emphasized that this prediction is an extrapolation from a small dataset and relatively short period of investigation. It would appear that the permanent fouling rate of activated sludge is at least twice that of the AnMBR (Ramphao et al., 2004); however the operating flux of the AnMBR at 4.3 L/m^2/h was significantly below that of the AS system (10 – 15 L/m^2/h) (Section 4.5.3).

7.1.3 Performance Evaluation

In response to the positive outcomes of the feasibility study, a lab-scale down-flow Anaerobic Packed Bed Reactor (AnPBR) was also constructed and operated to benchmark the performance of the AnMBR. The AnPBR was a scaled-down version of a pilot plant system currently under development by Sasol - its volume was exactly the same as the AnMBR (23 L) and its packing density and down flow velocity the same as the pilot plant (Section 3.2). Both systems are fed the same artificial FTRW and nutrient mix. The two systems were operated at a steady state organic loading rate (OLR) = 15 kgCOD/m^3/d for a period of 35 days and their performance compared. The flowing conclusions were drawn:

- The AnMBR effluent (35 mgCOD/L) is free of particulates and TSS compared with the AnPBR where 57 % of the effluent COD (1750 mgCOD/L) is in particulate form. Furthermore the total COD of the AnMBR is only 2% of the total effluent COD of the AnPBR at an OLR of 15 kgCOD/m^3/d. This difference would result in a significantly reduced operating and capital cost for the downstream processing system (Section 4.6.1).

- The membranes act as a positive barrier retaining biomass in the AnMBR. Because of this and the long sludge age, the dead biomass in the reactor gets hydrolyzed and is reintroduced as substrate to be utilized by the anaerobic biomass. This re-utilization of biomass results in a ~30% lower sludge production - and sludge incineration cost - if compared to the AnPBR (0.022 gTSS/$gCOD_{removed}$ vs. 0.031 gTSS/$gCOD_{removed}$ at OLR = 15 kgCOD/m^3_{Vr}/d) (Section 4.6.1).

- The main operating cost in anaerobic systems treating acidic waste water is the alkalinity (NaOH) dosing cost. Because of the high effluent SCFA and slightly higher reactor pH of the AnPBR to maintain a SCFA/Alkalinity < 0.3, the alkalinity consumption of the AnMBR system was ~40 % higher than that of the AnMBR under the same operating conditions (0.067 gNaOH/$gCOD_{removed}$ vs. 0.11 gNaOH/$gCOD_{removed}$) (Section 4.6.2).

- The AnPBR can handle far greater (3 times) shock loads than the AnMBR and also show a 30% shorter recovery period before complete recovery. From an operational point of view it

was also found that the AnPBR was significantly easier to operate and control than the AnMBR (Section 4.6.3).

- The AnMBR study indicates that steady state design loading rate of ~30 kgCOD/m^3/d is feasable, compared with ~8 kgCOD/m^3/d for the AnPBR. This implies a 3 times smaller reactor volume than required with the AnPBR for the same organic load. This and the significant savings capital and main operating costs namely; reactor volume (60%), alkalinity (40%), sludge incineration (30 %) and downstream processing (± 95%) indicates that the AnMBR might be a financially competitive treatment option for FTRW, despite the current high ultra filtration membrane costs and more complex control strategies.

7.1.4 Steady State AD-FTRW Modeling

In this research project, a general steady state model was developed for the anaerobic conversion of an alkalinity and nutrient deficient biodegradable substrate (including weak organic acids/bases) to biomass, carbon dioxide and methane (Section 5.1). The primary use of this model is reactor design i.e. the prediction of (i) mixed liquor concentration (MLSS) or (ii) reactor volume, (iii) reactor operational pH, (iv) alkalinity, (v) nutrient requirements and (vi) biogas production and (vii) composition for a given sludge age (R_s) organic loading rate (OLR) and influent pH and influent organic composition ($C_xH_yO_z$) – in this case FTRW. Data collected on the AnMBR during the feasibility and performance evaluation was used to calibrate the model to produce the steady state AD-FTRW model. Conclusions drawn from this part of the project were as follows:

- The model was calibrated with a 35 day steady state data set for the AnMBR. It was found that the model predicts the steady state system outputs with a large degree of accuracy, with biogas production, alkalinity requirements and reactor pH all well within the 5% error margin. However, due to the extremely long sludge age (>200d), the predicted mixed liquor concentrations (MLSS) shows a deviation of as much as 25%. (Section 5.2)

- After calibration the steady state model was validated against a 200 day data set for both the AnMBR and parallel AnPBR. It was found that the model predicts parameters like biogas production, alkalinity requirements and pH to within 10% of that measured. However,

parameters like MLSS and nutrient requirements shows deviations as large as 30% (Section 5.3)

- In the performance evaluation the AnPBR was operated in parallel to the AnMBR. Assuming the same stoichiometric and kinetic constants determined for the AnMBR (growth yield coefficient, Y_{AR} = 0.044 gCOD biomass/ gCOD substrate utilized, biomass unbiodegradable particulate fraction f_{AR} = 0.08, COD/VSS ratio, f_{cv} = 1.53 gCOD/gVSS and VSS/TSS ratio, f_i = 0.78 gVSS/gTSS and endogenous respiration rate b_{AR} = 0.0377 /d also to the AnPBR, then the effective MLSS concentration and sludge age for the AnPBR are around 25 gTSS/L and 32d (Section 5.3). The AnPBR system sludge age is an order of magnitude shorter than the AnMBR and because nutrient requirements increase with decreasing sludge age, the short sludge age of the AnPBR system is probably the main reason for the 50% higher nutrient requirements for the AnPBR.

- The predictive ability of the steady state AD-FTRW model can be used as a process control and monitoring tool *inter-alia* to identify operational problems including faulty pH control probes, OH overdosing, gas leaks and other operating and measurement equipment malfunction and bio-process, such as high SCFA, low Alkalinity, low pH, and low biogas production, to protect the stability of a delicately balanced biological system, in which NaOH dosing needs to be kept to a minimum to minimize operating costs.

- The two major assumptions in the steady state AD-FTRW model are; (i) all biodegradable COD (S_{bi}) that enters the system is utilized to completion and (ii) is directly and instantaneously converted to the final metabolic end products of anaerobic digestion (CO_2, CH_4 and Biomass). This two assumptions are also the major shortcomings in the steady state model:

    1. Since the entire influent biodegradable COD (S_{bi}) is utilized, the effluent biodegradable COD will always be predicted as zero (S_{be} =0). From the experimental data, this is not the case.

2. Inhibitory effects of temperature and pH fluctuations as well as the effects of the accumulation of accumulation of metabolic intermediates produced in the AD-FTRW cannot be predicted by the steady state model.
3. Reactor performance and effluent quality cannot be predicted under dynamic flow and load conditions.

7.1.5 Dynamic AD-FTRW Modeling

The dynamic AD-FTRW model was developed to complement the steady state model because it overcomes the deficiencies of the steady state model and can predict parameters such as; (i) effluent quality, (ii) system response to dynamic flow and load variations and (iii) inhibitory effects of pH, temperature and metabolic intermediates accumulating in the system. Analogous to the steady state model, the dynamic model was developed from balanced stoichiometric reactions describing the anaerobic metabolism. However, in this case each of the biodegradable fractions of the feed was assigned to its corresponding functional organism group (FOG), yielding a unique ratio of metabolic products for each of the biodegradable fractions in the feed. Alkalinity and pH predictions were done similarly to the steady state model.

The yield values of the individual FOGs were calibrated against the steady state model average composite yield (Y_{AR}). The half saturation constants for the individual FOGs were calibrated with West® against batch test experimental data from an experiment specifically designed for this purpose. The following conclusions were drawn;

- After calibration, the dynamic AD-FTRW was validated against dynamic flow and load experimental data. The model shows less variability in the predicted outputs than the experimental data. The model calculates daily averages, whereas the experimental data are grab samples obtained from the experimental system. Nevertheless parameters (i) alkalinity, (ii) pH, (iii) biogas production and (iv) composition and (v) MLSS are predicted within the ± 10 % error (Section 6.3).

- The largest variability in experimental data is observed in the effluent SCFA and COD (S_{be}). The experimental vs. predicted outputs for S_{be} and $SCFA_e$ are 190^S vs. 224^S mgCOD/L (P_{90} = 65%) and 134^S vs. 112^S mgAc/L (P_{90} = 75%) respectively. Thus it can be concluded that the

dynamic AD-FTRW model slightly over predicts the effluent COD (18%) and SCFA (20%). This slight over prediction is advantageous, since it will result in a more conservative design of downstream processes (Section 6.3).

- Even at long sludge ages, the endogenous (inactive) fraction of the sludge mass does not dominate the MLSS. Indeed it appears that even at a sludge age > 1000 days ~80% of the sludge mass is still active biomass. This is due to the very lo endogenous respiration rate (b) and residue fraction (f) of the anaerobic biomass (viz. 0.04/d and 0.08 respectively) (Section 6.3).

- During the experimental part of the project it was discovered that the AnMBR is prone to inhibition which can lead to system failure. Inhibitory parameters include pH, temperature, high SCFA concentrations and $H_{2(aq)}$ inhibition. Since these were not specifically investigated in the experimental part of the project, a literature survey was conducted to find the required inhibition functions for mesophillic anaerobic digestion and included in the simulation model. It was found that a temperature and pH variation of ± 4 ^{o}C and ± 0.3 pH units respectively can lead to a catastrophic system failure. Secondly a rapid (1 day) OLR increase of 17% also leads to a catastrophic failure. These findings correspond with observations on the experimental system (Section 6.4). It should however be emphasized that the inhibition functions obtained from literature were applied 'as is' and should still be validated experimentally if this research is continued.

- Irrespective of the inhibition type (pH, T, $SCFA_e$ or OLR increase) the $H_{2(aq)}$ always shows a fluctuation before the system fails catastrophically. It can also be noted that, if the $H_{2(aq)}$ recovers (i.e. decreases), the system also recovers from the inhibition of shock load. Secondly the $H_{2(aq)}$ also recovers far quicker than other parameters including effluent SCFA or effluent COD. Thus the $H_{2(aq)}$ concentration appears to the ideal pre-emptive parameter for predicting (i) inhibition, (ii) imminent reactor failure and also (iii) reactor recovery. Traditionally, the $H_{2(aq)}$ and the gas phase hydrogen partial pressure could not be measured economically due to its low concentrations. However, due to recent advances in hydrogen fuel cell technology inexpensive $H_{2(aq)}$-probes that can measure $H_{2(aq)}$ concentrations as low

as 90 nano-molls are currently available. It has also been proven that these probes can survive long term use in anaerobic digestion mixed liquor.

7.2 Recommendations

7.2.1 Membrane Performance: Evaluation & Enhancement

- Due to process constraints, the biogas recycle flow rate could not be accurately measured. It is thus recommended that a system be implemented for the accurate measurement of the biogas recycle and resultant membrane scouring rate. This will allow the investigation of the effect of scouring rate on membrane fouling, critical flux and reactor mixing.

- On-line trans membrane pressure and flow measurement can clarify this relationship, especially if it is logged on a regular (hourly) basis. This can then form the basis for a multi-parameter membrane performance model that can be included in the dynamic AD-FTRW model.

- The critical flux (CF) can be defined as the flux at which particle deposition on the membrane surface cannot be further controlled by the convective transport away from the membrane surface area induced by scour. Conversely, the CF is the maximum flux at which economical membrane operation can take place. This parameter should be measured on a regular (weekly) basis to identify parameters that might have an effect on the CF. One way of observing this parameter is to introduce an effluent recycle on the AnMBR (Figure 7.1).

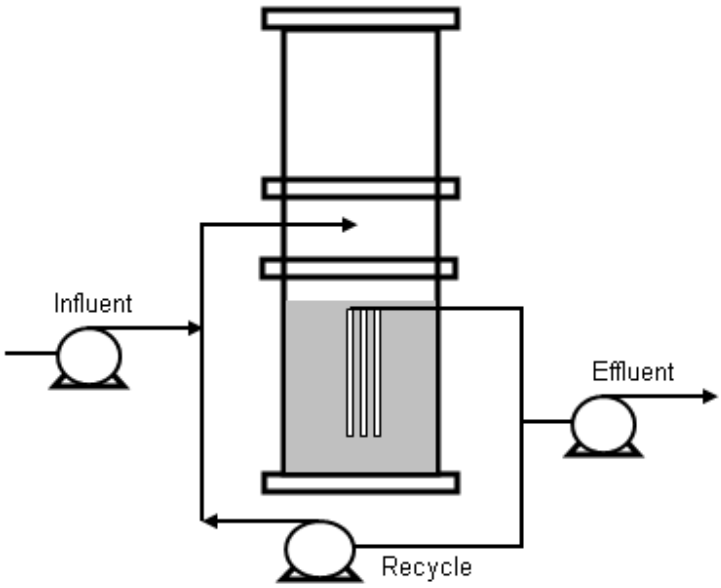

Figure 7.1, AnMBR with recycle for CF evaluation

- Parameters that might have an effect on membrane performance identified from literature include colloids, proteins, extra cellular polysaccharides (EPS), MLSS and also the change in microbial population with time. It is recommended that this investigation be initiated and the identified parameters measured on a regular (weekly) basis to quantify their effects on membrane performance and the critical flux.

- Research conducted on the addition of Powdered Activated Carbon (PAC) to submerged AnMBRs has proven to enhance membrane scour and increase the critical flux significantly. From the study conducted by Hu & Stuckey (2007) it appears that after PAC addition CFs > 20 L/m^2/h can be economically feasible.

7.2.2 Automated Control

For a high rate biological reactor treating a high concentration potentially inhibitory substrate, process control is critical. Organic overload and inhibitory conditions can occur in a matter of hours, as was observed in the AnMBR. Thus it is recommended that the investigation into process control of high rate AD-FTRW systems be continued. The investigation should include;

- Effluent SCFA control. An on-line effluent SCFA analyzer can be used to evaluate the SCFA concentration at an hourly rate. This can then be used to automatically control the influent flow rate. If the SCFA concentration increases above a high set-point (~200 mgAc/L), the feed (and resultant OLR) can be decreased and when the effluent SCFA decreases below a lower limit (~50 mgAc/L), the OLR can be increased. This system can perform two functions (i) protect the biomass against OLR overloads and (ii) automatically increase the OLR to the maximum for a given sludge age.

- Analogous to SCFA control, $H_{2(aq)}$ can also be used as process control parameter. Since $H_{2(aq)}$ (i) responds far more rapidly than effluent SCFA and (ii) can be used to diagnose a wide rage of inhibitions, this parameter appears to be the ideal control parameter for high rate anaerobic reactors. Recent advances in hydrogen fuel cell technology has yielded inexpensive $H_{2(aq)}$-probes that can measure $H_{2(aq)}$ concentrations as low as 90 nano-mols are currently available. It has also been proven that these probes can survive long term use in anaerobic digestion mixed liquor.

- The West® modeling platform in which the dynamic model was developed, gives the option of evaluating various control systems and strategies. This combined with the dynamic AD-FTRW model can be used to simulate various control strategies before it is physically implemented. It is thus recommended that a study on the simulation of control strategies be conducted before the experimental control systems are evaluated.

7.2.3 AD-FTRW Modeling

The dynamic model for the AD-FTRW appears to meet the expectations imposed on it in this research project. However, it should be emphasized that a significant amount of research can still be conducted on this model. These topics include;

- Inclusion of the mixed weak acid base relationships and mineral precipitation (Mosvoto et al. 2000), since this can have an effect on membrane performance and also nutrient availability for the micro-organisms.

- The validation of inhibition functions included in the dynamic AD-FTRW model. Experiments specifically designed for this purpose need to be conducted and used for inhibition function calibration and validation.

- Since the ADMBR operate at such long sludge ages, it is recommended that the dynamitic solids retention time (or dynamic sludge age) be incorporated into steady state model. This can now be done, since the yield (Y) and decay rate (b) has been characterized (Takacs et al., 2008).

7.2.4 Scaling up from Lab to Pilot Plant

The following recommendations are based on experience gained from lab-scale AnMBR operation and refinement.

- Inorganic foulants including rust, sand and concrete can have an adverse effect on membrane performance. These inorganics form a layer on top of the membranes and in so doing hinders the flow of effluent through them. If a significant amount of inorganics enters the system, a membrane performance decrease of > 90 % can be observed over night. Fortunately there is one characteristic that most inorganic foulants share, namely they have good settling properties. Thus it is recommended that a Primary Settling Tank (PST) be incorporated into the pilot plant AnMBR (Figure 7.2).

- It was observed that the AnMBR biomass is sensitive to over and under loading situations. To damp influent flow variations an equalization basin may be required. This equalization basin can double as a primary settling tank for the settling and disposal of possible inorganics in the feed stream. A hydraulic retention time of 12-24 hours is recommended for the PST/Equalization basin. It is recommended that the alkalinity and nutrients be dosed at a mixing point in the feed line just after the feed pump (P2 on Figure 7.2). Both the buffer and some nutrients (in excess) can be potentially poisonous to AD biomass in concentrated form.

- Unstable start-up conditions and system upsets such as NaOH overdosing can lead to excessive foaming in the AnMBR. It is therefore recommended that a gas head space of 50%

of the operational liquid volume be incorporated into the design. To further lessen the effect of foaming, foam baffles can be mounted on the membrane housing. These baffles protrude above the liquid level by about 3 cm (Figure 7.2). If the liquid level in the reactor is kept constant, the gas bubbling will induce a continuous flow of mixed liquor over the baffles which 'mixes' the foam back into the liquid phase. It was also found that these baffles enhance the mixing in the liquid volume. A third precautionary step against the effects of foaming is a moisture trap in the biogas recycle line, which traps any water spray or foam that gets sucked into the biogas recycle line. This moisture trap should be placed before the flow meter and compressor to protect these components from liquid damage.

- To quantify the gas scouring rate over the membranes, the biogas recycle rate should be measured. This was found to be quite cumbersome on the lab-scale AnMBR since the biogas that is being recycled has a 100% humidity and a high water spray content. It is recommended that a gas flow meter especially designed for the measurement of wet gas flow rates be used for this purpose.

- The compressor should be a sealed unit with minimal gas leakage, since the biogas is fairly flammable. The compressor must be able to suck biogas from the headspace via the biogas line and compress the biogas for reintroduction through the coarse bubble diffuser. It was found that ILMVAC Diaphragm Pumps (supplied by Air and Vacuum Technologies) give exceptional service. The compressor operated for 24 h/d for >600 days before the seals needed replacing. However it is highly recommended that two compressors are purchased, because the compressor is vital to the performance of the AnMBR.

- Finally it is highly recommended that some form of high rate control system be used to shield the AnMBR from overloading and NaOH poisoning. It was found that operator response time became too slow at OLRs > 20 kgCOD/m^3/d and that an electronic intervention system became necessary. Development and testing of the electronic control system on the AnMBR (Section 3.1.4) was not completed. If it is required that the AnMBR be operated at OLRs > 20 kgCOD/m^3/d it is important to have some kind of electronic failsafe in place to protect the biomass damage.

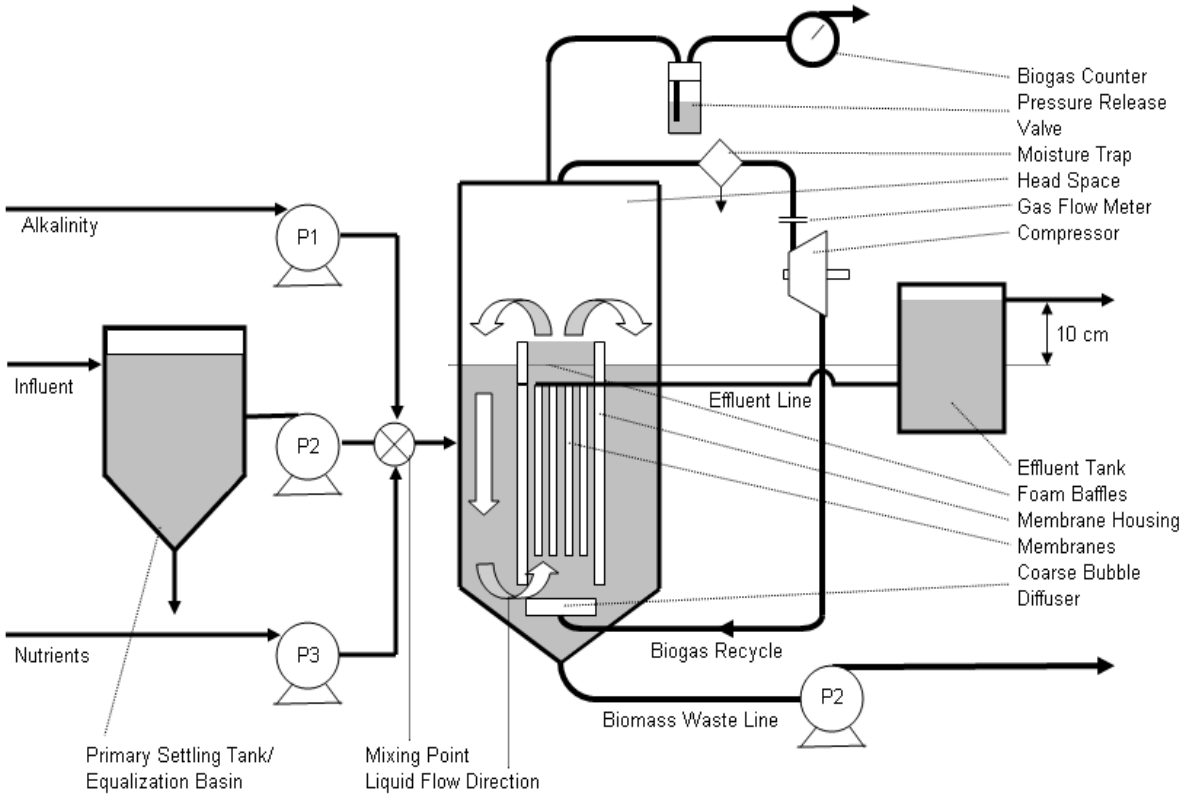

Figure 7.2, Suggested AnMBR Pilot Plant Layout

Reference list

Akram A, Stuckey DC (2007) *Batch assay to asses the microbial population in submerged anaerobic membrane bioreactors (SAMBRs).* 11th World Congress on Anaerobic Digestion, 23-27 Septemeber 2007, Brisbane , Australia.

Archer DB, Hilton MG, Adams P, Wiecko H (1986). *Hydrogen as process control index in a pilot-scale anaerobic digester*. Biotechnology Letters, Vol 8, No 3, pp 197-202

Alves M, Ferreira EC, Amaral AL, Pereira A, Novais JM, Mota M (2000) *Staged and non staged anaerobic filters: performance in relation to physical and biological characteristics of microbial aggregates*. Journal of Chemical Technology and Biotechnology, Vol. 75, pp 601-609

Avnimelech Y (2005). *Bio-filters: The need for a new comprehensive approach*. Aquacultural Engineering, Vol. 1341

Batstone DJ, Keller J, Angelidaki I, Kalyuznhyi SV, Pavlostathis SG, Rozzi A, Sanders WTM, Siegrist H and Vavilin VA (2002) *Anaerobic digestion model No 1* (ADM1), Scientific and Technical Report No 9, International Water Association (IWA), London, UK.

Beaubien A, Baty M, Jeannot F, Manem J (1995). *Design and operation of anaerobic membrane bioreactors: Development of a filtration testing strategy*. Journal of Membrane Science, Vol. 109, pp 173-184.

Brink IC, Ekama GA and Wentzel MC (2007) *A plant wide stoichiometric steady state WWTP model*. *Water Research* (submitted).

Britz TJ and Nel LH (1986), *The influence of different substrate pH values on the performance of a down-flow anaerobic fixed bed reactor treating petrochemical effluent.* Biotech Let, Vol 8, No 4, pp 293-298

Capri MG and Marais GvR (1974) pH adjustment in anaerobic digestion. *Water Research* **9**(3) 307-314.

Cheryan M, Rajagopalan N (1998). *Membrane processing of oily streams. Water treatment and waste reduction*. Journal of membrane Science, Vol 151. pp 13 – 28.

Cho J, Song KG, Yun H, Ahn KH, Kim JY, Chung TH (2005). *Quantitative analysis of biological effect on membrane fouling in submerged membrane bioreactor*. Water Science & Technology, Vol. 51, # 6-7

Churchouse S (1997). *Membrane bioreactors for water treatment – operating experiences with Kubota submenrged membrane activated sludge process*. Feature Article, Membrane Technology No. 83

Churchouse S, Wildgoose D (1999). *Membrane bioreactors progress from the laboratory to full-scale use*. Membrane Technology, No. 111, pp 4-8

Coulson JM, Richardson JF, (1998). *Chemical Engineering Volume 2: Particle Technology & Separation Processes*. Butterworth& Heinemann Publishers. 4th Edition.

De Zeeuw W, Lettinga G (1980), Accumulation of digested sewage sludge during start-up of an up-flow anaerobic sludge blanket (UASB) reactor. Biotechnology and Bioengineering Volume 22 Issue 4, Pages 699 - 734

Dochain D, Vanrolleghem P (2001) Dynamic modelling and estimation of wastewater treatment processes. IWA Publishing, Book, 400 pages.

Dold PL, Ekama GA and Maraisd GvR (1980*) A general model for the activated sludge process*. Progress Water Technology, Vol. **12**(Tor) 47-77.

Driessen WJBM, Habets LHA, Zumbragel M, Wasenuis CO (1999). *Anaerobic treatment of recycled paper mill effluent with internal circulation reactor*. 6th IAWQ Simposium on Forest Industry Wastewaters, Tampere, Finland, 6-10 June 1999

Du Plessis GH and Stegman P (1990), *Anaerobic treatment of Fischer-Tropsch Acid Water: Contents of bioreactor after 45 months of operation*, Sasol Technology, Research and Development Department, Water Research, Secunda

Du Preez (1987). Growth kinetic studies of acenetobacter calcoaceticus with special reference to acetate and ethanol as carbon sources. Internal Sasol Report.

Ekama GA (2004). *Motivation for research support – Anaerobic digestion membrane bioreactor treatment of Sasol reaction water.* Electronic mail correspondence between Prof GA Ekama of the University of Cape Town & Dr Peter Stegmann of Sastech Research and Development (Sasol)

Elmaleh S, Abdelmoumni L (1997). *Crow flow filtration of an anaerobic methanogenic suspension*. Journal of Membrane Science, Vol. 131, pp 261-274

Fane A, Chang S (2002). *Membrane Bioreactors: Design and operational options. MBR* Conference, Cranefield University UK, May 2002

Feijoo G, Soto M, Mendez R, Lema J (1995), *Sodium inhibition in the anaerobic digestion process: Antagonism and adaptation phenomena*. Enz. Mic. Tech., Vol 17, pp 180-188.

Fogler HS (1999), *Elements of Chemical Reaction Engineering*, Prentice Hall International Series, Physical and Chemical Engineering Sciences, 3rd Eddition 1000 pages

Hamdi M, Garcia JL (1991). *Comparison between anaerobic fiter and anaerobic contact process for fermented olive mill wastewaters*. Biosource Technology, Vol 38, pp 23-29.

Hellstrom D, Nordberg A, Olsson L-E, Jonsson L (2007). *Treatment of domestic wastewater and blackwater with food waste using a pilot anaerobic membrane bioreactor and reverse osmosis.* 11th World Congress on Anaerobic Digestion, 23-27 Septemeber 2007, Brisbane , Australia.

Hickey RF, Switzenbaum MS (1991). *The response and utility of hydrogen and carbon monoxide as process indicators of anaerobic digesters subject to organic and hydraulic overloads*. Research Journal Water Pollution Control Federation. Vol. 63, #2, pp 129-140

Howell JA (2003). *Future of membranes in green technologies and for water re-use*. Desalination Vol 162. pp 1-12.

Hu Y, Stuckey DC (2006). *Treatment of dilute waste waters using a novel submerged anaerobic membrane bioreactor*. Journal of Environmental Engineering, Vol. 132, No 2, pp 190 -198.

Hu Y, Stuckey DC (2007b). *Activated carbon addition to a submerged anaerobic membrane bioreactor: Effect on performance, trans membrane pressure and flux.* Journal of Environmental Engineering, Vol. 133, No. 1, pp 73-80

Hulshoff Pol L, Dorfling J, De Zeew W, Letinga G (1982). *Cultivation of well adapted palletized methanogenic sludge.* Biotechnology Letters, Vol. 4, # 5, pp 329-332.

Incropera FP, DeWitt DP, (1996). *Fundamentals of Heat and Mass Transfer*. John Wiley & Sons 4th Ed., 886 pages

Jiang T, Kennedy MD, Guinzbourg BF, Vanrollegem PA, Schippers JC (2005). *Optimizing the operation of a MBR pilot plant by quantitative analysis of the membrane fouling mechanism*. Water Science & Technology, Vol. 51, # 6-7

Jeison D, Van Lier JB (2006a). *Cake layer formation in anaerobic submerged membrane bioreactors (AnSMBR) for waste water treatment*. Journal of Membrane Science, Vol. 284. pp 227-236.

Jeison D, Van Lier JB (2006b). *On-line cake-layer management by trans-membrane pressure steady state assessment in Anaerobic Membrane Bioreactors for wastewater treatement*. Biochemical Engineering Journal, Vol 29, pp 204-209

Jeison D, Van Lier JB (2007a). *Cake formation and consolidation: Main factors governing the applicable flux in anaerobic membrane bioreactors (AnSMBRs) treating acidified waste waters*. Separation & Purification Technology, Vol 56. pp 71-78.

Jeison D, Van Lier JB (2007b). *Thermophillic treatment of acidified and partially acidified waste water using an anaerobic submerged MBR: Factors affecting long term operational flux*. Water Research Vol 41 pp 3868 – 3879.

Jeison D, Van Lier JB (2007c). *Anaerobic wastewater treatment and membrane filtration: a one night stand or a sustainable relationship?* 11th World Congress on Anaerobic Digestion, 23-27 Septemeber 2007, Brisbane , Australia.

Jones D (2006). *Anaerobic Digestion – The Basics*. Ag & Biological Engineering, Purdue. www.biogasworks.com

Judd S (2006). *Fouling control in submerged membrane bioreactors*. Water Science & Technology, Vol. 51, # 6-7

Kalyuznnyi SV, Davlaytshina MA (1997). *Batch anaerobic digestion of glucose and its mathematical modeling I: Kinetic investigations*. Biosource Technology, Vol. 59, pp 73-80.

Kalyuznnyi SV (1997). *Batch anaerobic digestion of glucose and its mathematical modeling II: Description verification and application of model*. Biosource Technology, Vol. 59, pp 249-258.

Kang IJ, Yoon SH, Lee CH (2002). *Comparison of the filtration characteristics of organic and inorganic membranes in a membrane coupled anaerobic bioreactor*. Water Research, Vol. 36, pp 1803-1813

Kansal A, Rajeshwari KV, Balakrishnan M, Lata K, Kishore VVN (1998). *Anaerobic digestion technologies for energy recovery from industrial wastewater – a study in the Indian context*. TERI Infromation Monitor on Environmental Science, Vol. 2, #3, pp 67-75.

Kataoka N, Tokiwa Y, Tanaka Y, Fujiki K, Tadora H, Takeda K (1992). *Examination of bacteria characteristics of anaerobic membrane bioreactors in three pilot scale plants for treating low strength waste water by application of the colony forming curve analysis method.* Applied Environmental Microbiology, Vol. 58, No. 9, pp 2751-2757

Lettinga G, Van Velsen AFM, Homba SW, De Zeew W, Klapwijk A (1980). *Use of the up-flow sludge blanket (UASB) reactor for biological wastewater treatment especially anaerobic treatment*. Biotechnology & bioengineering, Vol. XXII, pp 699-734

Li J, Sanderson RD, Hurndall MJ, Hallbauer DK, Hallbauer-Zadorozhnaya (2004). *Real-time observation of fouling in membrane filtration by non-evasive ultrasonic techniques*. South African Water Research Commission Report No. 166/1/04, 183 pages

Lim SJ (2007) *Comparisons between a UASB and EGSB reactor*. Website: http://home.eng.iastate.edu/~tge/ce421-521/seungjoo.pdf

Liesjean B, Rosenberger S (2004). *Correlation between membrane fouling and soluble organic substances in MBRs for municipal waste water treatment*. Water Science & Technology, Vol. 51, # 6-7

Liesjean B, Rosenberger S, Schrotter JC, Recherche A, (2004). *Membrane-aided biological wastewater treatment – an overview of applied systems*. Membrane Technology August 2004.

Lobos J, Wisniewski C, Heran M, Grasmick A (2005). *Effects of starvation conditions on biomass behavior for minimization of sludge production in membrane bioreactors.* Water Science & Technology, Vol. 51, # 6-7

Loewenthal RE, Wiechers HNS, Marais G (1996). *Softening and stabilization of municipal waste waters*, South African Water Research Commission

Loewenthal RE, Lahav O (2000). *Measurement of VFA in anaerobic digestion: Five-point titration method revisited*. Water SA, Vol 26, no 3

Metcalf & Eddy Inc. (1991). *Wastewater engineering: Treatment, disposal and reuse.* 3rd Eddition McGraw-Hill Inc. Civil Engineering Series.

McCarty PL (1967a). *Anaerobic waste treatment fundamentals. Part One: Chemistry and microbiology*. Public Works 95, September, pp 107-112

McCarty PL (1967b). *Anaerobic waste treatment fundamentals. Part Two: Environmental requirements & control.* Public Works 95, October, pp 123-126

McCarty PL (1967c). *Anaerobic waste treatment fundamentals. Part Three: Toxic materials & their control.* Public Works 95, November, pp 91-94

McCarty PL (1967d). *Anaerobic waste treatment fundamentals. Part Four: Process design.* Public Works 95, December, pp 95-99

McCarty PL (1974) Anaerobic processes. *Procs International Association of Water Pollution Research (IAWPR, now IWA) short course on Design Aspects of Biological Treatment*, Birmingham, UK, 18 Sept. 1974.

McCarty PL (1975). Stoichiometry of biological reactions. Progress in Water Technology, Vol. 7, #1, pp 157-172

Mignone NA (1995), *Biological inhibition/toxicity control in municipal anaerobic digestion facilities.* Website: http://www.awpca.net/Biological%20Inhibition.pdf

Monod, J. (1942). *Recherches sur la Croissance des Cultures Bactériennes*. Paris: Hermann & Co

Moosbrugger RE, Wentzel MC, Loewenthal RE, Ekama GA, Marais GvR (1991). *Weak acid/bases and pH control in an upflow anaerobic sludge bed reactor*. PhD Thesis, Dep Civ Eng, University of Cape Town.

Mosvoto EV, Wentzel MC, Loewenthal RE, Ekama GA (1997). *Kinetic-based model for mixed weak acid/base systems*. Water SA, Vol 23, No 4, pp 311-322

Mosvoto EV, Wentzel MC, Loewenthal RE, Ekama GA (2000). *Extension and application of the three-phase weak acid/base kinetic model to the aeration treatment of anaerobic digester liquors*. Water SA, Vol. 26, No. 4, pp 417-437

Oh SE, Iyer P, Bruns MA, Logan BE (2004). Biological hydrogen production using a membrane bioreactor. Biotechnology and Bioengineering, Vol. 87, No. 1, pp119 – 127

Parawira W, Murto M, Read JS, Mattiasson B (2005). *Profile of hydrolases and biogas production during two-stage mesophillic anaerobic digestion of solid potato waste*. Process Biochemistry, Vol. 40, # 4, pp 2945-2952

Pauss A, Guiot R (1993). Hydrogen monitoring in anaerobic sludge bed reactors at various hydraulic regimes and loading rates. Water Environment Research, Vol. 65, #3, pp 276-280

Perry RH, Green DW, Maloney JO, (1997). *Perry's Chemical Engineering Handbook*. Mc Graw-Hill, 7th Ed, 3600 pages.

Perez M, Romero LI, Sales D (1998). *Comparative performance of high rate anaerobic thermophillic technologies treating industrial wastewater*. Water Research, Vol 32, #3, pp 559-564.

Phillips TD, Du Toit FJ (2002). *Water reuse and recycle at Sasol*. 3rd International Conference & Exhibition on Integrated Environmental Management in Southern Africa, 27-40th August 2002, Johannesburg South Africa

Ramphao M, Ekama GA, Lakay MT, Mafungwa H, Wentzel M, (2004*). The performance and kinetics of biological nitrogen and phosphorous removal with ultra-filtration membranes for solid-liquid separation.* UCT Msc Thesis, 200 pages.

Reyes O, Sanchez E, Rovirosa N, Borja R, Cruz M, Colmenarejo MF, Escobedo R, Ruiz M, Rodriguez X, Correa O (1999). *Low-strength wastewater treatment by a multistage anaerobic filter packed with waste tire rubber*. Bioresource Technology, Vol. 70, pp 55-60.

Ripley LE, Boyle WC, Converse JC (1986). *Improved alkalimetric monitoring for anaerobic digestion of high strength wastes.* Journal of Water Pollution Control Federation, Vol. 58, # 5, pp406-411.

Rodríguez J, Kleerebezem R, Lema JM, Van Loosdrecht CM (2005) *Modeling product formation in anaerobic mixed culture fermentations*. Biotechnology & Bioengineering. Vol **93**(3) 592 – 606

Rosen C, Vrecko D, Gernaey KV, Pons MN, Jeppsson U (2006) *Implementing ADM 1 for plant-wide benchmark simulations in Matlab/Simulink.* Water Science & Technology, Vol. 54, no. 4.

Ross WR (1984). *The phenomenon of sludge pelletization in anaerobic treatment of maize process waste*. Water SA, Vol. 4, pp 197

Ross WR, Novella PH, Pitt AJ, Lund P, Thompson BA, King PB, Fawcett KS (1992). *Anaerobic digestion of wastewater sludge*. WRC Report No TT55/92

Rossouw N, Van Zyl PJ (2008) *Pilot scale evaluation for the treatment of low temperature Fischer-Tropsch (FT) Coal-to-liquids (CTL) reaction water using Paques BIPAQ® Internal Circulating (IC) Anaerobic Digestion (AD) technology*. Internal Sasol Report

Sam-Soon PLANS, Loewenthal RE, Wentzel MC, Marais GvR (1989). *Pelletization in the upflow anaerobic sludge bed reactor*. PhD Thesis, Dep Civ Eng, University of Cape Town.

Sasol Facts (2005). Sasol Corporate Affairs Department – May 2005. www.sasol.com

Siegrist H, Vogt D, Garcia-Heras JL, Gujer W (2002). Mathematical Modeling of Meso- and Thermophillic Anaerobic Sewage Sludge. Environmental Science & Technology, Vol 36, pp 1113-1123

Siegrist H, Hunziker W, Hofer H (2005). *Anaerobic digestion of slaughterhouse waste with UF-membrane separation and recycling permeate after free ammonia stripping.* Water Science & Technology, Vol. 52, No. 1-2, pp 531-536

Show KY, Tay JH (1999). *Influence of support media on biomass growth and retention in anaerobic filters*. Water Research, Vol. 33, # 6, pp 1471-1481.

Smith DP, McCarty PL (1990). *Factors governing methane fluctualtions following shock loading of digesters*. Research Journal Water Pollution Control Federation, Vol. 62, # 1, pp 58-64

Soares A, Fawehinmi F, Rogalla F, Laster JN, Jefferson B (2007). *Anaerobic wastewater treatment in a pilot scale membrane bioreactor: the effect of low temperature.* 11th World Congress on Anaerobic Digestion, 23-27 Septemeber 2007, Brisbane , Australia.

Sötemann SW, Ristow NE, Wentzel MC and Ekama GA (2005a) *A steady state model for anaerobic digestion of sewage sludges. Water SA* **31**(4) 511-528.

Sötemann SW, Van Rensburg P, Ristow NE, Wentzel MC and Ekama GA (2005b) *Integrated chemical/physical and biological process modeling Part 2 – Anaerobic digestion of sewage sludges*. *Water SA* **31**(4) 545-568.

Standard Methods in Water; Greenberg, Arnold E.; Trussell, R. Rhodes; Clesceri, Lenore S (1985) *Standard methods for the examination of water and wastewater*. Pollution; Water resources and management. Book, 1270 pages

Takacs I, Stricker AE, Achleitner S, Barrie A, Rauch W, Murthy S (2008). *Do you know your sludge age?* Water Environment Federation

Vavilin VA, Lokshina LYA (1996). Modeling of volatile fatty acid degradation kinetics and evaluation of micro-organism activity. Biores.Tech. 57 (1) 69-80

Van Zyl PJ, Britz TJ, Ellis ER, Lozenzen L (2005). *Preliminary design guidelines for the development of a granulating bioreactor*. South African Water Research Commission Report, No 1239/1/05, 104 pages

Van Zyl PJ, Wentzel MC, Ekama GA and Riedel K-H (2007) *Design and start up of a high rate anaerobic membrane bio-reactor for the treatment of a low pH, high strength dissolved organic wastewater.* 11th Anaerobic digestion (AD11) conference, Brisbane, 23-27 Sept.

Versprille B (2001). *Instrumentation and control of anaerobic plants*. Biothane Systems International, Presentation for COST, San Sebastian, March 2001

Wentzel MC (1988), *Biological excess phosphorous removal in activated sludge systems*. Msc. Thesis. UCT, ±400 pages.

Whitmore TN, Lioyd D (1986) *Mass spectrometric control of thermophillic anaerobic digestion process based on levels of dissolved hydrogen*. Biotechnology Letters. Vol. 8, #3, pp 203-208

Wasdworth HM (1998) *Handbook of statistical methods for engineers and scientists*. McGraw-Hill Professional, 688 pages

Yang W, Cicek N, Ilg J (2006). *State-of-the-art of membrane bioreactors: Worldwide research and commercial applications in North America*. Journal of Membrane Science, Vol. 270, pp 201-211

Yoon TI, Lee HS, Kim CG (2004), *Comparison of pilot scale performances between membrane bioreactor and hybrid conventional wastewater treatment systems*. Journal of membrane science Vol 242, pp 5-12.

You HS, Tseng CC, Peng SH, Chen YC, Peng SH (2005). *A novel application of an anaerobic membrane process in wastewater treatment*. Water Science & Technology, Vol. 51, # 6-7

Yuzir A, Sallis PJ (2007). *The effect of elevated (RS)-MCPP concentrations on the performance of an anerobic membrane bioreactor.* 11th World Congress on Anaerobic Digestion, 23-27 September 2007, Brisbane , Australia.

Zhang D, Lu P, Long T, Verstrate W (2005), *The integration of simultaneous nitrification and denitrification in a membrane bioreactor*. Process Biochemistry, Vol. 80, pp 541-547.

Zitomer DH, Bachman TC, Vogel DS (2005). Thermophillic anaerobic digester with ultrafilter for solids stabilization. Water Science & Technology, Vol. 52, No 1-2, pp 525-530.

Appendix

Table of Contents

Appendix 1.1 Current & Purposed Treatment System Comparison

Assumptions

- Energy density of Sasol Coal: 5.83 kWh/kgCoal. The thermodynamic efficiency of coal power plant: 33 %, thus a coal power plant generates **1.9 kWh/kgCoal**.

- 1kg coal consists of at least 0.5 kg carbon or 1/24 kmol carbon, resulting in 1/24 kmol CO_2, or (1/24 kmol)*(44 kg/kmol) = 1.83 $kgCO_2$/kgCoal. Thus the carbon cost of energy from coal is (1.83 $kgCO_2$/kgCoal)/(1.9 kWh/kgCoal) = **0.95 $kgCO_2$/kWh**

- Energy density of methane is rated at 887 kJ/mol or 55.6 MJ/kg or 39 MJ/m^3. Since 1kWh = 3600 kJ, methane is rated at 246 kWh/kmol current gas turbines operate at a thermodynamic efficiency of 30% thus, 39*0.30 = 11.7 MJ/m^3., **methane's electricity value is rated at 3.25 kWh/m^3 or 74 kWh/kmol**.

- Diffused aeration as used on the Sasol treatment plant is estimated at **1.5 kgO_2/kWh**.

Current System

- Currently treating 677 tCOD/d aerobically, activated sludge requires 0.71 tO_2/tCOD, thus (677 tCOD/d)*(0.71 tO_2/tCOD) = **480 tO_2/d Oxygen requirement for respiration.**

- And (480 tO_2/d)*(44/32) = **660 tCO_2 produced from respiration**

- **(677 tCOD/d)*(0.22 kgTSS/kgCOD) = 150 tTSS/d produced from aerobic COD removal**

- Thus (480 tO_2/d)/(1.5 tO_2/MWh) = **320 MWh/d required for oxygenation of activated sludge**

- (320 MWh/d)/(1.9 tCoal/MWh) = **170 tCoal/d for oxygenation power supply**

- (170 tCoal/d)*(1.83 $kgCO_2$/kgCoal) = **310 $kgCO_2$/d produced from coal burning**, and (310 $kgCO_2$/d)*(32/44 g/molO_2*molCO_2/g) = **225 kgO_2/d required for coal burning to produce energy for oxygenation of activated sludge**

Proposed – Part 1; Aerobic

- Only 154.7 tCOD/d will be treated aerobically, thus (154.7 tCOD/d)*(0.71 tO_2/tCOD) = **110 tO_2/d Oxygen requirement for respiration**

- And (110 tO_2/d)*(44/32) = **151 tCO_2 produced from respiration**

- **(154.7 tCOD/d)*(0.22 kgTSS/kgCOD) = 34 tTSS/d produced from aerobic COD removal**

- Thus (110 tO_2/d)/(1.5 tO_2/MWh) = **73.33 MWh/d required for oxygenation of activated sludge**

- (73.33 MWh/d)/(1.9 tCoal/MWh) = **39 tCoal/d for oxygenation power supply**

- (39 tCoal/d)*(1.83 $kgCO_2$/kgCoal) = **70.6 $kgCO_2$/d produced from coal burning**, and (70.6 $kgCO_2$/d)*(32/44 g/molO_2*molCO_2/g) = **51.4 kgO_2/d required for coal burning to produce energy for oxygenation of activated sludge.**

Proposed – Part 2; Anaerobic

- 522 tCOD/d will be treated anaerobically, 98% of COD will be converted to methane, thus 522*0.98 = 511 $tCOD_{Methane}$/d, or (511 000 $kgCOD_{Methane}$/d)/(64 kgCOD/$kmol_{Methane}$) = 8000 $kmol_{Methane}$/d or (8000 $kmol_{Methane}$/d)*(16 kgMethane/$kmol_{Methane}$) = 127.8 tonMethane/d or (8000 kmolMethane/d)*(22.4 m^3/kmol) = **179 000 m^3Metane/d from anaerobic digestion of FTRW**

- Thus (8000 $kmol_{Methane}$/d)*(887 kJ/$kmol_{Methane}$) = 6930 GJ/d or 1968 MWh/d or roughly **82 MW energy in methane. At 33% thermal efficiency, 27 MW (655 MWh/d) of electricity can be produced from the methane stream.**

- Experimental results obtained later in this project indicated that the AnMBR's power consumption is ± 15% of the energy produced from methane, thus 27*0.85 = **~23 MW excess energy produced from methane combustion**. Based on the assumption that a typical household consumes 1000 kWh/month or 33 kWh/d, the electricity generated from the methane stream will be enough to power (655 000*0.85 kWh/d)/(33 kWh/household/d) = 17 000 average SA households.

- If all the methane is used to produce electricity, less coal will be required; (655 MWh/d)/(1.9 MWh/tCoal) = **344 tCoal/d saved due to electricity production via methane combustion**

- Biogas is typically 50/50 CH_4 and CO_2 thus 8000 kmol CO_2 or (8000 kmolCO_2)*(44 kg/kmolCO_2) **= 352 tCO_2/d produced via anaerobic digestion**

- **(522 tCOD/d)*(0.04 kgTSS/kgCOD) = 21 tTSS/d produced from aerobic COD removal**

Appendix 1.2 Methane to Diesel

- The methane is firstly reformed to feedstock for the Fischer-Tropsch process viz.

  $CH_4 + H_2O \rightarrow CO + 3H_2$

- Next the feedstock is catalytically converted to long chain hydrocarbons, viz;

  $CO + 2H_2 \rightarrow -CH_2^- + H_2O$

- Since diesel is mostly polymer chains of length C_{11} to C_{20}, the heavies (polymers exceeding C_{20} in length) needs to undergo cracking.

- If cracking is included, 1 mol of methane produces approximately 1/15 mol diesel. The FT process efficiency is approximately 50%, thus 1 mol CH_4 = 1/30 mol diesel

- Thus (522 tCOD/d)*(0.98) = 511 tonCOD as Methane/d or (511 tCOD/d)/(64 kg/kmol$_{Methnae}$) = 8000 kmol$_{Methane}$/d, (8000 kmol$_{Methane}$/d)/(30 kmol$_{Diesel}$/kmol$_{Methane}$) = 266 kmol$_{Diesel}$/d

- Mr_{Diesel} = ± 167 kg/kmol$_{Diesel}$ & $Density_{Diesel}$ = 850 kg/m^3, thus (266 kmol$_{Diesel}$/d)*(167 kg/kmol$_{Diesel}$) = 44500 kg$_{Deisel}$/d or (44500 kg$_{Deisel}$/d)/(850 kg/m^3) = **52 000 L$_{Diesel}$/d**

Appendix 3.1: AnMBR P&ID

Figure A3.1 is a Piping and Instrumentation Diagram (P&ID) of the lab-scale AnMBR. Biogas gets extracted at the top of the reactor via the gas recycle line 1. The biogas is recompressed via a diaphragm-type compressor (PD1) and then recycled via the coarse bubble diffusers through the liquid volume of the reactor to induce gas scour over the flat panel membranes (M123). The biogas compressor is a ILMVAC MPC 1201 Ep with a maximum gas delivery rate of 8300 L/h. The biogas recycle flow rate is controlled with a bypass line and a valve (V1). If a higher flow rate is required V1 is closed and vice versa. This 'bypass' throttle is far less arduous on the compressor than normal 'in line' throttling to reduce flow rate

The reactor feed is introduced via line 5. A synthetic FTRW is fed to the system from feed tank (T3) via the feed pump (P2). P2 is a Masterflex Easy Load peristaltic pump with a flow speed adjustable to between 0 and 50 L/d, depending on the flow speed setting and the diameter of the tubing. The feed enters the reactor and is immediately mixed into the biomass where it is digested to produce biogas and active mass. The effluent exits the reactor through the membranes and into the effluent bucket (T1). To control the sludge age, biomass is wasted via line 7.

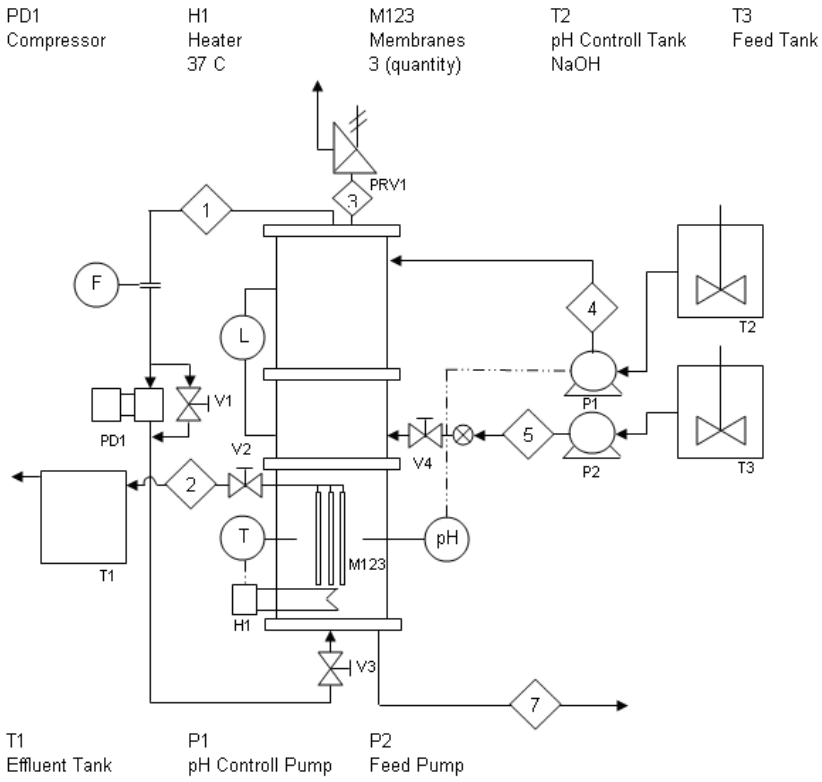

Figure A3.1, AnMBR Piping & Instrumentation Diagram

The gas volume pressure (above the membranes) and liquid level inside the reactor needs to be carefully controlled, because both add to the Trans Membrane Pressure (TMP) over the membranes, which in turn governs the flow out the reactor. By monitoring the liquid level with the level monitor (L) on the reactor and also by adjusting the pressure of the pressure relief valve (PRV1) the gas

pressure in the reactor headspace can be finely controlled. Therefore, the higher the PRV1 pressure, the faster effluent will exit the reactor and the lower the liquid level inside the reactor. The aim is to maintain the liquid volume of the reactor at 23 L.

The system temperature is controlled by an on/off type heater (H1) with a tolerance of approximately 1 ºC around 37 ºC. The pH is maintained at 7 via the pH control system. A pH probe submerged in the mixed liquor relays a signal to a control system which in turn switches the dosing pump (P1) on if the pH drops below a desired set point. The control system depicted in Figure A3.1 was the original design; after the reactor performance was evaluated at high loading rates (> 20 kgCOD/m^3/d) the pH control system was further modified. This will be discussed in the following section.

Appendix 3.2: AnMBR High OLR Control System

The dosing of buffer affects the anaerobic process in two ways. The first is that it increases the alkalinity to the desired level (± 2000 mg$CaCO_3$/ℓ) and thus for any given feed flow rate the required volume of buffer is constant and can be calculated (Q_{bAlk}). The second effect of the NaOH is the neutralization of unutilized SCFAs:

$$\mathbf{CH_3(CH_2)_XCOOH + OH^- + Na^+ => CH_3(CH_2)_XCOO^- + H_2O + Na^+} \quad \text{(A3.1)}$$

Because the anaerobic digestion process utilizes the acid form of the SCFAs, only the unutilized SCFAs, namely the SCFA concentration in the effluent, requires neutralization. So the volume of buffer required for neutralization (Q_{bSCFA}) can also be calculated. This implies that the total buffer requirement (Q_{btot}) is a function of the influent flow rate and effluent SCFA concentration:

$$\mathbf{Q_{btot} = Q_{bAlk} + Q_{bSCFA}} \quad \text{(A3.2)}$$

Thus for a given influent flow rate and desired effluent SCFA concentration (~100 mgAc/L) the Q_{btot} can be calculated and the buffer dosing pump flow rate can be set appropriately.

At the set buffer dosing, the system pH will be maintained if the flow rate stays constant and the effluent SCFA stays < 100 mgAc/L. However, if there is a system upset in the form of an increase in feed flow rate or effluent SCFA, Q_{btot} will not supply sufficient alkalinity and/or neutralization resulting in a decrease in pH. It is this, easily observable pH fluctuation that the control system is based on.

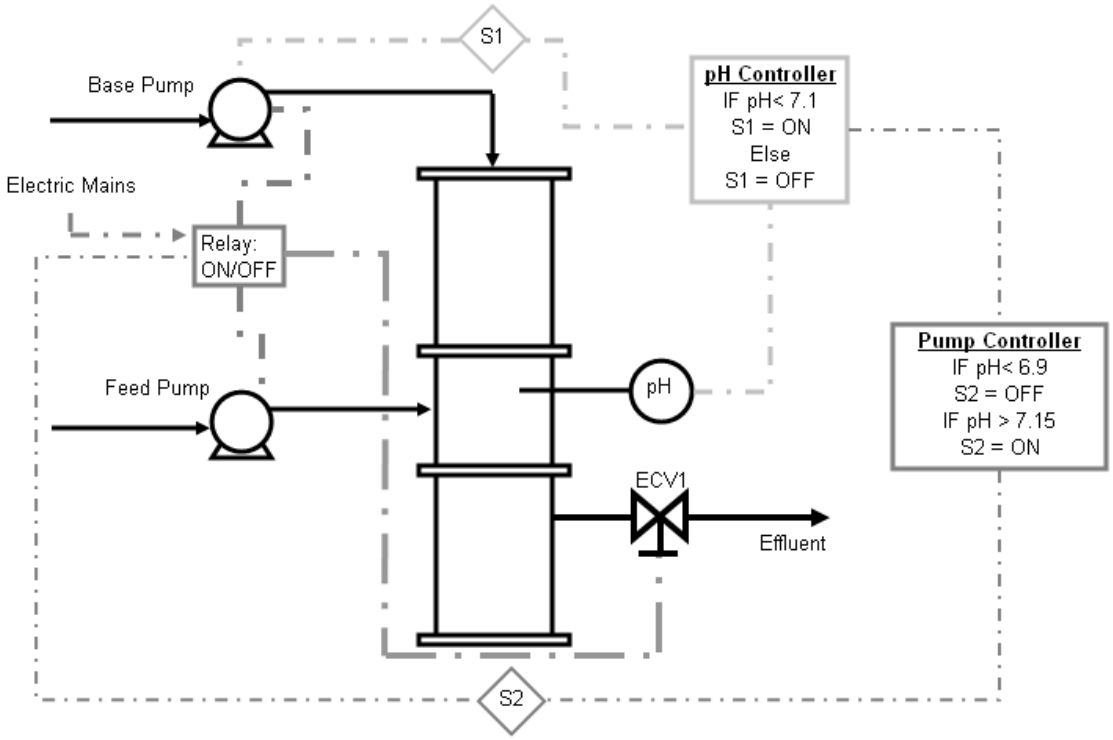

Figure A3.2, AnMBR: On-line Control System

The Buffer Pump Controller (BPC1) in Figure A3.2 measures the reactor pH and activates the buffer dosing pump (BP1) if the pH falls below a desired level (pH ±7.1). If the buffer requirement is less than Q_{btot} the pH will recover, but if the buffer requirement is higher due to a SCFA overload, the pH will continue to decrease. An electronic pH reading is relayed from BPC1 to the control system (C1) and if the reactor pH falls below a selected set point (S1 = 6.9) the buffer pump and the feed pump are deactivated and the Effluent Control Valve (ECV 1) is closed. This effectively turns the system into a batch reactor. Now since the intervention of C1 ensured that the reactor SCFA and sodium concentrations are still relatively low (<500 mgAc/L and <3000 mgNa/L) and the pH is still in the optimum anaerobic digestion range, the digestion processes will continue. As the anaerobic process continues in batch mode, biogas and alkalinity will be produced from the undigested SCFAs resulting in an increase in reactor pH. C1 will continue to monitor the pH and if it increases above a high set point (pH = 7.15), the feed and dosing pump will be switched back on, ECV1 will be opened and normal operation will continue. In so doing the on-line control system shields the biomass from overloading situations.

Appendix 3.3: Pilot Scale Fixed Media Reactor Design and Scale-Down Methodology

The original pilot plant design was done by Talbott & Talbott for the specific purpose of treating FTRW. The reactor is a 420 stainless steel cylinder with an operational volume of 5 m^3 and a diameter of 1.2 m. Diluted effluent enters the reactor from the top and then passes through a disperser plate and onto the fixed media which is housed inside the reactor. The effluent moves through the packing and comes into contact with the immobilized micro-organisms which are attached to this media. This is where the COD gets removed and biogas produced. At the bottom of the packed bed, another disperser plate is situated which holds the packing in place. The effluent passes through the disperser plate and out the reactor. A heater, which maintains the system at 37 ºC, is situated in the liquid below the bottom effluent collector. A P&ID of the pilot-scale AnPBR can be seen in Figure A3.3.

CLASIFIED

Figure A3.3, Pilot Scale AnPBR P&ID

Table A3.1, Known Parameters of pilot scale AnPBR

CLASIFIED

The down flow velocity, of liquid over the packing is has a major effect on the hydrodynamic shear and mass transfer phenomenon over the packing material. These two factors in turn dictate the catalyst/biological performance that can be expected from the system (Perry et al., 1997, Coulson & Richardson, 1998). Any scale-up or scale down of a packed bed system should be done so that this down flow velocity remains constant. This ensures that for the same packing, the boundary layer conditions are equal and thus heat and mass transfer phenomena should also be similar (Incropera & DeWitt, 1996).

Packing Properties

The packing voidage (ε) is the amount of "empty space" there exists between the packing material in the reactor. For a scale down to be successful this voidage, which is also related to the surface area per unit reactor volume, should remain constant (Coulson & Richardson, 1998). The voidage varies with reactor diameter, as can be seen from Figure A3.4.

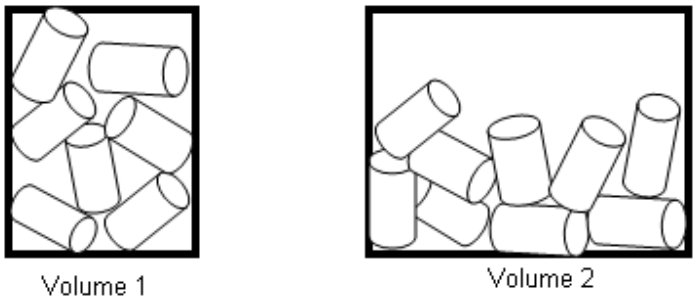

Figure A3.4, Voidage differences in "small" and "lager" diameter volumes

Because of the wall effects of the smaller diameter Volume 1, the packing is obstructed and the voidage is large. In the case of Volume 2, the wall effects are much less due to the larger diameter. The voidage is defined as follows:

$$\varepsilon = \frac{(V_b - V_s)}{V_b} \qquad [-] \qquad \text{(A3.3)}$$

With V_b being the total bed (or reactor) volume and V_s being the volume inside the bed occupied by packing. For the packing used in the AnPBR, one unit has a total cylindrical volume of $V_p = 2.7*10^{-5}$ m^3 and a surface area of $A_p = 0.0094$ m^2 (including inside area). The specific surface area of the packing (S_p) can then be calculated as:

$$S_p = \frac{A_p}{V_p} \qquad [m^2/m^3_{\text{packing material}}] \qquad \text{(A3.4)}$$

To observe how the voidage changes with diameter, the following experimental procedure was applied:

- Cylinders of different volumes and diameters were used
- These cylinders were then filled with the supplied packing to a known volume.
- The cylinder diameter (D_b) and volume (V_b) were logged, and
- the number of individual pieces of packing was counted (N_p).

The voidage was then calculated as follows:

$$\varepsilon = \frac{\left(V_b - N_p V_p\right)}{V_b} \qquad [-] \qquad \text{(A3.5)}$$

To observe how the specific surface area per unit volume (S_b) changes with diameter, eq 4 is used:

$$S_b = S_p(1-\varepsilon) \qquad [m^2/m^3_{\text{reactor volume}}] \qquad \text{(A3.6)}$$

S_b was then calculated for a range of cylinder diameters and Figure A3.5 displays the results that were obtained:

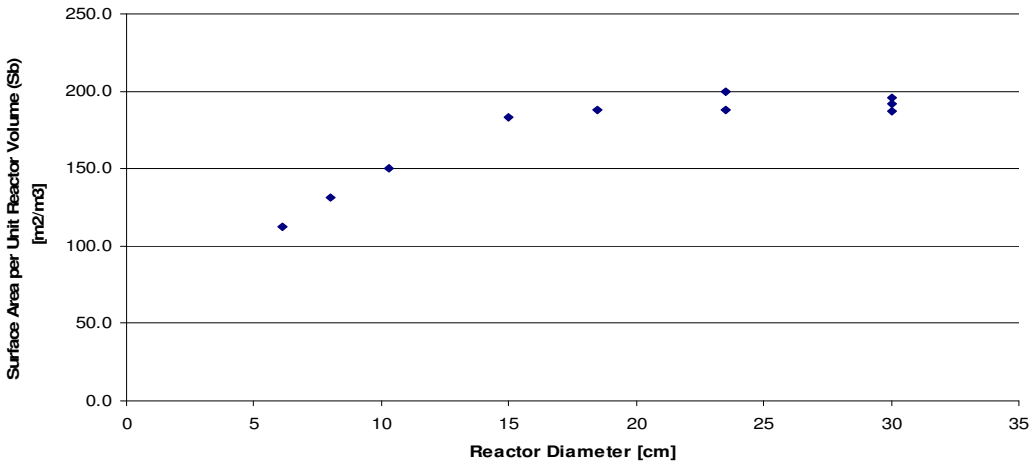

Figure A3.5, Packing surface area per unit reactor volume (S_p) as a function of reactor diameter

Note that at small diameters there is significant variation in surface area per unit volume as the diameter changes. However, for diameters of 0.015 m and larger the variance is nearly zero. This shows that for a surface area per unit reactor volume similar to that of the pilot-plant AnPBR, a lab-scale diameter limit is 0.015 m, but to be on the safe side a lab-scale diameter of 0.19 m was be chosen.

Appendix 3.4: COD, N & P Characterization

Any given wastewater sample (Influent, Effluent & MLSS) can be classified into COD fractions as depicted in Table A3.2. The biodegradable fractions (S_{bp} & S_{bs}) dictate the amount of methane and biomass that will be produced in the anaerobic system. The un-biodegradable soluble fraction dictates the minimum effluent quality and the un-biodegradable particulate fraction (Sup) combined with the biomass in the system (active and endogenous) dictates the mixed liquor concentration.

Table A3.2, Chemical Oxygen Demand (COD) Classification

COD Type	Abbreviation	Description	Equation
Total Unfiltered	S_t	COD of raw sample	-
Total Soluble	S_{ts}	COD of filtrate after Raw Sample has passed through a 0.45 um filter	-
Total Particulate	S_{tp}	Part of raw sample's COD that is in particulate form	$S_{tp} = S_t - S_{ts}$
Un-biodegradable Soluble	S_{us}	Part of raw sample's COD that is soluble and cannot be digested by biological processes **	
Un-biodegradable Particulate	S_{up}	Part of raw sample's COD that is in particulate form and cannot be digested by biological processes	$S_{up} = f_{up} * X_v / f_{cv}$
Biodegradable Particulate	S_{bp}	Part of raw sample's COD that is in particulate form and can be digested by biological processes	$S_{bp} = S_{tp} - S_{up}$

From the COD classification in Table A3.2, the various load parameters used to quantify a waste water stream or reactor performance can be calculated (Table A3.3).

** This is typically measured by digesting the waste water to be classified in a long sludge age activated sludge system and then measuring the filtered effluent COD

Table A3.3: Organic Loading & Performance Parameters.

Parameter	Abbreviation	Dimetion	Discription	Equation
COD Concentration	S	mgCOD/L	COD concentration of sample	Table (XXX)
COD Load	L	kgCOD/d	The Actual Mass of COD carried by a Effluent Stream	$S_{ti}*Q_i*24$
Organic Loading Rate	OLR	$kgCOD/m^3/d$	Mass of COD that can be supplied per unit reactor volume per day	$Q_{feed}*S_{ti}*24/V_r$
COD Removal Rate	RR	$kgCOD/m^3/d$	Mass of COD that can be removed per unit reactor volume per day	$(S_{ti} - S_{tse})*Q_{feed}*24 /(V_r*1000000)$
Removel Efficiency	RE	%	Persentage of COD Load that is removed by biological processes	RR*100/OLR

Analogously to the COD classification, nitrogen and phosphorous fractions can also be calculated for a given sample (Table 3.4).

Table A3.4, Nitrogen & Phosphate Classification

Parameter	Abbreviation	Dimetion	Discription	Equation
Free & Saline Ammonia	Na	mgN/L	FSA test done on Filtered Sample	-
Total Kedjal Nitrogen	Nt	mgN/L	TKN test done on Unfiltered Sample	-
Organic Nitrogen	OrgN	mgN/L	Organicall bound Nitrogen	N_t-N_a
Total Phosphates	Pt	mgP/L	Phosphate test done on Unfiltered Sample	-
Ortho Phosphates	Po	mgP/L	Phosphate Test done on Filtered Sample	-
Organic Phosphates	OrgP	mgP/L	Organically bound Phosphates	P_t-P_o

Appendix 3.5: Reactor Operation and Feedstock Preparation

Table A3.5 and A3.6 presents the parameters measured on the AnPBR and AnMBR and also the frequencies of the measurements

Table A3.5, Parameters measured on AnPBR

Measured Parameter	Daily	Twice Weekly	Monthly	As Required
Flow Rate	X			
Gas Production	X			
pH	X			
Buffer Usage	X			
COD (uf) (inf+eff)	X			
COD (f) (eff)	X			
TKN (inf + eff)		X		
FSA (inf + eff)		X		
Alkalinity (eff)	X			
VFA (eff)	X			
Biogas Composition				
HPLC Analysis (eff)				X
Metal Analysis				X

Table A3.6, Parameters measured on AnMBR

Measured Parameter	Daily	Twice Weekly	Monthly	As Required
Flow Rate	X			
Gas Production	X			
Sludge Wasting	X			
pH	X			
Buffer Usage	X			
Trans Membrane Pressure	X			
Reactor Volume	X			
TSS-VSS		X		
COD (uf) (inf)	X			
COD (uf) (eff)	X			
TKN (inf + eff)		X		
FSA (inf + eff)		X		
Alkalinity (eff)	X			
VFA (eff)	X			
Biogas Composition		X		
HPLC Analysis (eff)				X
Metal Analysis				X

The Synthetic Fischer-Tropsch Reaction Water is made up in a stock solution and in turn is diluted to18 gCOD/L. Since the mix consists mostly of $C_2 - C_6$ SCFAs, the pH is low (pH_{SFTAW} ± 2.5) and alkalinity (1.4 $gNaHCO_3/L$) needs to be added to increase the pH of synthetic FTRW to that of real FTRW (pH = 3.77). Table A3.7 displays the composition, recipe and characteristics of synthetic FTRW

Table A3.7, Synthetic Fischer-Tropsch Reaction Water: Specifics & Make-up

CLASIFIED

Appendix 3.6: Process Equipment Details

Table A3.8: Process Equipment Details

Process Unit	Abbre-viation	Description	Capacity	Medium
AnMBR				
Feed Pump	P1	Materflex Easy Load Peristaltic	0-50 L/h	Liquid
Waste Pump	P7	Materflex Easy Load Peristaltic	0-50 L/h	Liquid
Buffer Dosing Pump	BP1	Hanna Diaphragm	0-9 L/h	Liquid
pH Electrode	pH	Metrohm Vicotrode	0-14	Viscous Liquid
pH Controller	C1	Hanna	-	-
Pump Controller	PC1	Online Electronic (In-house Design)	-	-
Electronic Control Valve	ECV1	Fail-shut Electronic Control Valve	0/50 L/h	Liquid
Biogas Recycle Compressor	PD1	Ritter Drum-type	2-120 L/h	Gas
On/off Heater	H1	Fish tank-type	25-45 °C	Liquid
Pressure Release Valve	PRV1	Hydraulic Pressure Control	0-120 L/h	Gas
AnPBR				
Feed Pump	A	Materflex Easy Load Peristaltic	0-50 L/h	Liquid
Recycle Pump	C	Materflex Easy Load Peristaltic	0-50 L/h	Liquid
Buffer Dosing Pump	B	Hanna Diaphragm	0-9 L/h	Liquid
pH Electrode	pH	Metrohm Viscotrode	0-14	Viscous Liquid
pH Controller	C2	Hanna	-	-
5-Pt Titration Tests				
pH Electrode		Metrohm 477	0-14	Aqueous Solutions
Auto Titrator		Metrohm 715 Dosimat		
Biogas Composition Analysis				
Gas Chromatograph		Varian 330	0-100 %	CH_4, CO_2, N_2
Integrator				
Trace Metal Analysis				
Trace Metal Analyzer				

Appendix 4.1: AnMBR Restart – Adapted Biomass

Later in the study a second AnMBR start-up was done with waste sludge collected from the AnMBR over three months before hand. Figure A4.1 presents a comparison between AnMBR start-up times with un-adapted municipal digester sludge and with a well adapted biomass.

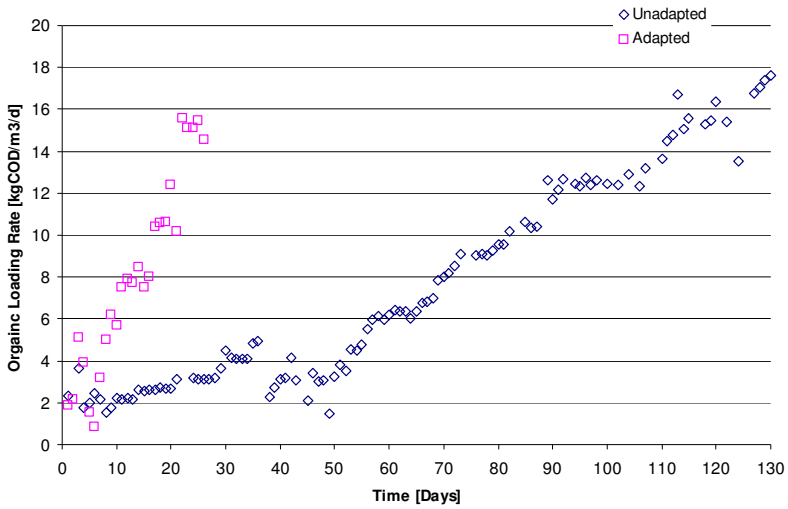

Figure A4.1, AnMBR Start-up time comparison for adapted & un-adapted biomass

Contrary to un-adapted anaerobic sludge, there is no observable lag phase in the start-up with an anaerobic sludge that is well adapted to the AD-FTRW climate. Secondly the slope of OLR increase in the adaptation phase is also much steeper, implying that the activity increase and resultant OLR increase was much faster than for the un-adapted biomass. A start-up period of 25 days was observed for the adapted biomass compared to 110 days for the municipal digester sludge.

Appendix 4.2: The Effect of Individual Nutrients on OLR

This section gives a discussion of the effect of nutrient concentration on reactor performance and thus OLR. The minimum required influent nutrient concentration will be identified as that at which the OLR reached 10 kgCOD/m^3/d. The data will be presented in scatter plots of the given nutrient concentration vs. OLR.

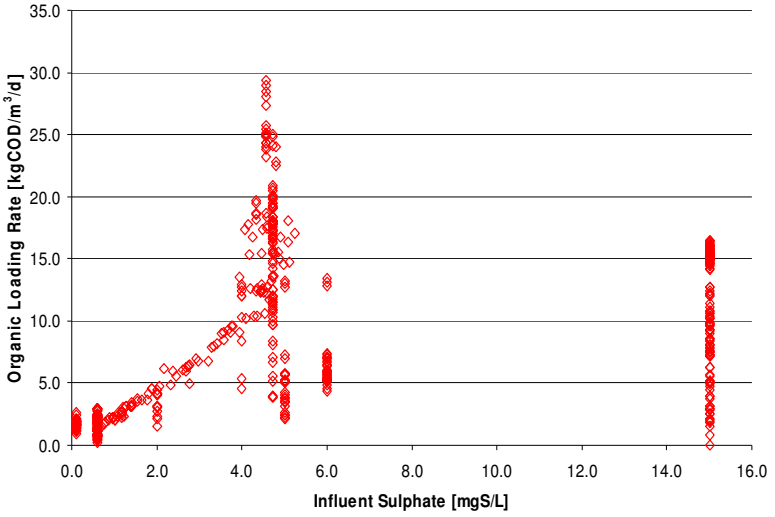

Figure A4.2, Influent Sulfate Concentration vs. OLR

Sulfate has a significant effect on the AnMBR performance. It can be noted from Figure A4.2 that a high OLR was never observed for an influent sulfate concentration lower than 4 mgSO_4-S/L, however once this minimum concentration limit was exceeded, the OLR increased dramatically. Figure A4.3 shows that the exact opposite is true for calcium:

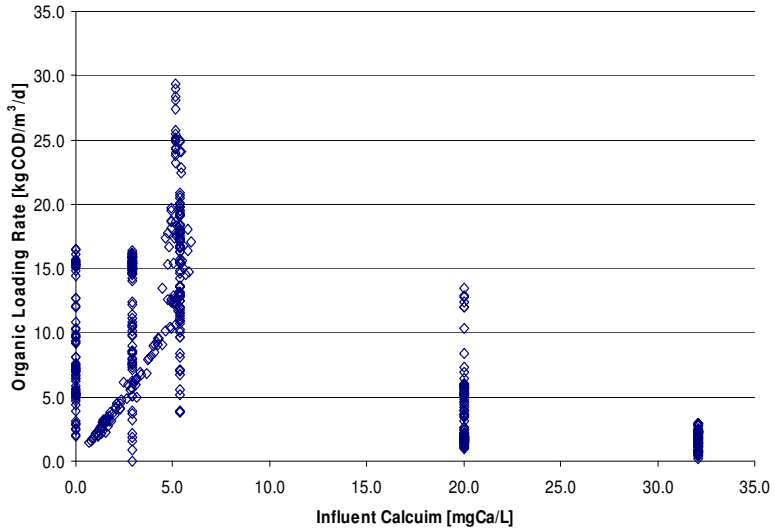

Figure A4.3, Influent Calcium Concentration vs. OLR

No correlation between the influent calcium concentration and the performance of the AnMBR could be identified. Even at concentrations as low as 0.0 mgCa/L OLRs of 10 kgCOD/m^3/d was observed. Thus results indicate that calcium need not be dosed as macro nutrient. The same observation can be concluded for magnesium from Figure A4.4:

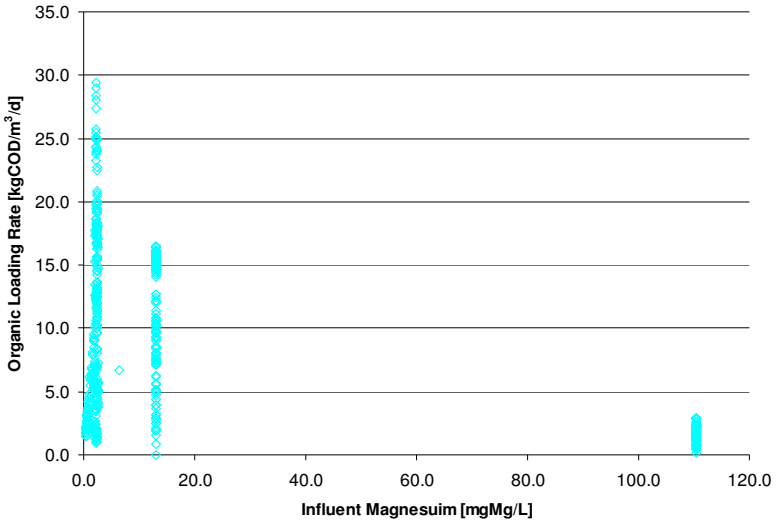

Figure A4.4, Influent Magnesium Concentration vs. OLR

No correlation was found between the influent magnesium concentration and the OLR, OLRs > 10 kgCOD/m^3/d was observed for influent magnesium concentrations as low as 2 mg/L. On the contrary, high OLRs were never observed for magnesium concentrations of >100 mgMg/L. This observation might point towards magnesium inhibition, but further investigation is required for conclusive evidence. Figure A4.5 displays the effect of Iron on OLR:

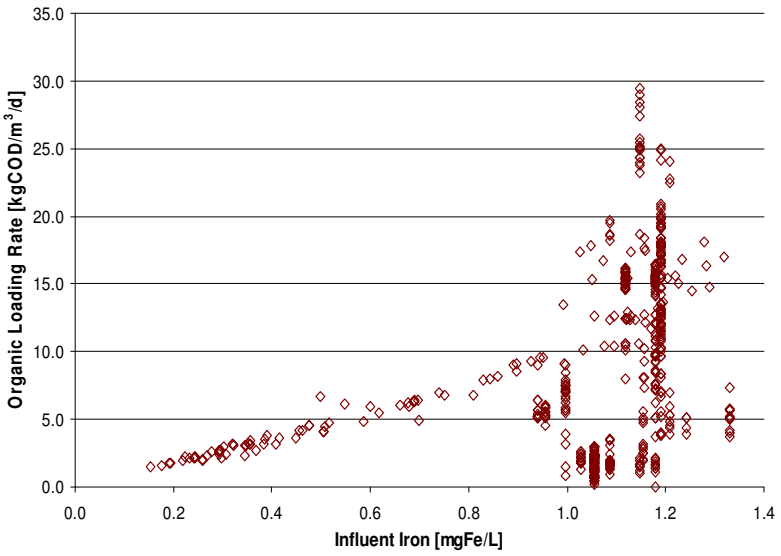

Figure A4.5, Influent Iron Concentration vs. OLR

A high OLR (>10 kgCOD/m^3/d) and influent iron concentration < 1 mgFe/L was never observed for the entire 685 day observational period. However, once a minimum influent iron concentration of 1 mgFe/L was exceeded, the OLR increased rapidly. Hence results indicate that Fe should be dosed as a macro nutrient at an influent concentration of at least 1 mgFe/L. The only micro nutrient that was evaluated was nickel. The reason for this is a debate in the literature on whether nickel is essential

for anaerobic digestion or not. Thus it was decided to include this micro nutrient in the nutrient optimization study (Figure A4.6):

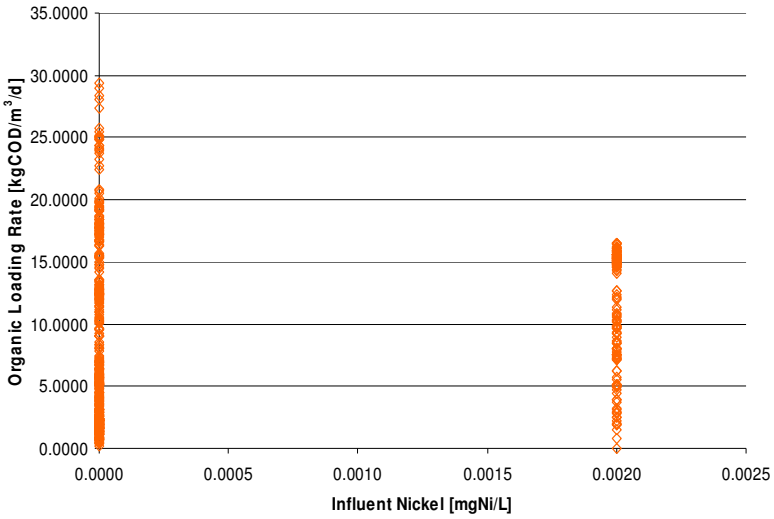

Figure A4.6, Influent Nickel Concentration vs. OLR

The AnMBR was operated at an influent nickel concentration of zero for more than 500 days; thereafter this concentration was upped to 2 µg/L. No correlation could be found between the influent Nickel concentration and the AnMBR performance.

Appendix 4.3: Membrane Life Span Calculation

The membrane life span is estimated by quantifying the change in the Tap Water Flux Slope (TFS) after a chemical clean. The decrease in the TFS over time gives an indication of the permanent fouling rate and thus lifespan of the membranes in the AD-FTRW environment. From Figure 4.7 it can be noted that the initial TFS slope for the system before commissioning was $TFS_i = 0.1336$ and after 530 days of operation this value has deteriorated to $TFS_{530} = 0.1152$. Thus the rate of slope change (RSC) can be expressed as follows:

$$RSC = \frac{TFS_i - TFS_{520}}{Time} \quad \text{(A3.7)}$$

Or

$$RSC = \frac{0.1336 - 0.1152}{520} = 3.471 * 10^{-5} \quad \text{(A3.8)}$$

If it is assumed that membranes will be replaced if permanent fouling has decreased the flux capacity by 50%:
$TFS_{50\%} = TFS_i/2$

And

$$MembraneLife = \frac{\left(\frac{TFS_i}{2}\right)}{RSC} \tag{A3.9}$$

Or

$$MembraneLife = \frac{\left(\frac{0.1336}{2}\right)}{3.471*10^{-5}} = 1924 \qquad \text{[days]} \tag{A3.10}$$

Giving an expected membrane life in the order of 7 years if the 18 months of operation in the activated sludge MBR is included.

Appendix 4.4: Steady State Data

A4.4.1 Submerged Membrane Anaerobic Bioreactor (AnMBR):

Table A4.1, AnMBR Steady State Data

Day	SS Organic Loading Rate	SS Influent COD	SS Influent Nitrogen	Reactor pH	MLSS [mgTSS/L]	MLVSS [mgVSS/L]	Sludge Age [Days]	Effluent COD [mgCOD/L]	Effluent Alkalinity	Effluent VFA [mgHAc/L]	Effluent N	Effluent Na	Effluent Specific	OLR [kgCOD/
650	15.58173665	18500	84	7.06	20.00	15.24	55.00	24.576	2357	0	63	878	0.045	15.58
651	15.13901627	18500	84	7.15	19.50	14.86	57.00	20.48	2331	48	32	1686	0.050	15.14
652	15.1103796	18500	84	7.12	19.18	14.61	56.00	28.672	2361	13	42	1452	0.099	15.11
653	15.43044791	18500	84	7.20	19.00	14.48	70.00	20.48	2209	21.9	35	1416	0.096	15.43
654	14.56055449	18500	84	7.18	18.70	14.25	195.83	18.432	2200	0	34	1012	0.058	14.56
655	15.31034483	18500	84	7.10	19.00	14.48	195.83	0	2180	0	37	1203	0.075	15.31
656	15.90666598	18500	84	7.08	19.20	14.63	195.83	12.288	2180	0	47	1117	0.067	15.91
657	15.84309943	18500	84	7.07	20.00	15.24	69.12	16.384	2170	0	35	885	0.046	15.84
658	15.3374686	18500	84	7.06	18.00	13.72	69.12	16.384	2153	38.6	32	1249	0.080	15.34
659	15.853632	18500	84	7.07	17.50	13.34	69.12	4.096	2165	0	28	1168	0.072	15.85
660	15.74635804	18500	84	7.05	17.12	13.05	69.12	37.728	2216	21	48	1149	0.070	15.75
661	15.8019872	18500	84	7.07	20.10	15.32	69.12	30	2158	0	52	899	0.047	15.80
662	16.07702723	18500	84	7.08	20.00	15.24	69.12	46.112	2160	0	41	1331	0.088	16.08
663	16.13369665	18500	84	7.08	21.00	16.00	69.12	45	2181	21	50	926	0.049	16.13
664	16.16389058	18500	84	7.07	20.50	15.62	69.12	35	2166	3.4	30	1129	0.069	16.16
665	15.99959688	18500	84	7.05	20.50	15.62	69.12	40	2228	0	32	998	0.056	16.00
666	14.74468085	18500	84	7.07	20.50	15.62	69.12	20	2197	37.3	46	1819	0.070	14.74
667	14.59295356	18500	84	7.07	20.80	15.85	55.55	50.304	2209	31	37	1059	0.062	14.59
668	15.05832831	18500	84	7.07	20.65	15.74	73.44	37.728	2343	4.6	43	1335	0.088	15.06
669	14.80124198	18500	84	7.07	21.00	16.00	61.84	88.032	2100	30	36	2242	0.072	14.80
670	15.40760518	18500	84	7.07	21.00	16.00	52.38	37.728	2211	0	41	1088	0.065	15.41
671	14.9156202	18500	84	7.07	22.00	16.76	50.00	41.92	2161	35	38	1507	0.104	14.92
672	14.91094995	18500	84	7.07	20.10	15.32	46.81	41.92	2160	0	39	2030	0.077	14.91
673	14.95269726	18500	84	7.05	20.50	15.62	47.73	28.672	2170	0	40	2111	0.051	14.95
674	14.6399839	18500	84	7.07	22.00	16.76	51.76	28.672	2200	0	40	2898	0.056	14.64
675	15.00390656	18500	84	7.06	22.00	16.76	52.38	73.728	2383	42	39	3004	0.077	15.00
676	14.65726182	18500	84	7.05	22.00	16.76	52.38	73.728	2200	0	39	1968	0.077	14.66
677	15.17535714	18500	84	7.07	21.45	16.34	52.38	40.96	2345	6.3	40	2020	0.052	15.18
678	15.54100547	18500	84	7.07	20.00	15.24	50.00	45.056	2400	0	41	1953	0.040	15.54
679	15.44560231	18500	84	7.07	20.23	15.42	50.00	16.384	2400	0	38	1590	0.040	15.45
680	15.29377143	18500	84	7.07	20.86	15.89	50.00	42	2200	0	38	1400	0.072	15.29
681	15.312	18500	84	7.07	20.40	15.54	50.00	20	2180	0	37	1230	0.071	15.31
682	15.22235238	18500	84	7.06	20.45	15.58	55.00	22	2100	7	40	1210	0.072	15.22
683	15.37916667	18500	84	7.07	20.85	15.89	52.00	45	2100	10	42	1100	0.078	15.38
684	15.33356429	18500	84	7.07	20.14	15.35	53.00	47	2210	0	18	1100	0.067	15.33
685	15.46285714	18500	84	7.05	20.50	15.62	49.00	50	2130	0	12	1090	0.064	15.46
686	15.10979048	18500	84	7.05	20.40	15.54	58.00	52	2050	15	14	1090	0.057	15.11
Avg	15.32	18500.00	84.00	7.08	20.19	15.39	69.74	35.09	2212.54	10.41	37.57	1441.08	0.07	15.32
Stdev	0.45	0.00	0.00	0.03	1.15	0.88	38.88	18.75	89.77	14.91	9.52	526.83	0.02	0.45
Number	37	37	37	37	37	37	37	37	37	37	37	37	37	37
Cnf Intvl	95	95	96	95	95	95	95	95	95	95	95	95	95	95
Alpha	0.050	0.050	0.040	0.050	0.050	0.050	0.050	0.050	0.050	0.050	0.050	0.050	0.050	0.050
Confidence	0.15			0.01	0.37	0.28	12.53	6.04	28.93	4.80	3.07	169.75	0.01	0.15
Min	15	18500	84	7.05	17.12	13.05	46.81	0	2050	0	12	878	0	15
Max	16	18500	84	7.20	22.00	16.76	195.83	88	2400	48	63	3004	0	16

A4.4.1 down Flow Anaerobic Packed Bed Reactor (AnPBR):

Table A4.2, AnPBR Steady State Data

Day	SS Organic Loading Rate [kgCOD/m3/d]	SS Influent COD [mgCOD/L]	SS Influent Nitrogen [mgN/L]	Reactor pH	MLSS [mgTSS/L]	MLVSS [mgVSS/L]	Sludge Age [Days]	Effluent COD [mgCOD/L]	Effluent Alkalinity [mgCaCO3/L]	Effluent VFA [mgHAc/L]	Effluent N [mgN/L]	Effluent Na [mgNa/L]	Effluent Specific NaOH Cons	OLR [kgCOD/m3/d]
296	15.2445	18500	84	7.19		777		1608	3200	725	21	1406	0.061	20.75676
297	14.8089	18500	84	7.2		600		1622	3121	713	43	1235	0.071	20.17993
298	14.7107	18500	84	7.15		763		1717	3200	770	17	2143	0.127	20.16
299	15.4920	18500	84	7.18		899		1921	3158	756	13	1500	0.080	21.49254
300	14.6794	18500	84	7.13		954		2030	3035	779	15	2195	0.126	20.5
301	14.5869	18500	84	7.2	360.1	1390		2357	3106	779	13	1429	0.082	20.78351
302	14.9470	18500	84	7.1		801		1837	3222	769	73	2041	0.139	20.63158
303	13.5240	18500	84	7.1		815		2031	2879	788	40	1357	0.092	18.88665
304	12.5903	18500	84	7.1		732		2017	2601	729	40	546	0.033	17.568
305	16.5569	18500	84	7.1	230	925		2072	2552	776	12	1082	0.062	23.18049
306	14.8379	18500	84	7.1		635		1713	2923	769	43	1348	0.078	20.32941
307	14.3137	18500	84	7.1		442		1671	2927	799	40	1377	0.074	19.56287
308	14.7133	18500	84	7.2	419	470		1519	2900	770	43	1282	0.072	19.92903
309	15.1136	18500	84	7.1		387		1464	2543	568	42	286	0.014	20.40486
310	15.2410	18500	84	7.1		746		1699	3046	761	43	2778	0.178	20.8644
311	15.5200	18500	84	7.1		649		1561	2710	718	43	1563	0.101	21.07317
312	15.6472	18500	84	7.1	311	580		1561	2372	1189	43	2222	0.107	21.2459
313	15.4699	18500	84	7.1		1036		2079	2912	779.6	39	2083	0.132	21.66771
314	15.1943	18500	84	7.1		1091		2051	2823	772	36	2000	0.121	21.2459
315	15.8531	18500	84	7	430.6	635		1513	2801	730	35	1519	0.079	21.46415
316	15.1678	18500	84	7.1		677		1388	2758	726	30	1519	0.083	20.3871
317	15.8191	18500	84	7.1		594		1595	2413	787	32	1190	0.066	21.52313
318	17.3316	18500	84	7.1		554		1600	2848	750	27	2073	0.107	21.54745
319	15.6027	18500	84	7.1		511		1678	2875	733.5	34	4250	0.230	21.33333
320	15.2175	18500	84	7.1		442		1485	2872	770	31	1909	0.125	20.57018
321	14.2355	18500	84	7.1	539	1305		2362	2948	802	47	2195	0.127	20.28866
322	14.6021	18500	84	7.2		1373		2499	3012	879	25	2326	0.137	20.98983
323	16.2872	18500	84	7.1		644		1686	3046	797.9	31	1951	0.103	22.27925
324	16.0940	18500	84	7.1		781		1727	3275	921	21	3000	0.155	22.06897
325	16.0870	18500	84	7.1		760		1720	3344	803	36	2500	0.135	20
326	14.4767	18500	84	7.1		740		1796	3410	791	37	2947	0.223	19.93263
327	14.0910	18500	84	7.1		631		1521	3548	664	37	2047	0.104	19.08837
328	14.6720	18500	84	7.1		699		1535	3410	791	59	5061	0.235	19.89153
329	16.0687	18500	84	7.1	1295.2	932		1521	3548	604	52	2774	0.167	21.76744
330	15.5247	18500	84	7.1		932		1288	3613	728	50	2280	0.040	20.74576
331	15.4850	18500	84	7.1		987		1686	3656	851	35	2629	0.192	21.18194
332	14.9712	18500	84	7.1		521		1563	3544	830	40	1857	0.106	20.33
Avg	15.16	18500.00	84.00	7.11	512.13	767.87		1748.53	3031.11	774.81	35.69	1997.33	0.11	20.70
Stdev	0.86	0.00	0.00	0.04	358.80	247.90		281.23	333.56	94.52	12.95	897.79	0.05	1.02
Number	37	37	37	37	7	37		37	37	37	37	37	37	37
Cnf Intvl	95	95	95	95	95	95		95	95	95	95	95	95	95
Alpha	0.050	0.050	0.050	0.050	0.050	0.050		0.050	0.050	0.050	0.050	0.050	0.050	0.050
Confidence	0.28			0.05	265.79	79.88		90.62	107.48	30.46	4.17	289.28	0.02	0.33
Min	13	18500	84	7.0	230.0	386.8		1288.4	2372.0	568.0	12.0	285.7	0.0	17.6
Max	17	18500	84	7.2	1295.2	1389.9		2499.5	3656.0	1189.0	72.8	5061.3	0.2	23.2

Appendix 5.1: Anaerobic Digestion of Glucose – Metabolic Pathways

Metabolism is defined as the biological conversion of a biodegradable substrate for both (i) energy production (catabolism) and (ii) biomass production (anabolism). In this example, glucose will act as model substrate to illustrate the functioning of both the catabolic and anabolic pathways of anaerobic digestion. Four possible catabolic pathways exist in the anaerobic digestion of glucose. The preference of which pathway is taken is governed primarily by the hydrogen partial pressure and secondarily by the amount of energy (electrons) that can be gained from the pathway. The exact definitions of 'high' and 'low' hydrogen partial pressure will be evaluated in Chapter 6.

Catabolic Pathway 1 (Low pH_2 & $H_{2(aq)}$):

In the 'Pathway 1' scenario, the hydrogen partial pressure in the anaerobic environment is low. If this is the case hydrogen production is at its maximum and glucose is converted – via acidogenesis (Z_{ad}) - to 2 mols of acetic acid and 4 mols of hydrogen:

$$C_6H_{12}O_6 + 2H_2O \rightarrow 2C_2H_4O_2 + 2CO_2 + 8H^+ + 8e^-$$
$$8H^+ + 8e^- \rightarrow 4H_2$$

$$C_6H_{12}O_6 + 2H_2O \rightarrow 2C_2H_4O_2 + 2CO_2 + 4H_2$$

In the second step the acetoclastic methanogens (Z_{am}) convert the acetic acid produced to carbon dioxide and methane:

$$2C_2H_4O_2 + 4H_2O \rightarrow 4CO_2 + 16H^+ + 16e^-$$
$$2CO_2 + 16H^+ + 16e^- \rightarrow 2CH_4 + 4H_2O$$

$$2C_2H_4O_2 + 4H_2O \rightarrow + 2CO_2 + 2CH_4$$

In the final step of pathway 1 the hydrogen produced is converted to methane and water by the hydrogenotrophic methanogens (Z_{hm}):

$$4H_2 \rightarrow 8H^+ + 8e^-$$
$$CO_2 + 8H^+ + 8e^- \rightarrow CH_4 + H_2O$$

$$4H_2 + CO_2 \rightarrow + CH_4 + 2H_2O$$

If the above three steps are combined the metabolic end products of Pathway 1 is:

$$\boldsymbol{C_6H_{12}O_6 \rightarrow + 3CH_4 + 3CO_2}$$

Catabolic Pathway 2 (Any pH_2 & $H_{2(aq)}$):

The 'Pathway 2' scenario is independent of the hydrogen partial pressure, in this case glucose is converted to butyric acid by Z_{ad}:

$$C_6H_{12}O_6 \rightarrow C_4H_8O_2 + 2CO_2 + 4H^+ + 4e^-$$
$$4H^+ + 4e^- \rightarrow 2H_2$$

$$C_6H_{12}O_6 \rightarrow C_4H_8O_2 + 2CO_2 + 2H_2$$

Note, significantly less hydrogen is produced, so Pathway 2 will continue even under high partial pressure scenario's. However, significantly less energy (electrons) is produced compared with Pathway 1, thus giving preference to the first catabolic pathway whenever possible. In the next step of Pathway 2, the butyric acid is converted – via butyrate reducing acetogens (Z_{acBu}) – to acetic acid and hydrogen:

$$C_4H_8O_2 \rightarrow 2C_2H_4O_2 + 4H^+ + 4e^-$$
$$4H^+ + 4e^- \rightarrow 2H_2$$

$$C_4H_8O_2 \rightarrow 2C_2H_4O_2 + 2H_2$$

In the third step the acetic acid produced above is utilized by Z_{am}:

$$2C_2H_4O_2 + 4H_2O \rightarrow + 2CO_2 + 2CH_4$$

Finally, the hydrogen produced is again converted to methane and water by Z_{hm}:

$$4H_2 + CO_2 \rightarrow + CH_4 + 2H_2O$$

If the four steps of Pathway 2 are combined the end products of Pathway 2 is:

$$\boldsymbol{C_6H_{12}O_6 \rightarrow 3CH_4 + 3CO_2}$$

Catabolic Pathway 3 (High pH_2 & $H_{2(aq)}$):

In the 'Pathway 3' scenario, the hydrogen partial pressure in the anaerobic environment is high, if this is the case hydrogen production is at its minimum and glucose is converted – via Z_{ad} - to 1 mol of propionic acid, 1 mol of acetic acid and 1 mol of hydrogen:

$$C_6H_{12}O_6 \rightarrow C_3H_6O_2 + C_2H_4O_2 + 2CO_2 + 2H^+ + 2e^-$$
$$2H^+ + 2e^- \rightarrow H_2$$

$$C_6H_{12}O_6 \rightarrow C_3H_6O_2 + C_2H_4O_2 + 2CO_2 + H_2$$

In the second step the propionic acid is converted to 1 mol of acetic acid and 3 mols of hydrogen by the propionate reducing acetogens (Z_{acPr}):

$$C_3H_6O_2 + 2H_2O \rightarrow C_2H_4O_2 + CO_2 + 6H^+ + 6e^-$$
$$6H^+ + 6e^- \rightarrow 3\,H_2$$

$$C_3H_6O_2 + 2H_2O \rightarrow C_2H_4O_2 + CO_2 + 2H_2$$

In the third step the acetic acid is again converted to methane:

$$2C_2H_4O_2 + 4H_2O \rightarrow 2CO_2 + 2CH_4$$

And finally, the hydrogen produced in Pathway 3 is converted to methane and water:

$$4H_2 + CO_2 \rightarrow CH_4 + 2H_2O$$

If the four steps of Pathway 3 are combined the end products of Pathway 3 is:

$$\boldsymbol{C_6H_{12}O_6 \rightarrow 3CH_4 + 3CO_2}$$

Even though the catabolic intermediates of the three pathways differ significantly, the end products of catabolism is identical for the three pathways.

Anabolic Pathway:

Anabolism is completely unaffected by hydrogen partial pressure, but requires energy from the catabolic processes. Hence metabolism (growth) will slow down as the hydrogen partial pressure increases and the energy production in catabolism slows down. Unlike catabolism, anabolism can be described by a single redox reaction:

$$C_6H_{12}O_6 + 6H_2O \rightarrow 6CO_2 + 24H^+ + 24e^-$$
$$24H^+ + 24e^- + 6CO_2 + 1.2NH_3 \rightarrow 1.2C_5H_7O_2N + 9.6H_2O$$

$$C_6H_{12}O_6 + 1.2NH_3 \rightarrow 1.2C_5H_7O_2N + 3.6H_2O$$

A nitrogen source is required for the production of biomass.

Appendix 5.2:

The method to calculate the catabolic end products of glucose (Appendix 5.1) can also be applied to calculate the end products for any other biodegradable substrate of known composition. Table A5.1 summarizes the end products for all the species of importance in this project:

Table A5.1 Catabolic End Products of Biodegradable Substrates

Compound [1 mol]	Composition $C_xH_yO_z$			D_s [electron molar equivalents]	COD [g/mol]	Catabolic End Products [mols]		
	x	y	z			H_2O	CH_4	CO_2
Glucose	6	12	6	24	192	0	3	3
Ethanol	2	6	1	12	96	0	1.5	0.5
Methanol	1	4	1	6	48	0.5	0.75	0.25
Hexanoic Acid	6	12	2	32	256	-2	4	2
Valeric Acid	5	10	2	26	208	-1.5	3.25	1.75
Butyric Acid	4	8	2	20	160	-1	2.5	1.5
Propionic Acid	3	6	2	14	112	-0.5	1.75	1.25
Acetic Acid	2	4	2	8	64	0	1	1

Where D_s = the e^-equivalents/$mol_{substrate}$ = (4x+y-2z).

Similarly, the stoichiometric relationships for anabolism can be applied to predict the anabolic end products for the species of importance in this study assuming a $C_5H_7O_2N$ biomass composition (Table A5.2):

Table A5.2 Anabolic End Products of Biodegradable Substrates

Compound [1 mol]	Composition $C_xH_yO_z$			D_s/D_b	Metabolic End Products [mols]			
	x	y	z		H_2O	NH_3	CO_2	$C_5H_7O_2N$
Glucose	6	12	6	1.2	3.6	-1.2	0	1.2
Ethanol	2	6	1	0.6	1.8	-0.6	-1	0.6
Methanol	1	4	1	0.3	1.4	-0.3	-0.5	0.3
Hexanoic Acid	6	12	2	1.6	2.8	-1.6	-2	1.6
Valeric Acid	5	10	2	1.3	2.4	-1.3	-1.5	1.3
Butyric Acid	4	8	2	1	2	-1	-1	1
Propionic Acid	3	6	2	0.7	1.6	-0.7	-0.5	0.7
Acetic Acid	2	4	2	0.4	1.2	-0.4	0	0.4

Where D_b = e^-equivalents/$mol_{biomass}$ for biomass $C_5H_7O_2N$ = 20

Appendix 5.3: Combination of Catabolic & Anabolic Pathways

The fraction of the electrons in the substrate that undergoes anabolism (E) is derived from the kinetic part of the model which is based on a single representative organism for the anaerobic consortium including hydrolysis and reuse of biodegradable organics released via the endogenous process (Figure A5.1):

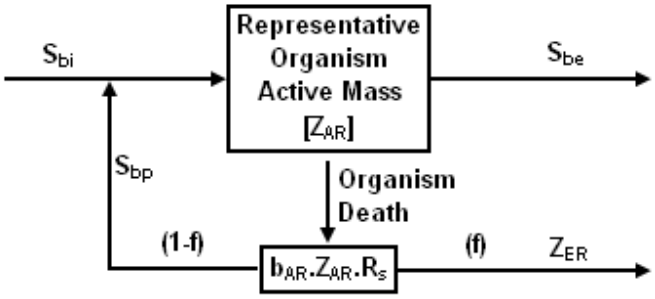

Figure A5.1, Single Surrogate Organism Death Regeneration Model

E is defined as the fraction of the COD (electrons) that is harvested from the reactor per day as active (Z_{AR}) and endogenous mass (Z_{ER}) per mass of biodegradable substrate utilized per day:

$$E = \frac{(Z_{AR} + Z_{ER})Q_w}{(S_{bi} - S_{be})Q_i} \tag{A5.1}$$

Since (Eq A5.1) is in terms of parameters that are supposed to be predicted by the steady state model, it is not of much use in this form and needs to be rewritten in terms of known parameters. This is done via a COD balance on various components formed in the anaerobic system. If a mass balance is done on the biodegradable substrate in the system the following is obtained (Figure A5.1):

$$[Accumulation] = [in] - [out] - [consumed] + [generated] \tag{A5.2}$$

$$V_r \frac{dS_b}{dt} = (S_{bi} - S_{be}).Q_i - S_{be}.Q_w - V_r.K.S_{be}. + (1-f).b_{AR}.Z_{AR}V_r \tag{A5.3}$$

With $K = \frac{\mu.Z_{AR}}{(K_s + S_{be})}$

Divide by V_r, $R_h = \frac{V_r}{Q_i}$ and $R_s = \frac{V_r}{Q_w}$ then:

$$\frac{dS_b}{dt} = \frac{(S_{bi} - S_{be})}{R_h} - \frac{S_{be}}{R_s} - K.S_{be} + (1 - f_{AR}).b_{AR}.Z_{AR} \quad \text{(A5.4)}$$

Similarly, a mass balance can be done on the active organisms mass (Z_{AR}) in the system:

$$V_r \frac{dZ_{AR}}{dt} = 0 - Z_{AR}.Q_w + V_r.Y.K.S_{be} - V_r.b_{AR}.Z_{AR} \quad \text{(A5.5)}$$

Or

$$\frac{dZ_{AR}}{dt} = -\frac{Z_{AR}}{R_s} + Y.K.S_{be} - b_{AR}.Z_{AR} \quad \text{(A5.6)}$$

At steady state $\frac{dZ_{AR}}{dt} = 0$ thus:

$$K.S_{be} = \frac{Z_{AR}\left(\frac{1}{R_s} + b_{AR}\right)}{Y_{AR}} \quad \text{(A5.7)}$$

At steady state $\frac{dS_b}{dt} = 0$ and if (A5.7) is substituted into (A5.4):

$$0 = \frac{(S_{bi} - S_{be})}{R_h} - \frac{S_{be}}{R_s} - \frac{Z_{AR}\left(\frac{1}{R_s} + b_{AR}\right)}{Y_{AR}} + (1 - f_{AR}).b_{AR}.Z_{AR} \quad \text{(A5.8)}$$

Rearranging Eq A5.8 for Z_{AR} yields:

$$Z_{AR} = \frac{\left(\frac{S_{bi} - S_{be}}{R_h}\right)}{\left(\frac{1}{Y_{AR}}\left(\frac{1}{R_s} + b_{AR}\right) - (1 - f_{AR}).b_{AR}\right)} \quad \text{(A5.9)}$$

The third mass balance that is required is on the endogenous mass (Z_{ER}) in the system:

$$V \frac{dZ_{ER}}{dt} = 0 - Z_{ER}.Q_w + V_r.f_{AR}.b_{ER}.Z_{ER} \quad \text{(A5.10)}$$

Divide by V_r, $R_h = \frac{V_r}{Q_i}$ and $R_s = \frac{V_r}{Q_w}$ then:

$$Z_{ER}\frac{1}{R_s} = f.b_{ER}.Z_{AR}$$

Rearrange:

$$Z_{ER} = f.b_{ER}.Z_{AR}.R_s \tag{A5.11}$$

Now we have the active (Z_{AR}) and endogenous mass (Z_{ER}) in terms of kinetic parameters.

$$Z_{VSS} = Z_{AR} + Z_{ER} = \frac{(S_{bi} - S_{be})}{R_h.\left(\frac{1}{Y_{AR}}\left(\frac{1}{R_s} + b_{AR}\right) - (1 - f_{AR}).b_{AR}\right)} + f.b_{AR}.Z_{AR}.R_s \tag{A5.12}$$

Rearrange

$$Z_{VSS} = Z_{AR} + Z_{ER} = \frac{(S_{bi} - S_{be}).(1 - f.b_{AR}.R_s)}{R_h.\left(\frac{1}{Y_{AR}}\left(\frac{1}{R_s} + b_{AR}\right) - (1 - f).b_{AR}\right)} \tag{A5.13}$$

Multiply by $\frac{R_s.Y_{AR}}{R_s Y_{AR}}$:

$$Z_{VSS} = Z_{AR} + Z_{ER} = \frac{Y_{AR}(S_{bi} - S_{be}).R_s(1 - f.b_{AR}.R_s)}{R_h.\left((1 - b_{AR}.R_s) - Y_{AR}(1 - f).b_{AR}.R_s\right)} \tag{A5.14}$$

Substituting Eq A5.14 into Eq A5.1 and $\frac{Q_w}{Q_i} = \frac{R_h}{R_s}$ yields:

$$E = \frac{Y_{AR}(1 - f.b_{AR}.R_s)}{\left(1 + b_{AR}R_s\left(1 - Y_{AR}\left(1 - f\right)\right)\right)} \tag{A5.15}$$

The above equations are general and apply to both the AnMBR and AnPBR.
For a system with (i) no unbiodegradable particulate organics in the feed and (ii) and fed only biodegradable soluble organics and (iii) the influent and effluent flow rates equal, as with the AnPBR, then $Q_w = Q_e$ i.e.

$$E = \frac{(Z_{AR} + Z_{ER})Q_w}{(S_{bi} - S_{be})Q_i} = \frac{Q_i\left(Z_{AR} + Z_{ER}\right)}{(S_{bi} - S_{be})Q_i} = \frac{S_{pe}}{\left(S_{bi} - S_{bse}\right)} \tag{A5.16}$$

Where

S_{pe}	= particulate effluent COD	[mgCOD/L]
S_{bi}	= influent biodegradable COD	[mgCOD/L]
S_{bse}	= biodegradable soluble effluent COD	[mgCOD/L]

Eq (A5.15) can be rearranged and in combination with (A5.16) can give the theoretical long term sludge age (R_{ST}) for the AnPBR system. Since $S_{te} = S_{pe} + S_{bse}$ = unfiltered effluent COD:

$$R_{ST} = \frac{(Y_{AR} - E)}{E.b_{AR}(1 - Y_{AR}(1 - f)) + Y_{AR}.b_{AR}} \quad \text{(A5.17)}$$

Eq A5.17 is valid only for long term (relative to sludge age) average values for S_{bi}, S_{bse} and S_{pe}.

Appendix 5.4: Anaerobic Metabolism of Biodegradable Organics

From Appendix 5.1 and Tables A5.1 and A5.2 it can be noted that there exists a relationship between the substrate composition and the ratio of metabolic end products produced from catabolism and anabolism. The catabolic and anabolic parts of the growth process will now be combined to give the overall metabolic process:

Catabolism:

$$C_xH_yO_z + (2x - z).H_2O \rightarrow x.CO_2 + D_s.H^+ + D_s.e^-$$

$$D_s.H^+ + D_s.e^- + \frac{D_s}{8}.CO_2 \rightarrow \frac{D_s}{8}.CH_4 + \frac{D_s}{4}.H_2O$$

$$C_xH_yO_z + \left(2x - \frac{D_s}{4} - z\right).H_2O \rightarrow \left(\frac{D_s}{8}\right).CH_4 + \left(x - \frac{D_s}{8}\right).CO_2 \quad \text{(A5.18)}$$

$$D_s = (4x + y - 2z)$$

Anabolism:

$$C_xH_yO_z + (2x - z).H_2O \rightarrow x.CO_2 + D_s.H^+ + D_s.e^-$$

$$D_b.e^- + D_b.H^+ + k.CO_2 + n.NH_3 \rightarrow C_kH_lO_mN_n + (2k - m).H_2O$$

$$C_xH_yO_z + \left((2x - z) - \frac{8.D_s}{D_b}\right).H_2O + \frac{D_s}{D_b}.NH_3 \rightarrow \left(x - \frac{5.D_s}{D_b}\right).CO_2 + \frac{D_s}{D_b}.C_5H_7O_2N \quad \text{(A5.19)}$$

$$D_b = (4.k + l - 2.m - 3.n) = 20 \text{ for } C_5H_7O_2N$$

The link between catabolism and anabolism is the E-value (Eq A5.15) as derived in Appendix 5.3 above, i.e. (1-E) catabolic reaction + (E) anabolic reaction equals the metabolic reaction.

Metabolism:

$$(1-E)\left[C_xH_yO_z+\left(2x-\frac{D_s}{4}-z\right).H_2O\rightarrow\left(\frac{D_s}{8}\right).CH_4+\left(x-\frac{D_s}{8}\right).CO_2\right]$$
$$+E\left[C_xH_yO_z+\left((2x-z)-\frac{8.D_s}{D_b}\right).H_2O+\frac{D_s}{D_b}.NH_3\rightarrow\left(x-\frac{5.D_s}{D_b}\right).CO_2+\frac{D_s}{D_b}.C_5H_7O_2N\right]$$

$$C_xH_yO_z+\left(2x-z-\frac{D_s}{4}(1-E)-\frac{8.E.D_s}{D_b}\right).H_2O+\frac{E.D_s}{D_b}NH_3\rightarrow$$
$$\frac{(1-E)D_s}{8}.CH_4+\left(x-\frac{D_s}{8}(1-E)-\frac{5.E.D_s}{D_b}\right).CO_2+\frac{E.D_s}{D_b}C_5H_7O_2N \quad \text{(A5.20)}$$

$$E=\frac{Y_{AR}(1-f.b_{AR}.R_s)}{\left(1+b_{AR}.R_s\left(1-Y_{AR}(1-f)\right)\right)}$$

Dissociated & Undissociated SCFAs:

F is defined as the split between the dissociated and undissociated forms of the SCFAs. This split (F) is governed by the dissociation constant (K_a) of the SCFAs. For any given pH:

$$[C_xH_yO_z]_{total}=[C_xH_yO_z]+[C_xH_{y-1}O_z^-] \quad \text{(A5.21)}$$

With $[C_xH_yO_z]_{total}$ being the total SCFAs concentration in the system. The equilibrium between the dissociated ($C_xH_{y-1}O_z^-$) and undissociated ($C_xH_yO_z$) forms are given by:

$$C_xH_yO_z \overset{K_{aFt}}{\rightleftharpoons} C_xH_{y-1}O_z^- + H^+$$

Or

$$K_{aFt}=\frac{\left[C_xH_{y-1}O_z^-\right]\left[H^+\right]_{feed}}{\left[C_xH_yO_z\right]} \quad \text{(A5.22)}$$

If Eq A5.21 and Eq A5.22 are combined, the fraction of the SCFAs in the dissociated form (F) is given by:

$$F=\frac{\left[C_xH_{y-1}O_z^-\right]}{\left[C_xH_yO_{ztotal}\right]}=\frac{1}{\left(1+\frac{K_{aFt}}{\left[H^+\right]_{feed}}\right)} \quad \text{(A5.23)}$$

Eq A5.20 can now be rewritten to include the effect of the dissociated SCFAs:

$$C_xH_yO_z + \left(2x - z - \frac{D_s}{4}(1-E) - \frac{8.E.D_s}{D_b}\right).H_2O + \frac{E.D_s}{D_b}NH_3 \rightarrow$$
$$\frac{(1-E)D_s}{8}.CH_4 + \left(x - \frac{D_s}{8}(1-E) - \frac{5.E.D_s}{D_b}\right).CO_2 + \frac{E.D_s}{D_b}C_5H_7O_2N \quad \text{(A5.24)}$$

$$CO_{2(gas)} + H_2O + C_xH_{y-1}O_z^- \rightarrow C_xH_yO_z + HCO_3^- \quad \text{(A5.25)}$$

$$C_xH_{y-1}O_z^- + \left(2x - z - \frac{D_s}{4}(1-E) - \frac{8.E.D_s}{D_b} + 1\right).H_2O + \frac{E.D_s}{D_b}NH_3 \rightarrow$$
$$\frac{(1-E)D_s}{8}.CH_4 + \left(x - \frac{D_s}{8}(1-E) - \frac{5.E.D_s}{D_b} - 1\right).CO_2 + HCO_3^- + \frac{E.D_s}{D_b}C_5H_7O_2N \quad \text{(A5.26)}$$

Now Eq A5.24 to A5.26 can be combined to yield the stoichiometric conversion of dissociated (F) and undissociated (1-F) SCFAs:

$$(F)\left(\begin{array}{l} C_xH_{y-1}O_z^- + \left(2x - z - \frac{D_s}{4}(1-E) - \frac{8.E.D_s}{D_b} + 1\right).H_2O \\ + \frac{E.D_s}{D_b}NH_3 \rightarrow \frac{(1-E)D_s}{8}.CH_4 + \left(x - \frac{D_s}{8}(1-E) - \frac{5.E.D_s}{D_b} - 1\right).CO_2 \\ + HCO_3^- + \frac{E.D_s}{D_b}C_5H_7O_2N \end{array}\right)$$
$$(1-F)\left(\begin{array}{l} C_xH_yO_z + \left(2x - z - \frac{D_s}{4}(1-E) - \frac{8.E.D_s}{D_b}\right).H_2O + \frac{E.D_s}{D_b}NH_3 \rightarrow \\ \frac{(1-E)D_s}{8}.CH_4 + \left(x - \frac{D_s}{8}(1-E) - \frac{5.E.D_s}{D_b}\right).CO_2 + \frac{E.D_s}{D_b}C_5H_7O_2N \end{array}\right)$$

$$\begin{array}{l} (1-F).C_xH_yO_z + F.C_xH_{y-1}O_z^- \\ + \left(2x + F - z - \frac{D_s}{4}(1-E) - \frac{8E.D_s}{D_b}\right).H_2O + \left(E\frac{D_s}{D_b}\right).NH_3 \rightarrow \\ (1-E)\left(\frac{D_s}{8}\right).CH_4 + \left(x - F - \frac{D_s}{8}(1-E) - \frac{E.5.D_s}{D_b}\right).CO_{2AD} + F.HCO_3^-{}_{AD} \\ + \left(E\frac{D_s}{D_b}\right).C_5H_7O_2N \end{array} \quad \text{(A5.27)}$$

Urea ($CO(NH_2)_2$) is used as nitrogen source in this study. Thus the NH_3 in Eq A5.27 needs to be substituted for urea and converted to NH_4^+. The dissociation of Urea is described as follows:

$$b.CO(NH_2)_2 + 3.b.H_2O + b.CO_2 \rightarrow 2.b.NH_4^+ + 2.b.HCO_3^- \quad \text{(A5.28)}$$

Secondly, alkalinity is dosed as NaOH, thus hydroxide (OH^-) dosing also needs be incorporated into Eq A5.27:

$$d.OH^- + d.CO_2 \rightarrow d.HCO_3^- \quad \text{(A5.29)}$$

The inclusion of Eqs A5.28 and A5.29 in A5.27 yields:

$$\begin{aligned}&(1-F).C_xH_yO_z + F.C_xH_{(y-1)}O_z^- + b.CO(NH_2)_2 + d.OH^- \\ &+\left(2.x + 3.b + F - z - \frac{E.D_s}{D_b}(2.k - m + n) - \frac{(1-E)D_s}{4}\right).H_2O \rightarrow \\ &\left(x - b - F - d - \frac{E.D_s}{D_b}(k-n) - \frac{(1-E)D_s}{8}\right).CO_{2\,AD} + \frac{(1-E)D_s}{8}.CH_4 \\ &+\left(2.b + F + d - \frac{n.E.D_s}{D_b}\right).HCO_3^-{}_{AD} + \left(2.b - \frac{n.E.D_s}{D_b}\right).NH_4^+ + \frac{E.D_s}{D_b}C_kH_lO_mN_n\end{aligned} \quad \text{(A5.30)}$$

Where
k = 5; l = 7; m = 2; n = 1 and D_b = 20 for $C_5H_7O_2N$ for the biomass

Appendix 5.5: Proton Balance for pH Prediction

This pH prediction method takes into account the bicarbonate produced from (i) the anaerobic digestion of dissociated SCFAs (HCO^-_{3Inf}), (ii) the hydrolysis of urea (HCO^-_{3Urea}), (ii) OH^--dosing for pH control ($HCO_3^-{}_{NaOH}$), (iii) the alkalinity required to neutralize undigested SCFAs ($HCO_3^-{}_{SCFA}$) and (iv) the carbon dioxide partial pressure (P_{CO2}). SCFAs that are not digested dissociates in the reactor because of the high reactor pH (7 compared with the feed pH of 3.77), this consumes alkalinity:

$$\begin{aligned}C_xH_yO_z &\rightarrow H^+ + C_xH_{(y-1)}O_z^- \\ HCO_3^-{}_{SCFA} + H^+ &\rightarrow H_2CO_3^* \rightarrow CO_{2SCFA} + H_2O \\ \hline C_xH_yO_z + HCO_3^-{}_{SCFA} &\rightarrow C_xH_{(y-1)}O_z^- + CO_{2SCFA} + H_2O\end{aligned} \quad \text{(A5.31)}$$

Since the optimal pH for anaerobic digestion is in the 6.8 to 7.5 range, it can be assumed that virtually all the inorganic carbon is in HCO_3^- form. Therefore the total inorganic carbon can be defined as:

$$C_t = \left[HCO_3^-\right]_{Total} = \left[HCO_3^-\right]_{AD} - \left[HCO_3^-\right]_{SCFA} \quad \text{(A5.32)}$$

Where

$$\left[HCO_3^-\right]_{AD} = \left[HCO_3^-\right]_{Inf} + \left[HCO_3^-\right]_{Alk} + \left[HCO_3^-\right]_{Urea} \quad \text{(A5.33)}$$

With
$[HCO_3^-{}_{AD}]$ = bicarbonate produced via Eq 5.30
$[HCO_3^-{}_{Inf}]$ = bicarbonate produced from the anaerobic digestion of dissociated SCFAs
$[HCO_3^-{}_{Alk}]$ = bicarbonate produced from OH^- dosing
$[HCO_3^-{}_{Urea}]$ = bicarbonate produced via urea hydrolysis
$[HCO_3^-{}_{SCFA}]$ = bicarbonate consumed for undissociated SCFA neutralization

The second parameter required for pH prediction is the partial pressure of CO_2 in the gas phase. This partial pressure is nothing more than the mol fraction of the CO_2 in the gas phase:

$$P_{CO2} = \frac{CO_2}{(CO_2 + CH_4)} = \frac{(CO_{2AD} + CO_{2SCFA})}{(CH_4 + CO_{2AD} + CO_{2SCFA})} \quad \text{(A5.34)}$$

Where
CO_{2AD} = carbon dioxide produced in Eq 5.30
CO_{2SCFA} = carbon dioxide produced from neutralization of undissociated SCFAs not utilized in the in the anaerobic digestion process (effluent SCFA) (Eq 5.28)

Now the pH relationship can be defined in terms of C_t and P_{CO2}. For any given pH:

$$C_t = \left[H_2CO_3^*\right] + \left[HCO_3^-\right] + \left[CO_3^{2-}\right] \quad \text{(A5.35)}$$

And if this is combined with Henry's law and the carbonate equilibrium relationships:

$$P_{CO2} = K_h.[H_2CO_3^*] \quad \text{(A5.36)}$$

And

$$K_{c1} = \frac{\left[HCO_3^-\right]\left[H^+\right]}{\left[H_2CO_3^*\right]} \quad \text{(A5.37)}$$

And

$$K_{c2} = \frac{\left[HCO_3^-\right]\left[H^+\right]}{\left[CO_3^{2-}\right]} \quad \text{(A5.38)}$$

Thus

$$C_t = K_h.P_{CO2} + \frac{K_{c1}.K_h.P_{CO2}}{[H^+]_{reactor}} + \frac{K_{c1}.K_{c2}.K_h.P_{CO2}}{[H^+]^2_{reactor}} \quad \text{(A5.39)}$$

If Eq 5.39 is rearranged and combined with $pH = \log_{10}[H^+]$ then:

$$pH = -log_{10}\left(\frac{K_h + \left(K_h^{\,2} - 8\left(\frac{C_t}{K_{c1}.P_{CO2}} - 1\right).K_{c2}\right)^{\frac{1}{2}}}{2.\left(\frac{C_t}{K_{c1}.P_{CO2}} - 1\right)}\right) \qquad \text{(A5.40)}$$

Eq A5.40 can now be solved along with Eq 5.30, Eq A5.34 and Eqs A5.32 and 5.33 to yield the system P_{CO2}, $H_2CO_3^*$ Alkalinity and reactor pH respectively.

Appendix 6.1: Dynamic AD-FTRW Model Constants

Table A6.1: Final Stoichiometric & Kinetic Constants for Individual FOGs in Model

Functional Organism Group		Stoichiometric		Kinetic	
		Biomass Yield (Y)	Endogenous Respiration Rate (b)	Maximum Specific Growth Rate (μ_{max})	Half Saturation Coefficient (K_s)
		[$mol_{Biomass}$ /$mol_{Substrate}$]	[1/d]	[1/d]	[mol/L]
Acidogenesis	Z_{ad}	0.1465	0.041	0.8	0.001
Acetogenesis (Hx)	Z_{acHx}	0.0303	0.015	1.18	0.00021
Acetogenesis (Va)	Z_{acVa}	0.0301	0.015	1.53	0.009
Acetogenesis (Bu)	Z_{acBu}	0.0301	0.015	2.268	0.005
Acetogenesis (Pr)	Z_{acPr}	0.0205	0.015	1.1	0.0002
Acetogenesis (EtOH)	Z_{acEtOH}	0.0125	0.015	1.15	0.001
Acetoclastic Methanogenesis	Z_{am}	0.02	0.037	1.5	0.0005
Methanogenesis (MeOH)	Z_{mm}	0.0181	0.037	1.15	0.001
Hydrogenotrophic Methanogenesis	Z_{hm}	0.0029	0.01	1.2	0.001

fcv = 1.52, fi = 0.78, f = 0.08

Table A6.2: Weak Acid Dissociation Constants at 25 ^{o}C (expressed as their negative log value pK) and Their Temperature Dependency. pK = A/T-B-C.T (Helgeson., 1976)

Thermodynamic Weak Acid Dissociation Constants		pK 25^{o}C	A	B	C	Apparent Weak Acid Dissociation Constants	
Carbonate	**pK_{c1}**	6.352	3404.7	14.844	0.0328	**pK'_{c1}**	$pK_{c1} + Log(f_m)$
	pK_{c2}	10.329	2902.4	6.498	0.0238	**pK'_{c2}**	$pK_{c2}- log(f_m)+log(f_d)$
Henry's Constant	**pK_h**	1.47	-1760	-9.619	-0.0075	**pK'_h**	pKh
Short Chain Fatty Acids:							
Acetic Acid (C_2)	**pK_{Ac}**	4.765	1170.5	3.165	0.0134	**pK'_{Ac}**	$pK_{Ac} + Log(f_m)$
Propionic Acid (C_3)	**pK_{Pr}**	4.874	1213.3	3.386	0.0141	**pK'_{Pr}**	$pK_{Pr} + Log(f_m)$
Butyric Acid (C_4)	**pK_{Bu}**	4.82				**pK'_{Bu}**	$pK_{Bu} + Log(f_m)$
Valeric Acid (C_5)	**pK_{Va}**	4.8				**pK'_{Va}**	$pK_{Va} + Log(f_m)$
Hexanoic Acid (C_6)	**pK_{Hx}**	4.85				**pK'_{Hx}**	$pK_{Hx} + Log(f_m)$

Table A6.3: Calculation of Activity Coefficients with Davies Eqs (Butler., 1964)

Activity Coefficients		
$log(f_m) = -A.((u^{1/2}/(1+u^{1/2}))-0.3u)$	**f_m**	Monovalent Ion Activity Coefficient
$log(f_d) = -A.4.((u^{1/2}/(1+u^{1/2}))-0.3u)$	**f_d**	Divalent Ion Activity Coefficient
	u	Ionic Strength Approximation (Kemp., 1971)
u = 0.00025.(TDS-20)	**A**	Temperature Dependant Constant
$A = 1.825*10^6.(78.3.T)^{-1.5}$	**T**	Temperature (Kelvin)
	TDS	Total Inorganic Dissolved Salts [mg/L]

Table A6.4: Inhibition Function Constants

Temperature		
T_{UL}	315	K
T_{LL}	305	K
pH		
$pH_{ULZadZac}$	8	
$pH_{LLZadZac}$	4	
$pH_{ULZamZmm}$	8	
$pH_{LLZamZmm}$	6.5	
pH_{ULZhm}	8	
pH_{LLZhm}	6.8	
Hydrogen		
k_{IH2Zad}	6.25E-04	mol/L
k_{IH2Zac}	1.00E-05	mol/L
$k_{IH2ZacPr}$	3.50E-06	mol/L
Total SCFA		
$k_{IAtZacPr}$	0.018	mol/L
k_{IAtZam}	0.1	mol/L

Appendix 6.2: Materials & Methods – Batch Test for Kinetic Parameter Optimization

The aim of this part of the project was to observe the utilization and product formation during the anaerobic digestion of the SCFAs in FTRW. The data collected was applied to calibrate the Monod half saturation constants (K_{sj}) in the dynamic AD-FTRW model.

A biomass sample was taken form the AnMBR after a stable operational period of longer than two weeks. The biomass was then transferred to a 1 L completely mixed batch reactor. Environmental conditions (T, pH and Alkalinity) in the batch reactor were a direct replica of the conditions in the AnMBR. After transfer the biomass was allowed to mix for 20 minutes to insure all residual SCFAs in the sample was completely utilized.

FTRW was then injected into the batch reactor via port 1 (Figure A6.1). The time was logged as the time of injection (t_{inj}). The amount of FTRW injected was estimated from the mass of biomass in the bacth reactor and the F/M ratio of the AnMBR during the stable period;

$$M_{FTRW} = (F/M)_{AnMBR}.MX_{VSS} \quad \text{(A6.1)}$$

Immediately after t_{inj} the first sample was drawn from port 2. It is assumed that no substrate utilization occurred up to this point. Samples were then taken at regular

intervals (every 60 min) and analysed for filtered COD, SCFA, Alkalinity and also the individual SCFAs were tested with an HPLC.

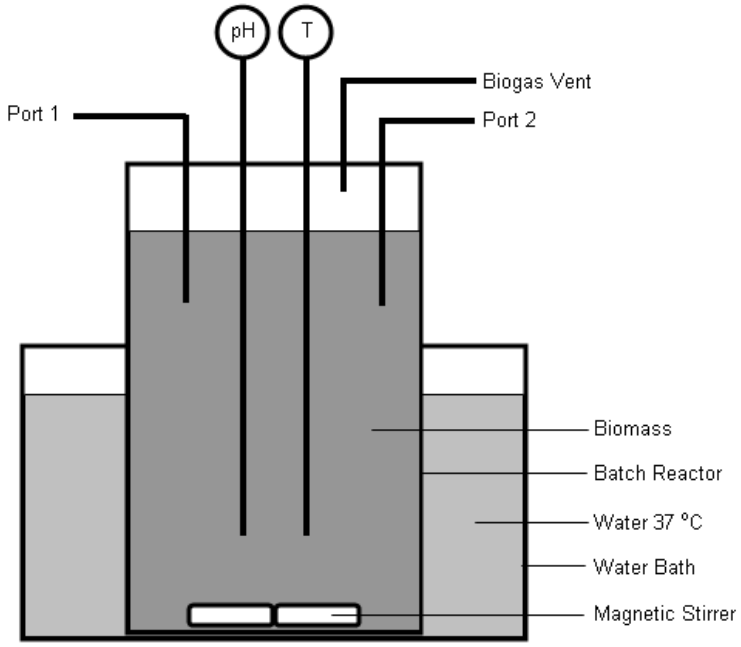

Figure A6.1, Batch Test Experimental Setup

Hourly samples are drawn until the effluent SCFA and COD approached zero. The length of time it takes for the biomass to utilize all the substrate is a function of the mass of biomass in the batch reactor. Typical output data is as follows (Figure A6.2):

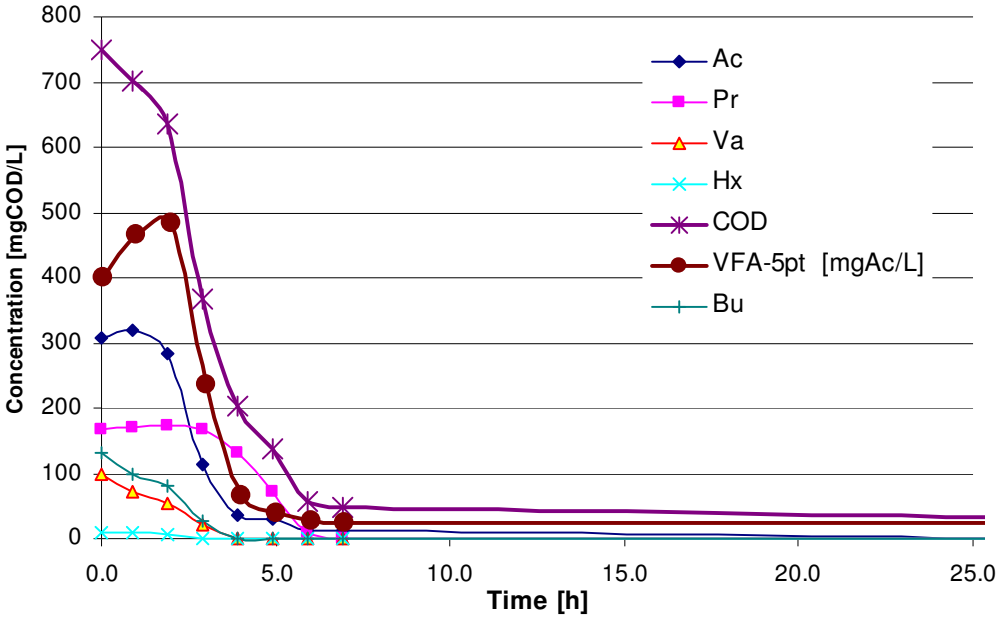

Figure A6.2: Substrate Utilization in Batch Test

Output data include COD, VFA-5pt, and the individual SCFA concentration time-concentration profiles after $t_{injection}$. Note acetate (Ac) and propionate (Pr) initially increases and then decrease because significant amounts of these compounds are

produced by the utilization of the C_6 to C_4 SCFAs in FTRW. It should be noted that the HPLC was only calibrated to a lower limit of 0.00025 mol/L (15 mg/L for Ac) and values recorded below this limit can be regarded as an extrapolation below the Method Detection Limit (MDL). Some caution should be taken with the use of such data since it might have a negative effect on parameter calibrations.

Appendix 6.3: Derivation of Dynamic AD-FTRW Stoichiometry

Acetogenesis of Hexanoic (Ha), Valeric (Va), Butyric (Bu), Propionic (Pr) Acid and Ethanol;

Catabolism

$$C_xH_{2x}O_z + (2+2p+z)H_2O \rightarrow C_2H_4O_2 + p.C_{(x-2)}H_{2(x-2)q}O_2 + 2r.H^+ + 2r.e^-$$
$$2r.H^+ + 2r.e^- \rightarrow r.H_2$$

$$C_xH_{2x}O_z + (2+2p+z)H_2O \rightarrow C_2H_4O_2 + pC_{(x-2)}H_{2(x-2)q}O_2 + r.H_2 \quad \text{(A6.2)}$$

Where

$$r = \left(x + 2p - z - \frac{pq(x-2)}{2}\right) \quad \text{(A6.3)}$$

If $\frac{x}{3} \geq 1$ then p = 1 else p = 0

If x=3 then q = 0 else q = 1

Anabolism

$$C_xH_yO_z + \left(\frac{5.D_s}{20} - x\right).CO_2 + \frac{D_s}{20}.NH_3 \rightarrow \left(\frac{8.D_s}{20} - (2x-z)\right).H_2O + \frac{D_s}{20}.C_5H_7O_2N \quad \text{(A6.4)}$$

Where

D_s = *(4x+y-2z)* = Substrate electron donating capacity [e^-/mol]

Metabolism

The catabolic and anabolic processes are combined through the true organism yield (Y_j);

$$(1-Y_{acj})\left(C_xH_{2x}O_z + (2+2p+z)H_2O \rightarrow C_2H_4O_2 + pC_{(x-2)}H_{2(x-2)q}O_2 + r.H_2\right) \quad \text{(A6.5)}$$
$$+Y_{acj}.\left(C_xH_yO_z + \left(\frac{5.D_s}{20} - x\right).CO_2 + \frac{D_s}{20}.NH_3 \rightarrow \left(\frac{8.D_s}{20} - (2x-z)\right).H_2O + \frac{D_s}{20}.C_5H_7O_2N\right)$$

(A6.6)

Secondly the WABC relationships are also incorporated into the metabolism;

$$F = \frac{\left[C_x H_{2x-1} O_z^-\right]}{\left[C_x H_{2x} O_z\right]_{total}} = \frac{1}{\left(1 + \frac{K_{acj}}{\left[H^+\right]_{feed}}\right)} \tag{A6.7}$$

$$C_x H_{2x} O_{zTotal} = (1-F) C_x H_{2x} O_z + F.C_x H_{(2x-1)} O_z^- \tag{A6.8}$$

$$F.C_x H_{(2x-1)} O_z^- + F.H_2 CO_3 \rightarrow F.C_x H_{2x} O_z + F.HCO_3^- \tag{A6.9}$$

$$\left(\frac{5D_s}{20} - x\right) H_2 CO_3 \rightarrow \left(\frac{5D_s}{20} - x\right).CO_2 + \left(\frac{5D_s}{20} - x\right).H_2 O \tag{A6.10}$$

$$HCO_3^- + NH_4^+ \rightarrow NH_3 + H_2 CO_3 \tag{A6.11}$$

By combining Eq's A6.6.5 to A6.11 the following expression is obtained for the description of the acetogenesis of FTRW;

$$\begin{aligned}
&(1-F) C_x H_{2x} O_z + F.C_x H_{(2x-1)} O^- + \left(E\left(\frac{5.D_s}{20} - x\right) + F - \left(\frac{E.D_s}{20}\right)\right).H_2 CO_3 \\
&+ \left((1-E)(2 - z + 2.p) - E\left(\left(\frac{8.D_s}{20}\right) - (2.x - z)\right) - E\left(\left(\frac{5.D_s}{20}\right) - x\right)\right).H_2 O + \frac{E.D_s}{20} NH_4^- \rightarrow \\
&(1-E) C_2 H_4 O_2 + (1-E) C_{xp} H_{ypq} O_2 + (1-E)\left(x + 2.p - z - \left(q.z\left(\frac{(x-2)}{2}\right)\right)\right) H_2 \\
&+ \left(F - \left(\frac{E.D_s}{20}\right)\right) HCO_3^- + \left(\frac{E.D_s}{20}\right) C_5 H_7 O_2 N
\end{aligned} \tag{A6.12}$$

If $\frac{x}{3} \geq 1$ then p = 1 else p = 0

If x=3 then q = 0 else q = 1

Appendix 6.4: Dynamic AD-FTRW Petersen Matrix & External Calculations

Processes →	Components →	1	2	3	4	5	6	7	8	9	10	11	12	13	14	15	16	17	18	19	20	21	22	23	24	25	26	27	Process Rates
		H_2O	CH_4	H_2	CO_2	H_2CO_3	HCO_3^-	NH_4^+	Ac	MeOH	EtOH	Pr	Bu	Va	Hx	$(NH_2)_2CO$	OH^-	S_{bp}	Z_{ad}	Z_{acHx}	Z_{acVa}	Z_{acBu}	Z_{acPr}	Z_{acEt}	Z_{mm}	Z_{am}	Z_{hm}	Z_e	
1	Acidogenesis (Z_{ad}) Growth	$\frac{-5(1-Y_{ad})}{Y_{ad}}$		$\frac{2(1-Y_{ad})}{Y_{ad}}$			$\frac{(1-Y_{ad})}{Y_{ad}}$	$\frac{(1-Y_{ad})}{Y_{ad}}$	$\frac{2(1-Y_{ad})}{Y_{ad}}$									$-\frac{1}{Y_{ad}}$	1										$\frac{\mu_{max,ad}S_{bp}Z_{ad}}{(K_{sad}+S_{bp})}\left(Sin\left(\frac{((T_k-273.15)-22)\pi}{30}\right)\right)\left(\frac{1+10^{-0.43(pH_{LLimAc}-pH_{LLimAc})}}{(1+10^{pH_L-pH_{LLimAc}}+10^{pH_{LLimAc}-pH_L})}\right)\left(1+\frac{H_2}{(k_{H_2Z_{ad}}+H_2)}\right)$
2	Acidogenesis (Z_{ad}) Death																	$(1-f)$	-1									f	$b_{ad}Z_{ad}$
3	Hexanoic Acid Acetogenisis (Z_{acHx}) Growth	$\frac{-(10-34Y_{acH_2})}{8Y_{acHx}}$		$\frac{8(1-Y_{acH_2})}{8Y_{acHx}}$		$-\frac{(5F_{acHx}+2Y_{acHx})}{8Y_{acHx}}$	$\frac{(5F_{acHx}-8Y_{acHx})}{8Y_{acHx}}$	-1	$\frac{5(1-Y_{acHx})}{8Y_{acHx}}$				$\frac{5(1-Y_{acHx})}{8Y_{acHx}}$		$-\frac{5}{8Y_{acHx}}$					1									$\frac{\mu_{max,acHx}HxZ_{acHx}}{(K_{acHx}+Hx)}\left(Sin\left(\frac{((T_k-273.15)-22)\pi}{30}\right)\right)\left(\frac{1+10^{-0.43(pH_{LLimHx}-pH_{LLimHx})}}{(1+10^{pH_L-pH_{LLimHx}}+10^{pH_{LLimHx}-pH_L})}\right)\left(\frac{1}{1+\frac{H_2}{k_{HxZ_{ac}}}}\right)$
4	Hexanoic Acid Acetogenisis (Z_{acHx}) Death																	$(1-f)$		-1								f	$b_{acHx}Z_{acHx}$
5	Valeric Acid Acetogenisis (Z_{acVa}) Growth	$-\frac{(20-59Y_{acVa})}{13Y_{acVa}}$		$\frac{20(1-Y_{acVa})}{13Y_{acVa}}$		$-\frac{(10F_{acVa}+2Y_{acVa})}{13Y_{acVa}}$	$\frac{(10F_{acVa}-13Y_{acVa})}{13Y_{acVa}}$	-1	$\frac{10(1-Y_{acVa})}{13Y_{acVa}}$			$\frac{10(1-Y_{acVa})}{13Y_{acVa}}$		$-\frac{10}{13Y_{acVa}}$							1								$\frac{\mu_{max,acVa}VaZ_{acVa}}{(K_{acVa}+Va)}\left(Sin\left(\frac{((T_k-273.15)-22)\pi}{30}\right)\right)\left(\frac{1+10^{-0.43(pH_{LLimAc}-pH_{LLimAc})}}{(1+10^{pH_L-pH_{LLimAc}}+10^{pH_{LLimAc}-pH_L})}\right)\left(\frac{1}{1+\frac{H_2}{k_{HH_2Z_{ac}}}}\right)$
6	Valeric Acid Acetogenisis (Z_{acVa}) Death																	$(1-f)$			-1							f	$b_{acVa}Z_{acVa}$
7	Butyric Acid Acetogenisis (Z_{acBu}) Growth	$-\frac{(2-5Y_{acBu})}{13Y_{acBu}}$		$\frac{2(1-Y_{acBu})}{Y_{acBu}}$		$-\frac{F_{acBu}}{Y_{acBu}}$	$\frac{F_{acBu}}{Y_{acBu}}-1$	-1	$\frac{2(1-Y_{acBu})}{Y_{acBu}}$				$-\frac{1}{Y_{acBu}}$									1						$\frac{\mu_{max,acBu}BuZ_{acBu}}{(K_{acBu}+Bu)}\left(Sin\left(\frac{((T_k-273.15)-22)\pi}{30}\right)\right)\left(\frac{1+10^{-0.43(pH_{LLimAc}-pH_{LLimAc})}}{(1+10^{pH_L-pH_{LLimAc}}+10^{pH_{LLimAc}-pH_L})}\right)\left(\frac{1}{1+\frac{H_2}{k_{HH_2Z_{ac}}}}\right)$
8	Butyric Acid Acetogenisis (Z_{acBu}) Death																	$(1-f)$				-1						f	$b_{acBu}Z_{acBu}$
9	Propionic Acid Acetogenisis (Z_{acPr}) Growth	$-\frac{(30-51Y_{acPr})}{7Y_{acPr}}$		$\frac{30(1-Y_{acPr})}{7Y_{acPr}}$		$-\frac{(10-8Y_{acPr}-10F_{acPr})}{7Y_{acPr}}$	$\frac{(10F_{acPr}-7Y_{acPr})}{7Y_{acPr}}$	-1	$\frac{10(1-Y_{acPr})}{7Y_{acPr}}$			$-\frac{10}{7Y_{acPr}}$											1						$\frac{\mu_{max,acPr}PrZ_{acPr}}{(K_{acPr}+Pr)}\left(Sin\left(\frac{((T_k-273.15)-22)\pi}{30}\right)\right)\left(\frac{1+10^{-0.43(pH_{LLimAc}-pH_{LLimAc})}}{(1+10^{pH_L-pH_{LLimAc}}+10^{pH_{LLimAc}-pH_L})}\right)\left(\frac{1}{1+\frac{H_2}{k_{HH_2Z_{ac}Pr}}}\right)\left(\frac{1}{1+\frac{SCFA}{k_{ISCFAZ_{ac}Pr}}}\right)$
10	Propionic Acid Acetogenisis (Z_{acPr}) Death																	$(1-f)$					-1					f	$b_{acPr}Z_{acPr}$
11	Ethanol Acetogenisis (Z_{acEt}) Growth	$-5\frac{(5-19Y_{acEt})}{15Y_{acEt}}$		$\frac{10(1-Y_{acEt})}{3Y_{acEt}}$		$-\frac{2}{3}$	-1	-1	$\frac{5(1-Y_{acEt})}{3Y_{acEt}}$		$-\frac{5}{3Y_{acEt}}$													1					$\frac{\mu_{max,acEt}EtZ_{acEt}}{(K_{acEt}+Et)}\left(Sin\left(\frac{((T_k-273.15)-22)\pi}{30}\right)\right)\left(\frac{1+10^{-0.43(pH_{LLimAc}-pH_{LLimAc})}}{(1+10^{pH_L-pH_{LLimAc}}+10^{pH_{LLimAc}-pH_L})}\right)\left(\frac{1}{1+\frac{H_2}{k_{HH_2Z_{ac}}Et}}\right)$
12	Ethanol Acetogenisis (Z_{acEt}) Death																	$(1-f)$						-1				f	$b_{acEt}Z_{acEt}$
13	Methanol Methanogenesis (Z_{mm}) Growth	$\frac{(5-33Y_{mm})}{6Y_{mm}}$	$\frac{(30-30Y_{mm})}{12Y_{mm}}$			$-\frac{(5-9Y_{mm})}{6Y_{mm}}$	-1	-1		$-\frac{10}{3Y_{mm}}$															1			$\frac{\mu_{max,mm}MeZ_{mm}}{(K_{Zmm}+Me)}\left(\frac{1+10^{-0.5(T_{LL}-T_{LL})}}{(1+10^{(T_k-T_L)}+10^{(T_L-T_k)})}\right)\left(\frac{1+10^{-0.43(pH_{LLZmm}-pH_{LLZmm})}}{(1+10^{pH_L-pH_{LLZmm}}+10^{pH_{LLZmm}-pH_L})}\right)$
14	Methanol Methanogenesis (Z_{mm}) Death																	$(1-f)$								-1		f	$b_{mm}Z_{mm}$
15	Acetoclastic Methanogenesis (Z_{am}) Growth	$-\frac{(5-11Y_{am})}{2Y_{am}}$	$\frac{(5-5Y_{am})}{2Y_{am}}$			$-\frac{(5-3Y_{am}-5F_{am})}{2Y_{am}}$	$\frac{(5F_{am}-2Y_{am})}{2Y_{am}}$	-1	$-\frac{5}{2Y_{am}}$																1			$\frac{\mu_{max,am}AcZ_{am}}{(K_{Sam}+Ac)}\left(\frac{1+10^{-0.5(T_{LL}-T_{LL})}}{(1+10^{(T_k-T_L)}+10^{(T_L-T_k)})}\right)\left(\frac{1+10^{-0.43(pH_{LLZam}-pH_{LLZam})}}{(1+10^{pH_L-pH_{LLZam}}+10^{pH_{LLZam}-pH_L})}\right)\left(\frac{1}{1+\frac{SCFA}{k_{ISCFAZam}}}\right)$
16	Acetoclastic Methanogenesis (Z_{am}) Death																	$(1-f)$								-1		f	$b_{am}Z_{am}$
17	Hydrogenotrophic Methanogenesis (Z_{hm}) Growth	$-10\frac{(15+11Y_{hm})}{20Y_{hm}}$	$\frac{(10-10Y_{hm})}{4Y_{hm}}$	$-\frac{10}{Y_{hm}}$		$-10\frac{(5-3Y_{hm})}{20Y_{hm}}$	-1	-1																		1		$\frac{\mu_{max,hm}H_2Z_{hm}}{(K_{Shm}+H_2)}\left(Sin\left(\frac{((T_k-273.15)-22)\pi}{30}\right)\right)\left(\frac{1+10^{-0.43(pH_{LLHm}-pH_{LLHm})}}{(1+10^{pH_L-pH_{LLHm}}+10^{pH_{LLHm}-pH_L})}\right)$
18	Hydrogenotrophic Methanogenesis (Zhm) Death																	$(1-f)$									-1	f	$b_{hm}Z_{hm}$
19	Carbon Dioxide (CO2) Expulsion/Dissolution	1			1	-1																							$K_{lCO_2}\left(H_cCO_g-K_{eqCO_2}CO_L\right)$
20	Hydroxide to Carbonate	1				-1	1										-1												$K_{lgOH^-}OH^-$
21	Urea Hydrolyis	-2				-1	2	2																					$K_{Urea}(NH_2)_2CO$

External Calculations

Reactor pH

$$pH = -log_{10}\left(\frac{K_h + \left(K_h{}^2 - 8\left(\frac{C_t}{K_{c1}.P_{CO2}} - 1\right).K_{c2}\right)^{\frac{1}{2}}}{2.\left(\frac{C_t}{K_{c1}.P_{CO2}} - 1\right)}\right) \quad \text{(A6.13)}$$

Alkalinity

$$H_2CO_3{}^{*}\,Alkalinity = \left[HCO_3{}^{-}\right] * 50000 \quad \text{(A6.14)}$$

Effluent Soluble COD

$$S_{bs} = \begin{pmatrix}[Hx]*256 + [Va]*208 + [Bu]*160 + [\mathrm{Pr}]*112 \\ +[Ac]*64 + [Me]*48 + [Et]*96\end{pmatrix}.1000 \quad \text{(A6.15)}$$

Short Chain Fatty Acids

$$SCFA = \left([Hx] + [Va] + [Bu] + [\mathrm{Pr}] + [Ac] + [Me] + [Et]\right) * 60000 \quad \text{(A6.16)}$$

Effluent Total Nitrogen

$$N_{te} = \left(2 * [Urea] + [NH_4]\right) * 14000 \quad \text{(A6.17)}$$

Mixed Liquor Suspended Solids

$$MLSS = \begin{pmatrix}[Z_{ad}] + [Z_{acHx}] + [Z_{acVa}] + [Z_{acBu}] + [Z_{ac\,\mathrm{Pr}}] \\ +[Z_{acEt}] + [Z_{am}] + [Z_{mm}] + [Z_{hm}] + [S_{bp}]\end{pmatrix}\left(\frac{160000}{f_{cv}.f_i}\right) \quad \text{(A6.18)}$$

Carbon Dioxide in Biogas

$$CO_2 = \frac{[CO_2].T_k.8314}{P_{atm}} \quad \text{(A6.19)}$$

Methane in Biogas

$$CO_2 = \frac{[CH_4].T_k.8314}{P_{atm}} \quad \text{(A6.20)}$$